Global heat adaptation among urban populations and its evolution under different climate futures

---

Linda Krummenauer

Kumulative Dissertation

zur Erlangung des akademischen Grades
"doctor rerum naturalium" (Dr. rer. nat.)

in der Wissenschaftsdisziplin
Klimafolgenforschung (Geoökologie)

eingereicht an der
Mathematisch-Naturwissenschaftlichen Fakultät
Institut für Umweltwissenschaften und Geographie
Universität Potsdam

Datum der Disputation
16. Juni 2022

Linda Krummenauer
Global heat adaptation among urban populations and its evolution under different climate Futures

Tag der Einreichung: Potsdam, den 31. August 2021
Tag der Disputation: Potsdam, den 16. Juni 2022

Gutachterinnen und Gutachter

Prof. Dr. Jurgen P. Kropp
Potsdam-Institut fur Klimafolgenforschung, Forschungsbereich II Climate Resilience
Universitat Potsdam, Institut fur Umweltwissenschaften und Geographie
Prof. Dr. Annegret Thieken
Universitat Potsdam, Institut fur Umweltwissenschaften und Geographie
Prof. Dr. Diana Reckien
University of Twente, Department of Urban and Regional Planning and Geo-Information Management

Published online on the
Publication Server of the University of Potsdam:
https://doi.org/10.25932/publishup-55929
https://nbn-resolving.org/urn:nbn:de:kobv:517-opus4-559294

Abstract

Heat and increasing ambient temperatures under climate change represent a serious threat to human health in cities. Heat exposure has been studied extensively at a global scale. Studies comparing a defined temperature threshold with the future daytime temperature during a certain period of time, had concluded an increase in threat to human health. Such findings however do not explicitly account for possible changes in future human heat adaptation and might even overestimate heat exposure. Thus, heat adaptation and its development is still unclear. Human heat adaptation refers to the local temperature to which populations are adjusted to. It can be inferred from the lowest point of the U- or V-shaped heat-mortality relationship (HMR), the Minimum Mortality Temperature (MMT). While epidemiological studies inform on the MMT at the city scale for case studies, a general model applicable at the global scale to infer on temporal change in MMTs had not yet been realised. The conventional approach depends on data availability, their robustness, and on the access to daily mortality records at the city scale. Thorough analysis however must account for future changes in the MMT as heat adaptation happens partially passively. Human heat adaptation consists of two aspects: (1) the intensity of the heat hazard that is still tolerated by human populations, meaning the heat burden they can bear and (2) the wealth-induced technological, social and behavioural measures that can be employed to avoid heat exposure. The objective of this thesis is to investigate and quantify human heat adaptation among urban populations at a global scale under the current climate and to project future adaptation under climate change until the end of the century. To date, this has not yet been accomplished. The evaluation of global heat adaptation among urban populations and its evolution under climate change comprises three levels of analysis. First, using the example of Germany, the MMT is calculated at the city level by applying the conventional method. Second, this thesis compiles a data pool of 400 urban MMTs to develop and train a new model capable of estimating MMTs on the basis of physical and socio-economic city characteristics using multivariate non-linear multivariate regression. The MMT is successfully described as a function of the current climate, the topography and the socio-economic standard, independently of daily mortality data for cities around the world. The city-specific MMT estimates represents a measure of human heat adaptation among the urban population. In a final third analysis, the model to derive human heat adaptation was adjusted to be driven by projected climate and socio-economic variables for the future. This allowed for estimation of the MMT and its change for 3 820 cities worldwide for different combinations of climate trajectories and socio-economic pathways until 2100. The knowledge on the evolution of heat adaptation in the future is a novelty as mostly heat exposure and its future development had been researched. In this work, changes in heat adaptation and exposure were analysed jointly. A wide range of possible health-related outcomes up to 2100 was the result, of which two scenarios with the highest socio-economic developments but opposing strong warming levels were highlighted for comparison. Strong economic growth based upon fossil fuel exploitation is associated with a high gain in heat adaptation, but may not be able to compensate for the associated negative health effects due to increased heat exposure in 30% to 40% of the cities investigated caused by severe climate change. A slightly less strong, but sustainable growth brings moderate gains in heat adaptation but a lower heat exposure and exposure reductions in 80% to 84% of the cities in terms of frequency (number of days exceeding the MMT) and intensity (magnitude of the MMT exceedance) due to a milder global warming. Choosing a 2 °C compatible development by 2100 would therefore lower the risk of heat-related mortality at the end of the century. In summary, this thesis makes diverse and multidisciplinary contributions to a deeper understanding of human adaptation to heat under the current and the future climate. It is one of the first studies to carry out a systematic and statistical analysis of urban characteristics which are useful as MMT drivers to establish a generalised model of human heat adaptation, applicable at the global level. A broad range of possible heat-related health options for various future scenarios was shown for the first time. This work is of relevance for the assessment of heat-health impacts in regions where mortality data are not accessible or missing. The results are useful for health care planning at the meso- and macro-level and to urban- and climate change adaptation planning. Lastly, beyond having met the posed objective, this thesis advances research towards a global future impact assessment of heat on human health by providing an alternative method of MMT estimation, that is spatially and temporally flexible in its application.

Zusammenfassung

Hitze und steigende Umgebungstemperaturen im Zuge des Klimawandels stellen eine ernsthafte Bedrohung für die menschliche Gesundheit in Städten dar. Die Hitzeexposition wurde umfassend auf globaler Ebene untersucht. Studien, die eine definierte Temperaturschwelle mit der zukünftigen Tagestemperatur während eines bestimmten Zeitraums verglichen, hatten eine Zunahme der Gefährdung der menschlichen Gesundheit ergeben. Solche Ergebnisse berücksichtigen jedoch nicht explizit mögliche Veränderungen der zukünftigen menschlichen Hitzeadaption und könnten daher sogar die Hitzeexposition überschätzen. Somit ist die menschliche Adaption an Hitze und ihre zukünftige Entwicklung noch unklar. Die menschliche Hitzeadaption bezieht sich auf die lokale Temperatur, an die sich die Bevölkerung angepasst hat. Sie lässt sich aus dem Tiefpunkt der U- oder V-förmigen Relation zwischen Hitze und Mortalität (HMR), der Mortalitätsminimaltemperatur (MMT), ableiten. Während epidemiologische Fallstudien über die MMT auf Stadtebene informieren, wurde ein auf globaler Ebene anwendbares allgemeines Modell, um auf die zeitliche Veränderung der MMTs zu schließen, bisher noch nicht realisiert. Der konventionelle Ansatz ist abhängig von der Datenverfügbarkeit, ihrer Robustheit und dem Zugang zu täglichen Mortalitätsdaten auf Stadtebene. Eine gründliche Analyse muss jedoch zukünftige Veränderungen in der MMT berücksichtigen, da die menschliche Hitzeanpassung teils passiv erfolgt. Die menschliche Hitzeanpassung besteht aus zwei Aspekten: (1) aus der Intensität der Hitze, die von der menschlichen Bevölkerung noch toleriert wird, also die Hitzebelastung, die sie ertragen kann, und (2) aus vermögensbedingten technologischen, sozialen und verhaltensbezogenen Maßnahmen, die zur Vermeidung von Hitzeexposition eingesetzt werden können. Das Ziel dieser Arbeit ist es, die menschliche Hitzeanpassung der städtischen Bevölkerung unter dem aktuellen Klima auf globaler Ebene zu untersuchen und zu quantifizieren und die zukünftige Anpassung an den Klimawandel bis zum Ende des Jahrhunderts zu projizieren. Dies wurde bis heute noch nicht erreicht. Die Bewertung der globalen Hitzeanpassung städtischer Bevölkerungen und ihrer Entwicklung unter dem Klimawandel umfasst drei Analyseebenen. Erstens wird am Beispiel Deutschlands die MMT auf Stadtebene nach der konventionellen Methode berechnet. Zweitens trägt diese Arbeit einen Datenpool von 400 städtischen MMTs zusammen, um auf dessen Basis ein neues Modell zu entwickeln und zu trainieren, das in der Lage ist, MMTs auf der Grundlage von physischen und sozioökonomischen Stadtmerkmalen mittels multivariater nichtlinearer multivariater Regression zu schätzen. Es wird gezeigt, dass die MMT als Funktion des aktuellen Klimas, der Topographie und des sozioökonomischen Standards beschrieben werden kann, unabhängig von täglichen Sterblichkeitsdaten für Städte auf der ganzen Welt. Die stadtspezifischen MMT-Schätzungen stellen ein Maß für die menschliche Hitzeeanpassung der städtischen Bevölkerung dar. In einer letzten dritten Analyse wurde das Modell zur Schätzung der menschlichen Hitzeadaption angepasst, um von für die Zukunft projizierten Klima- und sozioökonomischen Variablen angetrieben zu werden. Dies ermöglichte eine Schätzung des MMT und seiner Veränderung für 3 820 Städte

weltweit für verschiedene Kombinationen aus Klimatrajektorien und sozioökonomischen Entwicklungspfaden bis 2100. Das Wissen über die Entwicklung der menschlichen Hitzeanpassung in der Zukunft ist ein Novum, da bisher hauptsächlich die Hitzeexposition und ihre zukünftige Entwicklung erforscht wurden. In dieser Arbeit wurden die Veränderungen der menschlichen Hitzeadaptation und der Hitzeexposition gemeinsam analysiert. Das Ergebnis ist ein breites Spektrum möglicher gesundheitsbezogener Zukünfte bis 2100, von denen zum Vergleich zwei Szenarienkombinationen mit den höchsten sozioökonomischen Entwicklungen, aber gegensätzlichen starken Erwärmungsniveaus hervorgehoben wurden. Ein starkes Wirtschaftswachstum auf der Grundlage der Nutzung fossiler Brennstoffe fördert zwar einen hohen Zugewinn an Hitzeanpassung, kann jedoch die damit verbundenen negativen gesundheitlichen Auswirkungen aufgrund der erhöhten Exposition in rund 30% bis 40% der untersuchten Städte aufgrund eines starken Klimawandels möglicherweise nicht ausgleichen. Ein etwas weniger starkes, dafür aber nachhaltiges Wachstum bringt aufgrund einer milderen globalen Erwärmung eine moderate Hitzeanpassung und eine geringere Hitzeexposition und sogar eine Abnahme der Exposition in 80% bis 84% der Städte in Bezug auf Häufigkeit (Anzahl der Tage über der MMT) und Intensität (Magnitude der MMT-Überschreitung). Die Wahl einer 2 °C-kompatiblen Entwicklung bis 2100 würde daher das Risiko einer hitzebedingten Sterblichkeit am Ende des Jahrhunderts senken. Zusammenfassend liefert diese Dissertation vielfältige und multidisziplinäre Beiträge zu einem tieferen Verständnis der menschlichen Hitzeanpassung unter dem gegenwärtigen und zukünftigen Klima. Es ist eine der ersten Studien, die eine systematische und statistische Analyse städtischer Merkmale durchführt, die sich als MMT-Treiber verwenden lassen, um ein verallgemeinertes Modell der menschlichen Hitzeanpassung zu erarbeiten, das auf globaler Ebene anwendbar ist. Erstmals wurde ein breites Spektrum möglicher hitzebedingter Gesundheitsoptionen für verschiedene Zukunftsszenarien aufgezeigt. Diese Arbeit ist von Bedeutung für die Bewertung von hitzebezogener Gesundheitsauswirkungen in Regionen, in denen Mortalitätsdaten nicht zugänglich sind oder fehlen. Die Ergebnisse sind nützlich für die Gesundheitsplanung auf Meso- und Makroebene sowie für die Stadtplanung und die Planung der Anpassung an den Klimawandel. Über das Erreichen des gestellten Ziels hinaus treibt diese Dissertation die Forschung in Richtung einer globalen zukünftigen Folgenabschätzung von Hitze auf die menschliche Gesundheit voran, indem eine alternative Methode der MMT-Schätzung bereitgestellt wird, die in ihrer Anwendung räumlich und zeitlich flexibel ist.

Publications

This cumulative dissertation comprises the following research articles that were published in ISI-indexed journals:

Chapter 3: Huber, V., Krummenauer, L., Lange, S., Pena Ortiz, C., Gasparrini, A., Vicedo-Cabrera, A., Garcia Herrera, R. and K. Frieler. Temperature-related excess mortality in German cities at 2 °C and higher degrees of global warming. In: *Environmental Research, (186:109447) July 2020.* https://doi.org/10.1016/j.envres.2020.109447

Chapter 4: Krummenauer, L., Prahl, B.F., Costa, L., Holsten, A. Walther, C. and J.P. Kropp (2019): Global drivers of minimum mortality temperatures in cities. In: *Science of the Total Environment (695:133560), December 2019*. https://doi.org/10.1016/j.scitotenv.2019.07.366.

Chapter 5: Krummenauer, L., Costa, L., Prahl, B.F. and J.P. Kropp (2021): Future heat adaptation and exposure among urban populations and why a prospering economy alone won't save us. In: *Scientific Reports (11:20309), October 2021*. https://doi.org/10.1038/s41598-021-99757-0.

Minor adjustments in spelling and grammar have been made to the articles as presented here in chapters 3, 4, and 5 to create a uniform style across this thesis. For reader-friendly referencing of appendix material, slight modifications have been made in the articles and in the appendices.

Acknowledgements

I would like to thank Prof. Dr. Jürgen Kropp for the opportunity of writing my doctoral thesis at the Potsdam Institute for Climate Impact Research (PIK). In particular, I thank him for his valuable advice and his support to let me work freely on such an interesting topic that was quite novel to our working group at PIK. I would like to thank Prof. Dr. Annegret Thieken for her supervision at the University of Potsdam.

Further, I thank Prof. Jürgen Kropp, Prof. Dr. Annegret Thieken and Prof. Dr. Diana Reckien for having reviewed my work; Prof. Dr. Manfred Rolfes for having chaired my doctoral defense, and Prof. Dr. Oliver Korup and Prof. Dr. Hubert Wiggering for having joined the examination committee.

I am very grateful to Dr. Luís Costa and to Dr. Boris Prahl for the regular meetings, fruitful discussions and their critical feeback on my work and for their guidance.

Enriching overarching discussions with Dr. Mathias Lüdeke and great methodological advice by Dr. Diego Rybski were always very much appreciated. Acknowledgements to Dr. Anne Holsten, who initiated my first contact to today's dissertation topic.

Many thanks to Prof. Dr. Cristina Pena Ortiz for hosting me at Universidad Pablo de Olavide in Sevilla, Spain. I am very much obliged to Dr. Veronika Huber for letting me contribute to her fantastic work and for having me in Sevilla.

Thanks to our working group members for the good company and joyful moments, especially during Pappelallee times. I am very happy that some of you became my very dear friends, a special thank you to Boris Prahl, Markus Böttle and Manon Glockmann, but also to Bin Zhou, Luís Costa, Carsten Walther, Ramana Gudipudi, Yunfei Li, David Landholm, Tabea Lissner and Anne Holsten. The same holds for Nuria Plaza Martín and Ana Fernández Ayuso, thank you for your friendship at UPO Sevilla and far beyond.

I am thankful to have received funding from the Potsdam Graduate School at the University of Potsdam and the DAAD.

Last but not least, I am deeply grateful to my family for their support and patience. I thank my father to have triggered my interest in geography and climate. Thank you Alejandro for all your support and your care.

Contents

List of Figures

List of Tables

Acronyms and Abbreviations

MMT Minimum Mortality Temperature
HMR Heat-mortality Relationship
UHI Urban Heat Island
WBT Wet Bulb Temperature
WBTmax Maximum Wet Bulb Temperature
RMSE Root Mean Square Error
AICc Akaike Information Criterion
CI Confidence Interval
eCI Empirical Confidence Interval
GMT Global Mean Temperature
RR Risk Ratio
CMIP Coupled Model Intercomparison Project
GCM General Circulation Model
RCP Representative Concentration Pathway
DLNM Distributed-lag non-linear model
QAIC Quasi-Akaike Information Criterion
BLUP Best linear unbiased predictor
SD Standard deviation
SDgcm Standard deviation of mean excess mortality estimates based on central BLUPs across GCMs
SDrcp Standard deviation of mean excess mortality estimates based on central BLUPs across RCPs
SDepi Standard Deviation resulting from Monte Carlo simulations considering GCMs and RCPs one at a time
GHG Greenhouse Gas
SSP Shared Socio-Economic Pathway
RH Relative Humidity (%)
MCC Multicountry Multicommunity Collaborative Network
ICD International Classification of Diseases

Introduction

Transforming knowledge into a global model to project future human heat adaptation

1

1.1 The essence of heat-related mortality and heat adaptation among urban populations

During the 2000s, the warmest decade globally since the beginning of the records, some world regions had experienced a number of record-breaking heat waves and the monthly temperature extremes had been five times larger than in a climate without long-term warming (Coumou et al., 2013). Conditions that were associated with severe heat waves such as in 2003, 2006 and 2015, have increased over recent decades (Kornhuber et al., 2019). There is evidence that human-induced climate change has increased the probability of occurrence and magnitude of such severe heat waves in the recent climate (Ciavarella et al., 2021). Prominent examples of severe heat waves of the recent past that were associated with increased mortality are the 1995 heat wave in Chicago (USA), where more than 700 people lost their lives within five days (Semenza et al., 1996), during the 2003 European heatwave an excess mortality of 140% was found for the highly urbanised Paris area in contrast to other French regions (Fouillet et al., 2006). India was severely impacted in 2015 with location-specific temperatures exceeding 50 °C resulting in 2 248 death cases across the country (Sarath Chandran et al., 2017). A recent study attributed 37% of the death cases in the warm seasons during the period 1991 to 2018 to anthropogenic climate change in 732 cities across all continents (Vicedo-Cabrera et al., 2021). A slightly increasing trend in heat-related mortality in 2000–2019 was observed in 750 cities across the globe (Zhao et al., 2021b).

In the future, with an increasing trend in the global mean temperature, heatwaves are projected to become more frequent, severe, and longer-lasting until the end of the 21st century (Meehl, 2004; Coumou and Robinson, 2013; Masson-Delmotte et al., 2021). They will be accompanied by larger uncertainty and climate variability, also at the regional scale (Ganguly et al., 2009). For Chicago (USA), a broad range of excess mortality estimates from future heat waves, between 166 and 2 217 cases per year, was provided (Peng et al., 2011). Heat particularly concerns cities due to a higher heat burden in urban areas compared to their surroundings, which is called the Urban Heat Island (UHI) (Oke, 1973). Details on this phenomenon follow in Chapter 1.1.1.

However, not only heat extremes, but generally also medium temperatures are going to rise with global warming. Under a climate trajectory representing high Greenhouse Gas (GHG) concentrations Representative Concentration Pathway (RCP) 8.5, cities in the USA, the Middle East, northern-central Asia, northeastern China as well as continental cities in South America and Africa were projected to experience a substantial warming (Zhao et al., 2021a). Such conditions constitute a threat to human heat in cities. Future heat-related excess mortality in cities in the USA, south-central Europe, Mexico, and South Africa was projected to increase, especially under RCP 8.5 (Lee et al., 2020). For cities in Northern Europe, East Asia, and Australia, where heat-related excess mortality is relatively low as of 2010–2019 (0.3–0.5%), a moderate increase in heat-related excess mortality (2.5–3.2%) is projected in 2090–2099 (Gasparrini et al., 2017). Cities in hotter regions, i.e. Central and South America, Southern Europe and Southeast Asia already show a relatively high level of heat-related excess mortality today (0.6–1.7%). For the future, a considerable increase is estimated up to 10.5% in Southern Europe and culminating at 16.7% in southeast Asia (Gasparrini et al., 2017). For ten US cities, totals of temperature-related deaths and the Empirical Confidence Intervals (eCIs) are given (Weinberger et al., 2017) and the following pattern detectable: In any RCP, the mortality is going to increase, whereas the higher the forcing, the more fatalities are projected to occur in the future. For RCP8.5 and concerning the year 2090, almost three times as many death cases are projected for the ten US cities in total as had occurred in 1997. This work exemplarily demonstrates how impact projections of future heat-related mortality are derived from future exposure metrics. Adaptation to heat however, is not taken into account in the modelling strategy, as also practised by a number of further studies (Baccini et al., 2011; Peng et al., 2011; Wu et al., 2014; Hajat et al., 2014; Gasparrini et al., 2017). Most authors assume no changes in adaptation and population and thus either continue observed mortality pattern until the end of the century (Gasparrini et al., 2017). Still, it would be important to consider heat adaptation as it functions, besides heat exposure, as a second control for heat-related health outcomes. A review study suggested the integration of adaptation was advantageous over excluding it (Gosling et al., 2017). The objective of this thesis is to establish a method to assess global heat adaptation among urban populations and inform about its development considering different climate futures. Hence, in this work it is argued that it is pivotal to appraise both aspects, human heat adaptation and exposure, jointly in context. A plain change in climate or exposure does not necessarily lead to a change in mortality because societies might be able to adapt over time, attenuating mortality risk. Neglecting adaptation in impact assessments on heat-related mortality likely leads to an overestimation of heat impacts (Gosling et al., 2017; Huang et al., 2011).

In this thesis, the definition of 'human heat adaptation' diverges from established broader definitions of 'adaptation' in context of overall climate change adaptation, such as the definition given in the IPCC's Fifth Assessment Report (WGII AR5) (Agard et al., 2014). The quantification of human adaptation to elevated temperature can be inferred from the Heat-mortality Relationship (HMR), which is commonly derived by impact studies on heat-related mortality. The HMR is location-specific and usually represented by U- or V-shaped curve in most cases showing the dependency of daily mortality records or mortality Risk Ratios (RRs) against daily temperature data (McMichael et al., 2008; Bao et al., 2016) (see Figure 1.2 A). Mortality or risk is highest with low and high temperatures. The lowest point on the HMR, also called exposure-response function, is the Minimum Mortality Temperature (MMT). It is also referred to as 'optimum temperature', where health outcomes from heat are lowest for a population (Iñiguez et al., 2010; Bao et al., 2016; Gasparrini et al., 2015). Studies have proposed the use of the MMT as indication of human long-term adaptation to heat (Folkerts et al., 2020; Åström et al., 2016). As it indicates the temperature associated with the minimum mortality on the HMR, it is therefore currently the best empirical measure of the temperature level to which a city's population is adapted to at a specific point in time. Temperatures significantly higher or lower than the MMT are associated with disproportional increases in excess mortality. Upward changes in the MMT were found to shift the entirety of the curve representing the HMR as well as associated indicators such as threshold values defining national heat-wave warnings (López-Bueno et al., 2021), hence suggesting that heat adaptation is taking place (Follos et al., 2020). In this thesis, the MMT is considered as an initial information to address the posed challenge of developing a method to estimate the MMT as a backbone of this work and to evaluating the evolution of future human heat adaptation. So far, its use in future impact assessments on heat-related mortality remains debatable, as such studies often show deficits in how they assume changes in the HMR and the MMT until the future. Most commonly, the MMT and the HMR are 'shifted' into higher temperatures (see Gosling et al., 2017). This means that mortality in the future will remain the same and the projected U- or V-shaped HMR will remain in its original shape as it was established for observed mortality and temperature data. More details on this critical topic are presented in Chapter 1.1.2. Here in contrast, it is assumed that human adaptation to any location-specific temperature is continuously given and partially autonomous (Turek-Hankins et al., 2021; Petkova et al., 2014; Gosling et al., 2017) but may alter with changes in temperature and other influential factors. These characteristics distinguish human heat adaptation from the adaptation to other types of climate-related hazards. It contains a component of adaptation that is rooted in an individual or a group of population. These features demonstrate the uniqueness of the population's heat adaptation, which is presented in more details in Chapter 1.1.2.

As of today, the present day MMT has been established for more than 660 case study cities from 43 countries, by applying a common methodology, while at the time the work at hand was initiated in 2015, a number of 272 cities were considered (Gasparrini et al., 2015; London School of Hygiene and Tropical Medicine, 2021). This considerable effort, having assembled the data and analysis, was led by the Multicountry Multicommunity Collaborative Network (MCC) and must be acknowledged here. Despite of this growing pool of cities across the globe for which the HMR and the MMT have been established for the recent past and lately for the future, the information offered by this data pool is spatially incoherent. Many smaller cities around the globe have not yet been investigated and even larger cities from some world regions are still underrepresented (Gasparrini et al., 2017; Egondi et al., 2012; El-Zein et al., 2004). This is either due to the unavailability of continuous time series of mortality and temperature records on a daily basis in the first place, the reliability of such health outcome data, or it might even be due to a lack of research interest or funding in those locations (El-Zein et al., 2004; Egondi et al., 2012). Most obviously, data is available in developed and emerging economies (Guo et al., 2018; Gasparrini et al., 2017). However, so far, not many MMTs existed for German cities, despite being a 'typical' country of research interest in this field: First, death cases are officially registered at the city-level, which could easily be exploited to establish the HMR. Second, a share of 77.4% of Germany's population lives in cities as of 2019 (The World Bank, 2019), which makes the establishment of the urban HMR a legitimate research pursuit. Munich, Nuremberg and Augsburg had already been covered (D'Ippoliti et al., 2010; Breitner et al., 2014; Chen et al., 2019; Rai et al., 2019).

This thesis seeks to complement the data pool with MMTs for German case studies and aims to demonstrate the data-induced challenges despite of given data availability, and to underline the need for a simpler and more generalised method to derive the MMT for larger amounts of cities at a time. While at the case study scale, the input data to estimate the MMT is clear, the generic drivers of MMTs at the global urban scale has received little scrutiny. The necessity to better understand the mechanism between heat impacts and the city environment becomes obvious. It is crucial to make MMT visible and understandable at the global level and investigate beyond case studies in data-rich and economically wealthy regions. After all, the MMT is key to determining the populations' level of heat adaptation at present and in the future climate (López-Bueno et al., 2021; Folkerts et al., 2020; Follos et al., 2020). This endeavour addresses the quest for a better understanding of heat-related adaptation, that had been put forward earlier (Arbuthnott et al., 2016; Gosling et al., 2017; Liu and Ma, 2019) and a quest to identify which factors majorly influence human heat adaptation in order to promote them by heat adaptation policies (Folkerts et al., 2020). The outcomes serve to foster urban resilience and support to avert heat-related mortality in the future, which is of utmost importance since cities have to cope with a higher heat burden than their surrounding, see Chapter 1.1.1.

As an overarching goal, this work is motivated by investigating human heat adaptation in different urban settings under recent and future climate conditions and by understanding in which way different trajectories of global warming will take its influence on human health outcomes. A general and flexible model to estimate the MMT for recent and future climate conditions is the major prerequisite to achieve this goal. This thesis acknowledges the value of locally-specific MMTs and the data-related challenges to generate the HMR for case studies, which is a precondition to further scale the MMT to the global level. Further, it recognises the MMT as precondition to research recent and future human heat adaptation at the global urban level and to adjust its application for use with the future climate and socio-economic development. The latter exercise is particularly interesting due to the coverage of multiple climate futures and socio-economic pathways that might take influence on the future MMT. This thesis aims at assessing how future heat adaptation is influenced by changes in climate and socio-economy. It seeks to contextualise the evolution of adaptation with changes in heat exposure to robustly project possible health outcomes at the end of the 21st century. Such knowledge enables the identification of locations that are particularly in danger due to small gains in collective heat adaptation but simultaneously large alterations in heat exposure across various climate futures. As a side product, this thesis informs future impact studies on spatially accurately disaggregated MMTs and their change magnitudes

Besides its scientific advancement in this field, this thesis provides a basis to build a knowledge pool to minimise fatalities from heat in the future by separating the contributions of different components of heat adaptation to overall human heat adaptation. The usefulness of the insights generated here is not only constrained to decision-makers in the health sector, but is also valuable information for urban and infrastructure planning to create resilient cities in the future. Additionally, it serves capacity building in terms of institutional and public preparedness and awareness, which is still lacking among many citizens, the elderly and even local policymakers (Beckmann and Hiete, 2020; Lenzholzer et al., 2020; Valois et al., 2020). Already today, fatalities could be avoided, e.g. the death of a 17-year old boy in Cordoba (Spain) who jumped into a swimming pool to refresh himself after heat exposure during a 2019 heatwave with temperatures of about 40 °C over days (El Mundo, 2019).

This thesis seeks to raise awareness towards heat as a hazard to human health among the scientific community and policymakers in various fields by distilling the core knowledge from different disciplines and driving it further.

The thematic focus of this thesis is multifaceted, which makes it a very interesting yet interwoven subject to investigate. It comprises health aspects, research about cities and urban planning, physical and climate science, as well as social and economic factors. Thus, a careful preparation and brief introduction of each of these aspects in the following sections serves for a better understanding of the overall topic and mechanisms.

1.1.1 Heat in the urban built-up area

Extreme heat events and elevated ambient temperatures constitute a threat for urban areas as they are amplified by the Urban Heat Island, the phenomenon where urban built-up environments heat up more than the rural surrounding (Oke, 1973; Zhou et al., 2013; Zhou et al., 2017). Under a changing climate, heat stress increases in urban areas are projected twice as large as in their surrounding rural areas, which is driven by the UHI itself, its concurrence with heat waves, and urban expansion due to increasing urbanisation (Wouters et al., 2017). The authors calculated a heat stress multiplication by a factor between 1.4 and 15 depending on the scenario (Wouters et al., 2017).

The core of heat being problematic in cities roots in urban land use, surfaces and materials used in the built-up area of cities. Dark surfaces and materials, such as roofs, asphalt roads, concrete and metal are characterised by increased heat capacity and thermal conductivity as well as a low albedo but a high emissivity (Oke, 1973). These surfaces absorb and store energy from solar radiation during daytime. During nighttime, they release the energy leading to an increase in temperature during the night over the city compared to the surrounding of the city. Additionally, a lack of evapotranspiration above urban land uses from missing vegetation spurs the UHI as well as the use of building materials that create a mirror effect, e.g. glass facades and heat up quickly, e.g. steel construction (Oke, 1973; Susca et al., 2011). The release of anthropogenic heat from vehicles, industry, heating and air-conditioning (Sailor and Lu, 2004; Sailor et al., 2011). Air-conditioning, a means used to reduce temperature in buildings, was modelled to contribute an additional 0.7 °C to the urban heat island intensity at 1pm in a typical office building cluster and entailed a daily average rise of outdoor air temperature by 0.53 °C (Liu et al., 2011).

Further, the city morphology has an effect on the UHI. The urban street canyon and its energy balance further amplify the UHI by its diurnal pattern. A study (Nunez and Oke, 1977) found that during the day, a radiative surplus exists in the urban street canyon which is dissipated by turbulent transfer, while about 25–30% of the energy is stored in the canyon materials, such as in the walls of buildings. During the night, a radiative deficit is balanced by the release of the heat stored in the subsurface. Wind direction and speed and the surrounding thermal environment take influence on the advective contribution to the air volume energy balance (Nunez and Oke, 1977). Apart from the city size, which has the strongest influence on UHI intensity among morphological factors, the compactness of a city has a reinforcing effect (Zhou et al., 2017). According to this work, the intensity decreases with anisometry, the degree to which the cities stretch. A recent study concluded for simulated artificial cities of the same setting, that a higher building density will lead to a stronger UHI intensity (Li

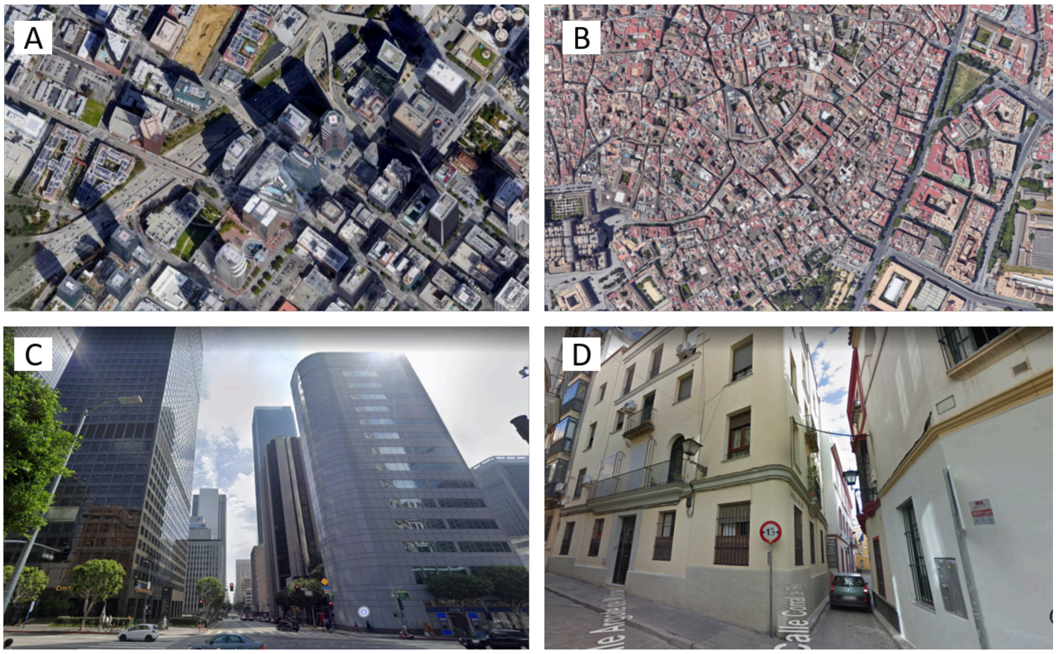

Fig. 1.1.: Impressions of diverging city morphologies. Downtown Los Angeles, dominated by wide open streets organised in a gridded pattern (A) and the Sevilla city centre, with small winding alleys and high building density (B). Urban street canyons in downtown Los Angeles with large building heights and low albedo surfaces (C) and in Sevilla city centre, with very low building height and narrow shaded streets and traditional building materials (D). (Source: Googlemaps 2020)

et al., 2019). Further the authors state that, an increasing urban fraction and building height will reinforce the UHI intensity. The 'western city' (Figure 1.1 A and C), its architecture, and building style, choice of building materials as well as the urban planning paradigms thus contribute to the formation of the UHI above cities. Such city type is likely prone to the UHI effect. A traditional architecture, compact morphology with narrow streets and adequate building materials in hot climates developed as form of cultural adaptation to heat. This is visible e.g. in the historic city centre of Sevilla (Spain, Figure 1.1 B and D). Small, disperse and stretched out city design was found to be most beneficial in terms of UHI alleviation (Zhou et al., 2017). Chapter 2 will present an overview of background knowledge on how cities and their inhabitants can adapt to heat. Evidence from cities in an ever-hot region, the Middle East, is introduced.

1.1.2 The uniqueness of adaptation to heat and the challenges related to its quantification

Human heat adaptation is very unique. It becomes obvious that the 'damage' caused by heat and the adaptation measures differ fundamentally from those related to other climatic, meteorologic, or hydrologic hazards, i.e. to storms, flooding, or heavy precipitation. In these cases, damage usually concerns property or infrastructure and is measured in monetary values, while in case of heat, no lasting reminder of physical devastation is left in their wake and thus less collective memory (Luber and McGeehin, 2008; Johnson et al., 2009). This becomes particularly evident in the case of flooding, which is seen as a more prominent issue (Lenzholzer et al., 2020). The losses from heat or temperature-related hazards as well as the benefit from adaptation to heat is usually about the individuals' lives or health status but never monetised. The closest it gets to a monetised assessment, is to evaluate the years of life lost (Huang et al., 2012; Odhiambo Sewe et al., 2018; Arbuthnott et al., 2020). This information can be used to derive a monetary value for e.g. productivity losses due to the death of employees or human capital, savings in pensions, life insurances, health care costs, or welfare losses per hot day as in (Karlsson and Ziebarth, 2018).

The adaptation to heat is a continuous and complex process and may refer to multiple levels of intervention: the individual and the interpersonal levels, the community and institutional level; as well as the environmental level and the public policy level (Wight et al., 2016; Guo et al., 2018). Across all levels of intervention, heat adaptation measures are not able to control or alleviate the heat hazard as such. Further, for example in the case of flooding, the nature of the suitable repertoire of planned 'hard' adaptation measures, e.g. dykes, coastal defences, and retention basins is somewhat binary. So to say, adaptation in such cases is either present or absent. With heat adaptation, this is not the case. A deeper comparative discourse at this point is out of scope of this thesis and is not further pursued here. It was worth mentioning to underline that in the case of heat, human heat adaptation is very challenging to grasp or quantify (Boeckmann and Rohn, 2014) and that it is unique compared to other types of adaptation in context of climate change.

Adaptation to heat points at the collective adaptation of the city population, which is a composite of two components, physiological acclimatisation, also referred to as intrinsic adaptation (Achebak et al., 2019; Guo et al., 2018), and wealth-enabled technological, social, or behavioural measures, which is considered as extrinsic adaptation (Achebak et al., 2019). In more concrete terms, this refers to (1) the intensity of the heat hazard that is still tolerated by human populations, meaning the heat burden they can bear and (2) the wealth-induced technological, social and behavioural measures that can be employed to avoid heat exposure. Physiological acclimatisation is defined as the natural process of gradual physiological adjustment of the human body as it gets used to new climatic conditions (Freitas and Grigorieva, 2015). It signifies the ability of the human body to undergo physiological adaptations to attenuate stress of a new climatic environment (Freitas and Grigorieva, 2015). Acclimatisation to the local climate is activated during childhood but it can also be acquired or lost during a lifetime (Bae et al., 2006; Mercereau et al., 2017). Age, health predispositions and obesity or a large body size are disadvantageous for successful physiologic acclimatisation to heat (Klenk et al., 2010; Rai et al., 2019; Hanna and Brown, 1983; Hanna and Tait, 2015). Generally, acclimatisation is an ongoing independent process and happens rather spontaneously or passively, as an individual or the population as a whole cannot evade to adapt (Petkova et al., 2014; Gosling et al., 2017). Thus, acclimatisation is here defined as autonomous adaptation that occurs without coordinated planning in individuals or communities and it is usually reactive by nature (Turek-Hankins et al., 2021; Petkova et al., 2014). The increase in the MMT in Stockholm (Sweden) over time (1901–2009) was understood as occurring autonomous adaptation in previous literature (Åström et al., 2016). Wealth-enabled adaptation comprises the facilitated access to technology, a social status, or behaviour, that contributes to avoid heat strain, for example adequate building standards and construction measures or air conditioning and a highly-developed health system, pursuing a white-collar work, or the daily siesta held all over Spain. The access to this type of adaptation requires financial resources among the society and is closely related to the development status. Such adaptation is mainly introduced at the community, institutional, environmental and public policy levels, but also overlaps with the individual level (Wight et al., 2016). Thus, this type of adaptation can be considered rather as planned adaptation, which usually involves deliberate policy actions that are based on anticipated climate risks (Petkova et al., 2014). These two components comprised by overall heat adaptation might however function with different magnitudes, the mechanisms might impact locations heterogeneously, and they might develop at different spatial and temporal scales (Gosling et al., 2017), which is still obscure to date. Chapter 2 provides an overview of human adaptation in in cities in the Middle East, an ever-hot region, where humans have been adapting for centuries to a hot environment.

Most studies in public health research do not directly measure and analyse adaptive behaviours in response to temperature extremes (Deschenes, 2014). According to this review, only some studies explain changes observed in mortality effects over time as an adaptation effect (Deschenes, 2014). Examples are studies about Japan 1972–2010 (Ng et al., 2016) and France 2003–2008 (Fouillet et al., 2008), which both report a decrease of heat-related mortality over time and interpret it as adaptation. Other studies used the prevalence of air conditioning or energy consumption over the summer as indicators for adaptation in economic research on heat adaptation as reported by a review (Deschenes, 2014). Evidence for health-preserving effects of adaptation in response to extreme temperatures are scarce and proof of effective reductions in adverse health outcomes still unclear, this concerns even prominent adaptation measures such as early warning systems and public outreach (Deschenes, 2014; Boeckmann and Rohn, 2014). A separation of autonomous adaptation and planned adaptation as proposed by Petkova et al., 2014 would serve to elucidate the contributions of each adaptation component to overall human heat adaptation. This however, has not yet been accomplished. Further, methodological challenges were identified that relate to nonlinear exposure-response functions representing heat-health outcomes or adaptation, such as complicated dynamic relationships, confounding factors, variables bias and heterogeneity across time, location and socio-economic settings (Deschenes, 2014; Gosling et al., 2017).

The most common methods to model adaptation in future impact studies comprise absolute 'shifts' by fixed temperature magnitudes (e.g. Gosling et al., 2009) or relative 'shifts' of the MMT and its respective HMR based upon the same percentiles in the observed and the future temperature distributions (e.g. Honda et al., 2014). Alternatively, the HMR and its corresponding MMT are 'shifted' by estimating the HMR anew using climate projections and assuming constant mortality (Gasparrini et al., 2017). Continued mortality time series from the past are used due to lacking mortality projections. A caveat of these methods is that they assume either the HMR itself, or at least components of it, are static and do not change until the future, which means that no change in heat adaptation is assumed until the future, or adaptation is neglected in the modelling. Such methods require a critical delta value, the difference between the future and the historical MMTs, by which the MMT shifts into higher temperature regimes (Figure 1.2 B), which has so far not yet been supported by empirical evidence and is thus chosen arbitrarily (Gosling et al., 2017). Further, it can be doubted that this delta value is the same across locations. Less common among earlier impact studies is to reduce the slope of the HMR, or combine this technique with a shift in MMT (Gosling et al., 2017) (see example in Figure 1.2 B). These methods account for the change in the population's sensitivity to heat with time, but also ground on a hypothetical change in slope as reviewed by Gosling et al., 2017.

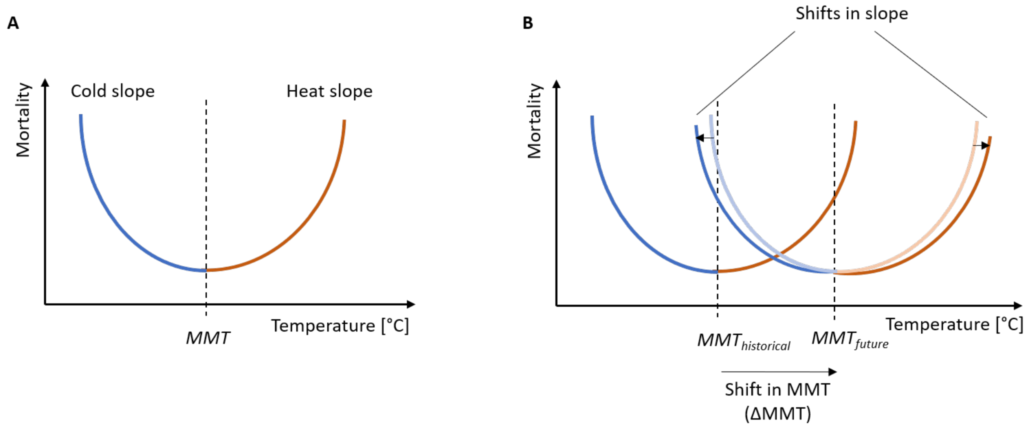

Fig. 1.2.: **Scheme of an example of an U-shaped heat-mortality relationship.** The U-shaped curve representing the heat-mortality relationship is separated by the MMT into a heat and a cold slope (A). The MMT is the lowest point on the curve indicating the minimum mortality at a defined point in time. A deviation from the MMT into warmer or colder temperatures leads to excess mortality. Thus, the MMT recently serves as best empirical measure of the temperature level to which a city population is adapted to. For future impact analysis, the MMT is commonly 'shifted' into higher temperature regimes (B). The difference between the past and the future MMTs is the critical delta value (ΔMMT later on in this thesis). Upon the MMT shift, the heat slope (and the cold slope) however, likely do not remain in the same shape. Thus, the heat-mortality relationship cannot be considered as static. A static heat-mortality relationship would not take into account human heat adaptation until the future.

A thorough impact assessment on future heat-related mortality, however, has to consider that the HMR changes due to changes in human heat adaptation from acclimatisation and due to socio-economic development, which enables the access to adaptation measures. Thus, the HMR does not remain static concerning the slopes in temperature ranges above and below the MMT. A precondition to achieve a more robust impact assessment on future heat-related mortality is the knowledge of the delta shift in MMT. This thesis will provide this delta value as an important side product while aiming at its own objective, appraising the evolution of human heat adaptation at the global urban scale under different climate futures, a challenge that has not yet been taken on at the global level.

1.2 Advancing the knowledge on the human heat-mortality relationship

Prior to advancing the knowledge on human heat adaptation, an illustration of background knowledge on heat and human heat adaptation in cities in an ever-hot environment and their options of technological, social, and behavioural measures towards heat adaptation is presented in Chapter 2. This chapter underlines the importance to address heat as a challenge for cities and their population, especially in regard of climate change. An outlook on the future habitability of Middle Eastern cities is provided. This chapter serves as a foundation, where the three following research questions can be based upon.

1.2.1 Overcoming data-related challenges and extending the urban MMT pool

Given that the HMRs and the MMTs in German cities are lacking and no large-scale evidence for heat adaptation for German cities had been quantified, in contrast to several cities in neighbouring countries, the need to establish the HMR for this densely-populated country is growing. The data availability should not pose an obstacle to establish the HMR for major German cities and determine their level of adaptation, since mortality records are available from the Research Data Center of the German Federal Statistical Office and the Statistical Offices of the Federal States. Provided that not many German case studies have been investigated so far, the question arises which potential challenges concerning the data preparation prior to carrying out the analysis will be encountered. Another motivation driving the research on the HMR in German cities is to make a contribution to the ever-growing pool of HMR curves assembled by the MCC to assess impacts of temperature on mortality internationally and complement the world map with the MMTs for German cities. For this purpose, the methodology used by researchers in this network can be adapted and applied for use of the daily mortality records and climate data. The research question resulting from this research gap is vital for the further course of this thesis since it constitutes a precondition at micro-level to generate a pool of MMTs that serves to generalise the data and identify the drivers for heat adaptation among populations across cities globally.

Research Question 1
Which challenges have to be overcome to extend the pool of MMTs by deriving the HMR for German case studies? ☞ Chapter 3

1.2.2 Generalising the MMT from case studies to the global level

Having gained the knowledge how to establish the HMR for case studies, such information pooled should be exploited to investigate on global drivers of the MMT and offer a solution how to estimate MMTs to create a global picture of the human heat adaptation across cities. So far, such investigation has not yet been undertaken. This solution should be a generalised and simple method, able to derive MMTs as a measure for human heat adaptation for any city without requiring daily mortality records. It should rely on open access data that is easily accessible and understandable. As the MMT gives an indication of an urban population's heat adaptation, it is an indispensable requirement for this global model to represent the multiple aspects of adaptation. These are physiologic acclimatisation on the one hand and wealth-enabled technological, social, and behavioural measures on the other hand. The acclimatisation of the human body and human survival is physiologically constrained. In case of high ambient temperatures, the human body cannot dissipate heat to the surrounding air. Transpiration as a cooling mechanism is also limited. Further, essential biophysical functions of the body fail. These deliberations are subject to the second research question to be addressed in this thesis.

Research Question 2
To which share do climatic, topographic, and socio-economic features influence the MMTs and how can MMTs be generalised from case study to the global level?
☞ Chapter 4

1.2.3 Future development of adaptation and heat exposure

The adaptation of an urban society or a population to heat is increasingly gaining in importance in the scientific discourse. Especially in regard of a changing climate, leading to more frequent and intense hazard exposure, i.e. extreme heat waves and generally elevated ambient temperatures, the question about the future development of human heat adaptation is a critical issue that requires investigation. Many studies have neglected adaptation in their heat impact modelling strategies, considering only changes in heat exposure. Various case studies have delivered an attempt to project the MMT in the future considering climate change. Some authors 'shift' the MMT into higher temperature regimes but the increment (°C) by which the MMT and its corresponding HMR are shifted has not yet sufficiently been evidenced. It is to be doubted that this increment is equal for all cities. This is why a final research question in this work aims at estimating future MMTs for cities around the globe independently from such increment. It is still an open research gap how adaptation in urban populations and hazard exposure (frequency and magnitude) across cities will develop in the future considering different climate trajectories and socio-economic options. It is intriguing to identify which futures will be beneficial to humankind and which will possibly threaten habitability of cities. These considerations shape the third and final research question.

Research Question 3
How will MMTs and heat exposure change in the future as response to 21st century warming in major cities? ☞ Chapter 5

1.3 Addressing the research questions

The MMT as an indication of the population's adaptation to the long-term climate and socio-economic conditions is the central theme of this work. The legitimate and yet open questions refer to (1) which data-related challenges have to be overcome to establish the MMT newly for case studies on the basis of daily mortality records and temperature, (2) based on case study information, how a generalisation of the MMT across global cities can be achieved and its principle drivers be identified, and (3) how the MMT as adaptation measure and heat exposure will develop under different climate and socio-economic futures until the end of the century. Each question is explored in a separate chapter in this thesis, as illustrated in Figure 1.3. Each chapter and the work presented therein contributes with different weight to two pivotal topics: (1) to the methodological development of a generalised model, presented as height of the chapter boxes and (2) to the assessment of human heat adaptation in cities under different futures, the overall objective of this thesis, indicated by the width of the chapter boxes. The subsequent Chapters 3 to 5 build on one another as indicated by the layers in Figure 1.3. The thickness of the lines surrounding each chapter box indicates the degree of topicality for the overall objective of this thesis, which culminates in Chapter 5. The Chapters 3 and 4, dealing with Research Questions 1 and 2, have each been published as a stand-alone and peer-reviewed research article. The work around 3 presented in 5 is a third article, which is currently under review. With each chapter and research question, the perspective on human heat adaptation and its representative, the MMT, is concretised and finally finds application in an investigation on the future development of heat adaptation and exposure considering a multitude of possible futures.

Subject to Chapter 3 is the question about data-related challenges to establish the HMR and provide the MMT as a measure for heat adaptation at the city-scale for particular cities in Germany. This is formulated in Research Question 1. An number of major German cities for which the HMR has not yet been derived provide the opportunity to serve for this purpose. The mortality records have been obtained from the Research Data Centres of the Federation and the Federal States of Germany and have been prepared for the principal analysis. This task comprised the adjustment of data to changes in political boundaries in certain cities and the correction of time series whenever bias was discovered, e.g. due to public holidays. The two-stage approach used here to establish the HMR, also referred to as exposure-response function, are adapted from previous studies that have established the conventional method to generate the HMR (Gasparrini et al., 2015; Gasparrini et al., 2010; Gasparrini et al., 2012a). The here calculated MMTs are subsequently contributed to a large pool of MMTs and useful for the following chapter.

In Chapter 4, a pool of MMTs at case-study level is used as fundamental resource to generalise and scale this adaptation measure to the global level as expressed in 2. First, the generic drivers motivated in literature were tested to which share they drive the MMTs. In an extensive model selection process, a linear model was tested against a sigmoid model and independent variables selected to best reproduce the MMTs. To support the choice of the sigmoid model, segmented linear models with asymptotes were tested. A multivariate maximum-likelihood regression was chosen to best describe the empirical MMT sample in a sigmoid form. It showed best results in nested and non-nested model comparisons, according to Root Mean Square Error (RMSE) and the Akaike Information Criterion (AICc), which were employed to identify the best model. A likelihood-ratio test ensured the significance criterion of each parameter in the model. The sigmoid model was tested for performance on world regions and climate zones. This approach is unique since it unifies many in literature proposed city-features and tests them against each other on their suitability to predict the MMT at the global urban scale.

Chapter 5 serves to adapt the model established in the previous chapter for application for the future climate trajectories and future socio-economic developments for an enlarged city sample, covering about nearly 4000 cities across the globe to assess the future change in MMT and heat exposure (3). The original model was re-calibrated to match the future projections of temperature and socio-economic input variables. The delta changes in MMT and in heat exposure, as the number of days above the MMT and the magnitude thereof, between the end of the 21st century and the beginning are recorded. The model was modified to isolate each individual effect of change in independent climate and socio-economic variables on the change in MMTs. This analysis allowed to discriminate the highest contributor to the change in MMT until the end of the century for each city. A spatial analysis serves to identify the critically endangered cities and regions. The product of this article is a large and novel data base on future heat adaptation and exposure for cities under multiple climate and socio-economic futures, which may be used by scientists and decision-makers equally for

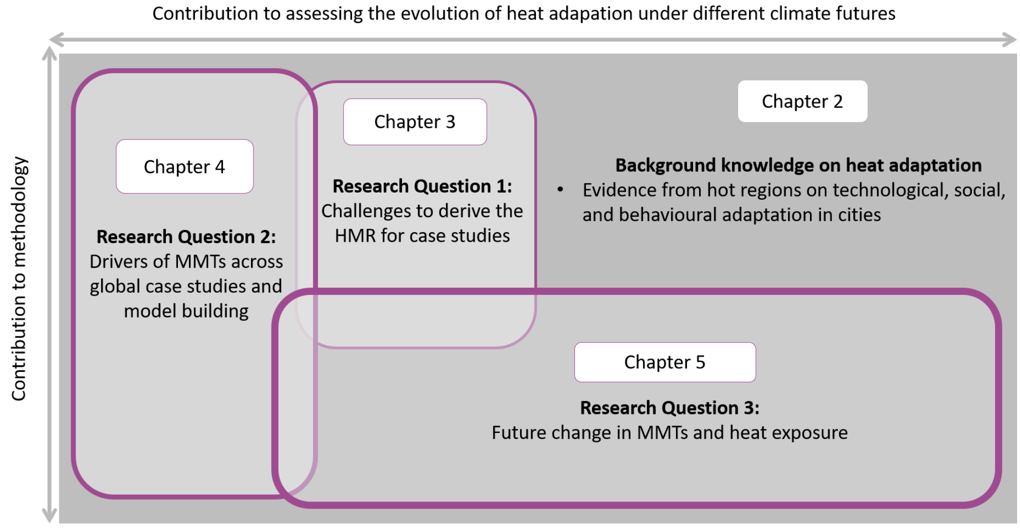

Fig. 1.3.: **The research questions in context of their contribution to the overall objective of the thesis and their contribution to the methodology to achieve this goal.** Each research question relates to an own chapter. Chapters 3 and 4 have been published as stand-alone articles. The article presented as Chapter 5 is currently under review. The literature review-based chapter 2 serves as a general prologue to the following original research work. The layers represent the rank from the thematic basis, via the MMT establishment for case studies, to the exploration of MMT drivers and the building of a global adaptation model, finally to the investigation of the future MMT and its evolution in context of heat exposure. The width of the chapter boxes indicates the contribution to the overall assessment of the evolution of adaptation under different climate futures, which is the overall objective of this thesis. The length of the chapter boxes represents the contribution to the methodology. The thickness of the box line signifies the overall topical focus in this thesis. Overlap of the boxes shows overlap among the research questions.

research and policy-making. To date, such comprehensive data has not yet been produced. The outcomes presented in this final chapter also inform future global impact studies of heat-related mortality by providing the delta change in human heat adaptation in cities worldwide. Further, a simple functional relationship is proposed how future changes in mortality could possible be assessed.

2

How cities and their inhabitants can adapt to heat

Evidence on heat adaptation in cities in the Middle East

Abstract. Already today, the Middle East is characterised by hot temperatures and low precipitation during the summer months. It is especially the lack of water resources that makes many parts of the region inhabitable. Climate change will cause an increase in average temperatures and a decrease in precipitation in many locations. The atmospheric uptake of water, e.g. over the Persian Gulf, paired with more extreme temperatures will lead to humidity conditions which would further constrain habitability. An increase in heat-related morbidity and mortality cases due to these future climate conditions is therefore very likely. A higher demand for water resources, but lower availability will cause a more severe scarcity of the resource. The rapid population growth and the urbanisation are causing further pressure on water and land resources. By the end of the century, the region, especially along the Gulf coast, will experience climate and resource conditions that likely put the survival of human kind without suitable technical measures into question.

The section presented in Chapter 2 has been translated from German to English with minor adjustments and updates on numbers from:

Krummenauer, L. and J. P. Kropp (2018): Grenze der Bewohnbarkeit in heißen Regionen am Beispiel des Nahen Ostens [The limits of habitability in hot regions - The example of the Middle East]. In: Lozán, J. L., Breckle, S.-W., Graßl, H., Kasang, D. and R. Weisse (Eds.): *Warnsignal Klima - Extremereignisse [Extreme events]. Verlag Wissenschaftliche Auswertungen*, Hamburg, pp. 326-332.

2.1 The physical geography of the Middle East

The Middle East comprises the states of Mashrek (Jordan, Palestine incl. The West Bank and Gaza, Lebanon and Syria as well as Israel and Sinai, as part of Egypt), the Arabian Peninsula (Kuwait, Bahrain, Qatar, Saudi Arabia, United Arab Emirates, Yemen, Oman) and Iran. In total, the region was home to around 250 million people in 2016 (The World Bank, 2018). Apart from the fertile crescent, the Nile valley and the Mediterranean coast as well as isolated oases, steppes and deserts dominate the natural area. Less than 300 mm of rainfall per year is characteristic of large parts of the region, which already makes drinking water otherwise available (e.g. extraction of fossil groundwater, wastewater treatment, seawater desalination). In addition, the region is highly dependent on food imports, because 50% of wheat and barley are imported, 70% of rice and 60% of maize (Waha et al., 2017). The Middle East covers several climate zones from north to south. Warm Mediterranean climate (winter rain region with hot summers) as in Tel Aviv-Jaffa (Israel) stretches along the coast of Israel via Syria and Iraq into western Iran to the Persian Gulf. Cool and hot steppe climates (above the drought limit, annual mean temperature $< 18\,^\circ$C or $> 18\,^\circ$C, e.g. in Damascus (Syria) and Kirkuk (Iran) follow to the south and dominate in the north and east of Iran. Towards southern Syria and Iraq, steppe climates turn into hot arid desert (no or very low rainfall and annual mean temperature $> 18\,^\circ$C). They also dominate the entire Arabian Peninsula and the Iranian highlands. Cities located in such a climate are the Saudi Arabian cities of Mecca, Jeddah, Riyadh, and Doha (Qatar) and Kuwait City (Kuwait). Scattered cool arid desert climates (annual mean temperature $< 18\,^\circ$C) can be found in high altitudes. Isfahan (Iran) and Sanaa (Yemen) are located in this climate zone. While the desert regions are already permanently uninhabitable, the majority of the population is concentrated in the cities of the Middle East. However, current and upcoming climate change makes it likely that the habitability of other regions will be restricted. Using selected sample cities, the long-term observed climatic conditions (1961–1990) in the Middle East can be shown (Table 2.1). While relatively moderate annual mean temperatures, hot summer months and moderate precipitation are observed in the cities of the Mediterranean climate and the cool steppe climates, the temperatures in the desert metropolises are on average warmer than 25 °C all year round. The average annual maximum temperature is higher than 30 °C. The mean of the maximum temperature of the hottest months in the desert cities even exceeds 40 °C, while the mean of the minimum temperature of the hottest month is not lower than 26 °C. The latter corresponds approximately to the average maximum temperature of Freiburg im Breisgau (Germany) in July. Daily temperature extremes above 50 °C have already been measured occasionally in these desert cities. The Middle East is also heavily influenced by seasonal precipitation. Large parts of the region are winter rain areas. In the Mediterranean and in steppe climates, the annual rainfall is increased compared to the desert climates (Table 2.1). The latter are characterised by summer periods with very little and often several months without precipitation. In terms of habitability, it is essentially the temperature in combination with the air humidity, the actual availability of water and soil fertility that allow human life and a sufficient livelihood in a geographical area or not. The habitability of a region can be enhanced through physiological, behavioural, social and cultural adaptation to the natural environmental conditions. Furthermore, technical measures such as air conditioning and room humidification can contribute to stretch the limits to habitability to a certain extent.

2.2 Adaptation and urban planning

Rural areas originally shaped the economy of the Middle East. In addition to agriculture practised in river valleys and around water points (oasis), the Bedouin tribes lived from cattle breeding. Their nomadic lifestyle was adapted to the availability of water and forage for the herds. Such livelihood was feasible due to the absence of fixed territorial ownership rights. Starting with the land reform of the Ottomans in the second half of the 19th century and the one initiated by the English and French after 1916, there was a compulsion to register land ownership, which increasingly eroded the Bedouin way of life and their livelihood. Private and state land purchases as well as military interventions against the prevailing tribal societies forced the Bedouins to restrict their livelihood to semi-nomadism or to abandon their lifestyle and sedentarise them. Oil discoveries in the 1920s further intensified the privatisation of the areas. A drought in the 1960s, in the territory what is today Syria, caused a large proportion of desert inhabitants to search for other employment opportunities in the cities (Kark and Frantzman, 2012). Even before the Syrian civil war began in 2011, the Levant was hit by one of the worst dry spells in 900 years (Cook et al., 2016). There are indications that a failed agricultural policy has further exacerbated living conditions and that climatic changes could have at least partially contributed to the outbreak of the Syrian civil war (Kelley et al., 2015). The secondary and tertiary sectors of the Middle East mainly concentrated on cities that had developed close to oasis, along rivers or coasts. Urban development in the region did not follow any regulations (apart from the values and norms of Islam, e.g. modesty, separation of residential area and work space, protection of private life). The urban morphology and construction were adapted to the predominant hot climate. High building densities with narrow, winding streets created shade in public spaces. The relatively low number of storeys, flat roofs and the exposition of the buildings guaranteed relatively moderate temperatures inside. Typical local building materials with a high albedo and a cooling effect on the interior, such as adobe, limestone and marble or palm fronds and wood, were used (Khalaf, 2012; Salama, 2015). Houses were usually built around one or multiple courtyards or patios framed by roofed arcades and with closed facades towards the outside (Abdulkareem, 2016; Dhingra and Chattopadhyay, 2016). Private and public buildings were passively and naturally cooled based on an air pressure gradient, which provided sufficient comfort despite the hot temperatures. Air was supplied and exchanged via so-called wind towers, an originally Persian architectural element (Salama, 2015). The air flow was often conducted over water surfaces in qanats, urban subsurface canals, or across in-house water basins and fountains in the courtyard to additionally take advantage of the evaporative cooling. The chimney effect was used in windless areas to create a draft of air masses in the houses (Amirkhani Aryan et al., 2010). Maschrabiyyas (carved wooden latticework) on unglazed windows and bay windows offered protection against direct sunlight (Abdulkareem, 2016; Khalaf, 2012) but allowed for circulation of air. The modernisation in urban planning according to western standards from 1916 replaced the traditional planning and building styles. The import of modern European urban planning (e.g. the functional city by Le Corbusier or the garden city by Howard) with the principles of zoning and functional separation altered the traditional urban structure and function. New European elites created a cityscape based on the European city models with representative houses and large openly designed public squares. The cities soon became a pull factor for internal labour migration from rural areas and the demand for housing grew. Western urban planning however, paid little attention to local and socio-cultural circumstances. The old town of Kuwait City (Kuwait) was torn down during the oil boom and new, modern, high-floor buildings and a traffic network with wide motorways based on western urban morphology were created (Yacobi and Shechter, 2005). Building materials unsuitable for hot climates, such as concrete, steel and large glass surfaces and facades were introduced. These materials store heat during the day and release it into the ambient air at night, thus contributing to the UHI (Khalaf, 2012). The use of air conditioning in buildings was introduced to counteract the overheating of the buildings' interior, which caused an enormous energy consumption. A lack of spatial planning and policies by local governments after the administration was taken over by the Europeans led to increased poverty, insufficient or degraded housing and in general, an eroding standard of living among a rapidly growing population. Up to date, informal settlements often shape the cityscape, i.e. in Cairo (Egypt) or Sanaa (Yemen). The region is characterised by rapid urbanisation. Already today around 60% of the population lives in urban areas (Dewachi et al., 2014). In the rich Gulf states, urban planning is still practised according to the western planning paradigms and cities are developed into naturally unsuitable desert areas (Yacobi and Shechter, 2005). However, a cautious return to traditional architectural features of hot climates can be noticed. Several efforts have been made in modern architecture to incorporate traditional elements to reduce the energy requirements in residential and public buildings. Examples are the Kuwait Investment Authority Headquarters building (Khalaf, 2012) or the site of the King Abdullah University of Science and Technology in Thuwal (Saudi Arabia) (Kamal, 2014). The development of completely new settlements, i.e. Masdar City, Abu Dhabi (UAE) according to the principles of emission avoidance and low energy consumption as well as according to traditional morphology is feasible but requires high financial expenditure (Ibrahim, 2016). These developments show that prosperity, technological measures and cost-intensive development projects allow adaptation to hot climates. However, the vulnerability concerns a population segment which cannot afford these amenities or which is exposed to the high outside temperatures due to outdoor labour.

2.3 Extreme temperatures today

Mean daytime temperatures in the Middle East during summer are very high (see above). For the period 2010 to 2018, the mean daily temperatures in summer were around 43 °C (e.g. Mogayra, Saudi Arabia; Kuwait City and Jahra, Kuwait; Nasiriya, Iraq; Minab, Iran). Extreme temperatures can reach 50 °C and above, e.g. on 29 June, 2017 in Ahwaz (Iran) with a daily maximum temperature of 53.7 °C (Independent, 2017; NOAA National Climatic Data Center, 2018) or the following day in Basra in Iraq with 53.9 °C (UN News, 2016). Temperatures exceeding 50 °C were also observed in Oman, Iran and the United Arab Emirates in 2017. However, they may also occur in more moderate Mediterranean climates. Tendentiously, recorded temperatures in the region are only a few degrees Celsius lower than the highest temperature ever measured and officially confirmed, a maximum of 56.7 °C[1] in Furnace Creek in Death Valley (USA) recorded on 10 July 1913 (WMO, 2018). High temperatures in combination with high RH constitute a critical condition because the thermal load on the human body increases. Cooling mechanisms of the body, especially the sweating via evaporative cooling is constrained or stops completely as the ambient air cannot absorb

[1] Officially confirmed as of 2018; At the same site 54.4 °C were measured on 16 August 2020 and could substitute the official record in case it was proven not valid

any additional moisture. The lowest temperature that can be achieved by direct evaporative cooling is the Wet Bulb Temperature (WBT). Due to the evaporative cooling, it is below the dry bulb air temperature and is a measure for the thermal load levied upon the body. Indices derived from the WBT are based upon the measured air temperature and the RH and are generally referred to as measures of perceived temperature (°C WBT). An extreme situation was given on 20 July 2017 in Jask (Iran). At a mean daily temperature of 35.3 °C and a mean RH of 84%, the heat index showed a thermal load of 61 °C TWB that day (NOAA National Climatic Data Center, 2018). In contrast, hot days with low RH are less stressful. For example, a mean daytime temperature of 43.3 °C with a RH of 4% in Mogayra (Saudi Arabia) was perceived as 38.8 °C TWB. In case there is no cooling at night and nocturnal temperatures remain high, an additional strain is put on the organism, as recovery phases are not sufficiently long. The highest night temperature ever of 44.2 °C was recorded in Khasab (Oman) on 27 June 2017 (Burt, 2017; Géoclimat, 2018; Al Jazeera, 2017). Overall, more than a third of all days in the region from 2010 to 2018 showed a temperature maximum > 30 °C and almost no nightly cooling (fluctuations between minimum and maximum temperature of no more than 3 K) (NOAA National Climatic Data Center, 2018).

Tab. 2.1.: **Climate parameters in Middle Eastern cities.** Annual mean temperatures, monthly mean temperatures of the hottest month in each case and precipitation (annual mean and number of months with less than 1 mm of precipitation) for selected cities. Further explanations in the text. Munich is given as a comparison (calculation based on data from Climate-Data.org (2018) and Wetterkontor (2018)).

Climate	**City**	**Temperature** Annual mean			**Hottest Month**				**Precipitation**	
					Month	Monthly mean			Annual mean	Months
		Tmean	*Tmin*	*Tmax*		*Tmean*	*Tmin*	*Tmax*	*mm*	*≤1 mm*
Mediterranean	Tel-Aviv Yaffa	20.2	14.9	25.5	August	27.0	22.1	32.0	562	4
cool steppe	Damascus	16.9	18.8	23.4	July	26.2	16.7	35.8	198	4
hot steppe	Kirkuk	21.6	14.9	28.3	July	34.6	26.3	42.9	365	4
cool desert	Isfahan	15.6	8.0	23.3	July	28.2	19.6	36.9	125	4
cool desert	Sanaa	16.2	8.2	24.3	July	20.0	13.4	26.6	265	0
hot desert	Mekka	30.0	23.5	36.6	July	35.2	29.1	41.3	70	4
hot desert	Jeddah	28.0	21.2	34.9	August	32.1	26.0	38.2	52	7
hot desert	Riad	25.4	18.1	32.8	July	34.7	26.9	42.6	111	5
hot desert	Doha	27.0	21.6	32.5	July	34.9	28.9	41.0	76	5
hot desert	Kuwait	25.3	19.3	31.3	July	36.0	29.4	42.7	103	4
Oceanic	Munich	8.0	3.5	11.6	July	17.4	12.1	22.8	930	0

2.4 The future climate conditions

Undoubtedly, human beings in particular are the drivers of global warming (Kelley et al., 2015) and the future climatic conditions in the region will increasingly be characterised by very hot summers. From 2050 onward, they will even become a new normal (Lelieveld et al., 2014). Under an optimistic climate trajectory (RCP2.6) with a global average warming of no more than 2 °C compared to the pre-industrial age (1850–1900), the Middle East could experience an increase in average summer temperatures of around 2.5 °C to 3 °C (Figure 2.1 A) between 2071 and 2100 (Waha et al., 2017). In the event of a more pessimistic climate scenario (RCP8.5) and a subsequent rise in global mean temperature of 4 °C, an increase in average summer temperatures of up to 8 °C is possible in the region (Figure 2.1 B) (Waha et

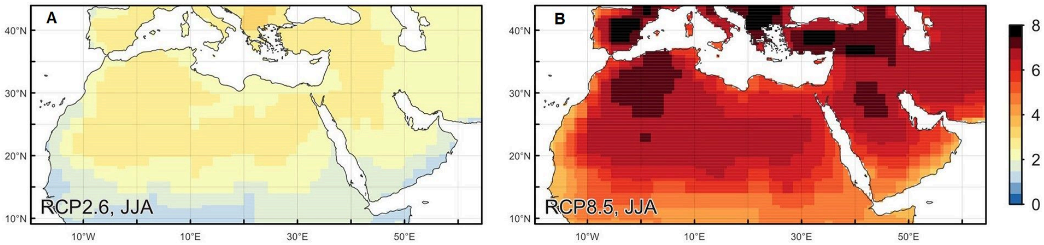

Fig. 2.1.: Projection of the average change in summer temperatures for the Middle East. Optimistic climate change scenario (RCP2.6, global change in mean temperature + 2 °C) (A); Pessimistic climate change scenario (RCP8.5, global change in mean temperature + 4 °C) (B). Shown are the expected temperatures for the months June-July-August (JJA) and the period 2071–2099 compared to the years 1850–1900 (courtesy of Alexander Robinson published in Waha et al. 2017).

al., 2017). The latter will primarily affect large parts of Saudi Arabia and Iraq. Furthermore, the frequency and intensity of extreme temperatures will change significantly compared to pre-industrial times. Previously rare extreme heat, e.g. comparable to the heat wave in Russia in 2010, can be expected for 30% of the summer months anywhere in the Middle East in the future. In a world with 4 °C warming compared to the pre-industrial average temperature (RCP8.5), around 65% of the summer months in the Middle East would be classified as extreme heat in the period 2071–2099 (Waha et al., 2017). Corresponding changes are also expected for the thermal load at night. During the period 1986–2005, the nocturnal temperatures were lower than 30 °C on average, but in case of the pessimistic RCP8.5, they are assumed to exceed 34 °C at the end of the 21st century (Lelieveld et al., 2016). The situation with regard to precipitation and the associated availability of water is expected to aggravate in the future. The low precipitation of 300 mm per year already today will continue to decrease in the future. In locations showing a future precipitation increase, positive effects through precipitation will directly be vanished due to increasing evaporation. In general, drought periods will increase in general (Waha et al., 2017). Under the optimistic climate trajectory RCP2.6, an increase in winter precipitation of 20% to 50% compared to the period 1951–1980 is projected for the interior of the Arabian Peninsula and the southwest, especially for Oman (Figure 2.1 A). In contrast, under the pessimistic scenario RCP8.5 (Figure 2.1 B), the increase in annual rainfall in the centre of the peninsula will be lower (20-40% compared to 1951–1980). Winter precipitation decreases by up to 20% (RCP2.6) or up to 30% (RCP8.5) (compared to 1951–1980) are expected for the areas north of 30 °C North on a Sinai-Kuwait line (Figure 2.2 A and B). For the summer months, decreases in precipitation of up to 60% to a large spatial extent can be expected for both climate trajectories compared to the years 1951 to 1980, especially between the Sinai-Baghdad line (Iraq) and the inner Arabian Peninsula (Figure 2.2 C and D). This comes in addition to an increasing temperature and a generally very low precipitation level (Waha et al., 2017).

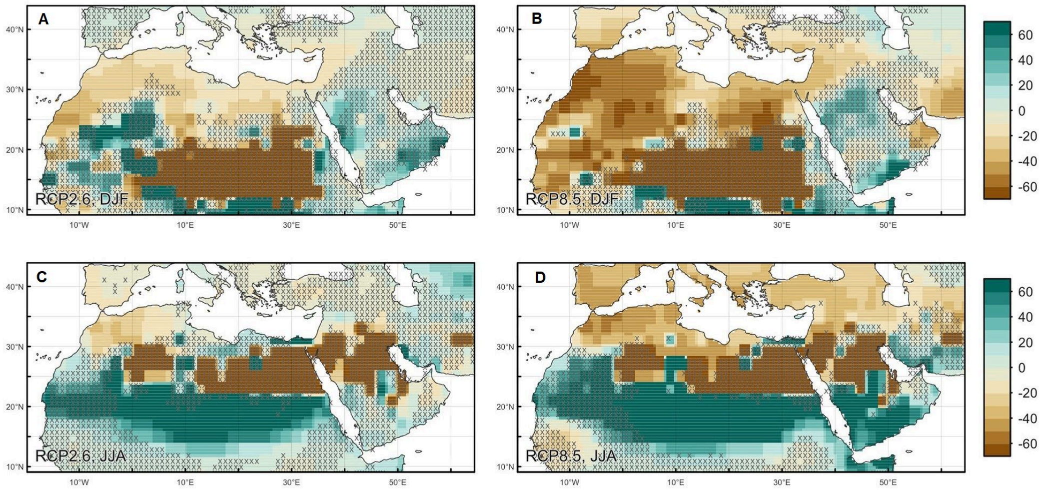

Fig. 2.2.: **Percentage change in the amount of precipitation under climate change scenarios in winter and in summer.** Scenario RCP2.6 (December-January-February, DJF) (A) and in summer (June-July-August, JJA) (C). Scenario RCP8.5 (December-January-February, DJF) (B) and in summer (June-July-August, JJA) (D). The periods 2071–2099 and 1951–1980 are compared. Since the absolute amounts of precipitation in the region are already very small, large relative changes can also mean very small absolute changes. Regions indicated with crosses are uncertain about the direction of change (two or more models out of an ensemble of five) (courtesy of Alexander Robinson published in Waha et al. 2017).

2.5 Implications for the habitability of the Middle East

If such temperature and precipitation conditions as discussed above occur, this will have far-reaching implications for the habitability of the Middle East. Above all, the increasing temperatures in combination with the RH will make some regions of the Middle East almost uninhabitable (Pal and Eltahir, 2016). A distinction must be made here whether people settle in rural or urban areas or whether they are physically active. For example, recent studies show that the number of hot days in cities is already twice as high as in rural regions (Wouters et al., 2017). This development will intensify with increasing warming. At the same time, structural elements such as the degree of compactness of a city, determine the thermal heat load in cities (Zhou et al., 2017). Since urban structures and infrastructures are designed to sustain in a long-term perspective, it is difficult to make short-term adjustments for adaptation. Still, well-planned urban structures could bring relief from the heat burden, if e.g. cooled rooms or urban green areas would be available. However, if the critical measure of 35 °C WBT is exceeded for more than 6 hours, this will usually trigger hyperthermia in the human body (Sherwood and Huber, 2010). This constitutes a serious condition especially for the elderly since a generally weaker cardiovascular system has to work more intensely to compensate the blood flow to the extremities to maintain the body's cooling mechanism. Longer exposure to such weather and climate conditions, especially for outside workers or athletes is not recommendable. The current situation in the Middle East is characterised by a maximum WBT of approximately 30 °C. In many regions, the WBT levels off at 26 °C–27 °C and rarely exceeds the 31 °C WBT mark (Pal and Eltahir, 2016; Sherwood and Huber, 2010). However, the Middle East is one of the most vulnerable regions worldwide when it comes to inhabitability of urban areas. Especially in low-lying coastal plains around the Persian Gulf, where high air temperatures are paired with high RH, the mean Maximum Wet Bulb Temperature (WBTmax) is already higher than 31 °C today (Pal and Eltahir, 2016). Therefore, as climate change progresses, the physiologically feasible acclimatisation limit of 35 °C WBT might be exceeded in large parts of the Middle East, according to the same study. Thus, the suitability of these regions as human habitat has to be questioned (Pal and Eltahir, 2016; Sherwood and Huber, 2010). Pessimistic climate projections show that by 2100, today's 95th percentile will become a normal state during the summer months of some Middle Eastern cities (e.g. for Abu Dhabi and Dubai (United Arab Emirates), Doha (Qatar), Dhahran (Saudi Arabia) and Bandar Abbas (south coast of Iran)). The WBTmax will exceed 35 °C more often during the course of the year in these cities. At the Arabian coast of the Red Sea, e.g. in Jeddah or Mecca, the TWBmax reaches 33 °C or 32 °C, which is a problematic state for people with a weak cardiovascular system (Ahmadalipour and Moradkhani, 2018). The upper limit of 35 °C WBT as the limit for human heat tolerance certainly only represents an approximation to reality, however local and individual factors should not be neglected. An approximation to a lower limit, i.e. the temperature that marks the first mortality cases due to heat in urban populations, is currently possible for cities worldwide. It is driven by socio-economic factors, the long-term climate and topography (Krummenauer et al., 2019). In 2010, approximately 3 000 cases of serious heat effects were recorded among workers in Abu Dhabi (Health Authority Abu Dhabi, 2011). Although an effective time management, regular interruptions of heat exposure or the provision of beverages might mitigate the effects of heat on the body, alarming figures are expected for the region. For example, the heat-related mortality rate for the age group older 65 is projected to rise from 1/100 000 (1961–1990) to 47 (2080) in Egypt and from 3/100 000 to 34 in Oman (UNESCWA and WHO, 2017). Since a continuous urbanisation is to be expected in the upcoming decades, the question arises whether changed urban planning paradigms can alleviate the critical circumstances. A return to traditional architecture and urban planning will likely not improve the limit of habitability and the general living conditions in the long-run. Still, such alterations might temporarily improve comfort conditions in regard of temperature indoors. The determination of the limit of habitability is an overall multi-criteria problem that cannot be defined solely by temperature or RH limits. In order to adapt to future conditions, it is not only physiological acclimatisation that has to be considered, but also the costs for the implementation of necessary technological measures (e.g. seawater desalination, cooling) have to be taken into account, as well as generally the local resource availability. Especially the available water resources are to be mentioned here. Due to the warming temperatures, demographic alterations and urbanisation, the demand for drinking water will rise in the future, while natural water resources are being increasingly overused. For coastal aquifers, the overuse is already happening and jointly with a rising sea level, this leads to the salinisation of groundwater resources already today (Waha et al., 2017; Dewachi et al., 2014). Overall, the available drinking water volume per capita has reduced to a quarter of the supply volume in 1960, while today the demand is 16% higher than the available renewable water resources (Dewachi et al., 2014). Above all, in Jordan, in Yemen and in most countries of the Arabian Peninsula, the ratio of withdrawal to availability of drinking water is greater than 100%, whereas a ratio of more than 40% at national level already constitutes 'Severe Water stress' (Waha et al., 2017; Damkjaer and Taylor, 2017). Due to the demographic development, in 2050 the demand for drinking water in most Arab countries will exceed the availability by 50%, so that large regions of the Middle East will face an absolute water stress (less than 500 m^3/person and year, or 1370 l/head and day). In Saudi Arabia, the average annual rainfall is less than 59 mm/year but the available drinking water resources only about 210 l/person a day (or 76 m^3/person and year) (FAO, 2017). Already today 79% of the drinking water in the Gulf States is obtained by desalination. This dependency will increase with changing climate conditions and as a result, the energy need will grow (Dewachi et al., 2014). A water shortage has long-term consequences for the region. Wherever agriculture can still be practised, the ecological boundaries will shift, growth periods of plants will be shortened and thus the grain harvests will be reduced. In addition to favouring desertification processes, this also means reduced water and feed availability for cattle breeding (Waha et al., 2017). This has negative consequences for domestic agriculture and thus for local food security and further increases the dependency on food imports.

2.6 Synopsis

Physiologically, at the end of the century, temperature and humid conditions will prevail in the coastal plains around the Persian Gulf that will reach the limit of a possible human acclimatisation and adaptation capacity. This problem can be addressed in cities by implementing technological measures such as air conditioning systems, but still, this remains only an option for the wealthy population segment. In rural regions, the large-scale implementation is likely not an alternative, i.e. the partially nomadic tribes in the desert regions will slowly reach the limits of their traditional lifestyle and livelihoods. Such traditional lifestyles will likely disappear while urbanisation and climate change advance. Urbanisation in particular leads to a further amplification of the problem, because urban lifestyles consume more resources, leaving less for other lifestyle options. Overall, future daily life and employment opportunities will largely be constrained to the interior of buildings, which constitutes a confinement of the quality of life. A return to traditional (behavioural, social and cultural) adaptations and the acknowledgement of experience will likely have only small mitigating effects on the consequences for the habitability of the Middle East regarding progressing climate change. In addition, the increasing resource scarcities must be taken into account. The increasing incapability of the region to meet domestic demand for basic food and water resources is driving up costs, making the region dependent on international markets and making its society more vulnerable. High food prices had already contributed to the Arab Spring uprisings in 2010, which shows how fragile such conditional systems can be.

Extending the pool of MMTs

3

Temperature-related excess mortality in German cities at 2° C and higher degrees of global warming

Abstract. Investigating future changes in temperature-related mortality as a function of GMT rise allows for the evaluation of policy-relevant climate change targets. So far, only few studies have taken this approach, and, in particular, no such assessments exist for Germany, the most populated country of Europe. We assess temperature-related mortality in 12 major German cities based on daily time-series of all-cause mortality and daily mean temperatures in the period 1993–2015, using distributed-lag non-linear models in a two-stage design. Resulting risk functions are applied to estimate excess mortality in terms of GMT rise relative to pre-industrial levels, assuming no change in demographics or population vulnerability. In the observational period, cold contributes stronger to temperature-related mortality than heat, with overall attributable fractions of 5.49% (95%CI: 3.82–7.19) and 0.81% (95%CI: 0.72–0.89), respectively. Future projections indicate that this pattern could be reversed under progressing global warming, with heat-related mortality starting to exceed cold-related mortality at 3 °C or higher GMT rise. Across cities, projected net increases in total temperature-related mortality were 0.45% (95%CI: -0.02–1.06) at 3 °C, 1.53% (95%CI: 0.96–2.06) at 4 °C, and 2.88% (95%CI: 1.60–4.10) at 5 °C, compared to today's warming level of 1 °C. By contrast, no significant difference was found between projected total temperature-related mortality at 2 °C versus 1 °C of GMT rise. Our results can inform current adaptation policies aimed at buffering the health risks from increased heat exposure under climate change. They also allow for the evaluation of global mitigation efforts in terms of local health benefits in some of Germany's most populated cities.

The article presented in Chapter 3 is published as:

Huber, V., Krummenauer, L., Lange, S., Pena Ortiz, C., Gasparrini, A., Vicedo-Cabrera, A., Garcia Herrera, R. and K. Frieler (2020). Temperature-related excess mortality in German cities at 2 °C and higher degrees of global warming. In: *Environmental Research, (186:109447) July 2020.* https://doi.org/10.1016/j.envres.2020.109447

3.1 Introduction

Climate change is expected to alter the currently observed pattern of temperature-related excess mortality around the globe. Quantitative assessments of temperature-related mortality under climate change scenarios have often focused on heat, concluding that heat-related excess mortality is likely to increase under global warming (Huang et al., 2011; Li et al., 2018; Sanderson et al., 2017; Wang et al., 2019). The fewer studies that investigated the entire temperature range generally estimated concomitant decreases in cold-related mortality (Martin et al., 2012; Li et al., 2013; Schwartz et al., 2015; Gasparrini et al., 2017; Weinberger et al., 2017; Martinez et al., 2018; Vicedo-Cabrera et al., 2018), albeit some of these results have been controversially discussed (Arbuthnott et al., 2018; Kinney et al., 2015). The majority of projection studies has presented changes in excess mortality for different emission scenarios and future time periods. Yet, given that the international climate change policy targets, as, e.g. implemented in the Paris Agreement, are expressed as temperature limits, there is a growing need to present mortality projections as a function of GMT rise (Ebi et al., 2018). In addition, the focus on temperature magnitudes rather than on time periods facilitates the construction of damage functions to integrate health impacts in integrated assessment models (Carleton et al., 2018), and allows for the derivation of impact emulators required to quickly judge emission pledges in terms of climate impacts (Ostberg et al., 2018). So far, there are few projection studies of temperature-related mortality focussing on the magnitudes of GMT change (Chen et al., 2019; Vicedo-Cabrera et al., 2018; Wang et al., 2019; Mitchell et al., 2018; Lo et al., 2019). Most of these studies consider only the lower levels of possible GMT rise within this century (1.5 °C, 2 °C, and 3 °C above pre-industrial levels), while we also take the higher global warming levels (4 °C and 5 °C) into account. Furthermore, we are the first to present projections of temperature-related mortality based on a newly assembled observational dataset of death counts and climate variables in 12 large cities of Germany, the most populated country of Europe. Although temperature-related excess mortality in Germany has been studied based on observational data for specific cities (Breitner et al., 2014), regions (Laschewski and Jendritzky, 2002; Muthers et al., 2017), and the entire country (Karlsson and Ziebarth, 2018), there is only a very limited number of quantitative climate change projection studies. The few existing ones are limited to specific cities or regions of Germany (Chen et al., 2019; Rai et al., 2019), neglect the effects of cold (Zacharias et al., 2015; Kendrovski et al., 2017), or use only one simplified model for the relationship between temperature and mortality for the entire country (Hübler et al., 2008). The main objective of this study is to evaluate the policy-relevant climate change target of limiting global warming to 2 °C compared to higher warming levels in terms of changes in temperature-related mortality in Germany. In this evaluation, we focus on the potential for local benefits versus damages of climate change. To this aim, we derive temperature-mortality associations in 12 large German cities, using state-of-the art statistical techniques developed in time-series modelling (Gasparrini et al., 2010; Gasparrini et al., 2012a). Based on these associations and an ensemble of locally bias-corrected climate projections (Frieler et al., 2017), we estimate temperature-related excess mortality at different degrees of global warming (1 °C, 2 °C, 3 °C, 4 °C, and 5 °C of GMT rise above pre-industrial levels). Since we make the counterfactual assumption of no future changes in adaptation and demography, our estimates are best interpreted as exposing the current population of Germany's major cities, embedded in current infrastructures and health care systems, to different possible temperature distributions of the future.

3.2 Materials and methods

3.2.1 Observational data

We obtained daily death counts of all-cause mortality in 12 major German cities ($> 500\,000$ inhabitants; see Appendix A.2 Table A.1 for city coding and population data) from the Research Data Centres of the Federation and the Federal States of Germany for the period 1 January 1993 to 31 December 2015 (individual datasets are available as https://doi.org/10.21242/23211.[year].00.00.1.1.0). The cities are spread across the entire country (Appendix A.2 Figure A.1), and represent around 16% of the total German population in 2015 (Appendix A.2 Table A.1). Given the susceptibility of a wide range of death causes to non-optimal temperatures (e.g. Anderson and Bell, 2009; Gasparrini et al., 2012b), it is a common approach in studies of temperature-related mortality to analyse total death counts. More specifically, it has been shown that results on temperature-mortality associations are practically insensitive to the use of all-cause versus non-accidental mortality data across a large number of locations (Gasparrini et al., 2015). Data of daily mean temperature (24-h averages) for the study period was derived from the Climate Data Centre of the German National Meteorological Service. If several weather stations existed within the city boundaries, stations closest to the city centre were chosen, provided that measurements were available for the whole study period (Appendix A.2 Table A.2). We decided to use temperature data from a single weather station, given that more spatially refined exposure data does not generally yield different estimates of temperature-mortality associations compared to simpler one-station data (Schaeffer et al., 2016; Weinberger et al., 2019). Details on the processing of missing values are given in Appendix A.1.

3.2.2 Temperature projections

Projections of daily mean temperatures for the 12 cities were derived from the second phase of the Inter-Sectoral Impact Model Intercomparison Project (ISIMIP2b) (Frieler et al., 2017), comprising gridded ($0.5\,^\circ C \times 0.5\,^\circ C$), bias-corrected data from 4 General Circulation Models (GCMs) (GFDL-ESM2M, HadGEM2-ES, IPSL-CM5A-LR, MIROC5), which contributed simulations to the 5th Coupled Model Intercomparison Project (CMIP)5. For each GCM, we considered the historical run in the period 1986–2005 and 4 different climate-change scenario runs (RCP2.6, RCP4.5, RCP 6.0, RCP8.5) in the period 2006–2099 (2006–2100 for RCP8.5 simulations from IPSL-CM5A-LR). Time-series from the grid cell enclosing the respective city coordinates were extracted, and the data was additionally bias-corrected using the local weather station data from each city following the approach by Lange (Lange, 2017). Through this additional bias-correction step we mapped the spatial temperature mean of the grid cell to the local scale of the city. The remaining bias in the distribution of daily mean temperatures was relatively small (Appendix A.2 Figure A.2). In addition to local projection data, we also considered annual averages of corresponding GMT series.

3.2.3 Defining global warming levels

To select time slices corresponding to the considered levels of global warming, we first computed a series of annual GMT differences against pre-industrial levels for each GCM and RCP (extended backwards in time using data from the historical run). In this step, given

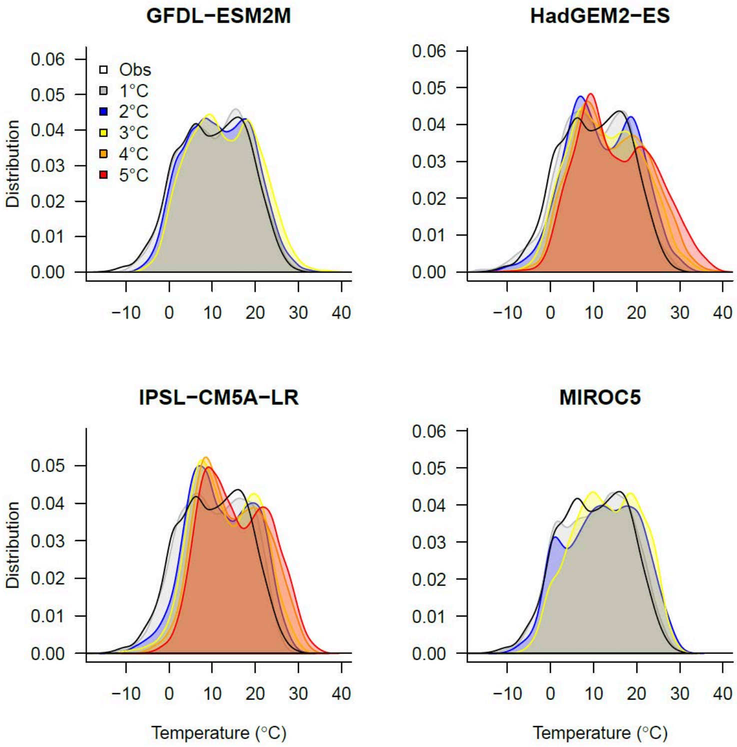

Fig. 3.1.: **Example distributions of observed (black) and projected (colours) mean daily temperatures at different levels of global warming in Berlin, by GCM.** Distributions were constructed based on daily simulation data (1986–2099, historical run combined with RCP8.5), mapped to global warming levels by considering 21-year running means of annual differences in GMT above pre-industrial levels (see Appendix A.2, Table A.3). (For interpretation of the references to colour in this figure legend, the reader is referred to the Web version of this article.)

that some of the GCMs considered (especially HadGEM2-ES and IPSL-CM5A-LR) simulate historical global warming trends that deviate substantially from the observed trend, we chose 1986–2005 as a reference period and added the observed global warming of 0.6 °C between this reference period and pre-industrial levels (following (Schleussner et al., 2016). Subsequently, we computed 21-year running means of GMT increases above pre-industrial levels and determined the corresponding temporal windows when the considered levels of global warming (1–5 °C) were reached for the first time (Appendix A.2, Table A.3 for selected time windows). Finally, we extracted the local temperature projections in these temporal windows (for an example of the resulting temperature distributions for Berlin based on RCP8.5, see Figure 3.1). It can be noted that only HadGEM2-ES and IPSL-CM5A-LR reached 4 °C and 5 °C above pre-industrial levels in the scenarios considered (Figure 3.1, Appendix A.2, Table A.3). We used the lowest warming level 1 °C, which roughly corresponds to the historical global warming up to present-day, as a reference to compute relative changes in projected mortalities.

3.2.4 Deriving temperature-mortality associations

Temperature-mortality associations were estimated with a two-stage approach, following Gasparrini et al. 2015 (Gasparrini et al., 2015). The details of the methodology are extensively documented in Gasparrini et al. (2010) (Gasparrini et al., 2010) and Gasparrini et al. (2012) (Gasparrini et al., 2012a). In the first stage, we used time-series quasi-Poisson regression to estimate city-specific exposure-response functions. Temperature-mortality associations were modelled with DLNMs. We fitted a natural cubic spline function with three internal knots placed at the 10th, 75th, and 90th percentiles of the local temperature distribution to model the exposure-response curve. This choice assures a log-linear extrapolation of the exposure-response curve beyond the observed temperature range (Vicedo-Cabrera et al., 2019). The lag-response curve was modelled with a natural cubic spline with an intercept and three internal knots equally distributed in the log-space, accounting for up to 21 days of lag. We controlled for day of the week with an indicator, and for seasonal and long-term trends with a natural cubic spline of time with 7 degrees of freedom per year. The chosen number of degrees of freedom for control of season and long-term trends corresponded to the minimum Quasi-Akaike Information Criterion (QAIC) summed across all (Appendix A.3, Figure A.3). Model choices were further tested in a sensitivity analysis (Appendix A.2, Table A.4). In the second stage, we performed a multivariate meta-regression on reduced coefficients from the first stage, which describe the overall cumulative exposure-response curve across the 21 days of lag. Long-term average temperature and temperature range (difference between maximum and minimum temperature) (Table 3.1) were included as meta-predictors in the model. Both meta-predictors explained part of the heterogeneity between cities (Appendix A.2, Table A.5). From the meta-regression model, we derived the best linear unbiased predictors Best linear unbiased predictors (BLUPs) for each city, which represent a trade-off between the location-specific association provided by the first-stage regression and the pooled association, and identified the MMT (Table 3.1).

Tab. 3.1.: Descriptive statistics, estimated minimum mortality temperatures (MMT), and attributable fractions in the observational period (1993–2015).

City	Total deaths	Daily Tmean		MMT		Attributable fractions					
						Total		Cold		Heat	
		°C	(min, max)	°C	(perc)	%	(95%CI)	%	(95%CI)	%	(95%CI)
Berlin	811 051	10.2	(-15.6,30.5)	18.9	(85th)	6.95	(5.24,8.61)	5.95	(4.25,7.61)	1.00	(0.89,1.13)
Bremen	150 608	9.8	(-14.1,27.6)	17.6	(87th)	3.56	(0.23,6.81)	3.21	(-0.07,6.39)	0.36	(0.16,0.55)
Cologne	229 457	10.6	(-16.5,29.3)	17.7	(84th)	6.78	(4.84,8.79)	5.70	(3.69,7.77)	1.08	(0.93,1.24)
Dortmund	155 233	10.5	(-15.2,28.9)	17.9	(86th)	6.23	(4.21,8.23)	5.44	(3.44,7.50)	0.79	(0.68,0.91)
Dresden	125 866	9.6	(-16.3,30.4)	18.7	(86th)	5.42	(2.41,8.37)	4.72	(1.68,7.7)	0.69	(0.53,0.87)
Dusseldorf	160 069	10.9	(-14.6,30.0)	17.9	(84th)	6.84	(4.60,9.05)	5.76	(3.42,8.08)	1.08	(0.90,1.27)
Frankfurt	168 417	11.0	(-12.9,29.9)	19.8	(87th)	9.59	(5.99,12.87)	8.50	(4.97,11.73)	1.09	(0.88,1.29)
Hamburg	445 338	9.6	(-13.5,28.8)	18.5	(90th)	4.93	(1.54,8.16)	4.63	(1.37,7.75)	0.31	(0.15,0.44)
Hannover	279 125	9.9	(-16.9,29.0)	17.2	(84th)	4.62	(2.81,6.46)	3.83	(1.99,5.75)	0.79	(0.64,0.95)
Leipzig	152 861	10.0	(-17.5,29.0)	17.7	(82nd)	5.09	(3.10,7.11)	4.03	(2.00,6.11)	1.07	(0.87,1.26)
Munich	290 962	10.0	(-13.4,29.5)	19.7	(88th)	7.23	(4.77,9.57)	6.62	(4.21,8.95)	0.61	(0.47,0.74)
Stuttgart	136 878	10.7	(-13.0,30.3)	19.2	(86th)	7.98	(5.54,10.34)	7.07	(4.57,9.50)	0.91	(0.76,1.08)
All cities	3 105 865	10.3	(-17.5,30.5)	18.4	(86th)[1]	6.30	(4.60,7.98)	5.49	(3.82,7.19)	0.81	(0.72,0.89)

[1] Median of city-specific estimates.

3.2.5 Computation of attributable mortality

All computations of daily mortality attributable to non-optimal temperatures, in the observational period and at different levels of GMT rise (1–5 °C) followed a similar setup. We used the exposure-response curve defined by the BLUPs and centred on the MMTs, and combined these with different daily series of temperature and mortality. To derive attributable mortality in the observational period (1993–2015), we used the observed temperature series and forward moving averages of observed deaths counts across the lag period as described in Gasparrini and Leone (2014) (Gasparrini and Leone, 2014). To estimate projected attributable mortality at different levels of global warming, we built upon the approach by Gasparrini et al. (2017) (Gasparrini et al., 2017) and Vicedo-Cabrera et al. (2018) (Vicedo-Cabrera et al., 2018). A series of projected daily mortality was constructed by averaging observed deaths counts per day of the year. We then replicated the annual pattern 21-times, in order to derive mortality series of the same length as the projected temperature series. We summed attributable numbers in the observational period or across each series of projected temperatures to derive total temperature-related excess mortality. We also separated components due to heat and cold by considering only days with temperatures higher or lower than the MMT. Dividing by the total number of observed deaths or the sum of projected mortality series we also derived the corresponding attributable fractions. Overall attributable fractions, for all cities combined, were derived by summing daily attributable numbers across all cities, and dividing by the sum of deaths across cities. The ensemble mean at each level of GMT rise was calculated as the average across all GCM-specific, and RCP-specific attributable fractions. In averaging across RCPs, we assumed that it did not matter when in time a specific warming level was reached (see also Appendix A.2, Table A.3), i.e. we assumed a scenario-independence of results.

3.2.6 Uncertainty estimation

To assess the uncertainty stemming from the fitted exposure-response functions, we conducted Monte Carlo simulations drawing 1000 times from a multivariate normal distribution defined by the BLUPs and the corresponding covariance matrix. We determined 95% eCIs by considering the 2.5th and 97.5th percentiles of the resulting sample. In the projections, we additionally determined the uncertainty stemming from the use of different GCMs, and RCPs. Total uncertainty, including epidemiological and climate uncertainties, was assessed by considering the 2.5th and 97.5th percentiles of mean excess mortality in each GMT bin across all Monte Carlo samples, GCMs, and RCPs. In addition, we were interested in determining the contribution of different sources of uncertainty to the overall variability in excess mortality estimates. To assess climate uncertainty, due to differences between GCMs and RCPs, we calculated the Standard deviation of mean excess mortality estimates based on central BLUPs across GCMs (SDgcm), and across RCPs (Standard deviation of mean excess mortality estimates based on central BLUPs across RCPs (SDrcp)), respectively. As a measure of epidemiological uncertainty, we computed the average of standard deviations resulting from Monte Carlo simulations, considering GCMs and RCPs one at a time (Standard Deviation resulting from Monte Carlo simulations considering GCMs and RCPs one at a time (SDepi)). We normalised these standard deviations (reflecting uncertainties in GCMs, RCPs, and exposure-response functions, respectively) dividing by their sum: SDgcm + SDrcp + SDepi. It can be noted that the differentiation between GCMs and RCPs in contributing to climate uncertainty was only possible for global warming levels 1–3 °C, because results for higher warming levels were based on RCP8.5 only (cf. Appendix A.2, Table A.3). Thus, for warming levels $> 3\,^{\circ}$C we only considered SDgcm and SDepi. All computations were done using R (version 3.4.3) with packages dlnm and mvmeta. The code was partly adapted from Gasparrini et al.(2015) (Gasparrini et al., 2015), Gasparrini et al. (2017) (Gasparrini et al., 2017), and Vicedo-Cabrera et al. (2019) (Vicedo-Cabrera et al., 2019), and is available on request from the first author.

3.3 Results

Our dataset of 12 major German cities included a total of 3 105 865 deaths in the period 1993–2015 (Table 3.1). The mean (min, max) of daily mean temperatures across cities was 10.3 °C (-17.5 °C, 30.5 °C). Overall cumulative temperature-mortality associations were relatively similar across cities (Figure 3.2), showing a gradually rising RR for cold (i.e., below the MMT), and a more steeply increasing RR for heat (i.e. above the MMT). MMT estimates fell in the range 17.2 °C–19.8 °C, corresponding to the 82nd to 90th percentiles of the distribution of daily mean temperatures in the individual cities (Table 3.1). All cities showed a similar temporal lag structure: The effect of cold peaked a few days after the exposure and lasted up to 3 weeks, while the effect of heat was more immediate and vanished (or reversed sign, indicative of mortality displacement) after a few days (Figure A.3, Figure A.4). Total excess mortality attributable to non-optimal temperatures across cities was 6.30% (95%CI: 4.60–7.98) (Table 3.1). Out of this, 0.81% (95%CI: 0.72–0.89) were attributable to heat, and 5.49% (95%CI: 3.82–7.19) to cold. Comparing city-specific estimates, the lowest total excess mortality was observed in Bremen (3.56%; 95%CI: 0.23–6.81) and the highest in Frankfurt (9.59%; 95%CI: 5.99–12.87) (Table 3.1, Figure 3.3). Confidence intervals of attributable fractions were significant (i.e.d̃id not include zero) in all cities, except for cold attributable mortality in Bremen. The sensitivity analysis showed that modelling choices only marginally affected our estimates of present-day attributable fractions (Appendix A.2, Table A.4). Projections of excess mortalities for 1° C of GMT rise above pre-industrial levels, roughly corresponding to historical global warming up to today, were very close to the estimates based on observational data (Figure 3.3). In all cities, heat excess mortality was projected to increase from today's GMT level towards higher magnitudes of global warming, while cold excess mortality was projected to decrease (Figure 3.3, Appendix A.2, Table A.6). Whereas at lower levels of GMT rise cold contributed considerably stronger to total excess mortality than heat, this pattern was reversed at higher levels of GMT rise (see crossing points of blue and red curves in Figure 3.3). For a 5 °C increase in GMT above pre-industrial levels total excess mortality attributable to non-optimal temperatures was projected to reach 9.02% (95%CI: 6.60–11.44) across cities, with heat contributing the larger part 5.75% (95%CI: 4.48–7.09), and cold contributing only 3.27% (95%CI: 1.93–4.60) (Table 3.2, Figure 3.3). In all cities, net changes in total excess mortality from today's 1 °C to a 2 °C increase in GMT above pre-industrial levels were marginal and not significant from zero (Figure 3.4). At this warming level, projected increases in heat-related mortality were largely compensated for by decreases in cold-related mortality. In most cities, significant net increases in total excess mortality started to appear at 3 °C or 4 °C of GMT rise above pre-industrial levels (Figure 3.4, Appendix A.2, Table A.6). For all cities combined, total excess mortality was estimated to increase by 0.45% (95%CI: -0.02–1.06) towards 3 °C, 1.53% (95%CI: 0.96–2.06) towards 4 °C and 2.88% (95%CI: 1.60–4.10) towards 5 °C, compared to the current 1 °C rise in GMT (Table 3.2, Figure 3.4). Underlying these net changes were marked increases in heat-related mortality by 1.68% (95%CI: 1.21–2.30) at 3 °C, 3.26% (95%CI: 2.81–3.70) at 4 °C, and 4.95% (95%CI: 3.84–6.10) at 5 °C, corresponding to a 2.8-fold (95%CI: 2.3–3.4), a 5.1-fold (95%CI: 4.6–6.0) and a 7.2-fold (95%CI: 6.5–7.9) rise in heat-related excess mortality, respectively, compared to today's warming of 1 °C (Table 3.2, Figure 3.4). The estimated standard deviations indicated that differences in climate simulations (originating from the use of various GCMs and from considering different RCPs) were the dominant source of uncertainty in projections of heat-

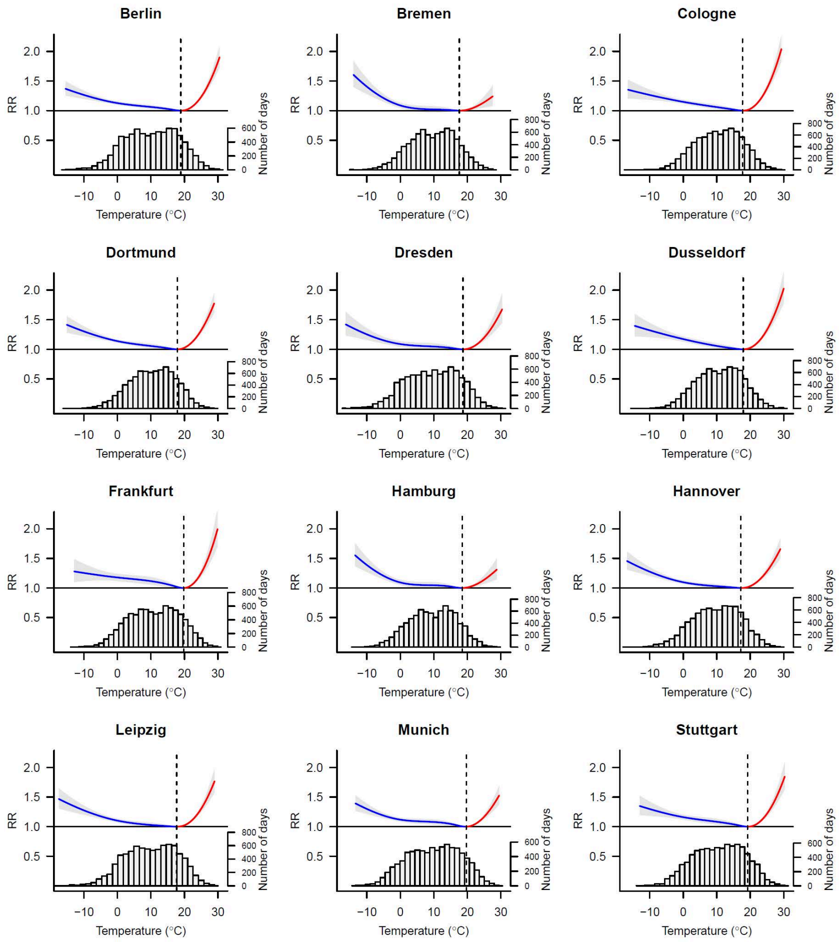

Fig. 3.2.: **Temperature-mortality associations in German cities estimated from observed deaths counts and mean daily temperatures in 1993–2015.** Mortality is reported as RR with respect to the MMT (dashed line). Cold-related RR (temperature < MMT) is shown in blue, heat-related RR (temperature > MMT) in red. Shading corresponds to empirical 95%CIs. Lower panels depict daily mean temperature distributions. (For interpretation of the references to colour in this figure legend, the reader is referred to the Web version of this article.)

related excess mortality (Figure 3.5). By contrast, uncertainties in the temperature-mortality associations were the main contributor to total uncertainty in projections of cold-related mortality. Climate uncertainty contributed increasingly to overall uncertainty in projected total excess mortality along the gradient of global warming considered. The choice of RCP was generally the least important source of uncertainty, compared to differences among GCMs and uncertainties inherent in exposure-response functions, with the exception of warming levels 1 °C and 2 °C for heat-related mortality (Figure 3.5).

3.4 Discussion

Here, we present for the first time a comprehensive assessment of temperature-related excess mortality under current and possible future climate conditions in major German cities, taking into account both heat- and cold-related mortality. Our findings indicate that while low temperatures currently contribute stronger to overall excess mortality than high

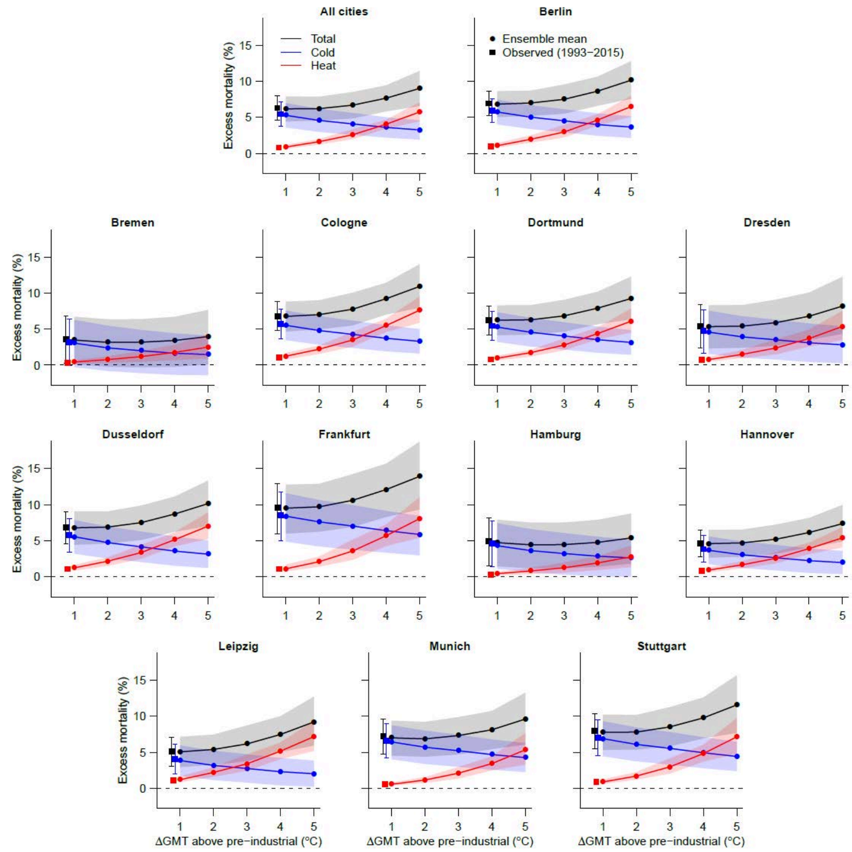

Fig. 3.3.: **Projected total (black), cold-related (blue) and heat-related (red) excess mortality at different levels of global warming, for all cities combined, and by individual city.** Circles show mean excess mortality averaged across GCMs and scenario types (RCPs) for considered increases in global mean temperature (ΔGMT) above pre-industrial levels. Squares depict excess mortality estimates based on observations (see Table 3.1). Shading and whiskers correspond to 95%CIs, taking into account uncertainty related to temperature-mortality associations and climate projections (GCMs and RCPs). (For interpretation of the references to colour in this figure legend, the reader is referred to the Web version of this article.)

Tab. 3.2.: **Projected excess mortality (GCM-RCP-ensemble averages) at different levels of GMT rise above pre-industrial for all 12 German cities combined.** Relative changes (net differences, change factor) are computed relative to 1 °C GMT rise.

GMT rise above pre-industrial	Temperature range	Attributable fractions		Net differences		Change factor	
		%	(95%CI)	%	(95%CI)	%	(95%CI)
1 °C	Heat	0.89	(0.66,1.18)	–		–	
	Cold	5.29	(3.61,6.99)	–		–	
	Total	6.19	(4.45,7.92)	–		–	
2 °C	Heat	1.64	(1.25,2.01)	0.73	(0.41,1.03)	1.8	(1.4,2.3)
	Cold	4.58	(3.00,6.18)	-0.74	(-1.03,-0.50)	0.9	(0.8,0.9)
	Total	6.22	(4.56,7.87)	-0.01	(-0.39,0.31)	1.0	(0.9,1.1)
3 °C	Heat	2.60	(2.00,3.36)	1.68	(1.21,2.30)	2.8	(2.3,3.4)
	Cold	4.10	(2.59,5.62)	-1.22	(-1.68,-0.87)	0.8	(0.7,0.8)
	Total	6.70	(4.87,8.51)	0.45	(-0.02,1.06)	1.1	(1.0,1.2)
4 °C	Heat	4.06	(3.44,4.69)	3.26	(2.81,3.70)	5.1	(4.6,6.0)
	Cold	3.61	(2.20,5.02)	-1.72	(-2.11,-1.35)	0.7	(0.6,0.7)
	Total	7.67	(5.83,9.45)	1.53	(0.96,2.06)	1.2	(1.1,1.4)
5 °C	Heat	5.75	(4.48,7.09)	4.95	(3.84,6.10)	7.2	(6.5,7.9)
	Cold	3.27	(1.93,4.60)	-2.07	(-2.56,-1.62)	0.6	(0.5,0.7)
	Total	9.02	(6.60,11.44)	2.88	(1.60,4.10)	1.5	(1.2,1.8)

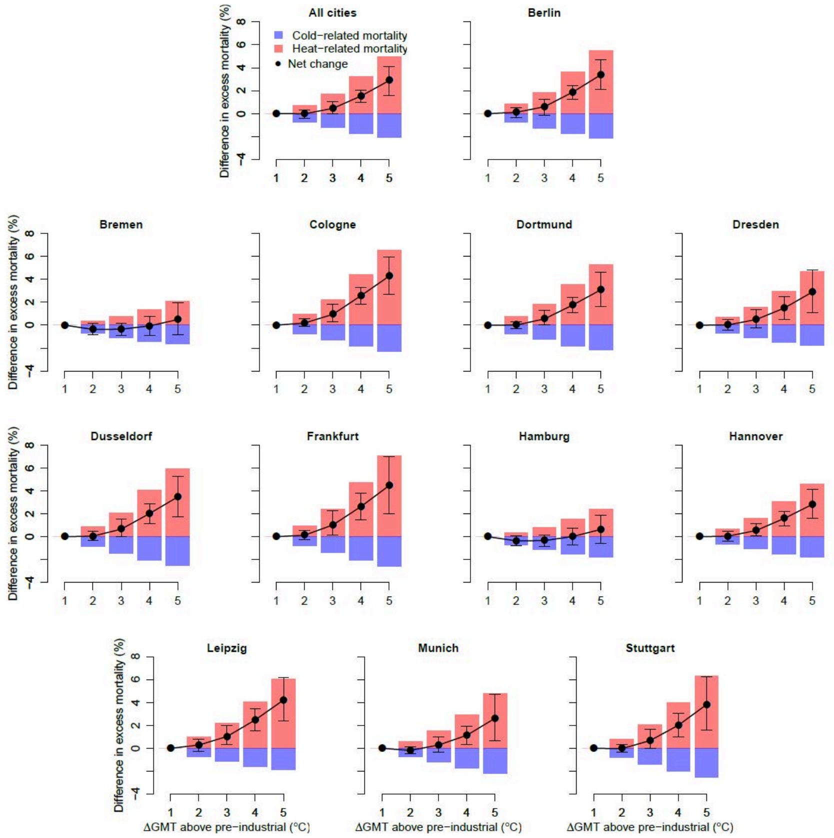

Fig. 3.4.: **Differences in excess mortality compared to today's 1 °C of global warming for all cities combined, and by individual city.** Bars and circles correspond to GCM-RCP-ensemble averages (cf. Figure 3.3). Whiskers show 95%CIs in net differences.)

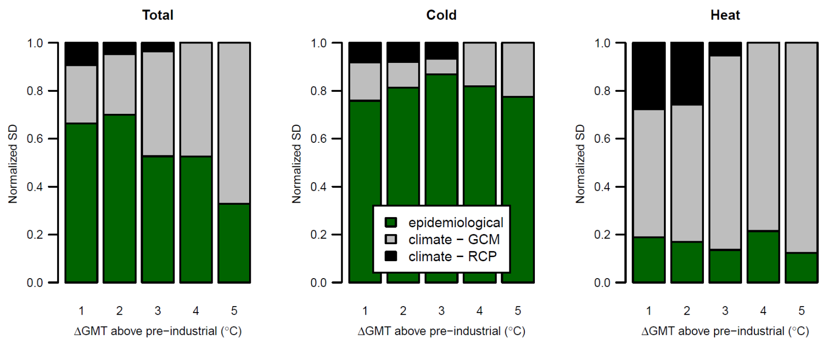

Fig. 3.5.: **Relative uncertainty in projections.** Relative uncertainty expressed as normalised Standard deviations (SDs) arising from GCMs and RCPs (climate uncertainty), and exposure-response functions (epidemiological uncertainty) in projections of total excess mortality (left), cold-related excess mortality (middle) and heat-related excess mortality (right), by level of global warming. Results shown are for all cities combined.

temperatures across the cities studied, this pattern could be reversed if GMT rise more than 3 °C relative to pre-industrial levels. Higher levels of global warming on the order of 3 °C, 4 °C and 5 °C are accompanied in our projections with marked net increases in total temperature-related excess mortality compared to today. By contrast, limiting the rise in GMT to 2 °C would avoid any significant change in total temperature-related mortality compared to today. Yet, underlying increases in heat-related mortality at this warming level are still considerable on a relative scale, with a mean projected 1.8-fold rise in the attributable fraction across cities. Our results on attributable mortality in the observational period (1993–2015) agree with Gasparrini et al. (2015) (Gasparrini et al., 2015), who found that a larger fraction of the current temperature-related excess mortality in cities around the world can be attributed to cold than to heat. The temperature-mortality associations estimated here are also in qualitative agreement with Breitner et al. (2014) (Breitner et al., 2014), who showed that both very low and very high ambient temperatures increase non-accidental mortality in three southern German cities. E.g. for Munich our RR estimates translate into a 8.7% and 19.9% increase in mortality between the 1st vs 10th, and 99th vs 90th percentiles of daily mean temperatures, respectively, compared to 8.5% and 6.8% estimated by Breitner et al. (2014) (Breitner et al., 2014). By contrast, a recent study on temperature-related mortality across all German counties (Karlsson and Ziebarth, 2018) found evidence for heat-related mortality, but remained inconclusive on the effect of cold. The difference with our findings might stem from methodological differences in modelling the lagged effects of temperature. In fact, Gasparrini (2017) (Gasparrini et al., 2017) suggested that simpler approaches such as moving averages or linear lag functions (as adopted by Karlsson and Ziebarth, 2018 (Karlsson and Ziebarth, 2018)) tend to underestimate cold effects on mortality, compared to more sophisticated methods such as the DLNMs used in our study. Our findings on projected mortality qualitatively match the estimates presented recently by Vicedo-Cabrera et al. (2018) (Vicedo-Cabrera et al., 2018), who found moderate increases in net excess mortality for warming levels 3 °C and 4 °C relative to 1.5 °C for cities in Central Europe (which in this analysis comprise France, Switzerland, Czech Republic, and Moldova as the countries geographically closest to Germany). Our results can also be compared to the only study that has so far presented quantitative projections on heat- and cold-related mortality for the whole of Germany (Hübler et al., 2008). Disregarding the effect of an aging population, this study found a doubling of heat-related fatalities for a scenario (SRES A1B) corresponding to approximately 3 °C global warming by the end of the century (conversion of scenario and time period into GMT level based on Ebi et al., 2018 (Ebi et al., 2018)). Our aggregated results across all cities are approximately in line with these findings (Table 3.2: we found a mean increment factor of 2.8 [95% CI: 2.3–3.4]). Furthermore, Hübler et al. (2008) (Hübler et al., 2008) found that at 3 °C the effects of cold and heat only roughly balanced each other, with a slight surplus of additional deaths due to heat, which is also in accordance with our results. Our study has several limitations. Most importantly, our projections do not take into account possible shifts in the vulnerability of the population towards non-optimal temperatures over time, which might occur due to demographic changes, alteration of health care services, physiological acclimatisation, or adaptation measures. These shifts have been documented for the past, especially regarding decreasing vulnerability towards heat (e.g. Achebak et al., 2018; Barreca et al., 2016; Chung et al., 2018). Some recent projection studies have also explicitly accounted for demographic changes, based on age-specific exposure response functions (Lee et al., 2019; Rai et al., 2019). However, our approach does not easily allow us to incorporate these changes in time.

By integrating different climate scenarios (RCPs) in our definition of global warming levels we break up the temporal structure of projections and thus cannot directly integrate possible future changes in demography or adaptive behaviour. Thus, our results should by no means be misinterpreted as future predictions of temperature-related excess mortality. Instead, our approach allows us to isolate the effect of climate from other socio-economic factors known to influence mortality. Consistently with previous published studies we estimated large uncertainties in projected excess mortalities (Gasparrini et al., 2017; Vicedo-Cabrera et al., 2018), stemming from the imprecision in estimated temperature-mortality associations, from differences among GCMs, and from sampling uncertainty related to different RCPs. Yet, even though we capture important elements of the total uncertainty, there are some limitations to our uncertainty measures. First, our approach does not account for the uncertainty in choosing the functional form for extrapolating exposure-response curves beyond the maximum temperatures in the observational datasets (Benmarhnia et al., 2014; Vicedo-Cabrera et al., 2018). This shortcoming would lead to an underestimation of the contribution of epidemiological uncertainty to total uncertainty in heat-related mortality projections (Figure 3.5). Second, by using temperature projections derived from transient climate simulations in a limited time period we base our estimates on an incomprehensive sampling of the temperature distributions corresponding to the different magnitudes of global warming considered. This concerns in particular the higher warming levels (4 °C and 5 °C), where our estimates are based on RCP8.5 simulations of two GCMs only (Appendix A.2, Table A.3), and, thus, the resulting bias in the estimation of climate uncertainty should be greatest. Last but not least, our study leaves to further research the more detailed investigation of observed heterogeneity between cities. Sera et al. (2019) (Sera et al., 2019) recently showed that some of the differences in the magnitude of attributable fractions observed among cities around the world can be related to variability in external factors such as demographic parameters, air pollution levels, socio-economic indicators, and urban infrastructure. In this regard, it is interesting to note that the two cities with the most maritime climate, and thus the comparatively coolest summers, Bremen and Hamburg, showed the lowest heat-related excess mortality (Table 3.1). Further analyses relating differences in exposure-response functions to local climate characteristics is a promising avenue to account for potential shifts in vulnerability to non-optimal temperature in more refined future projection studies.

3.5 Conclusions

In conclusion, our findings show that keeping global warming below 2 °C above pre-industrial levels implies considerable health benefits in German cities compared to higher warming levels, especially those to be reached if global greenhouse gas emissions are not drastically reduced in the coming decades. While we found marked net increases in temperature-related excess mortality for global warming by 3 °C and more, ambitious mitigation in accordance with the Paris Agreement would avoid a net increase in overall excess mortality compared to today. At the same time, even at 2 °C of global warming, adaptation efforts would need to be implemented in order to buffer the estimated increase in heat-related mortality, which, independent of concomitant shifts in cold-related mortality, appears as a considerable future public health risk in Germany.

From case study to global level

4

Global drivers of minimum mortality temperatures in cities

Abstract. Human mortality shows a pronounced temperature dependence. The minimum mortality temperature (MMT) as a characteristic point of the temperature-mortality relationship is influenced by many factors. As MMT estimates are based on case studies, they are sporadic, limited to data-rich regions, and their drivers have not yet been clearly identified across case studies. This impedes the elaboration of spatially comprehensive impact studies on heat-related mortality and hampers the temporal transfer required to assess climate change impacts. Using 400 MMTs from cities, we systematically establish a generalised model that is able to estimate MMTs (in daily apparent temperature) for cities, based on a set of climatic, topographic and socio-economic drivers. A sigmoid model prevailed against alternative model setups due to having the lowest AICc and the smallest RMSE. We find the long-term climate, the elevation, and the socio-economy to be relevant drivers of our MMT sample within the non-linear parametric regression model. A first model application estimated MMTs for 599 European cities ($>$ 100 000 inhabitants) and reveals a pronounced decrease in MMTs (27.8–16 °C) from southern to northern cities. Disruptions of this pattern across regions of similar mean temperatures can be explained by socio-economic standards as noted for central eastern Europe. Our alternative method allows to approximate MMTs independently from the availability of daily mortality records. For the first time, a quantification of climatic and non-climatic MMT drivers has been achieved, which allows to consider changes in socio-economic conditions and climate. This work contributes to the comparability among MMTs beyond location-specific and regional limits and, hence, towards a spatially comprehensive impact assessment for heat-related mortality.

The article presented in Chapter 4 is published as:

Krummenauer, L., Prahl, B.F., Costa, L., Holsten, A. Walther, C. and J.P. Kropp (2019): Global drivers of minimum mortality temperatures in cities. In: *Science of the Total Environment (695:133560), December 2019*. https://doi.org/10.1016/j.scitotenv.2019.07.366.

4.1 Introduction

The location-specific MMT gives an indication of an urban population's level of sensitivity to elevated ambient temperature (Harlan et al., 2014). Present-day climate MMTs have been determined by associating daily temperatures with daily mortality records in spatially incoherent case studies (Curriero, 2002; Iñiguez et al., 2010; Gasparrini et al., 2015; Seposo et al., 2016; Wichmann, 2017). Studies delivering MMTs for a larger amount of case study cities around the globe exist (Gosling et al., 2007; McMichael et al., 2008; Gasparrini et al., 2015), but only for data-rich regions. However, they fall short of distilling the information contained within MMTs to achieve a continuous spatial coverage of MMTs for cities, region- or world-wide. To date, this constitutes an obstacle for an elaboration of spatially extended impact studies on heat-related mortality, e.g. in central Europe, Africa or for global impact assessment initiatives. In this work, we establish a modelling approach to accomplish a coherent quantification of MMTs. First explorations of heterogeneity in drivers of heat risks at the city-level have been based on a meta-regression for 64 locations (Hajat and Kosatky, 2010). We seek to provide MMTs for even more cities than available from these extended studies and to reduce the number of previously suggested climatic and non-climatic MMT drivers across case studies to a significant minimum.

MMTs differ regionally among cities, according to their climate (Ballester et al., 2011; Hajat and Kosatky, 2010). Populations are to some extent acclimatised and, as far as their socio-economic standard allows, behaviourally and technically adapted to their local climate (Medina-Ramon and Schwartz, 2007; Guo et al., 2014; Harlan et al., 2014; Zaninović and Matzarakis, 2014; Tobías et al., 2017), even to extremes (Hajat and Kosatky, 2010; Chung et al., 2015). However, this adaptation is incomplete (Medina-Ramon and Schwartz, 2007; Hajat and Kosatky, 2010; Guo et al., 2014) since mortality occurs below and above the MMT. Another potential climatic driver is the annual temperature variability (Iñiguez et al., 2010; Zaninović and Matzarakis, 2014). Further MMT drivers related to topography, demography, city-structure, as well as the socio-economy, and the health status have been put forward in literature. See appendix for details on drivers and references. To clarify the importance of each driver, we use 400 MMT estimates for cities (we refrain from MMTs given as fixed percentiles) from a range of epidemiological studies and corresponding climatic, topographic, demographic and socio-economic data for each city. MMT estimates from previous studies are heterogeneous concerning time scales (years or seasons) and temperature metrics (daily mean or maximum temperature or their apparent temperature equivalents), which impedes the comparability and interpretation of findings. We homogenise the MMTs and construct a non-linear parametric regression model expressing the functional relationship between MMTs and a set of demographic and socio-economic drivers, complementary to climatic and topographic ones. We aim at a non-linear model because a physiologically constrained absolute limit to human acclimatisation to the local climate was suggested (Sherwood and Huber, 2010; Hanna and Tait, 2015). Further, socio-economic adaptive capacity is neither absolutely complete, nor is it able to overcome the physiologic limit. Hence, MMTs are likely to have a maximum. Crucially, we provide a generalised method that enables the spatially continuous estimation of MMTs for cities worldwide for present climate conditions. We provide a first MMT dataset for European cities resulting from our model.

4.2 Materials and methods

4.2.1 City-specific minimum mortality temperatures

To construct a model, we investigate 400 empirical MMTs derived from daily mortality and air temperatures in cities via the time-series or time-stratified case-crossover designs in peer-reviewed publications. Both methods were reported comparable (Hajat and Kosatky, 2010; Lu and Zeger, 2007). MMTs either given in mean or maximum temperatures (Tmean, Tmax), or their apparent temperature equivalents (ATmean, ATmax) were considered. We convert MMT metrics to ATmean, a commonly used metric by some original studies (Michelozzi et al., 2007; Sun et al., 2012; Wichmann, 2017), to ensure comparability among estimates, whereas MMTs given in ATmean remain unchanged. To do so, we use homogenised time-series of daily observed Tmean, Tmax, dew point temperature (Tdewp), and daily mean wind speed from the Global Summary of the Day (GSOD), see appendix for climate stations. AT equivalents are calculated from the drybulb air temperature (Tmean or Tmax) and the dew point temperature (Tdewp) in $^\circ$C using the equation $\mathrm{AT} = -2.653 + (0.994 * \mathrm{T}) + (0.0153 * \mathrm{T}^2_{\mathrm{dewp}})$ (Michelozzi et al., 2007) and adjusted for wind speed $[\mathrm{m/s}]$ (Steadman, 1984). The conversion is based on the average daily Tmean or Tmax of those days within the original study period that display similar values to the corresponding MMTs ($+/-$ 0.5 $^\circ$C). To change MMTs in ATmax to ATmean, we first convert the GSOD Tmax time-series to ATmax and then apply the first step as above. For the corresponding days, we continue using the respective Tmean observations for the second and third steps.

4.2.2 Regression variables

For each city related to an MMT, we collect climate station data containing time-series of the mean, maximum, minimum and dew point temperatures on a daily resolution from the Global Summary of the Day (GSOD). We obtain time-series on socio-economic indicators, health-status, and age stratification on an annual resolution at country-level from the World Bank Open Data (WBOD), the World Income Inequality Database, and the Millennium Development Goals Lebanon Report (MDGLR). We attribute the indicators' 1995–2005 averages to each city, for GDP per capita and improved urban water we use data for 2000. City coordinates, coastline, and population density (as of 2000) are taken from the Center or International Earth Science Information Network (CIESIN) and elevation from a SRTM 90m DEM (as of 2000). Thirteen variables (Table 4.1) on the cities' long-term climate, topography, and demography are computed from these datasets. All independent variables are supported in previous studies. They equally feed into the multivariate regression analysis. See appendix for full dataset references, calculation of variables, and supporting references.

4.2.3 Multivariate regression analysis

We determine the curve best describing the empirical MMT sample via multivariate maximum-likelihood regression. For all variable combinations, we primarily compare a linear and a non-linear sigmoid model. A sigmoid model (Equation 4.1) is motivated by the hypothesis that MMTs might have a maximum due to physiological constraints of the human capacity to acclimatise to heat (Sherwood and Huber, 2010) and the incompleteness of socio-economically driven adaptive capacity. We therefore assume the curve representing the

Tab. 4.1.: **Information on independent variables used in the regression analysis.** GSOD = Global Summary of the Day, CIESIN = Center for International Earth Science Information Network, GRUMP = Global Rural-Urban Mapping Project, SRTM = Shuttle Radar, DEM = Digital Elevation Model, GPW = Gridded Population of the World, WBOD = World Bank Open Data, WIID = World Income Inequality Database, MDGLR = Millennium Development Goals Lebanon Report. Find full references for datasets and supporting references in the appendix.

Type	Independent variables	Source Data	Years
Climate	30-year average of daily mean temperature	GSOD	various, cf. appendix
Climate	30-year average of annual amplitude	GSOD	various, cf. appendix
Climate	30-year average of hottest month's temperature	GSOD	various, cf. appendix
Topography	Distance to coast	CIESIN GRUMP	2000
Topography	Latitude	CIESIN GRUMP	2000
Topography	Elevation in meters a.s.l.	SRTM 90m DEM	2000
Demography	Population density	CIESIN GPW	2000
Socio-economy	GDP per capita (current international Dollars in PPP)	WBOD	2000
Socio-economy	GINI Coefficient	WBOD, WIID, MDGLR	1995-2005 average
Socio-economy	Improved urban water source (% of urban population with access)	WBOD	2000
Socio-economy	Health expenditure (% of GDP)	WBOD	1995-2005 average
Socio-economy	Life expectancy (at birth)	WBOD	1995-2005 average
Socio-economy	Share of population older 65 (%)	WBOD	1995-2005 average

MMTs is bound by constant upper and lower asymptotes. To further support or reject our hypothesis we add three simple segmented linear models to the comparison: with a constant asymptote at the top (I), at the bottom (II), and both combined (III). A schematic illustration of these models can be found in the appendix, Figure 1. As in the sigmoid case, all asymptotes are expressed as model parameters and are determined from regression against the MMT data.

We employ the Akaike information criterion corrected for small sample sizes (AICc) to select the best model. Unlike traditional statistical hypothesis tests, e.g. likelihood-ratio test (LRT), the AICc also allows comparison of non-nested models. The parameters of a nested model are a subset of the parameters of another model. As this condition does not apply for the linear and sigmoid models in this study, these two models are non-nested. The AICc may be used if the ratio of n observations and k variables is less than 40. It is 26 in our case. Before selecting the best model via the AICc, we impose two restrictions on suitable model candidates. Firstly, we restrict collinearity by excluding variable pairings with a Pearson's correlation coefficient $\rho > 0.75$. Secondly, we assess for each model candidate individually the significance of each model parameter via the LRT with a significance level of 0.99. Model candidates that include insignificant parameters are removed. The remaining model candidates are ranked with regard to their AICc and the model with the lowest is selected. The LRT restriction ensures that no spurious random variables remain in the model. An AICc-based model selection alone might fall short on doing so and additional model inspection is required (Arnold, 2010). Although arguments against the combination of AICc and LRT have been brought forward (Burnham and Anderson, 2002) we find that the LRT restriction consistently rejects model candidates that include additional parameters but only exhibit small increases in AICc scores (AICc difference < 2) compared to the candidates without the additional variables. As one of our objectives is model interpretation, we choose this approach to dismiss models that would contain uninformative parameters.

An out-of-sample test against 40 MMTs separated from the training data (n=360) prior to the analysis serves to assess the predictive skill of our final model. The validation data was chosen randomly, while maintaining the approximate proportional distribution in climatic zones of the full dataset of 400 MMTs. Further, we characterise our model for eight world regions and eleven climate zones and test statistically for each set of MMTs whether the model performs significantly better or worse than for the remaining data. All variables were standardised prior to the analysis by subtracting their mean value and dividing the difference by its standard deviation. For parameters see appendix.

$$\mathrm{Y} = \frac{\mathrm{c} - \mathrm{d}}{1 + \exp(-\mathrm{z})} + \mathrm{d} + \varepsilon \tag{4.1}$$

where
Y is the dependent variable
z is the linear term $\beta_0 + \beta_1 \mathrm{X}_1 + \beta_2 \mathrm{X}_2 + \ldots + \beta_\mathrm{m} \mathrm{X}_\mathrm{m}$ with
$\mathrm{X}_1, \ldots, \mathrm{X}_\mathrm{m}$ as the regressors
β_0 as the regression constant and intercept
β_i as the partial regression coefficients for $\mathrm{X}_1 (1 \leq \mathrm{i} \leq \mathrm{m})$
ε is a random or disturbance variable
c is the upper asymptote
d is the lower asymptote

4.2.4 Model application to European cities under present conditions

We estimate MMTs for major European cities using the proposed sigmoid model. E-OBS climate data (at a resolution 0.25 °C x 0.25 °C) for 1981–2010 serve to calculate the independent climate variables. The elevation raster resolution is adjusted to that of the climate. Socio-economic variables are employed at the national level. We consider only MMT estimates within the range of empirically available data used to establish the model (daily mean AT of 10.8 °C to 36.4 °C). MMTs are estimated for cities $>$ 100 000 inhabitants, selected via the GRUMP coordinates from CIESIN. See appendix for full references of datasets.

4.3 Results

4.3.1 MMT data

Most of the 400 MMTs in our sample are from southern Europe, North America, and East Asia (Figure 4.1). The general lack of MMTs from other regions, e.g. Africa is attributable to the unavailability of mortality records in the first place (El-Zein et al., 2004; Egondi et al., 2012). After the metric conversion, MMTs in $\mathrm{AT_{mean}}$ range from 36.4 °C in Haikou (China) to 10.8 °C in Edmonton (Canada). High MMTs occur in the tropics e.g. Bangkok (Thailand, 35.7 °C) or Manila (Philippines, 35.6 °C) and in the arid subtropics, e.g. Phoenix (USA, 34.5 °C), and Monterrey (Mexico, 34.6 °C). Low MMTs occur in Canada and New Zealand. See appendix for MMTs.

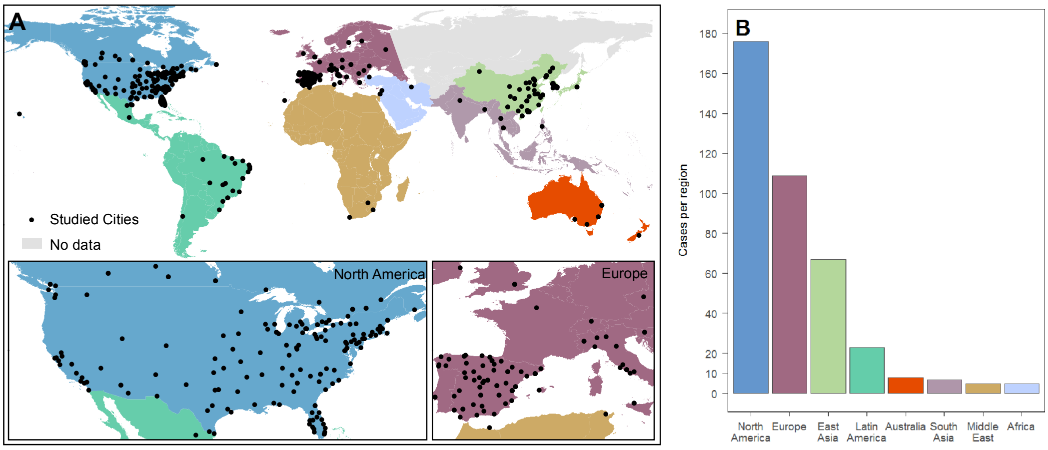

Fig. 4.1.: **Location of cities for which MMTs have been calculated and that are considered in this study.** (A) 400 MMTs from 309 cities. (B) Number of MMTs by world region.

4.3.2 Multivariate regression analysis

Our systematic comparison of the linear, sigmoid and segmented models across all variable combinations reveals that a sigmoid model best fits our regression dataset of 360 MMTs. Substantially, the sigmoid model displays the lowest and therefore most optimal AICc at 1782 and a low RMSE of 2.81 (Figure 4.2 A). Five significant variables are returned: the 30-year average of the daily mean temperature, the 30-year average of the annual amplitude, the elevation, the GDP per capita and improved urban water. The same variables in the linear model show less optimal AICc and RMSE values (AICc 1840, RMSE 3.05). The difference of AICc scores can be used to calculate an evidence ratio by calculating $\mathrm{Q_{i,j}} = \exp((\mathrm{AICc_j} - \mathrm{AICc_i})/2)$. It represents the evidence as to which model is better in a Kullback-Leibler information sense (Burnham and Anderson, 2002) and can be interpreted as the likelihood that a model *i* is superior in minimising the information loss than the reference model *j*. The resulting evidence ratio of $> \approx\ 10^{12}$ from the AICc difference of the linear to the sigmoid reference model indicates that the sigmoid model is $\approx\ 10^{12}$ times more likely to minimise the information loss than the linear model. Both segmented model variants with one asymptote (models I and II, cf. section 4.2.3) exhibit more optimal AICcs and RMSEs than the linear model but are less optimal than the segmented model with both asymptotes (model III, cf. section 4.2.3), with an AICc of 1790 and the RMSE of 2.83. The remaining AICc difference of ≈ 8 between the segmented model with both asymptotes (III) and the sigmoid reference model implies that the sigmoid model is ≈ 51 times more likely to minimise information loss than the segmented model III with both asymptotes. The coefficients of the sigmoid model are shown in Table 4.2. The fixed term β_0 was not found significant.

The sigmoid model resulting as the optimal model from the previous model comparison is seen as an indication for a general asymptotic behaviour at the top and the bottom of the MMT distribution in our sample. To support this finding, we demonstrate that the sigmoid behaviour is not restricted to a particular variable selection. A comparison of the 20 best returned sigmoid variable setups against their linear and segmented equivalents shows that the sigmoid models are significantly better in AICc (Figure 4.2 A). The average AICc deviations from the sigmoid reference model (Figure 4.2 B) is highest for the linear models

Tab. 4.2.: **Coefficients for the sigmoid model based on 360 MMTs and valid for standardised input variables** (see appendix for standardisation parameters). For this setup, the RMSE is 2.81 and the AICc is 1782. Temperature = 30-year average of the daily mean temperature, Amplitude = 30-year average of the annual amplitude, GDP per capita= GDP per capita in current int. Dollars in PPP, Improved Urban Water = Improved urban water source (% of urban population with access).

Parameters	Estimate	Std. Error	P-Value
Temperature	1.77	0.26	< 0.0001
Amplitude	1.03	0.16	< 0.0001
Elevation	-0.25	0.06	< 0.0001
GDP per capita	0.43	0.09	< 0.0001
Improved Urban Water	-0.68	0.13	< 0.0001
Upper asymptote	33.26	0.76	-
Lower asymptote	15.89	0.75	-

with 41.3, (evidence ratio of $\approx 9.3 * 10^9$). Adding the asymptotes decreases the average AICc deviation. The minimum average AICc deviation of 11.1 (evidence ratio of 257) is reached upon employing both asymptotes.

Comparing the MMTs estimates by the sigmoid model against the observed MMTs (Figure 4.3 A) reveals the majority of values is within the RMSE range $+/-$ 2.81 °C. Three outliers already had high or low MMTs in the original studies (Martin et al., 2012; Bao et al., 2016). We aggregate MMTs in bins of ten to reduce the variance and improve the signal. Binned MMTs show small deviations from the optimum line, indicating that our model estimate is free from systematic bias (Figure 4.3 A). Running the model on 40 independent MMTs results in a comparable model performance concerning scattering and location of data points (Figure 4.3 B) with an RMSE of 2.63 °C. This underlines the general applicability of the model, particularly with regard to cities that are not included in the regression data. Potentially systematic deviations are only seen for four cities (Busan, Shanghai_a, Hefei, Brisbane_b) located in temperate fully humid climates with high observed MMTs. We do not see a clear mechanism or obvious reason for this, while noting relatively low values for the elevation and GPD per capita. The characterisation of the model for climate zones and world regions (see Appendix B.3 Figures B.2 and B.3) supports that the model has no systematic bias in any of the subsets. In one case the subset RMSE is significantly different (at 99% confidence level) from the RMSE of the remaining sets. Our model has a smaller RMSE than expected for the oceanic fully humid climate.

Some authors employ percentiles of the temperature distribution as thresholds for emergency or to assess the change in mortality risk (Lowe et al., 2015; Yang et al., 2015; Chen et al., 2016). We searched for the optimum percentile in our daily mean temperature dataset and found a minimum RMSE of 3.5 at the 89th percentile. We conclude that our model displaying a smaller RMSE is better.

4.3.3 MMT Estimates for European cities from model application

Modelled MMTs in AT_{mean} for 599 European cities estimated by our model are displayed in Figure 4.4. A pronounced decline in MMTs from the Mediterranean in the south to the north is obvious with the exception of cities in higher altitudes. Sevilla (Spain) has the maximum MMT, 27.8 °C. The model produces lower MMTs for central eastern Europe compared to

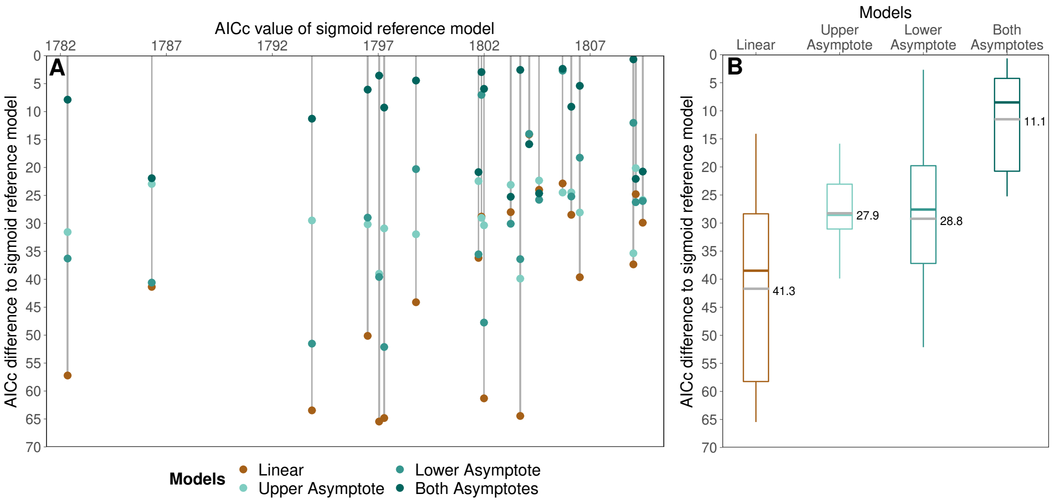

Fig. 4.2.: **Differences in AICc values between the 20 best fits of the sigmoid reference model and corresponding fits for the other variants.** Differences in AICc values compared to the sigmoid reference models typically decrease from the linear to the segmented model with both asymptotes. (A) Detailed comparison for the 20 best sigmoid reference fits and its variants, the one on the left with an AICc of 1782 being our selected model. (B) Distribution and average values of the AICc differences of the model variants related to the 20 best sigmoid reference models.

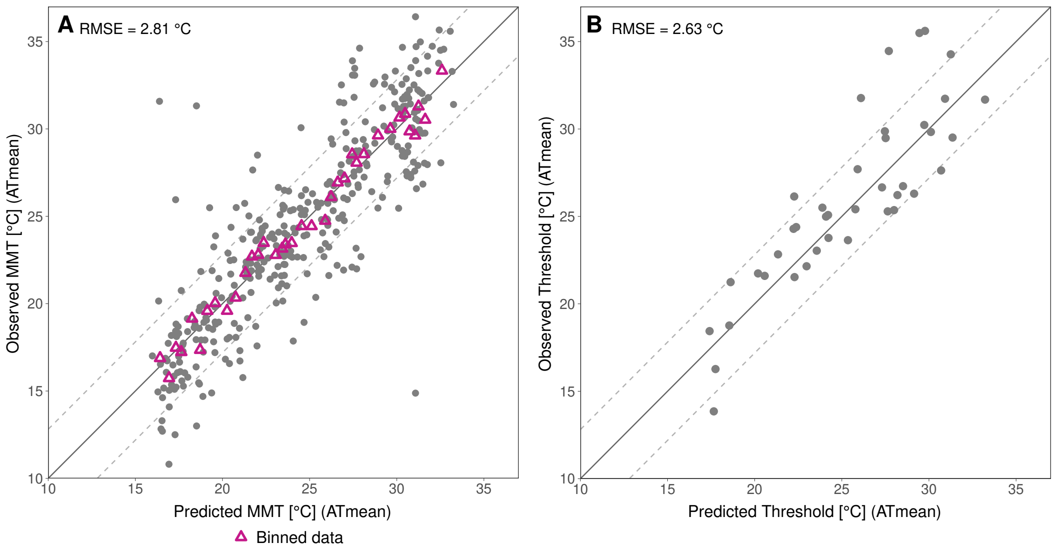

Fig. 4.3.: **Examination of the selected sigmoid model.** (A) MMT observations plotted against the predictions produced by the selected sigmoid model including binned values. (B) Out-of-sample validation of the selected sigmoid model using 40 independent validation cases with the same proportional distribution in climatic zones as the full MMT dataset. (A and in B for comparison) Solid line: optimal fit line, dotted lines: residual mean square error range of the sigmoid model.

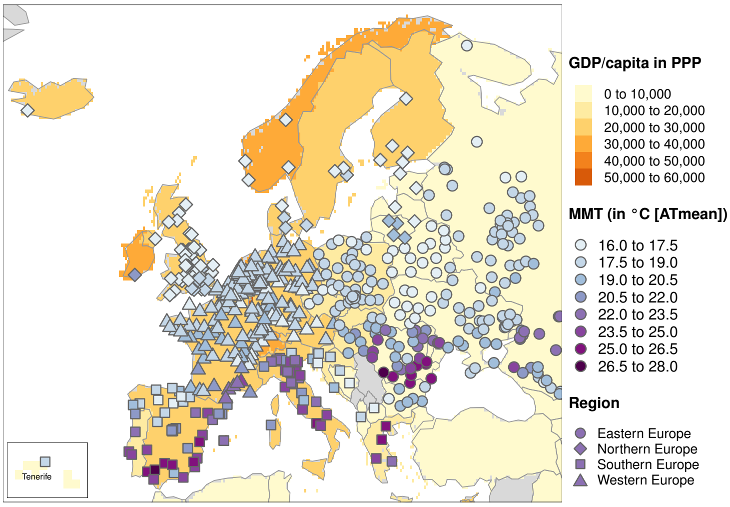

Fig. 4.4.: **Model application results for the current climate.** Estimated MMTs for 599 European settlements (population > 100 000) produced by our model. Estimates are within the range of observations.

most of central western Europe. This is likely due to low GDP per capita values in the east, since the influence of low long-term temperature on the MMT is balanced by that of the highest amplitudes in Europe (see histograms in Appendix B.3 Figure B.5). To demonstrate the force behind the GDP per capita, we examine Vienna (Austria) and Bratislava (Slovakia), a spatially close city pair ($\approx$ 55 km apart). The cities exhibit different MMTs of 20.5 °C and 18.4 °C AT, similar climate conditions (long-term mean temperatures of 10.9 °C and 10.3 °C and amplitudes of 22.7 °C and 23.2 °C), but a higher GDP per capita in Austria (29301.1) than in Slovakia (11347.9). The bulk of the European urban population, $\approx$ 95 million, lives in cities where MMTs range between 17.5 °C and 19.5 °C (Appendix B.3 Figure B.4).

4.4 Discussion

We propose a general sigmoid function based on long-term climate, topography, and socio-economic indicators that enables the estimation of MMTs at the city-level. The sigmoid model established on 360 MMTs results from a rigorous model selection process. It was better than linear and segmented linear models regarding AICc and the RMSE for the same variable combinations and data. When applying our model to estimate present-day MMTs for European cities, we find lower MMTs in high altitudes and a south-north decline in MMT magnitude. Some central eastern MMTs are lower than central western MMTs of comparable mean temperature regimes and even than northern MMTs related to high socio-economic standards. Major achievements of this work are the independence from daily mortality records and the option to generate spatially continuous MMT estimates for cities. Moreover, the model accounts for physiological constraints and the incompleteness of adaptation via wealth-induced adaptive capacity.

4.4.1 Drivers of MMTs

Our method identifies location-specific features that drive MMTs across different case studies and complements investigations of larger spatial extents at provincial or city-levels (Ballester et al., 2011; Gasparrini et al., 2015). We find that the climate has a significant role in determining the MMTs. The long-term mean temperature is strongly and positively correlated with our MMT sample, which is in line with a previous elemental analysis for urban MMTs (Hajat and Kosatky, 2010). The level of acclimatisation to temperature is significantly determined by regular exposure to a certain temperature (Medina-Ramon and Schwartz, 2007; Hajat and Kosatky, 2010; Guo et al., 2014; Harlan et al., 2014; Zaninović and Matzarakis, 2014; Tobías et al., 2017). We find a positive correlation between the MMT sample and the long-term amplitude as an indicator for maritimity and continentality. Previous evidence confirmed that regular exposure of populations to high temperature variability builds resilience to extremes (Iñiguez et al., 2010; Zaninović and Matzarakis, 2014).

Our findings suggest a slight negative significant correlation between the elevation and the MMT sample and that contrary to other studies (Bai et al., 2016), the latitude is unsuitable as predictor. A positive correlation between socio-economy, especially GDP per capita, and the MMT sample indicates that higher socio-economic standards equip urban populations with capacity to behaviourally and technically adapt and with the privilege to avoid exposure to heat. This was confirmed for wealth indicators, such as annual mean income, poverty or savings indicators (Curriero, 2002; Hajat and Kosatky, 2010; Arbuthnott et al., 2016; Chung et al., 2017; Kim and Kim, 2017) and indirect ones, e.g. low occupational exposure to heat as a consequence of high education levels (Heo et al., 2016; Liu et al., 2015; Kim and Kim, 2017), and high air conditioning prevalence (AC) (Curriero, 2002; Chung et al., 2017). The latter is critical, as AC in European homes is less common. Other still unknown factors may account for the residual error of the model. Further climatic, topographic, demographic, and socio-economic factors tested were not returned as significant predictors of MMTs in our most optimal sigmoid model, see appendix for details. Among those are the health status and age stratification of the population. We assume, they are already implicitly reflected by the two relevant socio-economic variables.

4.4.2 Uncertainties related to MMTs and the methodology

To incorporate the aspect of human discomfort but keep model complexity as low as possible, we chose AT as MMT unit. This has been done before in some temperature-related mortality studies (Michelozzi et al., 2007; Sun et al., 2012; Wichmann, 2017). Uncertainties might have been caused by averaging the AT over the identified days when carrying out the metric conversion. Employing daily means for the conversion could be a source of error. We tested this against the AT converted from 24 hourly values and subsequently averaged for each day over a ten-year period for a station at LaGuardia Airport (USA). This comparison displayed a small difference of 0.15 °C ($R^2 \approx 1$) and therefore supports our method to convert daily mean temperatures to daily AT.

A test on the association of the model results and the maximum lags used in the original studies showed that different lags are associated across the entire range of the MMT magnitudes. Model results were not systematically biased in this regard and could be used for our purpose. We have to acknowledge that some degree of uncertainty had been brought about by the original MMTs from the studies. They depend on the shape of the mortality relationship with temperature, which is influenced by fitting parameters, e.g. the degrees of freedom for the spline functions or the placement of the knots in the functions. See appendix for further details and discussion points.

4.4.3 Model choice

We found the additional segmented linear models less optimal concerning their AICc as compared to the sigmoid model with the equivalent variable setup. This was confirmed when tested on a smaller sample size of MMTs derived via the same methodology. Comparing the 20 best variable setups in the linear and segmented asymptotic variants against the prevailing sigmoid model suggests that even though the complexity increases from linear via segmented asymptotic to sigmoid models, the AICc improves by decreasing. This pattern gives an indication that MMTs might be constrained in the hot and in the cold ranges, as we hypothesised and described as possible limit of human physiological acclimatisation to heat (Sherwood and Huber, 2010) and a constraint due to the incompleteness of adaptation enabled by socio-economic standards. A broader coverage of MMTs especially in the global south and warmer regions would possibly increase precision and possibly reduce the remaining error in the model. Our model performs equally well for data-rich regions in different climate zones. We see this as indication that our estimates constitute plausible MMT approximations for such regions not covered by our training sample. We acknowledge that some authors employ percentiles of the temperature distribution as thresholds for emergency or to assess the change in mortality risk (Lowe et al., 2015; Yang et al., 2015; Chen et al., 2016). None of the percentiles (1st to 99th) was able to better approximate the observed MMTs in terms of RMSE than our model.

4.5 Concluding Remarks

Our suggested sigmoid model to estimate minimum mortality temperatures among city populations for recent climate conditions is not only driven by temperature measures but also by topography and socio-economic factors. As a composite of majorly physiological acclimatisation and socio-economy driven adaptive capacity, the MMT goes beyond a plain physiological heat tolerance. Our findings hint at the existence of a maximum and a minimum value of MMTs, which allows to consider constraints posed by acclimatisation and adaptive capacity. This should be subject to further research. Our alternative, generalised method is applicable for larger and smaller cities around the globe, and in regions that are usually not considered in case studies. We derive MMTs for 599 European cities with our model and provide the first spatially continuous dataset to researchers and stakeholders. For the first time, the spatially fragmented availability of MMTs from single case studies is overcome and a comprehensive assessment of the climatic and non-climatic MMT drivers is achieved. It is a major advantage that the required input data is easier accessible than daily mortality records conventionally used to estimate MMTs. Beyond assessing the present situation the model could be employed to investigate hypothetical conditions. Here, development status and changes in climate constitute potentially interesting issues. This work constitutes a coherent quantification of the level of urban populations' coping potential with and the onset of their susceptibility to warm temperatures in cities today across spatial scales and regions. It is intriguing to learn about how MMTs will change in the future considering climate change and different socio-economic pathways. This will be subject to our future work.

Projecting future adaptation

Future heat adaptation and exposure among urban populations and why a prospering economy alone won’t save us

5

Abstract. When inferring on the magnitude of future heat-related mortality due to climate change, human adaptation to heat should be accounted for. We model long-term changes in Minimum Mortality Temperatures (MMT), a well-established metric denoting the lowest risk of heat-related mortality, as a function of climate change and socio-economic progress across 3 820 cities. Depending on the combination of climate trajectories and socio-economic pathways evaluated, by 2100 the risk to human health is expected to decline in 60% to 80% of the cities against contemporary conditions. This is caused by an average global increase in MMTs driven by long-term human acclimatisation to future climatic conditions and economic development of countries. While our adaptation model suggests that negative effects on health from global warming can broadly be kept in check, the trade-offs are highly contingent to the scenario path and location-specific. For high-forcing climate scenarios (e.g. RCP8.5) the maintenance of uninterrupted high economic growth by 2100 is a hard requirement to increase MMTs and level-off the negative health effects from additional scenario-driven heat exposure. Choosing a 2 °C-compatible climate trajectory alleviates the dependence on fast growth, leaving room for a sustainable economy, and leads to higher reductions of mortality risk.

The article presented in Chapter 5 is published as:

Krummenauer, L., Costa, L., Prahl, B.F., and J.P. Kropp (2021): Future heat adaptation and exposure among urban populations and why a prospering economy alone won’t save us.
In: *Scientific Reports (11:20309), October 2021*.
https://doi.org/10.1038/s41598-021-99757-0.

5.1 Introduction

Apart from an increasing temperature trend in a warming climate, heat events will become more frequent, intense and longer lasting (Meehl, 2004; Ganguly et al., 2009; Coumou and Robinson, 2013). In response, human populations will have to adapt to higher future temperatures to ensure their survival (Ahima, 2020). The absence of adaptation to heat in urban populations would lead to an substantial increase in excess mortality in the future (Guo et al., 2018). These new conditions will challenge human health and the habitability of some world regions (Pal and Eltahir, 2016). Considerable efforts have been made to estimate future heat-related mortality risk (Mishra et al., 2015; Gasparrini et al., 2017), excess mortality (Guo et al., 2018), and future heat exposure (Liu et al., 2017; Mora et al., 2017b; Christidis et al., 2019), or burden of heat-related mortality attributable to recent anthropogenic climate change (Vicedo-Cabrera et al., 2021) among urban populations at a global scale. A comprehensive global projection of lethal conditions and their occurrence in the future considering possible climate futures from three Representative Concentration Pathways (RCPs) has been delivered by Mora et al. (2017) (Mora et al., 2017b). However, a better understanding of heat-related adaptation (Arbuthnott et al., 2016; Liu and Ma, 2019) is required.

Studies have proposed the use of the Minimum Mortality Temperature (MMT) as indication of human long-term adaptation to heat (Folkerts et al., 2020; Åström et al., 2016). The MMT quantifies the lowest point of the temperature-mortality curve (Gasparrini et al., 2017; Guo et al., 2018; Yin et al., 2019) and therefore it currently is the best empirical measure of the temperature level to which a city/region is adapted to. Temperatures significantly higher or lower than the MMT come associated with disproportional increases in excess mortality. Upward changes in the MMT were found to shift the entirety of the temperature-mortality curve as well as associated indicators such as threshold values defining national heat-wave warnings (López-Bueno et al., 2021), hence indicating that heat adaptation is taking place (Follos et al., 2020). In our understanding, both aspects, physiological acclimatisation and a socio-economic standard facilitating the access to technological, social or behavioural measures to avoid heat exposure are jointly considered in the minimum mortality temperature (MMT) (Krummenauer et al., 2019). This has been acknowledged by separating physiological acclimatisation and non-climate driven adaptation mechanisms (Vicedo-Cabrera et al., 2018) for observed mortality in the recent climate.

A principal method has been proposed to model the future heat-mortality relationship in cities. The exposure-response function remains in its shape and is entirely shifted to higher temperature regimes (Ballester et al., 2011; Gosling et al., 2017). This method relies on a critical assumption of choosing a delta value quantifying the absolute shift of the curve. The delta value is however subject to uncertainty since it requires the knowledge of future mortality records (Gosling et al., 2017). Most authors circumvent this unknown by continuing past mortality patterns (Gasparrini et al., 2017).

Our research seeks to complement these previous efforts by contributing the delta value by which the MMT changes for the world's major cities. Further, we analyse both, the populations' adaptation to heat as the MMT, their heat exposure and the future changes in these measures. We understand a positive change in MMT as gain in adaptation. The exposure is measured as (1) frequency of MMT exceedance by the daily temperature and

(2) magnitude of this exceedance. We argue that only a contextualised analysis of adaptation and exposure captures the populations' potential to cope with heat, especially under varying climate trajectories and development pathways. A high adaptation eases the coping with high exposure, while high exposure might lead to many fatalities given a low adaptation level. Our analysis considers four possible Representative Concentration Pathways (RCPs) (Vuuren et al., 2011) from four Global Circulation Models (GCMs). We combine these different climate futures with five possible socio-economic pathways (SSPs) (O'Neill et al., 2014; Riahi et al., 2017) leant on the Scenario Matrix (Vuuren et al., 2014; Riahi et al., 2017). These RCP/SSP combinations cover a broad bandwidth of possible climatic and socio-economic futures with different health outcomes for urban populations. For the first time, we offer the full spectrum of future adaptation and exposure outcomes and their future changes depending on the underlying climate trajectories and socio-economic developments. This work shows which benefits and detriments these futures have in store concerning heat-related mortality until 2100. We identify the principal influences of adaptation change for two scenarios most beneficial in economic growth but contrary in their climate trajectory. It is our objective to determine the lesser of two evils regarding the change in mortality against an ideal future in absence of climate change and heat exposure. We aim at demonstrating the disadvantage for human health arising from high forcing levels driven by a rapid growth based on fossil-fuels. Our results help to inform the public and support decision-making concerning climate and human urban health.

5.2 Results

5.2.1 General observations across cities

We assessed the changes in adaptation to heat for 3 820 cities worldwide from 2000 to 2100. We considered feasible combinations of the long-term ensemble mean (ENSMEAN) of each RCP and the SSPs. The projected MMT and its 2000–2100 change, ΔMMT, were contextualised with the change in two heat exposure parameters: (1) the frequency of heat exposure (EXD) and (2) the exposure magnitude (MAG). They refer to how many days the MMT is exceeded by the daily temperature in the future and in the past annually and how large the exceedance magnitude is. We used the 1991–2000 and 2090–2099 decadal means of EXD and MAG. We evaluated the parameter changes ΔEXD and ΔMAG between the past and the future decades (see Appendix C.1 Table S1 for city parameters).

MMT distributions at the end of the century varied in range and median across the RCP/SSP combinations (Fig. 5.1 A). The distributions' medians increase with an rising forcing level, culminating in SSP5 combinations. Combinations with SSP1 and SSP4 display second and third largest median values. Distributions associated with SSP5 and SSP1 stretch towards high MMT values. More cities reach higher adaptation in 2100 than in other combinations. The contrary applies for SSP3. SSP5 combinations, especially with RCP8.5, cover an enormous ΔMMT range, while in SSP1 it is smaller (Fig. 5.1 B). Although most distributions show low EXD, the tail towards higher EXD enlarges with increasing forcing, as obvious in RCP8.5/SSP5, and in RCP6.0 combinations (Fig. 5.1 C). In RCP2.6 few cities show a positive ΔEXD towards additional EXD in 2090–2099 but many display a negative ΔEXD, a reduction in EXD (Fig. 5.1 D). A higher forcing relates to additional EXD in more cities. RCP8.5/SSP5 exhibits a tail into larger ΔEXD. Simultaneously, the number of cities experiencing reductions in EXD remains high across RCPs, notably in SSP5 and SSP1 combinations. A pattern similar to EXD is obvious in MAG (Fig. 5.1 E). Distributions involving SSP3 have largest tails towards high MAG. The median is lowest in SSP1 and SSP5 combinations. Reductions in ΔMAG are dominant in SSP1 and SSP5 combinations (Fig. 5.1 F). Contrary, SSP3 displays highest ΔMAG. The distribution of ΔMAG RCP8.5/SSP5 can be distinguished by prominent tails into both ΔMAG directions and by the highest median. This investigation implies, changes in adaptation and exposure across the city sample are divers, explicitly under RCP8.5/SSP5 conditions.

5.2.2 How RCPs and SSP influence adaptation and exposure

An investigation of mean adaptation and exposure across the cities supports the previous findings. Figure 5.2 summarises the effects on MMT and EXD and their changes in the cities across all feasible RCP/SSP combinations according to the Scenario Matrix (Vuuren et al., 2014; Riahi et al., 2017). For the city sample, the highest change in mean adaptation across all scenario combinations is a mean ΔMMT of 7.9 °C, which is reached by RCP8.5/SSP5, the highest forcing level and the most rapid unsustainable economic growth. This also yields the highest absolute mean MMT for the city sample, 34.4 °C. This combination shows a small ΔEXD of -7.6 until the decade 2090–2099 and thus deviates from SSP5 combinations paired with lower forcing (Fig. 5.2). The lowest mean ΔMMT (3.7 °C) and the lowest absolute mean MMT (30.2 °C) are displayed for RCPs 4.5 with SSP3. SSP3 is characterised by a low future socio-economic level. Combinations with RCPs 4.5 and 6.0 yield the smallest mean reductions in EXD (ΔEXDs of -5.2 and -1.4) across the city sample until the future. A small mean ΔMMT of 4.3 (and a moderate future mean MMT of 30.8 °C) across the cities is produced by RCP2.6/SSP1. This scenario combination relying on sustainable growth exhibits the second highest increment in socio-economic development until 2100. It yields a relatively large mean reduction of -16.6 ΔEXD until the future decade and equals ΔEXD in RCP6.0/SSP5.

We observe that with an increasing forcing, except for SSP5 combinations, the mean ΔMMT, but also the mean ΔEXD become larger across the city sample. The mean ΔMAG behaves likewise. It ranges between -0.2 °C in RCP2.6/SSP1 and +0.2 °C in RCP8.5/SSP5 (Appendix C.2, Figure C.1). Even though increasing forcing levels achieve higher adaptation and larger adaptation rates until 2100, they amplify heat exposure frequency and magnitude.

SSP5 combinations, excluding that with RCP8.5, show high socio-economic levels across the cities and perform well concerning exposure reductions and high future MMTs. Hence, a large projected GDP/capita is an advantageous precondition for high adaptation. For our city sample, SSP5 generates the highest future mean country-based GDP/capita (Int$ 101 205) compared to the beginning of the century (Int$ 9 849). The 2100 GDP/capita related to SSP1 is less, but still comparatively high (Int$ 63 346). This suggests a high GDP/capita does not automatically lead to a better bearable situation regarding future heat and its related mortality for urban populations. In the following, we contrast two scenario combinations that generate the most optimistic socio-economy and thus enable highest adaptation gains (SSP5 and SSP1) but that are contrary in future exposure (RCP8.5/SSP5 and RCP2.6/SSP1).

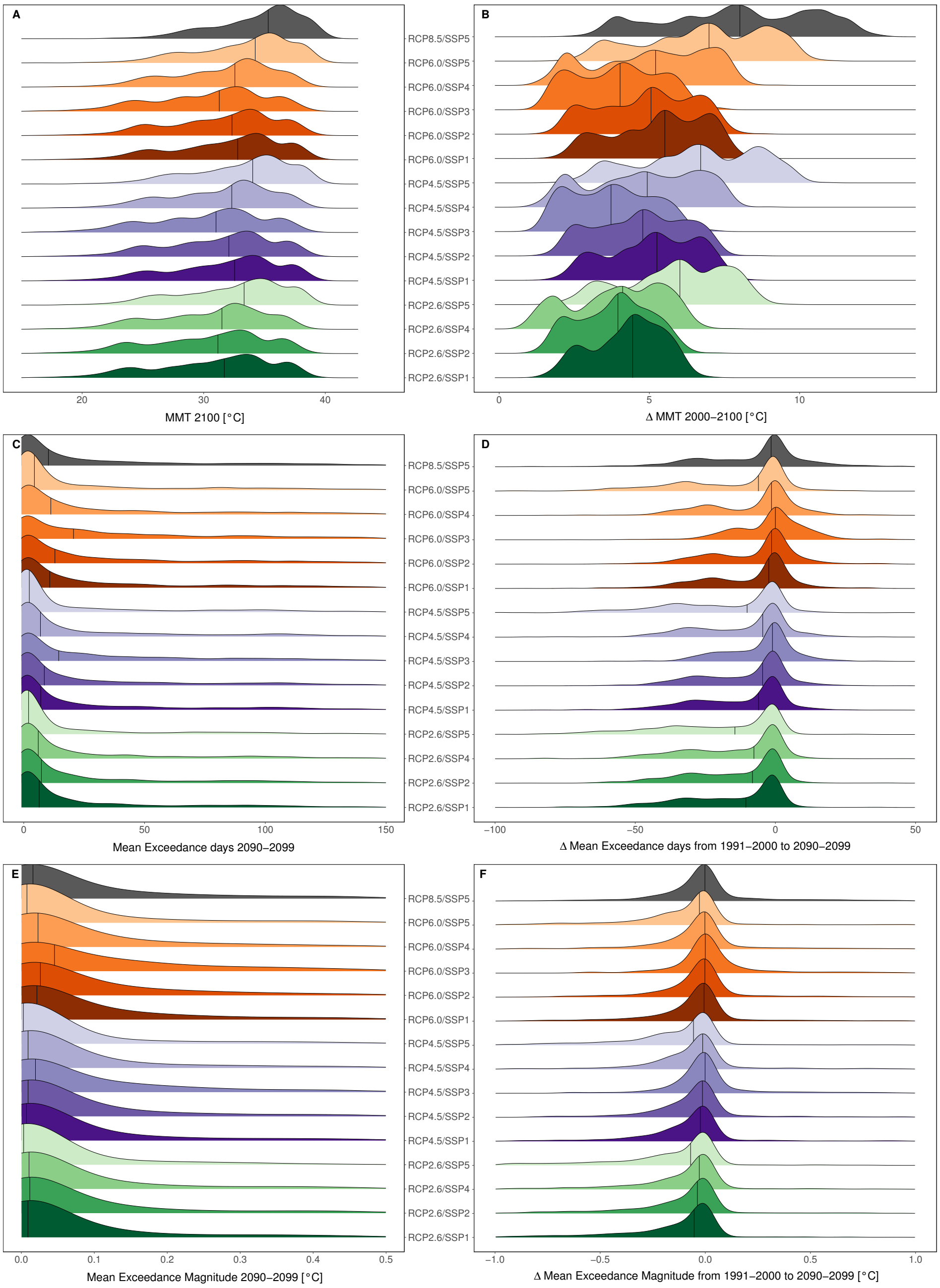

Fig. 5.1.: **Distributions of studied adaptation and exposure parameters for the RCP/SSP combinations.** Absolute MMT for 2100 (A), 2090–2099 exceedance days EXD (C), 2090–2099 exceedance magnitude MAG (E). Parameter changes are ΔMMT 2000–2100 (B), and exposure from 1991–2000 to 2090–2099: ΔEXD (D), ΔMAG (F). Vertical lines indicate the distributions' medians. Distributions c–f were trimmed.

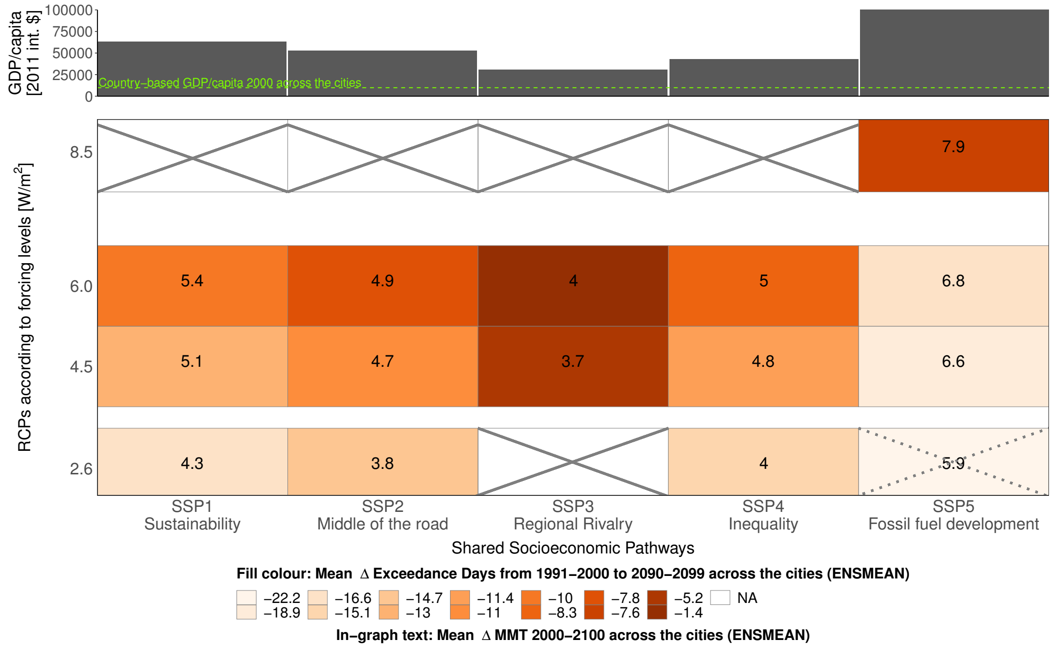

Fig. 5.2.: **Systematic overview of the change in adaptation and exposure for the city sample according to each RCP/SSP combination and the future socio-economic level per SSP.** Lower panel: The 1991–2000 to 2090–2099 ΔEXD (orange boxes) in context of ΔMMT (in-graph text annotations) for all possible RCP/SSP combinations. RCP2.6/SSP5 seems implausible (Riahi et al., 2017). Parameters of all scenario combinations are presented in Appendix C.1, Table S2. Upper panel: Unique country-based GDP/capita per SSP in 2100 (mean from IIASA and OECD data). Green line in upper panel denotes the country-based GDP/capita as of 2000 [in 2011 int.$].

5.2.3 Drivers of changes in adaptation 2000–2100

An analysis of adaptation change for the scenario combinations RCP2.6/SSP1 and RCP8.5/SSP5, unveils regionally distinct change pattern of ΔMMT (Figs. 5.3 A and 5.4 A). Cities in the northern hemisphere, especially in western Europe, show a larger ΔMMT than subtropical and tropical cities or cities in the southern hemisphere, except Oceania. Evidence from the top and the bottom of the ΔMMT distributions confirm these findings: Under RCP2.6/SSP1, highest ΔMMTs are 7.2 °C in Ostrava and Brno (Czech Republic), 7.1 °C in Olomouc (Czech Republic), 7.0 °C in Prague and Plzen (Czech Republic) and 6.9 °C in Râmnicu Vâlcea (Romania). Lowest ΔMMTs range between 1 °C (Nouakchott, Mauritania) and 1.5 °C (Umm Durman, Sudan) covering futher cities in Sudan and Chad. In a RCP8.5/SSP5 future, the highest adaptation gain is a ΔMMT of 13 °C in Râmnicu Vâlcea (Romania), followed by Ostrava (Czech Republic, 12.9 °C), Piatra Neamt and Olomouc (Romania and Czech Republic, 12.8 °C), and Kislovodsk and Uhta (Russia, 12.7 °C). The smallest gains in MMT range between 1.8 °C (Nouakchott, Mauritania) and 2.5 °C (Umm Durman, Sudan) and cover further cities in Sudan and Chad.

To shed light on the principal drivers behind ΔMMT across cities around the globe, we calculated the changes in each variable (climate variables and GDP/capita) until 2100 and their respective isolated effects on ΔMMT. The greatest weighted variable change was identified for each city and compared to the aggregated weight of the remaining variables' changes. The resulting primary contributors to ΔMMT, either a single variable's influence or the sum of two, are illustrated in Fig. 5.3 B for RCP2.6/SSP1 and Fig. 5.4 B for RCP8.5/SSP5. In the former case, large changes in adaptation are solely driven by high gains in GDP/capita cities in Western Europe, North America, East Asia, Oceania and coastal South America (Fig. 5.3 B). The change in climate as a primary driver leads to moderate increments in ΔMMT in Eastern European cities. Depending on the increment in variable change, this can also result in low ΔMMT, as in cities in Northern Africa, the Middle East and coastal Nigeria. This concerns cities in the Sahel, the Arabian Peninsula, and Pakistan and India, where climate-driven ΔMMTs range between 0 °C and 2 °C. Thus, the adaptation gain is lowest and slowest until 2100.

RCP8.5/SSP5 portrays higher increments in ΔMMT than RCP2.6/SSP1, while the regional distribution of change pattern roughly remains similar (Figs. 5.3 A and 5.4 A). However, completely different variable effects dominate ΔMMT in RCP8.5/SSP5 (Fig. 5.4 B). The extensive effect of GDP/capita on high ΔMMTs is either masked by an even larger climate influence or conjoined by the climate effect. Few cities in northwestern Europe, in China and in the southernmost latitudes remain whose large ΔMMT is uniquely defined by socio-economic gains until 2100. In RCP8.5/SSP5 the changes in climate variables until 2100 act as primary contributors to ΔMMT. Highest ΔMMTs across Europe are driven by the 30-year mean temperature in the east and additionally by the 30-year mean amplitude in southern Europe. In RCP8.5/SSP5, the 30-year mean temperature dominates the ΔMMT in a larger share of cities. Across African cities, Tmean30 is associated with rather low ΔMMTs.

Especially in a fossil-fuel-based future with rapid socio-economic growth as in RCP8.5/SSP5, the adaptation to heat will largely be driven by a strong physiological acclimatisation until 2100 and outweigh the already strong effect of economic growth. In a sustainable prosperous future, the gain in wealth until 2100 is the primary contributor to achieve heat adaptation.

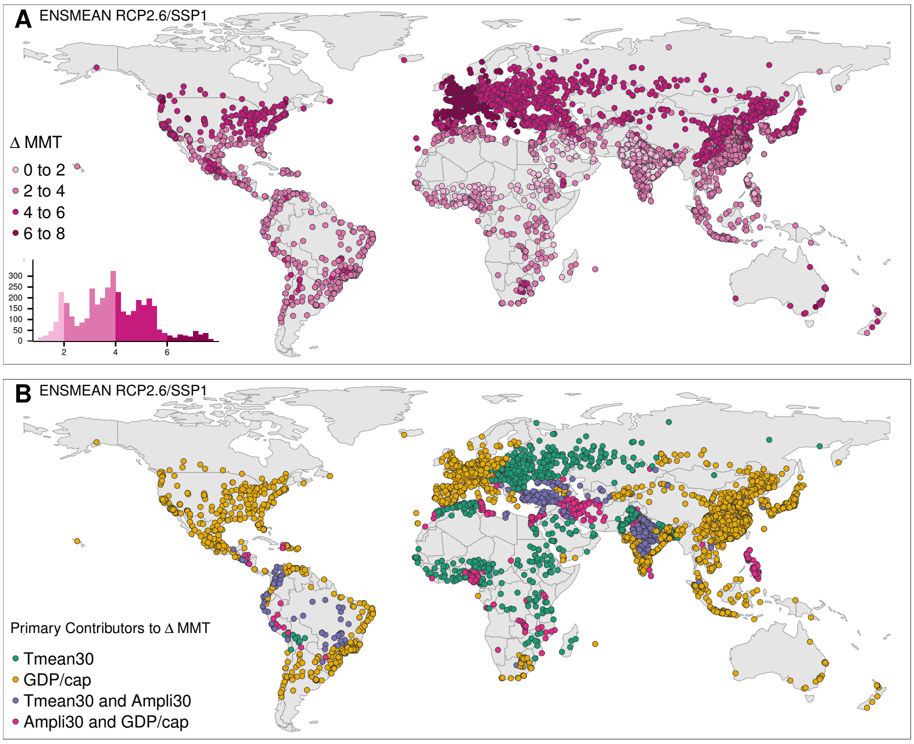

Fig. 5.3.: **Changes in adaptation until 2100 and their primary contributors to ΔMMT in a RCP2.6/SSP1 future.** ΔMMT 2000–2100 for RCP2.6/SSP1 for major world cities (A). Contributions of the single variables' 2000–2100 changes to ΔMMT 2000–2100 for RCP2.6/SSP1 (B).

5.2.4 Changes in exposure

Comparing the two highlighted scenario combinations regarding changes in exposure parameters until 2090–2099 across the cities reveals distinguished characteristics for ΔEXD and ΔMAG. In RCP2.6/SSP1, EXD reductions until 2090–2099 are largest with -140 EXD in the Chilean city Antofagasta, in Mossoró (Brazil, ΔEXD -128), Coquimbo and La Serena (Chile) with ΔEXD of -98 EXD. The maximum increase in EXD is projected for Jhang Maghiana (Pakistan, ΔEXD +40). Further Pakistani cities follow (Gojra ΔEXD +38, Faisalabad and Jaranwala, Sahiwal, and Okara ΔEXD +37). RCP8.5/SSP5 yields more extreme EXD changes than the sustainable scenario. Still, its mean ΔEXD across the cities remain twice as high (Figs. 5.1 D), and 5.2). The largest ΔEXDs reductions are -185 EXD in Antofagasta (Chile), -149 EXD in Coquimbo and La Serena (Chile). Mossoró (Brasil), Copiapó (Chile), Downey (USA) follow with -116, -109 and -104 EXD. The maximum EXD increase for this scenario is a ΔEXD of +92 EXD in Ciudad Obregón (Mexico), which exceeds the maximum increase in RCP2.6/SSP1 by factor 2.3. Further Pakistani cities rank high in ΔEXD: Faisalabad and Jaranwala (ΔEXD +86), Sahiwal, Okara and Bahawalnagar (ΔEXD +82).

The global perspective on ΔEXD shows prominent differences between the two highlighted scenario combinations in southern European, North American, Subsaharan, Indian, and East Asian cities, (Fig. 5.5). Here, in RCP2.6/SSP1, the negative ΔEXDs cause reduced future EXD (-50 – 0 EXD) (Fig. 5.5 A). In RCP8.5/SSP5, the positive ΔEXDs will yield additional EXDs (0 – 50 EXD) in those cities until 2090–2099 (Fig. 5.5 B). Large scenario disparities are obvious in cities in northwestern Mexico, Brazil, Pakistan, and India. In a fossil-fuel dependent

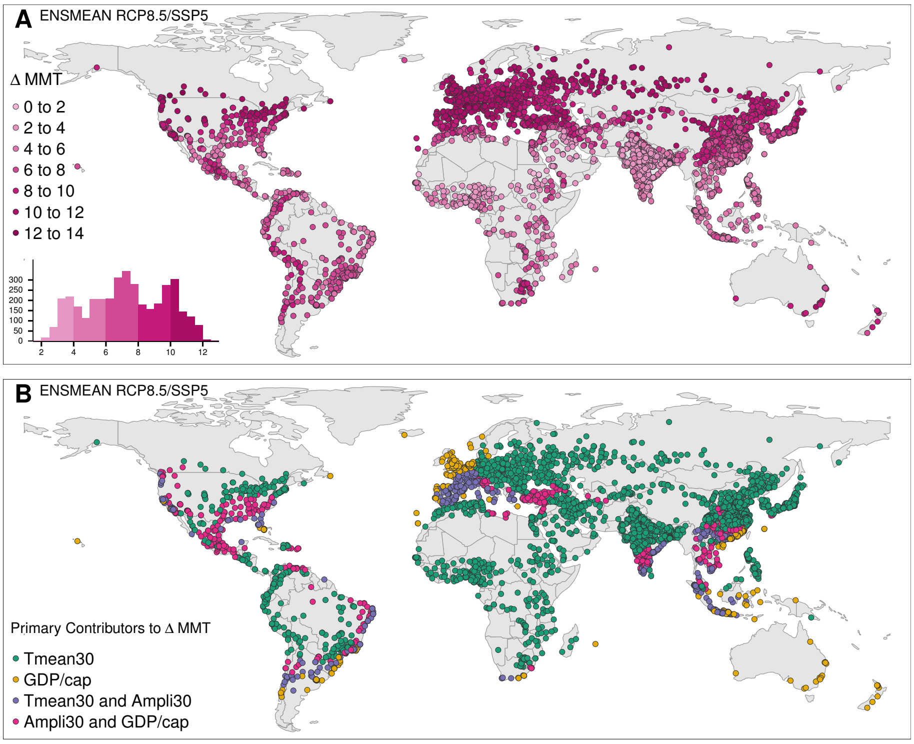

Fig. 5.4.: **Changes in adaptation until 2100 and their primary contributors to ΔMMT in a RCP8.5/SSP5 future.** ΔMMT 2000–2100 for RCP8.5/SSP5 for major world cities (A). Contributions of the single variables' 2000–2100 changes to ΔMMT 2000–2100 for RCP8.5/SSP5 (B).

future, these cities will have to cope with 50 to 92 additional EXD until 2090–2099. In RCP2.6/SSP1 ΔEXD will be less in and even bring EXD reductions in some of these cities (-50 – 0 EXD).

In terms of ΔMAG in the sustainable scenario, the largest MAG decreases concern Copiapó (Chile) with a ΔMAG of -3.5 °C, Dunhuang (China, ΔMAG -3.2 °C), Coquimbo and La Serena (Chile, ΔMAG -3° C), Geermu (China, ΔMAG -2.9 °C). The maximum increments in ΔMAG are expected in Pakistan (Fig. 5.6 A): Chishtian Mandi (ΔMAG +1.9 °C), Sahiwal, Okara, Bahawalnagar and Kamalia (ΔMAG +1.8 °C), and Gojra (ΔMAG +1.7 °C). Some of these cities overlap with highest ranks in ΔEXD. Generally, for RCP2.6/SSP1 we record a ΔMAG between -2 °C and 0 °C for most cities. Some cities in the subtropics and tropics display a positive ΔMAG between 0 °C and 2 °C until the future decade (Fig. 5.6 A). MAG reductions in RCP8.5/SSP5 are more extreme compared to the sustainable future. The mean of the RCP8.5/SSP5 ΔMAG across the cities is still higher and positive (Appendix C.2, Figure C.1). Maximum MAG reductions are projected in Copiapó and Antofagasta (Chile, ΔMAG -4.4 °C and -3.9 °C, Geermu (China, ΔMAG -3.8 °C), Coquimbo and La Serena (Chile, ΔMAG -3.5 °C) and Dunhuang (China, ΔMAG -3.2 °C). Maximum ΔMAG increments are observed in Bechar (Algeria, ΔMAG +5.4 °C), Karbala, al-Fallujah (Iraq) and Zambol (Iran) (ΔMAG +5 °C), ar-Ramadi and as-Samawah (Iraq, ΔMAG +4.8 °C). RCP8.5/SSP5 conveys an intensified situation concerning the extremes, while ΔMAG is still small in many cities (Fig. 5.6 B). Mainly cities in the Sahel, the Middle East into Pakistan and India, in northern and southern Africa, in the Southwestern USA and in northern Mexico show high increments in ΔMAG (+2 °C to +6 °C) until 2090-2099. Some severely exposed cities would profit from MAG reductions in RCP2.6/SSP1 instead (Figs. 5.6 A and B).

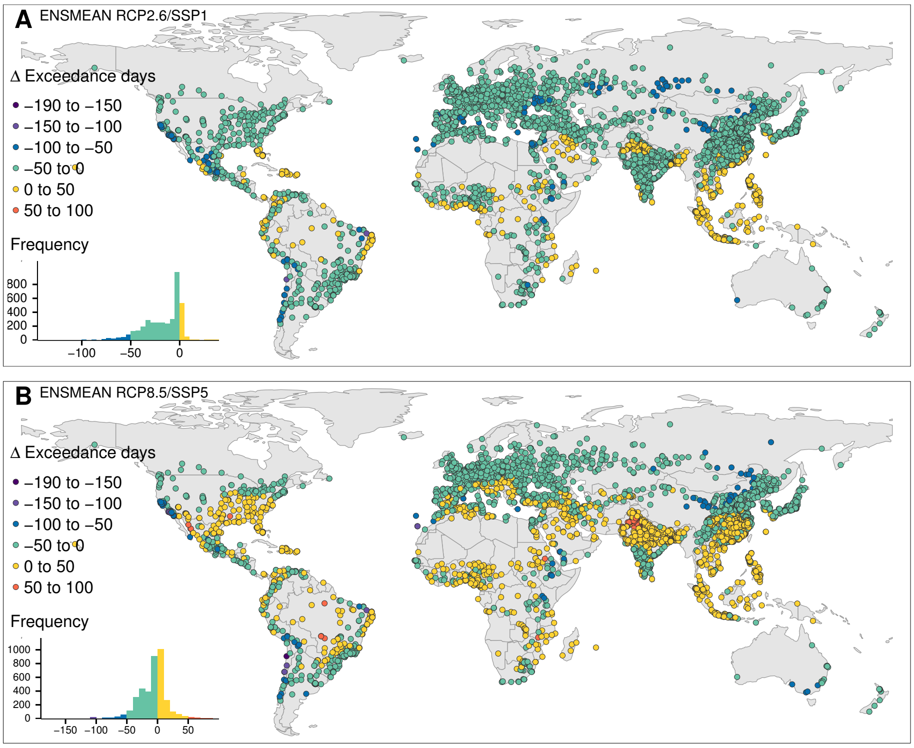

Fig. 5.5.: **Changes in future heat exposure frequency in major cities worldwide until 2100.** ΔEXD 1991–2000 to 2090–2099 in case of RCP2.6/SSP1 (A) and in case of RCP8.5/SSP5 (B).

Further evidence sharpens the disparity in future exposure concerning the selected scenario combinations (Table 5.1). In a RCP8.5/SSP5 future, a total of 2 285 (60%) cities in our sample will profit from an EXD reduction and 1 968 (51%) from a MAG reduction. Still, 1 150 (30%) cities will experience additional EXD and 1 459 (38%) a larger MAG. No EXD or MAG changes will concern 385 (10%) and 393 (10%) cities cities. In our sample, 705 (18%) cities will face more than one fourth of the year being EXD and 185 (5%) cities half the year being EXD. For five cities we project almost the entire year to be EXD (>350 EXD) considering such future. RCP2.6/SSP1 in contrast is associated with less cities experiencing aggravated exposure changes until 2090–2099. Only 224 (6%) cities will face additional EXD and 338 (9%) a higher MAG. The majority of cities in 2090–2099 will profit from less EXD (3 207 cities, 84%) and from a lower MAG (3 074 cities, 80%). No changes in EXD or MAG will affect 389 (10%) and 408 (11%) cities. These findings imply that a lower forcing yields a larger reducing effect on the heat exposure parameters for more cities due to a milder climate change. This suggests, in an ideal future without climate change but high wealth-driven adaptation, exposure measures would be minimised and a massive reduction in mortality could be expected. Against this ideal future, RCP2.6/SSP1 constitutes a slight impairment leading to a higher mortality. RCP8.5/SSP5 signifies a substantial worsening of prospects because positive wealth effects on adaptation are likely annihilated.

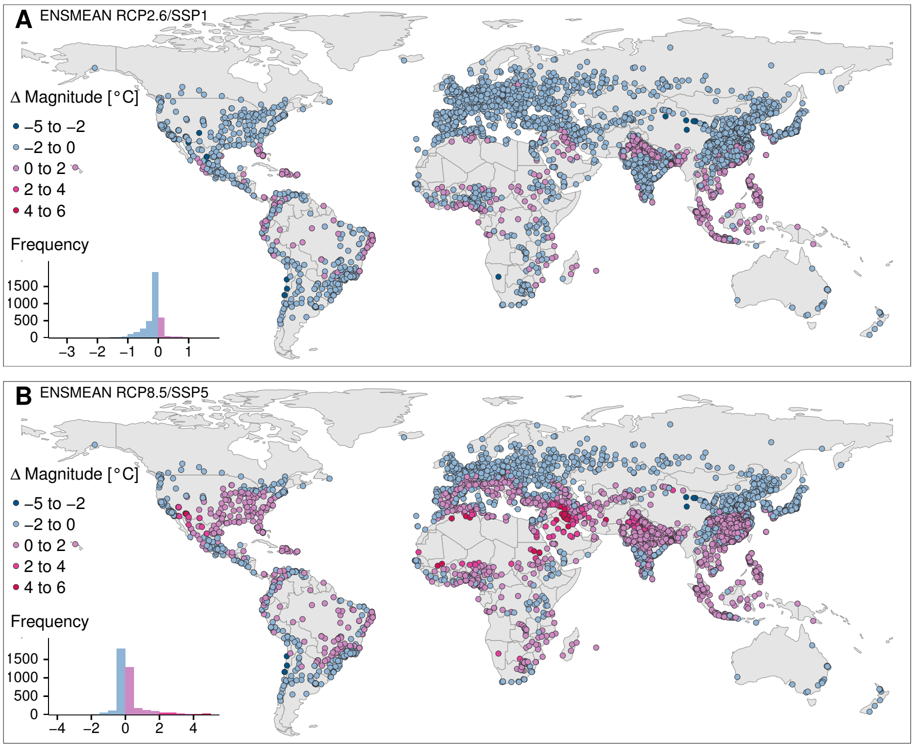

Fig. 5.6.: **Changes in future heat exposure magnitude in major cities worldwide until 2100.** ΔMAG 1991–2000 to 2090–2099 in case of RCP2.6/SSP1 (A) and in case of RCP8.5/SSP5 (B).

Tab. 5.1.: **Number and share of cities affected by changes in exposure from 1991–2000 to 2090–2099.** Exposure outcomes by indicator across the 3 820 world cities comparing RCP2.6/SSP1 and RCP8.5/SSP5

Indicator	**RCP2.6/SSP1**		**RCP8.5/SSP5**	
	No. of cities	**Percent (%)**	**No. of cities**	**Percent (%)**
Days reduction in EXD	3207	84	2285	59.8
Days increase in EXD	224	5.9	1150	30.1
No change in EXD	389	10.2	385	10.1
>25% of the year EXD	527	13.8	705	18.5
>50% of the year EXD	146	3.8	185	4.8
>350 EXD	0	0	5	0.1
Reduction in MAG [°C]	3074	80.5	1968	51.5
Increase in MAG [°C]	338	8.8	1459	38.2
No change in MAG	408	10.7	393	10.3

5.2.5 Adaptation and heat exposure in context

It is indispensable to view adaptation and exposure jointly. We aggregated the adaptation and exposure parameters across our sample of 3 820 cities and provide their outcomes (P05, P95, Mean, Min and Max) in Appendix C.1, Table S2. By 2100, a higher adaptation can be achieved by RCP8.5/SSP5 compared to RCP2.6/SSP1 because the ΔMMT increment is greater. This also requires a faster adaptation rate until 2100. However, a future according to RCP2.6/SSP1 is able to minimise heat exposure for our city sample in contrast to RCP8.5/SSP5. In both scenarios ΔEXD and ΔMAG values mostly correlate, as in cities in the Middle East, Pakistan and in parts of the USA and northern Mexico. High increases in heat exposure also coincide with small ΔMMTs in these regions (Fig. 5.7). Such circumstances are obvious in Asian cities at the tip of the distribution in RCP2.6/SSP1, and in Asian and African cities in RCP8.5/SSP5 (Fig. 5.7). This suggests these cities might be prone to increases in mortality until 2100.

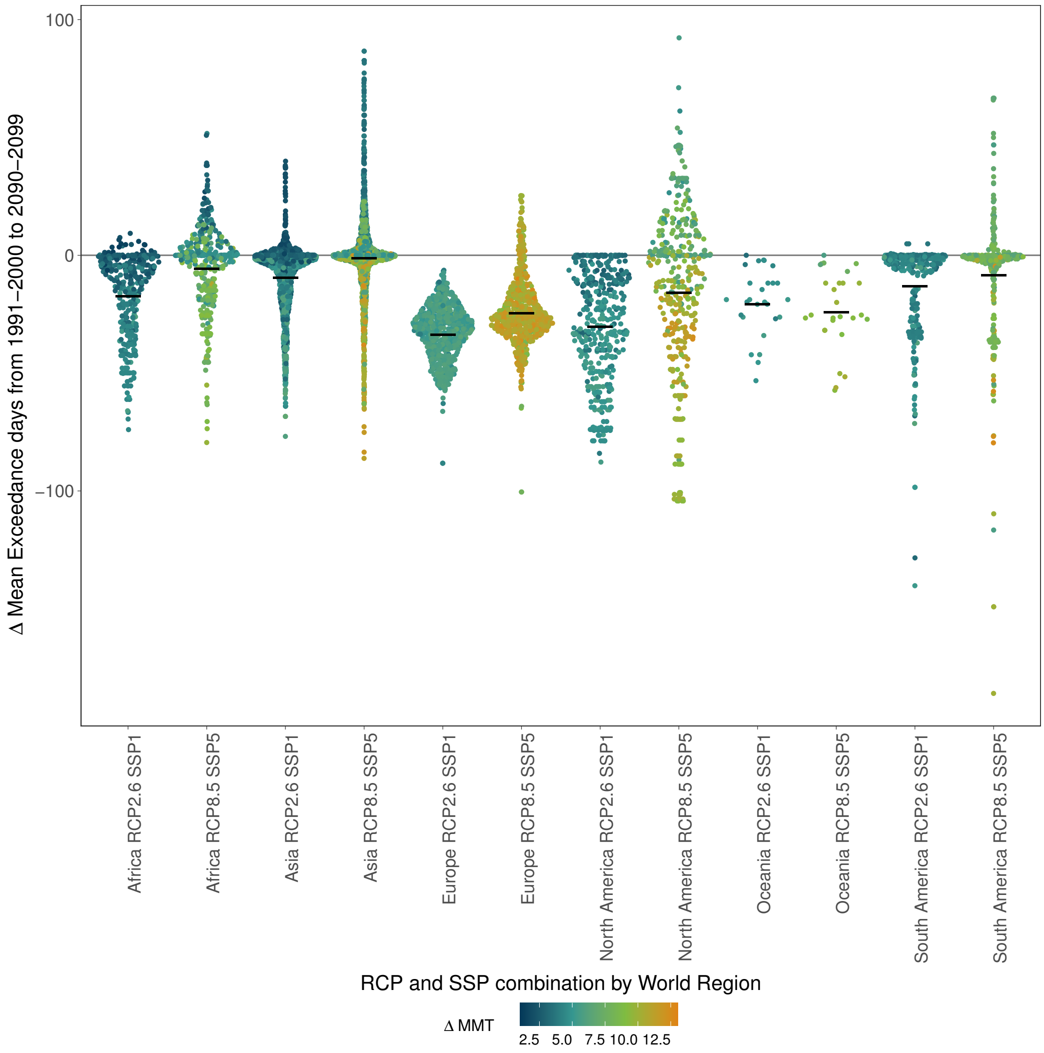

Fig. 5.7.: **Regional disparities in ΔMMT 2100–2000 and ΔEXD 1991–2000 to 2090–2099 for the selected scenario combinations RCP2.6 paired with SSP1 and RCP8.5 paired with SSP5.** Midbar indicates the mean of the ΔEXD distribution across the sample cities.

5.3 Discussion

For the first time, future adaptation and heat exposure for 3 820 cities worldwide have been assessed jointly. For the full spectrum of possible future climate trajectories (RCPs 2.6, 4.5, 6.0 and 8.5) and socio-economic pathways (SSPs 1-5) this analysis envisages potential adaptation and exposure changes until 2100. Considering that all options constitute an impairment against an ideal future assuming no climate change and thus only minimal exposure, we aimed to identify the least unfavourable choice for human health outcomes. We contrasted two options of highest socio-economic development facilitating wealth-enabled adaptation but diverging heat exposures: (1) The minimum forcing RCP2.6 reduces heat exposure in the majority of cities until the future decade (2090–2099) while a stable and sustainable socio-economic pathway SSP1 will equip most world cities with a moderately high adaptation. (2) A rapid socio-economic growth based on fossil fuels along with high forcing (RCP8.5/SSP5) will reach higher adaptation levels in 2100 for most cities against a sustainable future. Though, fewer cities will profit from decreases in heat exposure. In a RCP8.5/SSP5 future, 5.1 times as many cities will face more frequent heat exposures and 4.3 times as many will experience higher exposure magnitudes than in RCP2.6/SSP1. The high socio-economic level driven by fossil-fuel exploitation can only partly compensate for its own negative consequences for human health, especially as adaptation changes are rather climate-induced than by economic growth. A future according to RCP8.5/SSP5 would critically endanger cities in arid and semi-arid climates, i.e. cities in the southwestern USA, northern Mexico, in Brazil, in the Sahel, across the Arabian Peninsula and the Middle East, in Pakistan and India. All exhibit small gains in adaptation while heat exposures are projected to increase. Likely, this will raise heat-related mortality in those cities at the end of the century compared to its beginning. Even if heat exposure cannot be minimised as in a world without climate change, RCP2.6/SSP1, in contrast to RCP8.5/SSP5, has proven to be beneficial for urban populations' health. Its associated exposure decline until 2100 will outperform that in RCP8.5/SSP5. RCP2.6/SSP1 reaches moderate adaption levels without the expense of amplifying climate change. We conclude that socio-economic growth only contributes to future heat adaptation as long as it is generated sustainably.

The approach presented here takes stock of urban populations' adaptation and exposure to heat in 3 820 cities across the globe for the full spectrum of climate trajectories and socio-economic pathways. Recent approaches have either selectively established heat-mortality relationships for only few RCPs, falling short to provide a general overview, or they present the full RCP bandwidth (Gasparrini et al., 2017; Guo et al., 2018). They usually do not consider future socio-economic developments (Gasparrini et al., 2017). We demonstrated the necessity to integrate a socio-economic aspect to assess future adaptation. We found urban populations' heat adaptation is not purely climate-driven. Locally-extended SSPs were employed jointly with RCPs by a single study to estimate future summer excess mortality in Greater Houston (USA) (Rohat et al., 2019). They confirm other influences related to socio-economy.

So far, mostly single regions have been studied concerning habitability or heat burden. One global study considers humid heat, concluding that subtropical coastal areas are at risk (Raymond et al., 2020). For the Middle East, future habitability was questioned based on future temperature and humidity conditions regarding RCP8.5 (Pal and Eltahir, 2016; Raymond et al., 2020). Besides Middle Eastern cities, we identified further cities in warm arid and semi-arid regions to be prone to increased future heat exposure and low adaptation gains according to RCP8.5/SSP5. Following a sustainable pathway avoids exposure for most cities endangered in a RCP8.5/SSP5 future. Especially western European cities, North American, Central and Eastern Asian cities would benefit from considerable and sustainable economic growth-driven adaptation gains in a RCP2.6/SSP1 future. Sustainable and stable economic growth contributes to adaptation and maintains low forcing. Even though tropical and subtropical cities show relatively small and climate-driven increments in adaptation change until 2100, they profit from small exposure changes in a sustainable scenario. Additionally, their populations are acclimatised to high temperatures today. A strong socio-economic development based on fossil-fuel exploitation as in RCP8.5/SSP5 does not principally drive adaptation but amplifies extreme heat exposures in a larger number of cities, that would not be impacted as severely in a sustainable future.

It is common to investigate solely heat exposure in form of exposure days above a certain temperature threshold, e.g. high-risk days associated with mortality (Christidis et al., 2019). Such information is not quite sufficient to identify endangered locations for two reasons: First, adaptation is not accounted for, and second, because metrics describing adaptation and exposure changes matter rather than absolute values. Thus, our contextual assessment of future adaptation and exposure and most essentially, their changes until the end of the century is a novelty. We deliver a critical unknown required to determine the future HMR: ΔMMT is the denominator in the fraction to calculate the slope of the future HMR, which was up to date matter to uncertainty (Ballester et al., 2011; Gosling et al., 2017). Having shed light on this previously unknown delta value is a major achievement of our work.

The knowledge of the changes in heat exposure frequency and the exposure magnitude for a location leads us to conclude that a functional relationship between these parameters can be interpreted as a proxy for the change in heat-related mortality for this location. We propose a simple functional relation as a proxy for change in future heat-related mortality: $\Delta\text{MORT} = f(\Delta\text{EXD}, \Delta\text{MAG})$. ΔMORT is another critical metric still missing to derive the future HMR's slope. Given the present mortality of a location and assuming no changes in demography and health status, the change in mortality until 2100 can be roughly approached through the here introduced functional relationship between the changes in exposure parameters. Approaching the future HMR through a linear method, ΔMORT fills in the numerator of the slope fraction of the future HMR, which can now be solved: $m = \Delta\text{MMT}/\Delta\text{MORT}$. We encourage further research on this idea. Previous studies tried to circumvent the slope-related uncertainty in mortality changes by simply continuing past mortality pattern, which grounds on many assumptions (Gasparrini et al., 2017).

Our study has some limitations. Since to our knowledge there is no definite evidence about the time adaptation requires, we carry out our analysis under the premise that adaptation to heat, especially the wealth-enabled share, is instantaneous. We attempt to account for a lag in physiological acclimatisation by using mean climate variables over a 30-year period ending in 2094. Accordingly, our results denote a lower boundary of a wide adaptation margin. We assume no changes in health condition and heat-related mortality among the city populations until 2100. Further, the SSPs rely on assumptions and could be source of uncertainty in our projections. Still, the SSPs originate from an established framework developed to analyse different climate and socio-economic futures. We focused on ensemble means instead of scrutinising the influence of GCMs on our results. We are confident to present this information as an inter-model comparison in the future.

Urban populations will be able to adapt to increasing temperatures majorly in two ways. Either by a high socio-economic standard in a future related to sustainable economic growth. Or unfavourably, being forced to acclimatise to elevated heat exposure driven by high forcing which likely results in increased heat-related mortality in cities. We demonstrate the indispensability to appraise heat adaptation and exposure jointly to give recommendations for the public and decision-makers. We conclude that it is most beneficial to strive for a sustainable but prosperous future, which is compatible with the 2 °C limit, as for instance the scenario variant RCP2.6/SSP1 to avoid additional future heat exposure. The majority of the world's city population will profit from such choice. National health systems, particularly in poorer regions will not be as challenged as in less sustainable high-forcing futures.

Methods

5.3.1 Climate Data

Historical modelled data. Historical climate data from the Coupled Model Intercomparison Project 5 (CMIP5) experiments (Taylor et al., 2012) were available from the Inter-Sectoral Impact Model Intercomparison Project (ISIMIP) (*The Inter-Sectoral Impact Model Intercomparison Project (ISIMIP)* 2019) for four General Circulation Models (GCMs): GFDL_ESM2M, HadGEM2_ES, IPSL_CM5A-LR, and MIROC5. The gridded data were obtained with spatial resolution of 0.5°x 0.5°and the ensemble mean (ENSMEAN) across the four GCMs was calculated. **Climate projections.** Climate projections for four greenhouse gas concentration trajectories, the Representative Concentration Pathways (RCPS 2.6, 4.5, 6.0, and 8.5) were available from the same source as the historical modelled data. Data representing each RCP had been generated from four GCMs: GFDL_ESM2M, HadGEM2_ES, IPSL_CM5A-LR, and MIROC5. We calculated the ENSMEAN across the GCMs. The climate projections from 2006 to 2099 were provided as gridded data with a spatial resolution of 0.5°x 0.5°. **Climate variables.** We used the daily mean temperature (tas) of each GCM for all four RCPs to derive the required input climate variables for each city. The 30-year mean of the daily temperature and the annual amplitude were calculated for the past period 1965–1995 as input variables to estimate MMTs for 2000. The two climate variables were calculated for the future period 2064–2094 as input variables to estimate MMTs for 2099. The latter variable was calculated from the average of each annual amplitude between the warmest and the coldest monthly mean temperature for each year within the 30-year period. The daily mean apparent temperature (AT) was derived for 2000 and for the climate prediction year 2099. This enables to assess the frequency of days which show a daily ATmean exceeding the MMT in each city, and to measure the magnitude of the MMT exceedance. We use the climate parameters daily mean temperature (tas) and the daily mean humidity (hurs) to generate the daily mean dew point temperatures (tdewp) for the prediction years 2000, and 2099 as well as for ten consecutive years in 2090–2099 employing equation (5.1) (Lawrence, 2005). We proceed likewise with ten consecutive years in 1991–2000.

$$TD = B_l[ln(RH/100) + (A_l * T)/(B_l + T)]/A_l - ln(RH/100) - (A_l * T)/(B_l + T) \quad (5.1)$$

where A_l =7.625 and B_l =243.04°C

We subsequently use tas and the newly derived tdewp to calculate the daily ATmean according to the equation (5.2) by Michelozzi (2007) (Michelozzi et al., 2007)

$$AT = -2.653 - (0.994 * T) + (0.0153 * TD) \tag{5.2}$$

where T is the daily mean temperature and TD is the daily mean dew point temperature. We correct the AT for temperatures above 34 °C for wind speed using the climate variable daily mean wind speed (sfcWind) (Steadman, 1984).

5.3.2 Socio-economic data

Historical GDP/capita (2011 int. Dollars). This data was given in purchasing power parity (PPP) (The World Bank, 2017a) at country level and the data on improved urban water sources (% population with access) (The World Bank, 2017d) were obtained from the World Bank Open Database. We used the data for the year 2000. Projections for the GDP/capita (2005 int. Dollars, in PPP). Data was available at the country level representing five distinct Socio-economic Pathways (SSPs 1 to 5) from two modelling groups, IIASA (Crespo Cuaresma, 2017) and OECD (Dellink et al., 2017). The data for each SSP was adjusted to the historical GDP/capita (given in 2011 int. Dollar) using the common base year 2015 available in both, historic and projected data. Dividing the SSP data by the quotient of the SSP data and the historic data, as an adjustment factor, levelled the projected GDP/capita to the 2011 int. Dollar. We use the 2100 mean of the two SSP datasets to estimate the MMT in 2100.

5.3.3 Topographic data

Elevation data was obtained from a SRTM 90m DEM (Jarvis et al., 2008) at a spatial resolution of 0.25°x 0.25°. This data was aggregated to match the resolution of the climate data at 0.5°x 0.5°.

5.3.4 City coordinates

City coordinates were available from the from the Global Rural-Urban Mapping Project (GRUMP) Settlement Points (Center for International Earth Science Information Network (CIESIN) at Columbia University et al., 2008) from the Center or International Earth Science Information Network (CIESIN).

5.3.5 Model calibration

The methodology to estimate the future MMT grounds on our previously established generalised multivariate non-linear model to approximate the MMT for cities published in Krummenauer et al., 2019. Our approach estimates the MMT for cities independently from daily mortality records on the basis of a set of city-specific climatic, topographic and socio-economic variables (Krummenauer et al., 2019). This allows for spatially and temporally flexible model application. Details on the previous model, how it was established in our previous study as well as on its advantages and limitations are provided in Appendix C.3. The model to determine MMTs established in our previous study (Krummenauer et al., 2019) was adjusted for the use with the gridded historic and projected climate data from the ISIMIP project. For model calibration, we use the ENSMEAN historic 30-year mean of the daily temperature and the ENSMEAN 30-year mean of the annual amplitude calculated from the historic gridded data for the reference periods in accordance with the original work listed in the previous study (Krummenauer et al., 2019). The socio-economic variables for the year 2000 and the topography remained the same as in the previous study. The final selection of independent variables used in this paper, the treatment of co-linearity and the significance testing is discussed at lengths in Krummenauer et al., 2019. A total of 13 independent variables reflecting the topography (e.g., distance to coast, latitude) and socio-economy (e.g., health expenditure, share of population above 65) were originally tested in their ability in reproducing the observed MMT of the city. The same 400 cities across all climate zones and world regions were used for model calibration as in Krummenauer et al., 2019. We used a non-linear-least-squares fit to re-calibrate the model. The newly derived coefficients were then employed for MMT estimation in the historic and the future periods. We found that the re-calibrated model using gridded climate data preserves the relative importance of all independent variables as in Krummenauer et al., 2019 (Appendix C.3, Table C.1). The RMSE of the re-calibrated model ranked at 3.2°C while the RMSE of the original model was 2.8°C, this indicates only a minor penalty of using coarser gridded climate data.

5.3.6 Estimation of future minimum mortality temperatures

First, the newly calibrated model and the new coefficients were used to estimate the MMTs for the historic situation in 2000, employing the computed ENSMEAN long-term climate variables for 1965–1995 for each RCP, the socio-economic variables for 2000 and the topography. Second, the MMTs for the future situation in 2100 were estimated employing the computed ENSMEAN long-term climate variables for each RCP for 2065–2095, and the future socio-economic variable GDP/capita projecting the situation at the end of the century as in each SSP. The variable access to water and the topography remained constant. The future MMT estimation was carried out for each of the 15 feasible RCP and SSP combinations according to the Scenario Matrix (Vuuren et al., 2014; Riahi et al., 2017). This excludes the combination RCP 2.6. with SSP3 and RCP 8.5 may only be paired with SSP5. The feasibility of combination RCP2.6 and SSP5 is questionable in a real world (Riahi et al., 2017) and thus is rather neglected in our study. The MMTs are valid for the years around the prediction years 2000 and 2100 since long-term physiological acclimatisation is accounted for by employing long-term climate variables. Adaptation likely does not change significantly from one year to another. We determine the delta change in MMTs (ΔMMT) between the end and the beginning of the century for each city. We carry out this delta MMT calculation on the basis of the historic MMTs for the cities and the 15 sets of projected MMTs for the cities, each for one of the RCP/SSP combinations. Subsequently, we derive the mean MMT and the mean ΔMMT across the 3 820 cities for each of the RCP/SSP combinations.

5.3.7 Exposure Calculation

We use the estimated MMTs, a measure for human heat adaptation in cities, as a threshold to determine critical heat exposure that exceeds the MMTs and thus also the long-term acquired heat adaptation among the city population. We count the annual number of days that show a daily mean apparent temperature (ATmean) exceeding the MMT as adaptation measure. We do so for each year and city within the historic exposure reference period 1991–2000 and use the city-specific MMTs that are valid around the year 2000 as threshold. We calculate the mean number of exposure days (EXD) over the historic decade for each city. We repeat the procedure likewise for each year within the future exposure period 2090–2099 and each city under each of the four RCPs. For the future evaluation of EXD we employ the respective city-specific MMTs as thresholds that are valid around the year 2100. The choice of MMT sets that could be used as thresholds was determined by the RCP setting of the future decadal climate data. The RCP setting of the MMT sets (across the SSP settings) had to match that of the daily climate data within the decade. For example, four MMT sets for RCP2.6, combined with either SSP1, SSP2, SSP4 or SSP5 served one after another as threshold set. For the EXD analysis under RCP8.5, only MMTs for RCP8.5/SSP5 could be used. Subsequently, the mean number of exceedance days across the future decade is computed for each city and for each RCP/SSP combination. The EXD analysis resulted in 15 datasets, one for each RCP/SSP setting, covering 3 820 city-specific mean EXD values. We derive the delta changes in EXD (ΔEXD) for each city by subtracting the city-specific decadal mean EXD in 1991–2000 from the city-specific mean EXD in 2090–2099 under the 15 different RCP/SSP setups. This resulted in 15 different datasets, one for each RCP/SSP setup, each containing the ΔEXD for 3 820 cities. During the EXD evaluation, we record the exceedance magnitude as the difference between the MMT and the daily ATmean in each city and for each year within the historic and future decades. The annual mean exceedance magnitude (MAG) is computed for each city for the 15 RCP/SSP settings. The delta change in mean MAG (ΔMAG) for each city is derived by subtraction of the city-specific decadal mean MAG in 1991–2000 from the city-specific mean MAG in 2090–2099 under the 15 different RCP/SSP setups. Correspondingly, this resulted in 15 datasets containing the ΔMAG for 3 820 cities. Finally, we compute the RCP/SSP combination-specific mean values across the 3 830 cities for each of the four exposure parameters.

Discussion and Conclusions Contributions to a better understanding of human heat adaptation

6

6.1 General achievements and key findings

This thesis constitutes an assessment of the present and future human heat adaptation among urban populations around the globe and its evolution until the end of the 21st century considering different climate and socio-economic futures. Adaptation to heat is expressed as the Minimum Mortality Temperature (MMT). The MMT can be inferred from the lowest point on the exposure-response curve representing the Heat-mortality Relationship (HMR), a method that highly depends on robust and available daily mortality records at the city scale. Here it was aimed at providing a generalised method to derive the MMT based upon city features that are accessible for cities across the globe. Thus, in this thesis, the establishment of the urban MMT as a measure of human heat adaptation and the future projections of its changes until 2100 was achieved independently from daily mortality records or projections thereof, which makes it applicable across cities worldwide. This simple but solid method to assess heat adaptation in context of heat exposure was further developed to present the full spectrum of possible future health outcomes awaiting our society. Based on the results for 15 possible combinations of climate trajectories and socio-economic developments, it was recommended to strive for a 2 °C-compatible climate trajectory. This option performed best at gaining heat adaptation, due to a high share in sustainable wealth-driven adaptation gains, while the increase in heat exposure was kept small. Prosperous socio-economic growth based on fossil-fuels and high emissions was found to generate very high increments in adaptation gains. These gains would likely not be able to compensate high increases in heat exposure due to a high-end climate trajectory, leading to higher heat-related mortality at the end of the century. Such appraisal of human heat adaptation had not yet been accomplished so far. Heat adaptation had either often been neglected in the modelling strategies of previous global impact assessments on heat-related mortality, or it had been appraised based upon vague or deficient assumptions. Thus, this thesis contributed substantially to the understanding and the modelling of future human heat adaptation at a global urban scale by acknowledging that the HMR cannot be considered as static over time.

In this work, adaptation is captured in a multifaceted way by forging a bridge among three levels of analysis, each of which is preparatory to its following level and concretising the understanding of human heat adaptation, represented by the MMT. At the first level of analysis, it was demonstrated how data-related challenges at urban case study level impeded the measuring of the urban population’s adaptation and the extension of the existing pool of MMTs. Especially the access and robustness of daily mortality records and modified political boundaries over time concerning specific case studies were encountered and overcome. This suggested that the establishment of the urban MMT for a larger extent of cities or even major cities around the globe required a simpler and generalised method based upon easily accessible and less error-prone data. This was addressed within the subsequent second level of analysis. The MMT drivers were determined and a generalised model established to approximate the MMTs for cities around the globe, which is a *first key achievement* of this work. This novel method estimates the MMT based on simple city characteristics without requiring mortality records and builds the foundation to appraise the future evolution of heat adaptation. Further, the method unified the two components of heat adaptation, physiological acclimatisation and wealth-enabled adaptation measures but also allows to assess them separately. Building upon the previously established global model, as a third and final stage of analysis, the future urban MMT and its change until the end of the century is estimated in context with future heat adaptation and considering different climate trajectories and socio-economic pathways for nearly 4000 cities. This analysis depicts a wide range of choices for humankind concerning their future well-being in terms of future heat adaptation and exposure, which is a *second accomplishment* of this work. As this thesis appraised the evolution of heat adaptation until 2100, measured as the delta change in MMT for different climate futures, this major result informs global impact assessments on heat-related mortality on the value, by which the HMR may be 'shifted' into higher temperature regimes. This critical information had previously been lacking to define the future HMR for cities. The provision of this delta value further facilitates the derivation of the slope of the future HMR which constitutes a significant *third achievement* of this work. For this purpose, the change in exposure measures introduced here may be applied to infer the future change in mortality. Jointly, the measures of changes in adaptation and in exposure presented in this thesis allow for an initial establishment of the future HMR and constitute an advance towards a universal impact assessment on heat-related morality in cities in the future. A last and *fourth accomplishment* presented here is the possibility to separate autonomous and planned adaptation by having isolated the contributions of changes in climate and changes in socio-economy to the change in overall human heat adaptation in the model. This endeavour has never been carried out before at the global city scale. It reveals differences in adaptation drivers in cities across the globe and informs about which component of adaptation should be prioritised in the cities to strengthen overall heat adaptation.

This thesis has gotten to the very bottom of adaptation and its future development at the collective urban population level in cities around the globe. It unified health-related, geophysical and climatic features, urban characteristics as well as social and economic aspects for past or present periods as well as for the future. Therefore, this thesis may principally be attributed to global climate impact studies, geographic and social sciences, and shares overlap with the relatively new scientific field of planetary health. At the end of this unification stands the provision of spatially accurately aggregated information on adaptation in form of the MMT and its future development. This serves as tool to evaluate future adaptation and heat exposure measures in cities.

The methodology applied here ranged from a literature review via adapting the conventional way to derive the MMT to a multivariate non-linear data analysis with parameter estimation, and the calibration of the model for use with projected climate and socio-economic data. Statistical analysis was applied to compare the model outcomes and obtain threshold exceedances in frequency and intensity. Mathematical methods were applied to carry out the delta change analysis of adaptation and exposure measures. Statistical and mathematical methods were used to identify the major contributory variable driving adaptation gains in the future. The provision of two principal parameters of adaptation, the MMT and its change value across spatial and temporal scales at the global city level and their multifaceted and multi-disciplinary assessments are unique. This knowledge vitally contributes to the exploration and understanding of human heat adaptation and its interplay with heat exposure at the global city level, most essentially by providing the change in MMT. Thus, the overarching objective of this thesis, the appraisal of global heat adaptation among urban populations and its evolution under different climate futures been met.

6.1.1 The relevance of the model elaborated for future impact analysis and its usefulness beyond

The core of this thesis is the developed model to approximate the MMTs, as a measure of heat adaptation among urban populations, independently from the availability of daily mortality records across global cities. It is nourished by the knowledge gained from exploring the two components of human heat adaptation and their functioning, physiological acclimatisation, which is autonomous, and wealth-enabled adaptation, that refers to planned measures. Previous research efforts on the future HMR for single urban case studies or those at the global scale defined the MMT as a physiologic measure. The work achieved here complements such research efforts by appending the wealth-determined aspect of heat adaptation and by providing the increment by which the future MMT changes, which was chosen rather arbitrarily up to date.

Besides serving as foundation for three subsequent major achievements ((1) the appraisal of future adaptation under different futures, (2) facilitating the derivation of the future HMR's slope and (3) providing an option to separate the shares of autonomous and planned human heat adaptation), the elaborated model may be utilised for another relevant purpose: It allows the identification of those cities where populations will experience large disparities between a small gain in collective heat adaptation and high increments in heat exposure, which likely leads to increased heat-related mortality in the future. Cities in arid and semi-arid areas across the globe were classified to correspond to such critical future conditions. Such outcome and knowledge could be produced due to the joint and systematic quantification of adaptation and heat exposure for climate conditions today as well as under a multitude of climate and socio-economic futures, applying a consistent methodology. This approach constitutes a novelty in the research field on heat- or temperature-related mortality for various reasons: Particularly, because this joint assessment does not plainly rely on a city's climate parameters but also takes into account the socio-economic situation to evaluate the adaptation level. Additionally, it adds on to the findings provided by pure heat exposure assessments. It is not only the climate that is undergoing changes, but also adaptation will change and this is why an incorporation of adaptation in impact modelling is indispensable. Populations are able to acclimatise physiologically and due to increasing prosperity in societies, i.e. technological advancements, higher investments in infrastructural adaptation measures or higher investments in the health sector are possible.

Such joint analysis of the evolution of heat adaptation and exposure under different climate futures has been carried out in this thesis for an considerable amount of cities around the globe, enabling a direct comparison across cities and regions. The results presented in this thesis add value due to their topicality, generally considering the increased number of future heat events projected, greater severity and duration of these events in addition to a warming GMT. Most crucially however, the delta value of change in MMT that is independent from daily mortality records and projections as offered by this work spurs the progress of research towards a solid global impact assessment on heat-related mortality in cities. For past as well as for future climate conditions equally, the quantitative impact assessment of heat-related mortality is only carried out at the case study level and relied on vague assumptions. At the global city scale, a robust impact assessment on heat-related mortality still constitutes a methodological challenge. Nevertheless, the measures introduced here help to address this task by shading light on the future change increment in MMT, which is certainly not homogeneous in cities around the globe. Even beyond its value for scientific advancement, the work at hand and its findings deliver relevant information for the public and to support policy- and decision making, especially concerning urban development, national- and urban-scale infrastructure planning, the health sector in cities, and lastly for urban adaptation to heat and the avoidance of exposure across cities.

6.1.2 Key findings in summary

This thesis showed that the urban population's heat adaptation and its future evolution does not only depend on autonomous adaptation through physiological acclimatisation, but is also influenced by socio-economic growth. Case studies are not quite sufficient in creating a global picture on heat-related mortality and heat adaptation, since they are laborious and highly dependent on robust daily resolved mortality data. Thus, it was demonstrated that human heat adaptation can be approximated and generalised by using city-specific characteristics instead of error-prone daily mortality records that are difficult to access. This method relying on easily accessible climate, socio-economic and topographic data enables the estimation of adaptation for cities that have not yet been considered as case studies by conventional impact studies and allows a modification for application with climate projections. The analysis of future heat adaptation evidenced that the increment of change in future adaptation was heterogeneous across cities around the globe. The MMT as a measure for human heat adaptation cannot simply be 'shifted' into higher temperature regimes. Heat adaptation changes even varied across different climate futures for the same city. This is because changes in heat adaptation were driven by different model variables, depending on the combination of climate trajectory and the socio-economic pathway. Strongest contributor to moderate gains in adaptation (1 °C and 7.2 °C) in a 2 °C-compatible future was sustainable socio-economic growth. At the same time, the associated low-forcing climate trajectory showed only moderate increases in heat exposure in few cases while 80% of the cities even displayed a reduction in exposure (change in number of MMT exceedance days: -140 to +40; change in exceedance magnitude: -3.5 °C to +1.9 °C). Health outcomes in such future will likely be better manageable than in a future, where socio-economic growth is based on the exploitation of fossil fuels, which drives global warming. Even though in this unsustainable scenario, adaptation gains will be larger (between 1.8 °C and 13 °C), the resulting high-forcing climate change will decrease the share of cities tat benefit from exposure reductions to only 60%. Thus, higher heat exposure frequencies and magnitudes are expected in 30% – 40% of the cities, meaning the future adaptation levels will be exceeded in frequency and intensity (change in number of MMT exceedance days: -185 to +92; change in exceedance magnitude: -4.4 °C to +5.4 °C). A rise in future heat-related mortality until the end of the century can likely be expected as high exposure indicates. This is projected in cities across arid and semi-arid regions, such as in the Arabian Peninsula, across the Middle East into Pakistan and India, south of the Sahel and in Northern Africa, and in the Southwestern USA. This work proved that adaptation is a pivotal measure defining the degree of exposure by the frequency and severity of being transgressed. A joint research of adaptation and heat exposure in future heat impact studies is highly encouraged. Still, a certain quantity in heat-related mortality will always remain, even if the willingness to adapt is existent, despite of having implemented adaptive measures, having adapted physiologically and having adjusted the behaviour accordingly. In this regard, adaptation to heat fundamentally differs from the adaptation to other climate-related or meteorological hazards. Adaptation to heat is complex as many intrinsic factors from within the population as well as extrinsic environmental or socio-economic city characteristics influence the quantity of heat adaptation reached. These factors are reflected in all three levels of analysis in this thesis and jointly form the relationship of heat and mortality among urban populations.

In the following, the work accomplished in Chapters 3–5 will be revisited with regard to the corresponding research questions RQ1 through RQ3. The achievements, findings and scientific relevance of each chapter are embedded a broader context. Additionally, existing limitations are acknowledged. Lastly, Section 6.5 closes this chapter presenting relevant concluding remarks and an outlook on follow-up research.

6.2 Overcoming data-related challenges and extending the urban MMT pool (RQ1)

To establish the HMR for a city and derive its MMT as indicator for human heat adaptation, conventionally, daily mortality records and daily temperature data are used. Still, it can be difficult to derive the MMT due to missing, flawed or biased mortality records. Further, the access to these records is not always guaranteed. Even though for plenty of cities around the globe, the HMR and the MMT had already been established and fed into a pool of urban MMTs, the generation of the MMT remained challenging. So far, major German cities had not yet been considered in heat impact analysis and their MMT had not yet been calculated. Here, twelve German cities were chosen to demonstrate the data-related challenges that the conventional method of impact analysis brings along, how to overcome them and to motivate the establishment of a more generalised model to estimate the urban MMT. As a prerequisite for the endeavour to scale the MMT to the global city level, a pool of MMTs was required. The here derived MMTs for German cities served to extend this pool of urban MMTs. This interesting yet challenging experiment for a highly urbanised country has been addressed by the First Research Question RQ1 in this thesis:

> RQ1: *Which challenges have to be overcome to extend the pool of MMTs by deriving the HMR for German case studies?*

In Chapter 3, the HMR for twelve German cities was established and their MMTs identified using daily mortality records and daily temperature data over a period of 22 consecutive years. The daily mortality data was homogeneously obtained from the Research Data Centres of the Federation and the Federal States of Germany. The consistent methodology (Gasparrini et al., 2015) across the twelve cities was applied to derive the MMTs. The MMTs ranged between 17.6 °C in Bremen in northern Germany and 19.8 °C in Frankfurt (Main) in the centre of the country. These values corresponded to the 82th and the 90th percentiles of the daily mean temperature distributions in Bremen and Frankfurt. Generally, the MMTs were highest in southern German cities (Frankfurt, Stuttgart and Munich). The mean MMT across all twelve cities was 18.4 °C. The HMRs generated are in accordance with previous work on German cities and the HMR (Breitner et al., 2014)

On the one hand, this analysis enabled the contribution of the resulting MMTs to the ever-growing pool of city-level case studies established by the MCC, where German cities had not yet been represented, apart from very few Bavarian cities (Chen et al., 2019; Rai et al., 2019). This data pool is made available for further scientific purposes and helps to foster the research on heat-related mortality and other health outcomes under present and future climate conditions. At least seven studies have made use of the generated MMT data already (Vicedo-Cabrera et al., 2020; Vicedo-Cabrera et al., 2021; Chen et al., 2021; Meng et al., 2021; Urban et al., 2021; Zhao et al., 2021a; Zhao et al., 2021b), which is a success.

On the other hand, the work presented in Chapter 3 was related to four major challenges that had to be overcome concerning the acquisition and preparation of data. These data-related challenges especially concerned the time series of daily mortality records. First, such highly confidential and sensitive data of daily mortality records were not freely accessible for use. Time series on daily mortality data in German cities could only be obtained from the Research Data Centres of the Federation and the Federal States of Germany upon high expenses. Per statistic and year, the Research Data Centres of the Federation and the Federal States of Germany charged 250,00 Euros (Research Data Centres of the Federation and the Federal States of Germany, 2020). This made an analysis of 22 consecutive years a cost-intensive endeavour. Second, the mortality data could only be treated and prepared on site at the so-called 'safe center' for reasons of confidentiality (Research Data Centres of the Federation and the Federal States of Germany, 2020). Scripts and code to prepare the mortality records were controlled prior to their on-site use at the Research Data Centres of the Federation and the Federal States of Germany. Results had to be compliant with certain rules of anonymity. Output data was controlled for according to the four-eye principle prior to being provided for use outside of the Research Data Centres of the Federation and the Federal States of Germany. Further rules hampered rapid progress in workflow and data processing. Coding and debugging was made difficult since during the sessions at the Research Data Centres of the Federation and the Federal States of Germany, it was prohibited to take handwritten notes about the data or programming. Moreover, rapid and easy communication for queries about errors concerning the data or for accordance with co-authors were hindered because on-site computers did not have internet access and communication was only allowed outside of the 'safe center'. These restrictions for reasons of confidentiality and data protection are of utmost importance, however they made data preparation a rather laborious and time-intensive task. For researchers not based anywhere near a Research Data Centres of the Federation and the Federal States of Germany these restrictions might be an obstacle to work with such data. Besides the costs to obtain the data, this could be another reason why the HMR and the MMT had not yet been generated out covering several cities in Germany comparatively. The third challenge refers to the statistical bias and errors that were detected in the data. An unusually high daily mortality was recorded in Frankfurt (Main) on 1 January of each year. This was due to the closure of the registrar's office during the holidays and the week between Christmas and New Year's. All mortality cases that had occurred during that time of limited opening hours were registered for January 1st the following year. This bias was corrected by interpolating the mortality from the days prior and after this holiday period.

A last and fourth challenge consisted in altered district boundaries of studied cities during the studied years. Each statistical time series was linked to a particular political district indicated by a corresponding district code, called 'Amtlicher Gemeindeschlüssel' in Germany. The modification of political districts due to annexations of area or merging of districts entailed a modification in mortality time series as well as in population statistics. Such alteration concerned Hanover, where two districts were merged in 2001. The cities of Dresden and Leipzig each comprised four different district codes for different time periods. Such modifications had to be taken into account and incorporated in the analysis. This shows how error-prone statistical time series linked to a particular location can be, even in Germany, a country where data is well-documented.

When preparing the crude mortality records provided by the Research Data Centres of the Federation and the Federal States of Germany at the on-site 'safe center', it became obvious that according to the causes of death, only few death cases were associated to direct heat exposure, as coded under the T67 in the section "Effects of heat and light" in the International Classification of Diseases (ICD). The established heat-mortality associations for the German cities showed a pronounced increase in mortality for warm temperatures in the cities during the observation period 1993 to 2015, even if direct heat exposure as a cause of death was not recorded and all-cause mortality was used. The fact that all-cause mortality is conventionally associated with temperatures to establish the HMR is a common practice and is in line with other findings (Siebert et al., 2019; Guo et al., 2016; Gasparrini et al., 2017; Vicedo-Cabrera et al., 2021). Here, excess mortality refers to the share of mortality that is associated with temperatures above the MMT. Further, as the findings by an extensive study (Mora et al., 2017a) suggest, heat can impact human health in multiple indirect ways. Still, a more specific coding and recording system of death cases and same-day ambient conditions could contribute to discriminating heat-related death-cases and support more detailed analysis. Additionally, a web-based or real-time recording of death cases and causes paired with an automatic information flow from the registrars to the statistical offices would facilitate and fasten the collection and provision of data. This way, independence in recording from the registrar's office hours could be achieved and signals in the mortality data faster detected. This would also proof beneficial during a crisis situation as during the COVID-19 pandemic, where the information flow of case numbers lags during the weekend or depends on the operating hours of the registrar's offices and other involved administration (Bundeszentrale für Gesundheitliche Aufklärung, 2020). According to the Robert Koch Institute in Berlin, the German reporting system on incidences and death cases has already been improved during the pandemic in order to accelerate the publication of data, but still due to validation and quality control, a certain time lag in publication of cases remains (Robert Koch Institut, 2021). At present, a real-time monitoring of heat-related mortality in Germany is prevented due to the German Civil Status Act 'Personenstandsgesetz', as explained for the case of Hesse (Germany) in (Siebert et al., 2019). This legislation allows the reporting of a death case to the registrar up to three working days following the day of death, where it is subsequently recorded after a certification procedure. From there, the information is passed on to the local health authority and finally with a certain time lag to the statistical offices of the federal states. During the following week, about 90% of the death cases of the previous week are recorded (Siebert et al., 2019). A surveillance system for morbidity seems to be less bureaucratic and has already been implemented based on recorded and classified emergency services and rescue missions (Steul et al., 2019). The care capacity proof system 'Interdisziplinären Versorgungsnachweis (IVENA)' can thus be used to investigate the health effects of heat events in real time and can be used as an early warning system for prevention as its appliance in Frankfurt (Germany) implies (Steul et al., 2019). The work in Chapter 3 could also be modified for the appliance to morbidity data to generate valuable information of the long-term association of temperature and morbidity to support such real-time recording systems.

The work carried out in Chapter 3 goes far beyond contributing to clarify heat adaptation across urban populations in German cities by delivering their MMTs. It also reinforces the importance of the MMT for further and future research efforts related to health outcomes in cities. However, it also reveals the methodological and data-related challenges related to deriving the MMT and to establishing the HMR for cities applying the conventional approach put forward by previous work (Gasparrini et al., 2015). It became obvious, that despite of similarities in results across neighbouring cities or cities in adjacent countries, or similarities to outcomes of previous research, MMT data across different cities and countries is and was never perfectly coherent concerning their database, study period, location reference, methodologies and outcomes. Besides having illustrated how error-prone and data access-dependent this conventional approach to derive the MMT is, this work demonstrates that usually, this conventional analysis only adds few data points to the MMT pool at once. These circumstances support the need for a more generalised and simple approach to approximate the MMT for cities independently from cost-intensive and error-prone daily mortality records, which is presented in the next following Chapter 4. Thus, Chapter 3 can be considered methodology-related but also provides a contribution to ensuring the global assessment of the human heat adaptation and its evolution under different climates later on in this thesis (cf. Figure 1.3).

6.3 Generalising the MMT from case studies to the global level (RQ2)

After having demonstrated how challenging and error-prone it is to derive the MMT for cities based upon daily temperature and mortality records in Chapter 3, the motivation to develop a universal model to approximate heat adaptation that relies on easily accessible data and that is applicable for any city on the globe becomes obvious. Further, the established pool of urban MMTs across the globe encourages to exploit the entirety of the pooled MMT case-study data to withdraw generalised information about how to approximate the MMT. The advantage of a generalised model to approach the MMT as adaptation measure is that it allows the homogeneous estimation of MMTs across cities around the globe, independently from the existence and access to daily mortality (and temperature) records as supported by the methodology-related challenges portrayed in Chapter 3. The identification of city-specific features shaping the MMT constitutes a precondition to the model construction. For the purpose of closing this research gap, this topic has been condensed into the Second Research Question RQ2:

RQ2: *To which share do climatic, topographic, and socio-economic features influence the MMTs and how can MMTs be generalised from case study to the global level?*

The answer to this research question allowed the refinement and the quantification of the general qualitative knowledge about the two types of adaptation, autonomous and planned adaptation, and uses the information contained within the pool of MMTs extended in Chapter 3. Thirteen potential influential factors identified by previous literature were tested and reduced to five significant independent variables, that were able to describe the pool of MMTs most suitably according to the smallest RMSE and most optimal AICc in a multivariate non-linear regression model. The climate showed the largest and the socio-economy the second largest influences on the MMTs. The topography was least important but still significant. The model was able to estimate the urban MMT as measure of human heat adaptation based upon city features for a large number of cities that had not yet been investigated before in case studies. The MMT as described in Chapter 4, was far more than a plain temperature index, since it contained a climate and a socio-economic component. This confirms that physiologic acclimatisation constitutes one share of urban populations' overall adaptation to heat that is autonomous, which is here represented by climatic variables in the generalised model elaborated in Chapter 4. A high socio-economic status facilitates the access to technological, social and behavioural adaptation measures, which contributes planned adaptation as second component to the overall adaptation to heat. The model is established upon data from a multitude of studies on the HMR, delivering the MMTs for a pool of cities. A concern could be that empirical mortality data are not evenly reported across the sample of cities and studies or that there could be a lack of consistency in coding death cases. It is a common practice that studies investigating the HMR, as the peer-reviewed studies that were used to establish the model, do not specifically distinguish between causes of death, but rather refer to all-cause mortality in their studies (Guo et al., 2016; Gasparrini et al., 2017; Vicedo-Cabrera et al., 2021), even if explicit codes for 'Effects of heat and light' in the ICD exist. To include all-cause mortality likely mitigates any data bias from poorly reported death cases. Certainly, erroneous causes of death in the death certificate are among the mortality data employed, but also such errors will likely be smoothed by using all-cause mortality in the epidemiologic studies on the HMR. Thus, this issue should not constitute a limitation of the study presented here and should not influence further research on the future MMT.

In future research, the generalised model presented could be adapted to explore the city-specific drivers for heat-related morbidity. Following the model-building procedure in Chapter 4, a pool of morbidity indicators, such as hospital admissions or emergencies, from a set of cities could be used for such purposes. Multivariate non-linear regression could be employed to generalise the information and build a model to predict heat emergencies or morbidity thresholds. Such research could provide a first attempt to establish a globally homogeneous surveillance system for temperature- or heat-related morbidity in order to prevent mortality as health outcome in the first place, and inform the health system as well as urban infrastructure planning about morbidity risk. Research on temperature- or heat-related morbidity is less prominent than on mortality and thus, a pool of data has not yet been assembled. This however would overcome differences and warning definitions at the national level while at the same time it would be location-specific and it would contribute, besides national activities, to a more coherent spatial overview and record of heat-related morbidity and emergencies worldwide.

The work carried out in Chapter 3 complements earlier and ongoing large-scale conventional case-studies on temperature and mortality in cities as conducted by the MCC (Gasparrini et al., 2015; Guo et al., 2014) by providing a more general level of analysis deduced from the provided pool of MMTs. The identified city-specific features used to approximate the MMT can easily be obtained or calculated from data free of charge, while the MCC has to collect further daily mortality-based MMTs from cities or countries that have not yet been analysed in order to expand their MMT database. The model presented in this dissertation is a more flexible tool than what had been put forward up to date and offers further advantages: First, it is applicable to any urban area independently from political boundaries compared to what had been provided earlier by heat impact studies. This means, now, time series were independent from area codes or modifications of reference areas, a challenge that was encountered during the work presented in Chapter 3, to which – partially – the motivation to establish a generalised model was owed. A further advantage is that the model acknowledges the contribution of climate as autonomous adaptation and socio-economy as planned adaptation to overall adaptation (Turek-Hankins et al., 2021; Petkova et al., 2014), which points again at the uniqueness of human heat adaptation compared to the adaptation to other types of climatic hazards. The model established here made a contribution to further understanding the mechanism between heat, population and the city environment at a global scale, which was identified as a research need earlier (Arbuthnott et al., 2016; Gosling et al., 2017; Liu and Ma, 2019). A third major advantage of the presented method was that the model constituted a foundation and a scheme for application with climate and socio-economic projections to research the future adaptation under different climate and socio-economic settings. The future change of the MMT gives indication of how adaptation to heat will develop until the end of the 21st century. This task had remained challenging applying the conventional method to derive the future MMT (Gosling et al., 2017) and relied on many assumptions especially concerning future daily mortality data (Gasparrini et al., 2017). The future MMT could be used as a threshold value to investigate exposure frequencies and exposure severity on a daily basis. Accordingly, this parameter serves to appraise changes in heat exposure. The fact that the model was modifiable for application with climate and socio-economic projections strongly encouraged to carry out such final level of analysis to research the future adaptation in cities worldwide under different climate futures as undertaken and presented in Chapter 5. In this sense, the generalised model to approximate the MMT for cities worldwide established in Chapter 4 is a core achievement of this dissertation. The methodology elaborated in Chapter 4 is the foundation to pave the way for a global assessment of the future heat adaptation in cities around the globe as previously displayed in Figure 1.3.

6.4 Future development of adaptation and heat exposure (RQ3)

Having a generalised model at hand to estimate city-specific MMTs facilitated the investigation of the global assessment of the future adaptation and exposure changes among major cities, which was the third and final level of analysis in this dissertation and treated in Chapter 5. This research related once again to the two aspects of overall adaptation to heat.

Physiological acclimatisation is driven by the city-specific climate and thus is an autonomous adaptation. The socio-economically enabled adaptation measures are rather a planned type of adaptation. Both components of overall heat adaptation had been elaborated in Chapter 3 in form of the MMT and unified in the general model established in Chapter 4. As already signalised in the previous Section 6.3, in its form, the model could easily be adapted for use with projected climate and socio-economic data, to generate the future MMT. For such purpose, the last and Third Research Question RQ3 had been posed:

> RQ3: *How will MMTs and heat exposure change in the future as response to 21st century warming in major cities?*

To answer this research question, the development of the MMT as change in adaptation and the corresponding change in heat exposure was calculated and evaluated for a multitude of possible combinations of future climate trajectories and socio-economic pathways for a sample of nearly 4000 cities. This way, a wide spectrum of diverging future changes in adaptation and exposure was made available and comparable across RCPs (2.6, 4.5, 6.0, and 8.5) and SSPs1 to SSP5 for major cities around the globe. The results are standardised but still value the locally-specific information. The highest mean adaptation gain across the cities was reached in RCP8.5 and fossil fuel-driven SSP5 (+1.8 °C – 13 °C), while average exposure frequency and magnitude decreased only in 60% of the cities until 2100. In 30%–40% of the cities, the exposure increased. Changes in exposure frequencies and exposure magnitudes covered large ranges (-185 to +92 change in exposure days; -4.4 °C to 5.4 °C change in exposure magnitude). It is however questionable whether the gains in adaptation will compensate the strong increase in exposure in those cities. A moderate gain in adaptation was reached by sustainable and low-emission future RCP2.6 and SSP1, ranging between 1 °C and 7.2 °C. Simultaneously, the mean change in exposure frequency and magnitude was lower in 2100 in the majority of cities than in RCP8.5 and SSP5 (-140 to +40 change in exposure days; -3.5 °C to 1.9 °C change in exposure magnitude). About 80% of the cities were projected to profit from such developments until 2100. The share of cities in the sample experiencing an increase in exposure frequency only amounted to about 6% and 9% of the investigated cities were concerned with an increase in exposure magnitude. A RCP8.5 and SSP5 future produced higher heat exposure parameters for the majority of the cities, likely leading to higher heat-related mortality in 2100 as adaptation will probably not be able to compensate for the increment in exposure. Even though a RCP2.6 and SSP1 future was found more beneficial in terms of health outcomes compared to RCP8.5 and SSP5, both futures however constitute an aggravation against an ideal future without climate change but steady socio-economic growth. The large spectrum of possible health-related outcomes under different climatic and socio-economic settings is provided, which is considered a general accomplishment delivered by this thesis. Humanity should seize the opportunity to make its well-informed choice for future related to a minimum change in exposure and moderate adaptation.

The work presented in Chapter 5 offers a methodology to research future heat adaptation among urban populations and how it compares to the beginning of the century. It estimates the urban MMT anew based upon city features and projections of climate and socio-economy. Thus, this approach is spatially and temporally highly flexible because it is independent from daily mortality projections or continuation of observed time series, data that other heat impact studies use to derive the future HMR (Gasparrini et al., 2017). Most impact studies on heat-related mortality had not incorporated adaptation or adaptation effects (Gosling et al., 2017). Most certainly, to grasp and to measure human heat adaptation at the city level was a demanding task. This was especially due to, as demonstrated in this thesis, its non-binary nature, as one part of adaptation comes from within the population itself and is autonomous (Turek-Hankins et al., 2021; Petkova et al., 2014; Gosling et al., 2017) and hence, always existent (Freitas and Grigorieva, 2015). This once again hints at the uniqueness of human heat adaptation compared to other sorts of hazard adaptations. The work presented in Chapter 5 was able to propose a separation of the contributions of climate-driven autonomous adaptation through physiologic acclimatisation from socio-economy-enabled planned adaptation to overall heat adaptation, which is a major accomplishment, also for this thesis. Such separation of adaptation had been identified as an urgent research need in previous literature (Petkova et al., 2014; Gosling et al., 2017). The interplay of these two components of adaptation was unclear, especially the varying magnitudes of autonomous and planned adaptations and their heterogeneous impact across locations (Gosling et al., 2017). Within the analysis in Chapter 5, the information about the primary contributors to heat adaptation changes for particular combinations of RCP and SSP was provided. The change in socio-economic standard only contributed to high gains in human heat adaptation in a future dominated by sustainable economic growth and climate trajectory relating to the least warming covered in this analysis. Regions where the socio-economy was particularly prominent in driving adaptation were North America, Europe, East Asia and southern India, South Africa, and coastal communities across South America and the wealthiest South American countries Argentina and Uruguay. Strong economic growth as major driver for adaptation in a future based on fossil-fuel exploitation was exceeded by an even stronger contribution of the changes in climate. Only few cities in northwestern Europe, Asia, Oceania and South America remained, where the socio-economic change was primarily driving future changes in heat adaptation or masked the influence of the other variables. Such knowledge on the major drivers of human heat adaptation had not yet been elaborated before (Folkerts et al., 2020). It is useful to promote these major drivers through adequate policy-making (Folkerts et al., 2020).

The results presented in Chapter 5 suggested, that even within countries, the increment in adaptation change varied across cities and that such changes were driven by different forces across cities. In fact, adaptation changes were divers for each climate future. This helped to unravel further methodological uncertainties related to the modelling or incorporation of heat adaptation in impact studies. An absolute MMT shift into higher temperature regimes was recommended against a range of other options to model future adaptation (Gosling et al., 2017). However, up to date, the shift increment of the MMT was chosen arbitrarily or was predefined but never empirically proven (Gosling et al., 2017), which did not quite correspond to a realistic picture of the future development of adaptation. The method elaborated in Chapter 5 to derive future MMTs for cities was able to inform such impact studies on heat-related mortality on the critical increment by which the MMT will shift until the end of the century under the different scenarios. This work acknowledged that the HMR as non-linear response function was dynamic and could not be considered static or that observed mortality time series could be continued into the future as it was commonly assumed (Gasparrini et al., 2017; Deschenes, 2014; Gosling et al., 2017). This methodological clarification is a major achievement of this thesis because it also facilitates the derivation of the slope of the future HMR and hence, possibly even the future heat-related mortality.

The analysis demonstrated that the MMT for cities alone does not provide sufficient information on robust health risk outcomes without setting it into context with future heat exposure. Many studies lacked to do so or use the heat exposure as singular indicator for future heat risk, which fell short to include the information on the population's future adaptation. Such practice often lead to an overestimation of impacts (Gosling et al., 2017). A high heat exposure does not automatically lead to a high mortality risk in case the population is well-adapted to high heat exposure. Three conditions were identified that – if they jointly held true for a specific city – likely lead to an increased heat-related mortality in the future compared to the year 2000: (1) Additional or only slight reductions in exposure days, the number of days throughout a year that show a daily mean temperature exceeding the MMT in a city; (2) An increase in the annual mean temperature magnitude by which the MMT is exceeded by the daily mean temperature during an exposure day; and (3) only small gains in adaptation until 2100. Based upon these criteria, a number of endangered cities could be identified located in fully arid and semi-arid climates questioning their future habitability, which is in line with earlier studies (Pal and Eltahir, 2016; Milner et al., 2017). Here, especially in a future dominated by a strong socio-economic growth based on the exploitation of fossil fuels and high GHG concentration in the atmosphere, a strong climate change would cause a high exposure increment and a small gain in adaptation. This was projected to concern cities in the USA, northern Mexico, the Sahel and across the Arabian Peninsula and the Middle East into Pakistan and India. Findings on identified regions and cities at risk are partially in line with those regions and cities, for which a prior study found higher mortality risk associated with increases in the interactive effect of the mean temperature and the diurnal temperature range under RCP8.5 in 2090–2099 and a decreasing trend in RCP2.6 (Lee et al., 2020). Some results however diverge. The thesis at hand did not identify most cities across the USA at risk to experience increased mortality in RCP8.5/SSP5 in the future according to the three criteria stated above. This is possibly due to the consideration of increased future heat adaptation in this thesis, which is projected to be majorly driven by a combination of increases in climate and GDP/cap in those U.S. cities. A moderate increase in heat-related excess mortality was projected for cities in Northern Europe, East Asia and Australia under RCP8.5 (Gasparrini et al., 2017), which corresponds to the regions identified in this thesis, where cities show low or moderate exposure changes until 2090-2099 under RCP8.5/SSP5 and a large adaptation increment. Regarding similarities in cities associated with high increase in heat-related excess mortality in Gasparrini et al., 2017, only limited overlap was found with regions or cities that showed high exposure changes in this thesis. This could be due to the incorporation of heat adaptation in this the work at hand. Gasparrini et al., 2017 found that under a RCP2.6 future, the increase in heat-related mortality in warmer regions was smaller, which is roughly in line with the findings presented here about cities that show lower exceedance changes under RCP2.6/SSP1. Still, the results on increased exposure are in strong accordance with previous global projections on urban warming (Zhao et al., 2021a) and partially overlap with other findings at the global scale (Zheng et al., 2021), that only projected future urban heat waves and thus, only the exposure side. According to the findings presented in Chapter 5, a number of cities would profit from a large gain in adaptation and less severe increments in exposure change in a RCP8.5/SSP5 future. In contrast, in a future determined by a mild climate change based upon sustainable socio-economic growth and low GHG concentrations in the atmosphere, the sustainably generated economic growth component would primarily drive adaptation change in most cities to a moderate adaptation level in 2100 and mask the high effects of other variables.

Due to relatively low warming levels in this case, such scenario combination would even reduce exposure compared to 2000 in 80% of the cities investigated. A potential source of bias in the work presented here is that the exposure calculation strongly depends on the MMT, as the adaptation measure was used as a threshold to determine exposure frequency and magnitude. Still, as the MMT is indicative of the lowest point on the HMR (Folkerts et al., 2020), it can still used to determine exposure in the temperature ranges above the MMT. A reduction in heat exposure under SSP1-RCP2.6 and a new SSP1-RCP1.9 scenario was confirmed by the recent AR6 IPCC report as well as a limitation of the regions, where exceedances of dangerous heat thresholds will occur in the future (Masson-Delmotte et al., 2021). An increase in frequency and exceedance of dangerous heat thresholds in case of SSP5-RCP5 and in case of a newly established scenario SSP3-RCP7.0 was found, which corresponds to the findings here (Masson-Delmotte et al., 2021).

This work is somewhat limited by the use of gridded data. The coarseness of the data is a general limitation on impact studies. For urban analysis at a global scale, most certainly, trade-offs in detail have to be made. The analysis presented in this thesis does not claim to cover small details at the urban level but rather seeks to provide a first comparative global overview. Moreover, the resolution of the gridded data employed is identical to the resolution used in a number of urban impact studies (Gasparrini et al., 2017; Chen et al., 2019; Lee et al., 2020; Zhao et al., 2021b). One of those was recently able to disentangle the contribution of climate change and natural variability on past heat-related mortality in 732 cities (Vicedo-Cabrera et al., 2021) based on the same resolution as used in the work at hand. This indicates that such data could be used for urban analysis. However, when the model presented in Chapter 5 was re-calibrated, a RMSE of 3.2 °C was returned, that is very much identical to that of the original model, 2.81 °C, presented in Chapter 4. Thus, using coarse climate data did not seem to introduce any particular bias in the newly re-calibrated model.

Findings resulting from the analysis of future adaptation and heat exposure presented in Chapter 5 addressed the quest for a closer understanding of human heat-related adaptation (Arbuthnott et al., 2016; Liu and Ma, 2019; Folkerts et al., 2020). The results highlight the urgency and the complexity to approach adaptation to heat and most importantly to consider mitigation decisions (Ganguly et al., 2009). This way, a sustainable future can be achieved and the change in heat-related mortality can be kept low compared to other climate and socio-economic futures. Thus, a healthy planet is what ensures long-term human health. Here a fundamental link between this work and the concept and scientific field of Planetary Health is evident (Whitmee et al., 2015).

To add on to this work, the generated database could be exploited for investigations on the length of periods showing consecutive exposure days or whether the first exposure day of the year will be postponed until the end of the century. Further, it would be intriguing to bin warming levels of the GMT across RCPs and investigate which effects this would have on adaptation and exposure changes for the cities worldwide. Such methodology had been put forward by Vicedo-Cabrera et al., 2018 and Huber et al., 2020. Moreover, it is encouraged to research a 1.5 °C-compatible climate trajectory and its implication for human heat adaptation and exposure, which would be of value and importance for policy-making at the international stage. A 1.5 °C warming level could also be incorporated in the binning approach. Further, the establishment of a link between the future heat adaptation and exposure to a set of population scenarios could reveal the share of urban dwellers corresponding to different levels of heat adaptation and heat exposure for each climate and socio-economic future. This would help to identify the hotspots, where the most vulnerable towards heat will be concentrated and where the highest number of people with the least burden can be found. It would even be possible to adapt these population scenarios according to the results provided for the cities by the model established here. Population-related scenarios, i.e. on migration, could take into account that some cities might forfeit their habitability for their inhabitants and their pull-factor for migrants, while other cities will gain in attractiveness, depending on the climate trajectories and the socio-economic pathway combinations. The population scenarios underlying the five SSPs could be used for such purpose (Jones and O'Neill, 2016), they are available even at a resolution of 1km, which would be beneficial for such level of detail and were recommended for such undertaking over the UN population scenarios (Rozell, 2017). It would be intriguing to discriminate the share of heat-burden that is caused by the UHI and which effect the reduction of the UHI would have especially on exposure in the cities (Zhou et al., 2013; Zhou et al., 2017; Li et al., 2020) but also on changes in adaptation. Even a city growth model (Glockmann et al., 2021) could be integrated in such research idea. The effects of city growth on the exposure and adaptation change via the alteration of the UHI could be studied, which might deliver insights for innovative future urban planning to make cities more heat-proof, and for improving the well-being of citizens.

To sum up, the work presented in Chapter 5 constitutes the principal contribution to the global assessment of the future MMT as a measure of human heat adaptation and its change until the end of the century (cf. Figure 1.3). The provision of the change in MMT for the first time supports the understanding of future heat adaptation in cities. The scheme offered allows to explore possible combinations of climate and socio-economic futures in terms of heat adaptation and exposure and their developments until 2100. Thus it is supportive towards policy- and decision-makers from the local or community levels to the supranational level. The guidance by the Scenario Matrix (Vuuren et al., 2014; Riahi et al., 2017) to combine climate trajectories with socio-economic pathways in a meaningful way makes findings of this analysis easily relatable to other work and further climate impact assessments that use this framework as a basis. Results and achievements accomplished by the work in Chapter 5 are key to the overall objective of this thesis.

6.5 Concluding Remarks and Future Outlook

This thesis showed how human heat adaptation and its future development among urban populations worldwide can be assessed by using the city-specific minimum mortality temperature MMT. After having built a pool of MMTs, a model to estimate the MMT was presented, which achieved independence from daily mortality records and solely relied on city-specific climatic, topographic and socio-economic indicators. Employing the available indicators, the estimation of the city-specific MMT was possible with a small remaining error. This model overcame data-related challenges concerning daily mortality data, which was up to date a limitation that hampered the analysis at the global scale. Further, the indicator choice allowed spatial and temporal flexibility. The model was adjusted for use with climate and socio-economic projections. A systematic overview on the future changes in human heat adaptation and heat exposure among cities worldwide was provided for 15 combinations of climate trajectories and socio-economic pathways. A future under RCP8.5/SSP5, a scenario representing a strong climate change and very rapid socio-economic development based upon the exploitation of fossil fuels, was found to lead to largest improvements in adaptation, but also to strong increases in heat exposure in 30% to 40% of the cities. In this scenario, the strong economic development will likely not be able to compensate for its own negative consequences. In a future compatible with the 2 °C target of the Paris Agreement, such as RCP2.6/SSP1, 80% of the cities were projected to profit from a decrease in heat exposure. The findings presented here informed future impact studies on the increment in adaptation change, which was up to date matter to uncertainty. In addition, the importance to assess heat adaptation and heat exposure in context, which contributes to avoid an overestimation in heat impacts, was demonstrated in this thesis. The presented contributions of this thesis are useful for policy-making at various levels in regard of climate change adaptation and health infrastructure planning.

Overall, the findings of this thesis are somewhat limited by three issues. First, the evaluation of heat exposure depends on the heat adaptation measure, the MMT, as threshold. Nevertheless, the MMT is the lowest point on the heat-mortality relationship and thus divides the curve into a heat and a cold slope. Considering that any temperature above the MMT is associated with excess mortality, the MMT can still be used as threshold to determine exposure frequency and magnitude. By jointly analysing human heat adaptation and heat exposure, this thesis advanced previous studies, where only exposure as a measure of risk was considered and thus, the heat impact likely overestimated. After all, the exposure measures proposed here could contribute to the establishment of a first linear approach of the future heat-mortality relationship under consideration of human heat adaptation. Up to date, this had not been accomplished in epidemiological studies due to missing mortality projections. The results of this thesis vaguely suggest that the changes in exposure measures could possibly be used to approximate the change in future mortality. Using the change in mortality jointly with the change in heat adaptation, the slope of future heat-mortality relationship could be derived. Further research on this is strongly encouraged. Second, the analysis compares changes in human heat adaptation and heat exposure change between the beginning and the end of the 21^{st} century. The development of human heat adaptation and exposure parameters remains unclear in the time in between. Such knowledge would complement the work accomplished in this thesis. The establishment of a longer time-series on the MMT would have been desirable, but could not be realised so far, because the exact rate of the physiological acclimatisation is still unknown. A first attempt to approach such data could be to carry out the analysis presented here for the years 2050 or 2080 for example. This could deliver valuable information on the short-term developments and support near-term health-care planning and decision-making on urban and national adaptation planning. The data for such analysis is available and could be prepared for analysis as a next project. Third, the incorporation of additional socio-economic indicators at the city-level, such as GDP/capita or number of hospital beds, could inform cities better on their specific future health outcomes, which would be beneficial to support planned heat adaptation at the urban scale. A lack of consistent and highly resolved data across cities was an obstacle to such endeavour and lead to the choice of employing socio-economic indicators at national level. However, as socio-economic and health-related decisions are mostly taken at the national level, the use of national indicators in this thesis does still fulfil its purpose to give an overview of health-outcomes for cities at the global level.

To drive this research further in the future, a binning method on different warming levels of the GMT across climate trajectories and socio-economic scenarios is proposed, which would offer to study the pace at which heat adaptation in cities would have to be required. Moreover, a 1.5 °C-compatible scenario should be included to support the ongoing discourse on this warming constraint. Both research ideas have not yet been pursued. Additionally, it is desirable to learn about the quantitative effects that planned physical heat adaptation measures in cities contribute to avoiding heat-related mortality or at least on change in heat adaptation. Such investigation has not yet been carried out for the entirety of applicable adaptation measures to heat in cities. Further, it would be an intriguing task to adapt this work to heat-related morbidity. Such analysis would be complementary to what has been carried out in the thesis at hand in informing public actors and the urban population more concisely regarding future health infrastructure and urban planning. A consistent, digitalised and rapid information flow, at best in real time, from health facilities to statistical records would facilitate this research.

Appendix to Chapter 3

A

A.1 Supplementary methods

A.1.1 Handling of outliers and missing values in observational series

The mortality series were complete, with no missing values. Yet, we classified 7 data points (1 Jan during the 1990s) in the data for Frankfurt as outliers and removed them from the series. The temperature series included few missing values (Table A.2), which we chose not to interpolate. In the case of Dortmund, no complete series was available for neither of the nearby weather stations. We joined data from Hagen-Fley (available up to 2007) with data from Bochum (available from 2008 onwards). We tested for zero difference in means between these two stations during the overlapping period (1 Jan 1993 to 30 Apr 1994) using a Welch two sample t-test ($p > 0.1$), giving us confidence that the bias from joining two distinct series was small.

A.2 Supplementary tables

Tab. A.1.: Districts codes (Amtlicher Gemeindeschlüssel (AGS)) used to extract city-specific mortality data from archive of the German Statistical Offices, and city-specific population data from 2015 (Source: GENESIS-Online Datenbank, Statistisches Bundesamt 2018). Total population of Germany in 2015 was 81.2 million.

City	AGS years	AGS code	Population (2015)
Berlin	1993-2015	11000	3 520 031
Bremen	1993-2015	4011	557 464
Dortmund	1993-2015	5913	586 181
Dresden	1993	14002	543 825
	1994-1995	14062	
	1996-2007	14262	
	2008-2015	14612	
Dusseldorf	1993-2015	5111	612 178
Frankfurt	1993-2015	6412	732 688
Hamburg	1993-2015	2000	1 787 408
Hannover	1993-2000	03201 + 03253	1 144 481
	2001-2015	03241[1]	
Cologne	1993-2015	5315	1 060 582
Leipzig	1993	14004	560 472
	1994-1995	14065	
	1996-2007	14365	
	2008-2015	14713	
Munich	1993-2015	9162	1 450 381
Stuttgart	1993-2015	8111	623 738

[1] 01.01.2001: Merging of rural and urban districts

Tab. A.2.: Weather stations and number of missing values.

City	Weather station(s)	DWD code	Missing values
Berlin	Berlin-Tempelhof	433	None
Bremen	Bremen	691	None
Dortmund	Hagen-Fley	1920	9 days in 1993-2007
	Bochum	555	None in 2008-2016
Dresden	Dresden-Klotzsche	1048	None
Dusseldorf	Düsseldorf	1078	None
Frankfurt	Frankfurt-Main	1420	None
Hamburg	Hamburg-Fuhlsbüttel	1975	None
Hannover	Hannover	2014	None
Cologne	Köln-Bonn	2667	None
Leipzig	Leipzig-Holzhausen	2928	1 day
Munich	München-Stadt	3379	None
Stuttgart	Stuttgart-Schnarrenberg	4928	9 days

Tab. A.3.: Central year of 21-y windows where considered levels of GMT rise are reached, by GCM and RCP scenario

GCM	Δ GMT above pre-industrial	RCP2.6	RCP4.5	RCP6.0	RCP8.5
GFDL-ESM2M	1°C	2015	2015	2017	2016
	2°C	-	-	2076	2053
	3°C	-	-	-	2084
HadGEM2-ES	1°C	2007	2007	2006	2006
	2°C	2039	2038	2041	2031
	3°C	-	2070	2069	2052
	4°C	-	-	-	2068
	5°C	-	-	-	2085
IPSL-CM5A-LR	1°C	2008	2011	2010	2009
	2°C	-	2045	2048	2037
	3°C	-	-	2086	2056
	4°C	-	-	-	2073
	5°C	-	-	-	2090
MIROC5	1°C	2012	2012	2017	2011
	2°C	-	2063	2069	2047
	3°C	-	-	-	2069

Tab. A.4.: Sensitivity analysis.

Modelling choices	AF total (%)	AF cold (%)	AF warm (%)	MMT (percentile)
Default (all cities)	6.30	5.49	0.81	86th
Knots for exposure-response: 10th, 50th, and 90th	5.82	4.92	0.89	79th
Knots for exposure-response: 10th, 25th, 75th and 90th	6.00	5.21	0.79	88th
Cubic B-spline for exposure-response	4.36	3.81	0.54	89th
Quadratic B-spline for exposure-response	5.33	4.72	0.61	92nd
Df/year for seasonal control: 4	5.34	4.50	0.83	84th
Df/year for seasonal control: 6	5.36	4.60	0.75	86.5th
Df/year for seasonal control: 8	5.78	4.85	0.93	84th
Df/year for seasonal control: 10	5.38	4.46	0.92	84th

Tab. A.5.: Second-stage random-effects meta-regression model.

Model	Predictor	Test for predictor	Q test	I2
Intercept-only	-	-	<0.001	59.4%
Single predictor	Average temperature	<0.01	<0.01	42.3%
	Temperature range	<0.1	<0.001	48.1%
Full model	Average temperature	<0.001		
	Temperature range	<0.001	>0.1	22.3%

Tab. A.6.: Heat-related, cold-related and net change in excess mortality (%, 95%CI) by city and global warming level.

City		GMT rise above pre-industrial				
		1°C	2°C	3°C	4°C	5°C
Berlin	heat	1.09 (0.81 to 1.44)	1.97 (1.51 to 2.50)	2.98 (2.23 to 3.96)	4.64 (3.89 to 5.44)	6.50 (5.13 to 7.98)
	cold	5.75 (4.04 to 7.47)	5.03 (3.40 to 6.69)	4.53 (2.96 to 6.13)	4.01 (2.46 to 5.56)	3.66 (2.16 to 5.16)
	net	-	0.11 (-0.38 to 0.53)	0.6 (-0.14 to 1.23)	1.87 (1.23 to 2.47)	3.39 (2.09 to 4.70)
Bremen	heat	0.43 (0.17 to 0.70)	0.77 (0.31 to 1.22)	1.18 (0.47 to 1.96)	1.77 (0.70 to 2.82)	2.5 (0.92 to 4.26)
	cold	3.05 (-0.28 to 6.27)	2.39 (-0.8 to 5.47)	2 (-1.11 to 4.87)	1.65 (-1.34 to 4.4)	1.47 (-1.38 to 4.09)
	net	-	-0.37 (-0.85 to 0.13)	-0.36 (-0.9 to 0.15)	-0.06 (-0.9 to 0.76)	0.49 (-0.83 to 1.94)
Cologne	heat	1.24 (0.81 to 1.68)	2.21 (1.57 to 2.72)	3.49 (2.58 to 4.60)	5.49 (4.60 to 6.44)	7.61 (5.88 to 9.50)
	cold	5.52 (3.47 to 7.57)	4.79 (2.84 to 6.78)	4.26 (2.39 to 6.16)	3.72 (1.93 to 5.52)	3.30 (1.61 to 4.99)
	net	-	0.19 (-0.13 to 0.55)	0.94 (0.27 to 1.85)	2.58 (1.84 to 3.30)	4.28 (2.66 to 5.95)
Dortmund	heat	0.95 (0.64 to 1.30)	1.73 (1.19 to 2.12)	2.79 (2.06 to 3.70)	4.37 (3.59 to 5.22)	6.09 (4.51 to 7.84)
	cold	5.27 (3.22 to 7.33)	4.55 (2.58 to 6.55)	4.04 (2.16 to 5.93)	3.53 (1.72 to 5.34)	3.15 (1.44 to 4.85)
	net	-	0.01 (-0.28 to 0.32)	0.55 (0.04 to 1.26)	1.75 (1.10 to 2.39)	3.09 (1.64 to 4.61)
Dresden	heat	0.76 (0.50 to 1.13)	1.48 (0.98 to 2.10)	2.37 (1.49 to 3.54)	3.68 (2.58 to 4.92)	5.36 (3.48 to 7.52)
	cold	4.57 (1.56 to 7.54)	3.92 (1.04 to 6.78)	3.51 (0.78 to 6.29)	3.09 (0.44 to 5.77)	2.82 (0.28 to 5.37)
	net	-	0.02 (-0.41 to 0.47)	0.49 (-0.22 to 1.37)	1.49 (0.49 to 2.49)	2.9 (1.10 to 4.82)
Dusseldorf	heat	1.23 (0.85 to 1.64)	2.16 (1.52 to 2.68)	3.36 (2.49 to 4.43)	5.14 (4.22 to 6.14)	7.02 (5.27 to 8.94)
	cold	5.55 (3.21 to 7.86)	4.73 (2.53 to 6.96)	4.15 (2.05 to 6.28)	3.56 (1.54 to 5.57)	3.13 (1.23 to 5.04)
	net	-	0.05 (-0.29 to 0.46)	0.66 (0.01 to 1.55)	2.02 (1.15 to 2.88)	3.47 (1.74 to 5.26)
Frankfurt	heat	1.11 (0.73 to 1.68)	2.09 (1.40 to 2.80)	3.57 (2.35 to 5.15)	5.69 (4.28 to 7.25)	8.06 (5.42 to 11.02)
	cold	8.4 (4.89 to 11.6)	7.61 (4.20 to 10.64)	7.03 (3.76 to 9.92)	6.4 (3.34 to 9.14)	5.86 (2.97 to 8.44)
	net	-	0.14 (-0.22 to 0.54)	1.03 (0.15 to 2.24)	2.64 (1.47 to 3.81)	4.47 (2.02 to 7.02)
Hamburg	heat	0.43 (0.19 to 0.68)	0.80 (0.38 to 1.22)	1.24 (0.58 to 1.96)	1.92 (0.93 to 2.85)	2.77 (1.32 to 4.31)
	cold	4.30 (1.13 to 7.43)	3.62 (0.60 to 6.60)	3.22 (0.30 to 6.05)	2.85 (0.08 to 5.56)	2.61 (0.01 to 5.13)
	net	-	-0.35 (-0.77 to 0.09)	-0.34 (-0.86 to 0.13)	0.02 (-0.74 to 0.76)	0.64 (-0.58 to 1.88)
Hannover	heat	0.93 (0.63 to 1.25)	1.65 (1.19 to 2.15)	2.56 (1.85 to 3.41)	3.90 (3.16 to 4.73)	5.4 (4.08 to 6.86)
	cold	3.67 (1.75 to 5.59)	3.05 (1.22 to 4.89)	2.64 (0.89 to 4.42)	2.23 (0.54 to 3.93)	1.97 (0.37 to 3.57)
	net	-	0.05 (-0.37 to 0.50)	0.54 (0.08 to 1.14)	1.6 (0.94 to 2.23)	2.83 (1.60 to 4.10)
Leipzig	heat	1.21 (0.87 to 1.66)	2.21 (1.60 to 2.93)	3.41 (2.45 to 4.70)	5.16 (4.07 to 6.35)	7.17 (5.20 to 9.38)
	cold	3.86 (1.76 to 5.95)	3.19 (1.17 to 5.23)	2.76 (0.80 to 4.73)	2.31 (0.43 to 4.21)	2.03 (0.23 to 3.85)
	net	-	0.28 (-0.25 to 0.82)	1.03 (0.33 to 2.00)	2.48 (1.53 to 3.44)	4.21 (2.36 to 6.20)
Munich	heat	0.57 (0.39 to 0.81)	1.16 (0.77 to 1.56)	2.10 (1.37 to 2.96)	3.44 (2.49 to 4.44)	5.35 (3.30 to 7.66)
	cold	6.44 (4.05 to 8.75)	5.71 (3.39 to 8.01)	5.22 (3.00 to 7.43)	4.69 (2.60 to 6.78)	4.27 (2.27 to 6.28)
	net	-	-0.18 (-0.48 to 0.15)	0.29 (-0.31 to 0.98)	1.14 (0.30 to 1.94)	2.62 (0.68 to 4.7)

City		GMT rise above pre-industrial				
		1 °C	**2 °C**	**3 °C**	**4 °C**	**5 °C**
Stuttgart	heat	0.89 (0.63 to 1.24)	1.71 (1.22 to 2.27)	2.98 (2.06 to 4.17)	4.83 (3.72 to 6.05)	7.15 (4.81 to 9.75)
	cold	6.9 (4.46 to 9.31)	6.10 (3.76 to 8.45)	5.55 (3.31 to 7.80)	4.94 (2.80 to 7.09)	4.43 (2.39 to 6.46)
	net	-	-0.03 (-0.31 to 0.31)	0.68 (-0.03 to 1.69)	2.02 (1.01 to 3.05)	3.82 (1.57 to 6.24)

A.3 Supplementary figures

Fig. A.1.: Map of Germany showing the locations of the 12 cities included in the study.

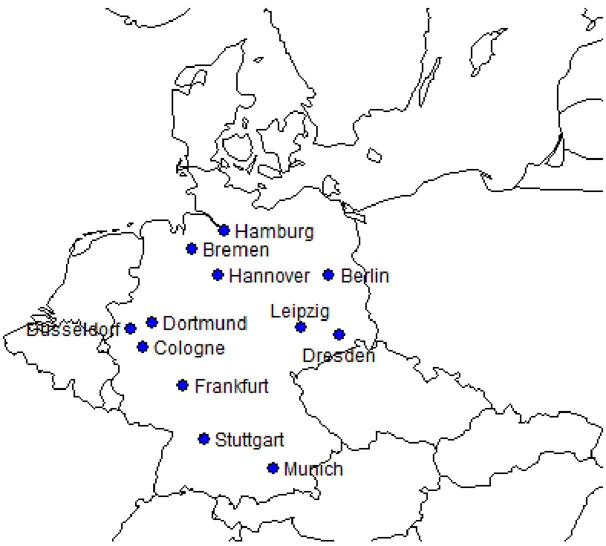

Fig. A.2.: Distribution of mean daily temperatures comparing weather station data with GCM data. We joined historical runs with RCP runs to derive complete series in the study period 1993–2015.

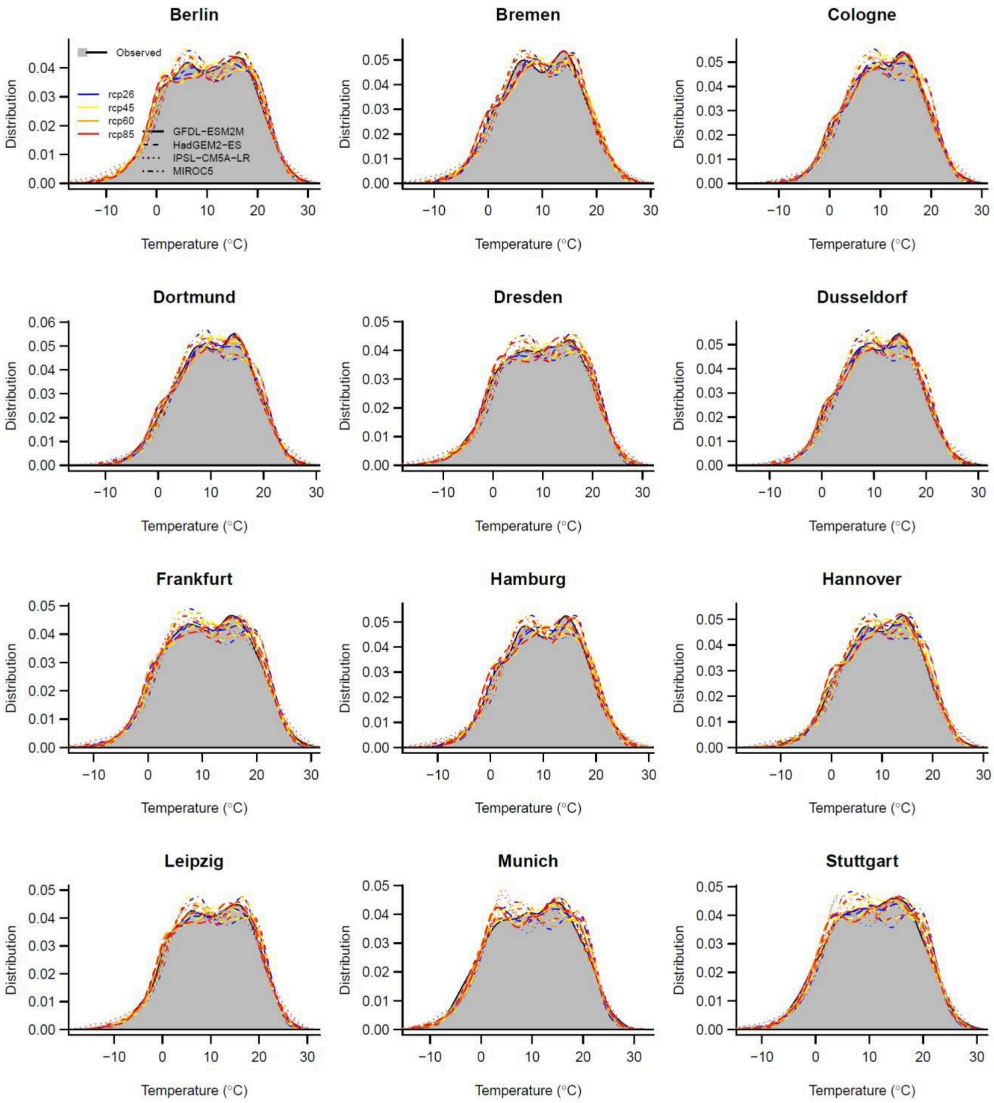

Fig. A.3.: Sum of quasi-Akaike information criterion (QAIC) across all cities for models differing in the degrees of freedoms (df) used to control for seasonality and long-term trends.

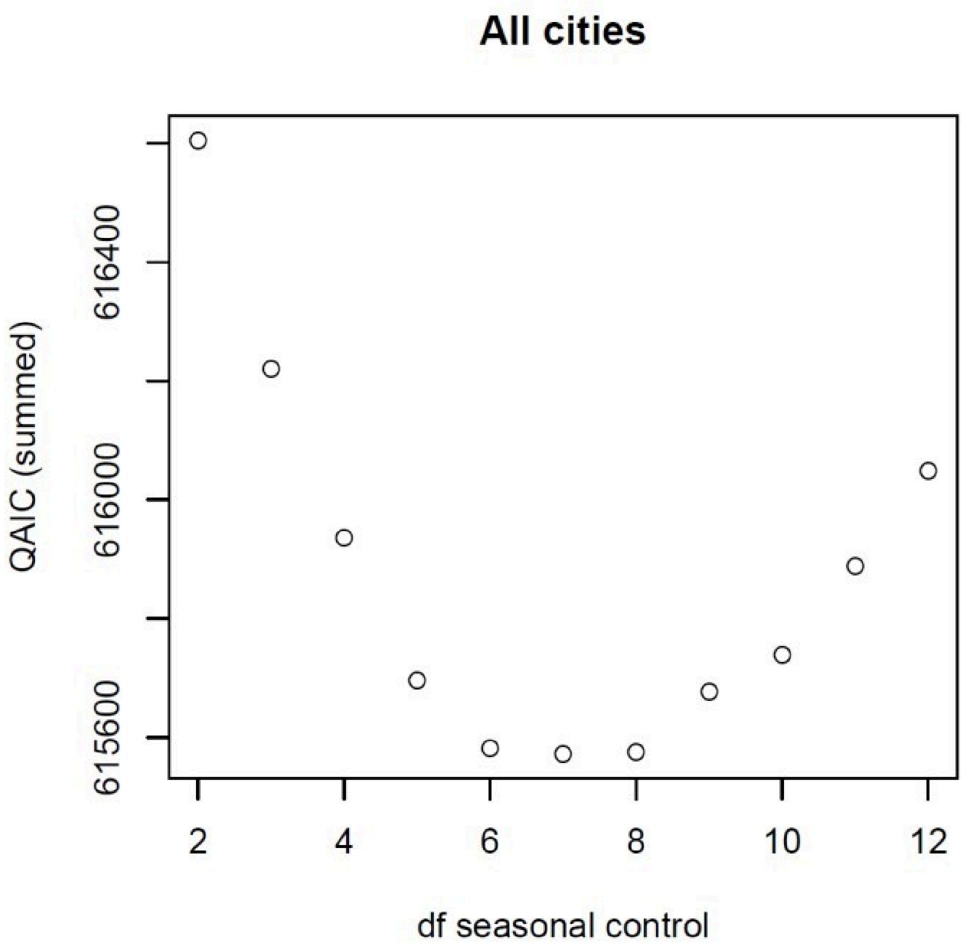

Fig. A.4.: Temporal lag structure underlying the overall cumulative temperature-mortality associations shown in Fig. 1. Depicted is the relative risk (RR) at each lag considered (0 to 21 days) for an exposure to cold (2.5th percentile of daily mean temperatures) and heat (97.5th percentile of daily mean temperatures) in each city.

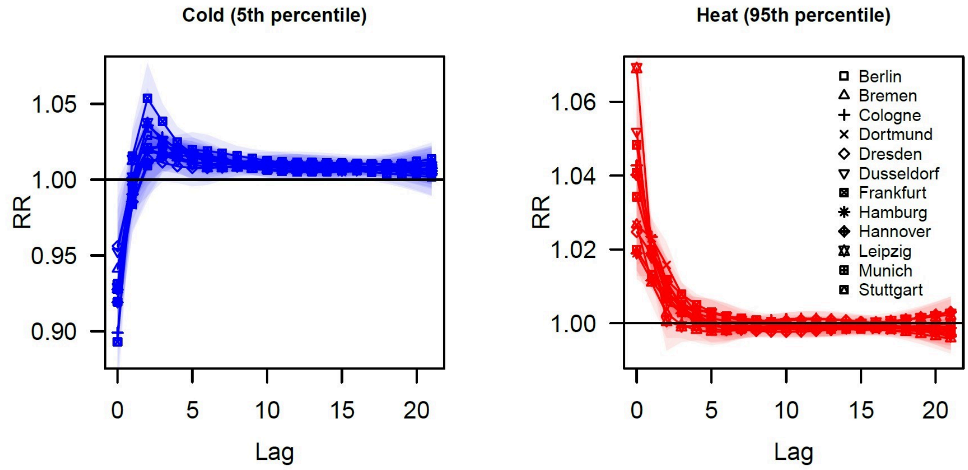

Appendix to Chapter 4

B

B.1 Metainformation on MMTs

Tab. B.1.: **Information on MMTs and details on the original studies** (For references see below).

Citation	MMT Cases	MMT Metric	Continent	Countries	Climate Zones	Notes
Baccini et al. (2008) (Baccini et al., 2008)	15	ATmax, ATmean	Europe	Czech Republic, Finland, France, Greece, Hungary, Ireland, Italy, Slovenia, Spain, Sweden, Switzerland, United Kingdom	Cf, Cs, Df	MMT for Barcelona given in ATmean
Bao et al. (2016) (Bao et al., 2016)	4	Tmean	Asia	China	Cf, Cw	
Burkart et al. (2011) (Burkart et al., 2011)	1	Tmean	Asia	Bangladesh	Aw	
Chung et al. (2009) (Chung et al., 2009)	2	ATmean	Asia	Japan, Republic of Korea	Cf, Dw	
Corobov et al. (2013) (Corobov et al., 2013)	1	Tmean	Europe	Republic of Moldova	Cf	Year 2007 is omitted in the study due to large temperature anomaly
Curriero et al. (2002) (Curriero, 2002)	11	Tmean	North America	United States of America	Am, Cf, Df	
El-Zein et al. (2004) (El-Zein et al., 2004)	1	Tmean	Asia	Lebanon	Cs	
Farajzadeh and Darand (2009) (Farajzadeh and Darand, 2009)	1	Tmean	Asia	Islamic Republic of Iran	Cs	
Gasparrini et al. (2015) (Gasparrini et al., 2015)	256	Tmean	North America, Europe, Asia, South America, Oceania	Australia, Brazil, Canada, China, Italy, Japan, Republic of Korea, Spain, Sweden, Thailand, United Kingdom, United States of America	Af, Am, As, Aw, BS, Bw, Cs, Cf, Cw, Df, Dw	Monmouth-Ocean, Nassau-Suffolk, Stamford-Norwalk, and country-, county-, provice- or district-level cases omitted (Japan, UK, Thailand, Sweden). Taiwanese cities excluded due to lacking World Bank Data. For Fort Pierce North, Gary, Lakeland, Naples, Nashua, Punta Gorda, York (all US), Kingston, London (both CA) GSOD data available only from 1980 or later, 30-year period adjusted.
Gosling et al. (2007) (Gosling et al., 2007)	6	Tmax	North America, Europe, Oceania	Australia, Hungary, Portugal, United Kingdom, United States of America	Cf, Cs, Df	
Gouveia et al. (2003) (Gouveia et al., 2003)	1	Tmean	South America	Brazil	Cf	
Ha and Kim (2012) (Ha and Kim, 2013)	1	Tmean	Asia	Republic of Korea	Dw	
Ha et al. (2011) (Ha et al., 2011)	3	Tmean	Asia	Republic of Korea	Cw, Dw	
Hales et al. (2000) (Hales et al., 2000)	1	Tmax	Oceania	New Zealand	Cf	
Harlan et al. (2013) (Harlan et al., 2014)	1	ATmax	North America	United States of America	BS	
Huang et al. (2017) (Huang et al., 2017)	4	Tmean	Asia	China	Cf, Cw	
Iniguez et al. (2010) (Iñiguez et al., 2010)	12	Tmean	Europe	Spain	BS, Cf, Cs	Vitoria, Cartagena omitted due to reported insignificant results. For Sevilla GSOD data available only from 1970s on, 30-year period adjusted.
Kan et al. (2003) (Kan et al., 2003)	1	Tmean	Asia	China	Cf	
Kim et al. (2006) (Kim et al., 2006)	4	Tmean	Asia	Republic of Korea	Cw, Df, Dw	
Kim et al. (2011) (Kim et al., 2011)	2	Tmean	Asia	Republic of Korea	Cw, Dw	
Leone et al. (2013) (Leone et al., 2013)	10	ATmax	Europe, Asia, Africa	Greece, Spain, Italy, Portugal, Israel, Tunisia	Cf, Cs	
Li et al. (2014) (Li et al., 2014)	4	Tmax	Asia	China	Cf, Cw, Dw	
Martin et al. (2012) (Martin et al., 2012)	13	Tmean	North America	Canada	Cf, Df	Halifax, Saskatoon omitted as no MMT similarity in temperature during study period found. For London GSOD data available only from 1980s, 30-year period adjusted.
McMichael et al. (2008) (McMichael et al., 2008)	11	Tmean	North America, Europe, Asia, South America, Africa	Brazil, Bulgaria, Chile, India, Mexico, Romania, Slovenia, South Africa, Thailand	Af, Aw, BS, Cf, Cs, Cw	
Montero et al. (2012) (Montero et al., 2012)	5	Tmax	Europe	Spain	Cs	For Albacete, Ciudad Real, Cuenca, Guadalajara, Toledo GSOD data available only from the 1970s on, 30-year period adjusted.
Perez et al. (2012) (Peretz et al., 2012)	1	ATmean	Asia	Israel	Cs	
Qiao et al. (2015) (Qiao et al., 2015)	1	Tmean	Oceania	Australia	Cf	
Revich and Shaposhnikov (2008) (Revich and Shaposhnikov, 2008)	1	Tmean	Europe	Russian Federation	Df	Monthly temperatures are used instead of daily temperatures
Seposo et al. (2015) (Seposo et al., 2016)	1	Tmean	Asia	Philippines	Af	
Sun et al. (2012) (Sun et al., 2012)	2	ATmean	Asia, Oceania	Australia, China	Cf, Dw	Cardivascular mortality
Wichmann (2017) (Wichmann, 2017)	3	ATmean	Africa	South Africa	Cf, Cs, Cw	
Williams et al. (2012) (Williams et al., 2012)	1	Tmean	Oceania	Australia	Cs	
Wu et al. (2013) (Wu et al., 2013)	4	Tmean	Asia	China	Cf	
Yang et al. (2015) (Yang et al., 2015)	15	Tmean	Asia	China	Cf, Cw, Dw	

B.2 Variables

B.2.1 Evidence on possible MMT drivers in literature

Climatic drivers. MMTs depend on the local climate (Ballester et al., 2011; Hajat and Kosatky, 2010). Higher MMTs are found for warmer cities closer to the equator compared to cooler ones in higher latitudes (Gosling et al., 2007; Hajat and Kosatky, 2010). In the US, southern cities are reported to have higher MMTs than northern cities (Curriero, 2002). This shows, that populations are in general acclimatised to their respective local climates (Hajat and Kosatky, 2010; Chung et al., 2015; Medina-Ramon and Schwartz, 2007; Guo et al., 2014; Harlan et al., 2014; Zaninović and Matzarakis, 2014; Guo et al., 2016; Tobías et al., 2017). Further, the annual temperature variability (Iñiguez et al., 2010; Zaninović and Matzarakis, 2014) and the humidity have been proposed, the latter either directly parameterised, e.g. (McMichael et al., 2008), or incorporated by using an humidity-adjusted metric, such as the AT or indices including humidity, e.g. the Heat Index (Kim et al., 2006) or the Discomfort Index (Peretz et al., 2012). No difference was found among both methods (Michelozzi et al., 2007).

Topographic, demographic and city-structural drivers. Topographic features, such as the distance to the nearest coast to account for a sea-breeze effect in coastal cities (Johansson and Emmanuel, 2006; Ng, 2012; Stewart et al., 2017), the elevation (Bai et al., 2016) and the latitude, e.g. (Hajat and Kosatky, 2010; Xiao et al., 2015) have been suggested as drivers of MMTs. Additionally, demographic and city-structural influences on the MMTs were found in previous studies. These were the population size (Medina-Ramon and Schwartz, 2007), and the city size (Oke, 1973) which is related to the urban heat island and consequently, the population density (Chen et al., 2016).

Socio-economic drivers. Socio-economic drivers influencing the MMTs are the Gross Domestic Product (GDP) per capita, annual mean income, poverty or savings indicators as well as deprivation and the GINI coefficient for income equality (Curriero, 2002; Hajat and Kosatky, 2010; Arbuthnott et al., 2016; Ng et al., 2016; Chung et al., 2017; Kim and Kim, 2017). The level of wealth gives indication on the capacity of populations to adapt to warm temperatures (e.g. air conditioning (AC), housing standards).

Drivers related to health status and age distribution. Health-related indicators also partly reflect the capacity to cope with elevated ambient temperatures, e.g. the share of households with access to safe water (Phung et al., 2016), the quality or access to health infrastructure (Kim and Kim, 2017), the number of hospital beds (Leone et al., 2013; Ng et al., 2016), the share of health expenditure of the GDP (Ha and Kim, 2013) or life expectancy (Leone et al., 2013) and could drive MMTs. Many studies identify the elderly as a vulnerable subpopulation, e.g. (Hajat and Kosatky, 2010; Iñiguez et al., 2010; Yu et al., 2012; Arbuthnott et al., 2016; Chen et al., 2016; Song et al., 2017; Wichmann, 2017).

B.2.2 Materials and datasets used to derive variables

Climate data. The Global Summary of the Day (GSOD), Version 7 (NOAA National Climatic Data Center, 2018) was chosen as a source for independent climate variables (See Appendix B.4, Table B.5) due to its comprehensive spatial and temporal coverage, although for some countries, constraints due to data restrictions have been noticed (NOAA National Climatic Data Center, 2018). We identified suitable climate stations within a ten kilometre radius to the cities' coordinates given by the Global Rural-Urban Mapping Project (GRUMP, Version 1) (Center for International Earth Science Information Network (CIESIN) at Columbia University et al., 2008) settlement points. We considered further away stations at airports due to their long time-series. Stations at buoys, lighthouses or beaches were neglected. The number of stations per city varies between one and eleven (See Appendix B.4, Table B.6). For most cities daily climate data was available from the 1940s or 1950s until 2018. We used homogenised series of the following surface meteorological elements in °C: (1) Daily mean temperatures, (2) Daily dew point temperatures, (3) Daily maximum temperatures, and (4) Daily minimum temperatures.

For the correlation and regression analysis, we calculate three climate variables per MMT case, characteristic for the local climate and supported by peer-reviewed literature. These are the 30-year averages of the daily mean temperature, the annual amplitude, and the monthly temperature maximum of each year. See Appendix B.2, Section B.2.3 for description, supporting references, and Appendix B.4, Table B.6 for data. Each variable is calculated from GSOD data within a 30-year period that ended five years before the observation period analysed in the respective heat-mortality study. Adjustments for this period were made for a few cities due to lacking data. To estimate MMTs for European settlements we use daily mean temperature values from the E-OBS data (Version 14) (Haylock et al., 2008). This 0.25 degree lat-long gridded climate data is available for entire Europe from January 1, 1950 until August 2016. We extract a 30-year period from January 1, 1981 to December 31, 2010 for all grid cells within Europe for the MMT approximation at city-level across Europe.

Topographic and demographic data. We extract topographic, demographic and city-structural regression variables via the city coordinates from the GRUMP settlement points (Center for International Earth Science Information Network (CIESIN) at Columbia University et al., 2008). The GRUMP (Version 1) coastline polygon shapefile (Center for International Earth Science Information Network (CIESIN) at Columbia University et al., 2008) allowed us to measure the cities' distances to the nearest coast in kilometres. The variable serves as proxy for comforting sea breezes. The cities' average elevation was extracted from a digital elevation model based on SRTM 90m data (Version 4) with approximately 90m spatial resolution (Jarvis et al., 2008). The cities' population density (year 2000) was derived from the Gridded Population of the World, Version 4, (GPW) (Center for International Earth Science Information Network (CIESIN) at Columbia University, 2016). See Appendix B.2 Section B.2.3 for methodology and Appendix B.4, Table B.5 for elevation data.

Socio-economic and development data. Socio-economic and development data at country-level are taken from World Bank Data (WBD). We employ the GDP per capita (in PPP, current international Dollars) (The World Bank, 2017a) as an indicator for overall welfare, and the GINI coefficient (The World Bank, 2017b) as a measure for inequality. For China, Japan, Switzerland, India, Korea, and New Zealand GINI data was available in the UNU-WIDER World Income Inequality Database (WIID) (World Income Inequality Database (WIID 3-4), 2017) and for Lebanon in Samad, 2008. Improved urban water sources and the percentage of urban population with access (The World Bank, 2017d) and the percentage of health expenditure of the GDP (The World Bank, 2017c) serve as development indicators. Likewise, we consider the life expectancy (The World Bank, 2017e) and the share of population > 65 years (The World Bank, 2017f) as indication of a population's health status. For our regression, we attribute the county-level data of the year 2000 to the respective cities, we use the average over the period from 1995 to 2000 for the GINI coefficient due to better data coverage. See Appendix B.4, Table B.5 for GDP/capita data.

B.2.3 Methodology to derive selected independent variables

1. **30-year average of daily mean temperature.** The average of daily mean temperature in °C within a period of 30 years indicates the temperature populations are generally exposed but also acclimatised to. A period of 30 years with a five year buffer to the start of the observation periods in the heat-mortality relationship studies was determined in GSOD data (NOAA National Climatic Data Center, 2018). Some cities were incompatible with this scheme. As their climate records do not date back so long, their 30-year periods adjusted as indicated in Appendix B.1. See Appendix B.4, Table B.5 for data.

2. **30-year average of the annual amplitude.** The average of the annual amplitude in °C (T_{mean}) within a period of 30 years serves as a measure of continentality. Each monthly average for this period was calculated. The annual amplitude was calculated by subtracting each year's monthly minimum from the monthly maximum temperature. The annual amplitudes for all 30 years were averaged. See Appendix B.4, Table B.5 for data.

3. **30-year average of the hottest month's temperature.** The average of the hottest month's temperature in °C (T_{mean}) over a period of 30 years are a measure of the magnitude of hot temperatures populations are exposed to once in a while. Annual monthly temperature maxima were averaged over 30 years in order to capture temperature extremes and the hottest month.

4. **Distance to the coast.** The distance from each GRUMP settlement point (Center for International Earth Science Information Network (CIESIN) at Columbia University et al., 2008) to the nearest coast in km indicates whether a comforting effect by a daytime sea breeze exists. We extracted the data from GIS by using the ACGIS10 Near-tool on the Homolosine Equal Area projection of settlement points layer (Center for International Earth Science Information Network (CIESIN) at Columbia University et al., 2008) and coastline polyline layer (European Environment Agency, 2013).

5. **Latitude.** The latitude has been employed as a explanatory variable before, e.g. in (Guo et al., 2013; Tobías et al., 2012) and a relationship between latitude and temperature was found. In another study, latitude was regressed on the

MMT in T_{mean} as an indication of climatic zones only (Hajat and Kosatky, 2010).

6. **Elevation in meters a.s.l.** The elevation in meters might have an effect on the heat-mortality relationship, as it has been reported before (Guo et al., 2013; Bai et al., 2016). We extract the elevation data within a 5 km buffer around the city coordinates from the elevation raster data (Jarvis et al., 2008) and average the cell values. See Appendix B.4, Table B.5 for data.

7. **Population Density.** The population density and temperature was found in Medina-Ramon and Schwartz, 2007; Hajat and Kosatky, 2010; Chen et al., 2016. A high population density likely leads to high mortality impact. Population density for the year 2000 was extracted for each city from the Gridded Population of the World, Version 4, (GPW) (Center for International Earth Science Information Network (CIESIN) at Columbia University, 2016). We use the average value for a 5 km buffer around the city coordinates.

Tab. B.2.: Summary of independent variables, supporting references and source datasets.

Type	Independent variables	Reference	Source Data
Climate	30-year average of daily mean temperature	e.g.Hajat and Kosatky, 2010; Iñiguez et al., 2010, Ballester et al., 2011; Guo et al., 2016	GSOD NOAA National Climatic Data Center, 2018
Climate	30-year average of annual amplitude	Iñiguez et al., 2010; Zaninović and Matzarakis, 2014	GSOD NOAA National Climatic Data Center, 2018
Climate	30-year average of hottest month's temperature	e.g. Kim et al., 2011; Peretz et al., 2012	GSOD NOAA National Climatic Data Center, 2018
Topography	Distance to coast	Johansson and Emmanuel, 2006; Ng, 2012; Guo et al., 2013; Stewart et al., 2017	CIESIN GRUMP Columbia University, 2018; Center for International Earth Science Information Network (CIESIN) at Columbia University et al., 2008
Topography	Latitude	e.g. Hajat and Kosatky, 2010; Guo et al., 2013; Xiao et al., 2015	CIESIN GRUMP Columbia University, 2018; Center for International Earth Science Information Network (CIESIN) at Columbia University et al., 2008
Topography	Elevation in meters a.s.l.	Guo et al., 2013; Bai et al., 2016	SRTM 90m DEM Jarvis et al., 2008
Demography	Population density	Medina-Ramon and Schwartz, 2007; Hajat and Kosatky, 2010; Chen et al., 2016	CIESIN GPW Columbia University, 2018; Center for International Earth Science Information Network (CIESIN) at Columbia University, 2016
Socio-economy	GDP per capita (current int. Dollars in PPP)	Hajat and Kosatky, 2010; Arbuthnott et al., 2016	WBOD The World Bank, 2017a
Socio-economy	GINI Coefficient	Ng et al., 2016	WBOD The World Bank, 2017b, WIID World Income Inequality Database (WIID 3-4), 2017, Samad, 2008
Socio-economy	Improved urban water source (% of urban population with access)	Phung et al., 2016	WBOD The World Bank, 2017d
Socio-economy	Health expenditure (% of GDP)	Ha and Kim, 2013	WBOD The World Bank, 2017c
Socio-economy	Life expectancy (at birth)	Leone et al., 2013	WBOD The World Bank, 2017e
Socio-economy	Share of population older 65 (%)	e.g.Hajat and Kosatky, 2010; Arbuthnott et al., 2016; Chen et al., 2016; Wichmann, 2017; Song et al., 2017	WBOD The World Bank, 2017f

B.3 The model

B.3.1 Schematic illustration of model variants tested

Fig. B.1.: Model variants tested in our analysis. We primarily carry out the analysis for the linear (A) and for the sigmoid (E) model variants, which are non-nested. To support our assumption of an upper and a lower limitation of the MMT, we test non-nested segmented linear models with an asymptote at the top (B), an asymptote at the bottom (C) and an asymptote at the top and bottom combined (D). The RMSE and the AICc continuously improve from the linear model (A) towards the sigmoid model variant (D).

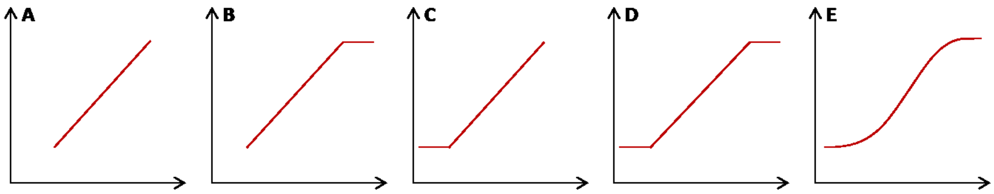

B.3.2 Standardisation parameters

Tab. B.3.: Mean and Standard Deviation of variables. Abbreviations: Tmean = 30-year mean temperature, Ampli = 30-year average of the annual amplitude, Elevation = elevation above sea level, GDP = GDP/capita in PPP, Urban Water = share of population with access to improved urban water sources in %.

Variable	Tmean	Ampli	Elevation	GDP	Urban Water
Mean	14.65318	19.97355	218.2881	24177.74	99.04625
Std. Deviation	5.575751	7.982493	321.5488	11894.17	1.593686

B.3.3 Discussion of variables not returned significant by the optimal sigmoid model

We found that the long-term average of the hottest month's temperature was not a relevant driver of our MMT sample considering our optimal model. Neither was the distance to the nearest coast even though it was reported to have a reductive effect on the heat burden in various cities (Ng, 2012; Stewart et al., 2017). As this variable is not particularly correlated with the annual amplitude ($\rho = 0.5$), this result might not be in conflict with our finding on the amplitude. Models including the distance to the coast instead of the amplitude did not show a lower AICc than those model setups without both variables.

Additionally, we did not find the population density to have significant influence on the MMTs. This is contrary to findings where the population size or density was reported as significant (Medina-Ramon and Schwartz, 2007; Guo et al., 2013) and to a recent study reporting the urbanisation level to be associated with decreased heat-related mortality risks and decreased vulnerability in China (Chen et al., 2016).

Our model does not support a significant influence of the GINI coefficient (Ng et al., 2016) as explanatory variable of MMTs. Socio-economic variables reflecting the population's health status or the capacity to react to elevated ambient temperatures are not represented in our model. This is contrary to studies reporting these factors significant, such as the share of households having access to safe water (Phung et al., 2016), quality or access to health infrastructure (Kim and Kim, 2017), number of hospital beds (Leone et al., 2013; Ng et al., 2016) or share of health expenditure of the GDP (Ha and Kim, 2013), and life expectancy (Leone et al., 2013). Indicators related to the age stratification of the population were not relevant in our model, even though many studies conclude that the elderly are one of the most vulnerable subpopulation (Hajat and Kosatky, 2010; Iñiguez et al., 2010; Yu et al., 2012; Arbuthnott et al., 2016; Chen et al., 2016; Song et al., 2017; Wichmann, 2017). These health and age characteristics are most likely already indirectly covered by other relevant overall development status variables, e.g. GDP per capita, a prevailing driver in our selected sigmoid model.

We did not find any confirmation for the relevance of the age distribution when testing the share of population older than 65 years for our MMT sample. Possibly, these health-related variables are already indirectly represented by other socio-economic variables in our model, which we assume according to high given collinearities. It is the share of health expenditure of the GDP being correlated with the GDP per capita ($\rho = 0.9$) as well as the share of population older 65 being correlated with the share of improved urban water sources ($\rho = 0.8$). The latter in return, is equally correlated with the life expectancy ($\rho = 0.8$). While both socio-economic variables are included in our most optimal model, the three health-related variables are not significant, but, however, contribute to the relevance of the socio-economic variables.

B.3.4 Discussion of minor uncertainties and limitations related to our findings and methods

Socio-economic variables may be employed either at country or city level. We chose to use the former due to a lack of comparable data at the city level, especially for smaller cities. Usually, country level data reflect the outcomes of national policies, e.g. the health status and age structure of populations, as well as the level of education and consequently the employment distribution among sectors. These factors contribute to and inform on a country's adaptive capacity and its ability for disaster response. In contrast to other drivers, these mechanisms are not limited to a location within a country and are not city-specific, even though some cities, but not all, have developed an adaptation plan to climate change (Reckien et al., 2015; Romero-Lankao and Gnatz, 2019). The employment of this data at the national level could possibly be a reason why indicators related to the health status of populations did not display such a strong signal in our optimal model.

An alternative approach to employing average long-term temperature is to use time series of temperature anomalies as input variable, which could be advantageous when attributing mortality for specific days or heat periods. Our choice is more indicative of the populations' current states of acclimatisation and consistent with the remaining climatic variables' time frame.

B.3.5 Model characterisation

We split the full dataset into a subset and the respective remaining data according to world regions (Figure B.2) and climate zones (Figure B.3). We use bootstrap estimates to derive lower and upper RMSE limits relating to a two-sided test at a 99% confidence level. We hypothesise that the RMSE values of the subsets are not significantly different from the RMSE values of the respective remaining datasets. As an example, we determine the RMSE for the model applied to the subset of all MMTs in Europe and compare it to the RMSE resulting from the model run on the remaining data that are not from Europe. We analyse the subsets for climate zones analogously.

Fig. B.2.: Model Characteristics for world regions. MMTs from each world region as independent sample of the remaining MMT data. Refer to Table B.4 to put the RMSE of each subset into context.

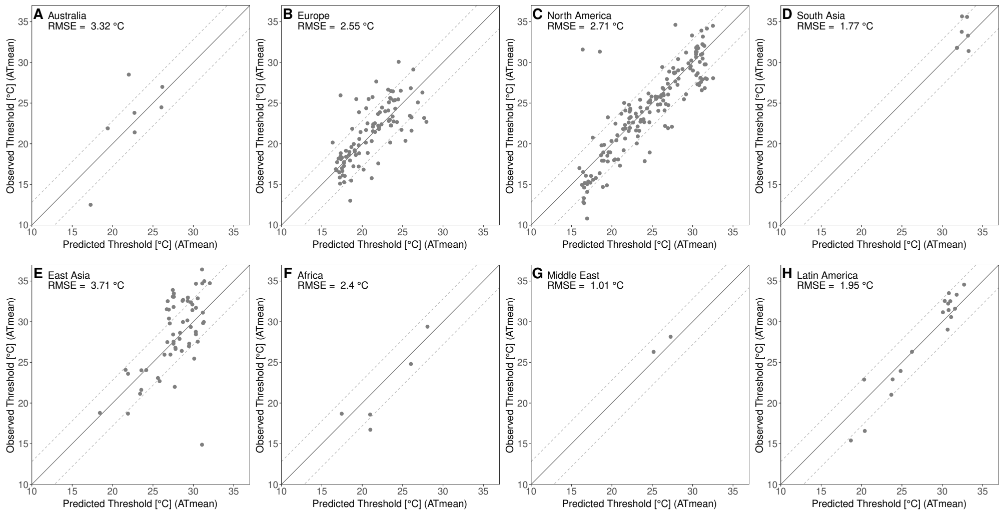

Tab. B.4.: Statistics according to world regions and climate zones. Subsets and their RMSE values in context of a 99% confidence level derived from the remaining data excluding the subset. World regions refer to Figure B.2, climate zones to Figure B.3.

Subset "World region"	Subset RMSE	Lower limit (P0.5)	Upper limit (P99.5)	Significant difference
Australia	3.32	0.81	6.79	no
Europe	2.55	2.05	4.08	no
North America	2.71	2.32	3.68	no
South Asia	1.77	0.85	6.79	no
East Asia	3.71	1.75	3.86	no
Africa	2.40	0.60	7.63	no
Middle East	1.01	0.13	11.46	no
Latin America	1.95	1.37	5.55	no

Subset "Climate zone"	Key	Subset RMSE	Lower limit (P0.5)	Upper limit (P99.5)	Significant difference
Mediterranean summer dry	Cs	2.70	1.97	4.11	no
Oceanic fully humid	Cf	2.18	2.30	4.12	yes
Tropical wet savanna	Aw	1.74	1.12	5.94	no
Continental winter dry	Dw	3.28	1.32	5.65	no
Continental fully humid	Df	3.36	1.90	3.85	no
Semi-arid steppe	BS	2.86	1.31	5.50	no
Subtropical winter dry	Cw	4.37	1.46	4.68	no
Tropical monsoonal	Am	1.94	0.74	7.10	no
Tropical rainforest	Af	2.93	0.51	8.36	no
Tropical dry savanna	As	2.66	0.11	11.46	no
Desert	Bw	3.80	0.01	15.19	no

Fig. B.3.: Model Characteristics for climate zones. MMTs from each climate zone as independent sample of the remaining MMT data. Refer to Table B.4 to put the RMSE of each subset into context.

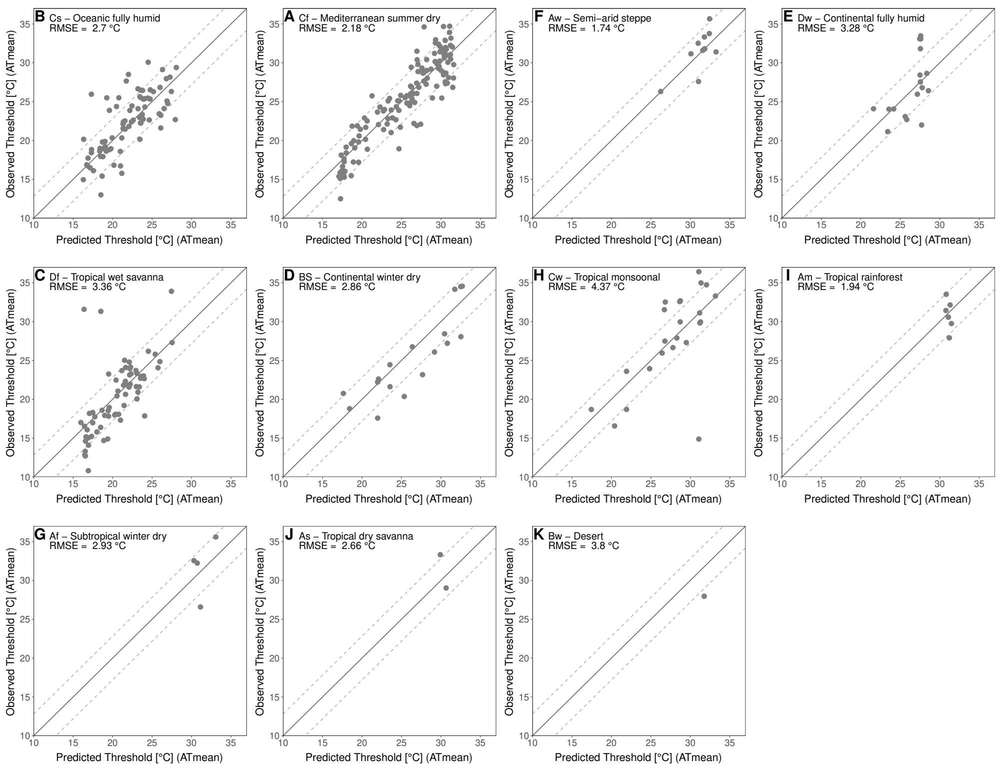

B.3.6 Model application: Estimation of MMTs for 599 European cities

Fig. B.4.: Cumulative population count per MMT class across all 599 European cities < 100 000 inhabitants included in the model application.

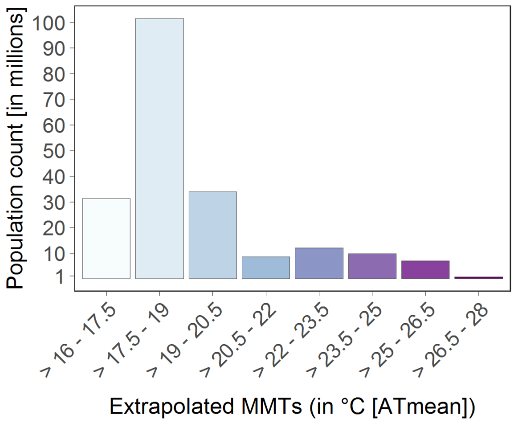

Fig. B.5.: Histograms for MMTs and the associated climate and socio-economic variables used in the model application for 599 European cities.

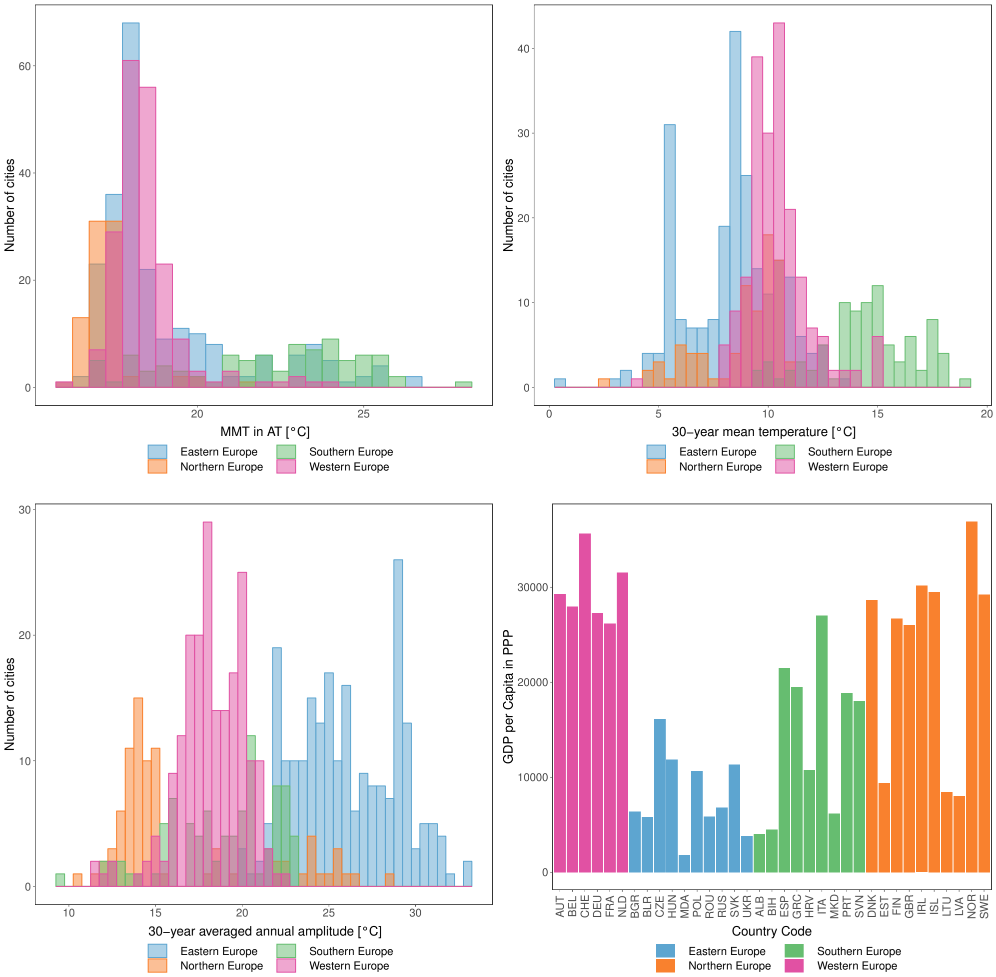

B.4 Data tables

Contents of the following appendix section:

Tab. B.5.: Cities, MMTs, and variables included in the analysis and meta information on each MMT case. Metric = original MMT metric in the study (daily mean or maximum temperatures Tmean, Tmax, and their apparent equivalents, ATmean and ATmax), MMT_{ori} = Original MMT in the study [°C], CZ = climate zone according to Köppen-Geiger classification, Start.SP and End.SP = start and end dates for respective MMT study period, Start30 and End30 = start and end dates for 30-year reference period, MMT_{AT} = to AT converted homogeneous MMT [°C], TMean = 30-year mean temperature [°C], Amp = 30-average of the annual amplitude [°C], T_{dewp} = dew point temperature [°C], Elev = elevation, GDP = GDP/capita in PPP, Water = share of urban population using safely managed drinking water services (%), Set = model calibration cases (M), validation sample cases (S)

Cities	ISO3	LAT	LON	Citation	Metric	MMT_{ori}	CZ	Start.SP	End.SP	Start30	End30	MMT_{AT}	TMean	Amp	T_{dewp}	Elev	GDP	Water	Set
Abbotsford	CAN	49.05	-122.33	Gasparrini et al. (2015)	Tmean	16.4	Cf	198601	200903	19510101	19811231	15.58	10.01	15.29	5.71	43	29185.4	100	M
Adelaide	AUS	-34.93	138.6	Williams et al. (2012)	Tmean	30	Cs	199310	200903	19580101	19881231	28.5	16.58	12.15	8.31	68	26374.7	100	M
Akron	USA	41.07	-81.52	Gasparrini et al. (2015)	Tmean	21.9	Df	198501	200612	19500101	19801231	23.32	10.1	27.5	4.04	312	36449.9	99.6	M
Albacete	ESP	39	-1.87	Gasparrini et al. (2015)	Tmean	22	Cs	199001	201009	19550101	19851231	21.45	14.54	21.05	6.27	685	21517.3	99.9	M
Albacete_a	ESP	39	-1.87	Montero et al. (2012)	Tmax	36	Cs	197501	200312	19730101	20031231	27.65	14.68	21	6.87	685	21517.3	99.9	M
Albuquerque	USA	35.11	-106.61	Gasparrini et al. (2015)	Tmean	24.2	BS	198501	200609	19500101	19801231	22.61	13.29	25.06	-1.63	1541	36449.9	99.6	M
Alicante	ESP	38.35	-0.48	Gasparrini et al. (2015)	Tmean	23.6	BS	199001	201012	19550101	19851231	24.99	17.58	14.51	10.94	57	21517.3	99.9	S
Allentown	USA	40.6	-75.48	Gasparrini et al. (2015)	Tmean	23.1	Df	198501	200612	19500101	19801231	25.08	10.87	26.46	4.7	116	36449.9	99.6	S
Almeria	ESP	36.83	-2.43	Gasparrini et al. (2015)	Tmean	24.1	Cs	199001	201012	19550101	19851231	26.52	18.31	13.9	12.02	54	21517.3	99.9	M
Anshan	CHN	41.12	122.99	Gasparrini et al. (2015)	Tmean	24.2	Dw	199601	200809	19610101	19911231	24.05	10.15	29.11	1.3	46	2933.3	97.2	M
Athens	GRC	37.98	23.73	Baccini et al. (2008)	ATmax	32.7	Cs	199204	199609	19570101	19871231	27.7	17.74	17.99	9.71	121	19503.9	99.8	S
Athens_a	GRC	37.98	23.73	Leone et al. (2013)	ATmax	31.7	Cs	199704	200409	19620101	19921231	26.83	17.68	18.33	9.63	121	19503.9	99.8	M
Atlanta	USA	33.76	-84.4	Curriero et al. (2002)	Tmean	24.61	Cf	197301	199412	19380101	19681231	27.66	16.41	20.66	9.91	291	36449.9	99.6	M
Atlanta_a	USA	33.76	-84.4	Gasparrini et al. (2015)	Tmean	25.6	Cf	198501	200612	19500101	19801231	28.74	16.08	21.1	9.76	291	36449.9	99.6	M
Atlantic	USA	39.36	-74.44	Gasparrini et al. (2015)	Tmean	23.1	Cf	198501	200609	19500101	19801231	25.8	12.07	24.07	6.79	3	36449.9	99.6	M
Austin	USA	30.3	-97.75	Gasparrini et al. (2015)	Tmean	28.3	Cf	198501	200609	19500101	19801231	32.24	20.1	20.37	12.86	184	36449.9	99.6	M
Avila	ESP	40.67	-4.7	Gasparrini et al. (2015)	Tmean	18.5	Cs	199001	201012	19550101	19851231	16.87	10.83	15.08	2.5	1101	21517.3	99.9	M
Badajoz	ESP	38.88	-6.97	Gasparrini et al. (2015)	Tmean	23.7	Cs	199001	201012	19550101	19851231	23.44	17.47	18.75	9.95	176	21517.3	99.9	M
Bakersfield	USA	35.36	-119.03	Gasparrini et al. (2015)	Tmean	29.2	BS	198501	200612	19500101	19801231	27.21	18.72	21.81	7.7	122	36449.9	99.6	M
Baltimore	USA	39.31	-76.62	Curriero et al. (2002)	Tmean	21.37	Cf	197301	199412	19380101	19681231	21.92	13.32	25.04	6.4	51	36449.9	99.6	M
Baltimore_a	USA	39.31	-76.62	Gasparrini et al. (2015)	Tmean	23.9	Cf	198501	200612	19500101	19801231	26.05	13.25	25.23	6.25	51	36449.9	99.6	M
Bangkok	THA	13.75	100.52	Gasparrini et al. (2015)	Tmean	29.9	Aw	199901	200812	19640101	19941231	35.66	28.33	4.81	22.68	2	7314.5	96.6	M
Bangkok_a	THA	13.75	100.52	McMichael et al. (2008)	Tmean	29	Aw	199101	199212	19560101	19861231	33.76	28.14	4.97	22.95	2	7314.5	96.6	M
Barcelona	ESP	41.4	2.17	Baccini et al. (2008)	ATmean	22.4	Cs	199204	200009	19570101	19871231	22.39	15.18	15.52	10.51	102	21517.3	99.9	M
Barcelona_a	ESP	41.4	2.17	Iniguez et al. (2010)	Tmean	20.32	Cs	199001	199612	19550101	19851231	21.54	15.21	15.38	10.51	102	21517.3	99.9	M
Barcelona_b	ESP	41.4	2.17	Leone et al. (2013)	ATmax	26.7	Cs	199104	200409	19560101	19861231	22.83	15.2	15.43	10.51	102	21517.3	99.9	S
Barcelona_c	ESP	41.4	2.17	Gasparrini et al. (2015)	Tmean	21	Cs	199001	201012	19550101	19851231	22.1	15.21	15.38	10.51	102	21517.3	99.9	M
Bari	ITA	41.12	16.87	Gasparrini et al. (2015)	Tmean	22.6	Cf	198701	201009	19520101	19821231	23.99	16.05	14.59	10.6	20	27006.4	100	M
Bari_a	ITA	41.12	16.87	Leone et al. (2013)	ATmax	30.1	Cf	199604	200409	19610101	19911231	25.09	15.97	15.64	10.5	20	27006.4	100	M
Barnstable	USA	41.66	-70.35	Gasparrini et al. (2015)	Tmean	22.2	Cf	198501	200612	19500101	19801231	24.31	10.75	22.61	5.52	19	36449.9	99.6	M
Batonrouge	USA	30.46	-91.14	Gasparrini et al. (2015)	Tmean	26.9	Cf	198501	200612	19500101	19801231	31.74	19.18	18.83	13.9	16	36449.9	99.6	M

Cities	ISO3	LAT	LON	Citation	Metric	MMT_{ori}	CZ	Start.SP	End.SP	Start30	End30	MMT_{AT}	TMean	Amp	T_{dewp}	Elev	GDP	Water	Set
Beijing	CHN	39.91	116.39	Sun et al. (2012)	ATmean	22	Dw	200501	200912	19700101	20001231	21.99	12.54	29.88	2.53	60	2933.3	97.2	M
Beijing_a	CHN	39.91	116.39	Gasparrini et al. (2015)	Tmean	25.5	Dw	199601	200812	19610101	19911231	28.43	12.35	29.94	2.48	60	2933.3	97.2	M
Beijing_b	CHN	39.91	116.39	Yang et al. (2015)	Tmean	24.9	Dw	200701	201312	19720101	20021231	26.8	12.56	29.99	2.54	60	2933.3	97.2	M
Beirut	LBN	33.87	35.51	El-Zein et al. (2004)	Tmean	27.5	Cs	199701	199912	19620101	19921231	31.68	19.64	12.73	13.48	42	9936.1	85.7	S
Belem	BRA	-1.45	-48.48	Gasparrini et al. (2015)	Tmean	26.7	Af	199701	201112	19620101	19921231	32.55	26.37	1.49	23.41	1	8987.2	97.6	M
Belohorizonte	BRA	-19.92	-43.93	Gasparrini et al. (2015)	Tmean	22.8	Cw	199701	201112	19620101	19921231	23.94	21.84	6.41	15.58	934	8987.2	97.6	M
Bilbao	ESP	43.25	-2.93	Gasparrini et al. (2015)	Tmean	19.6	Cf	199001	201012	19550101	19851231	19.81	14.64	12.98	9.02	153	21517.3	99.9	M
Bilbao_a	ESP	43.25	-2.93	Iniguez et al. (2010)	Tmean	17.58	Cf	199001	199612	19550101	19851231	17.2	14.64	12.98	9.02	153	21517.3	99.9	M
Birmingham	USA	33.52	-86.81	Gasparrini et al. (2015)	Tmean	25.6	Cf	198501	200609	19500101	19801231	29.18	16.77	21.14	10.59	193	36449.9	99.6	M
Bologna	ITA	44.5	11.34	Gasparrini et al. (2015)	Tmean	22.9	Cf	198701	201012	19520101	19821231	23.66	12.95	20.86	8.35	74	27006.4	100	M
Boston	USA	42.32	-71.09	Gasparrini et al. (2015)	Tmean	21.9	Df	198501	200612	19500101	19801231	22.94	10.67	25.33	3.94	27	36449.9	99.6	M
Boston_a	USA	42.32	-71.09	Curriero et al. (2002)	Tmean	20.95	Df	197301	199412	19380101	19681231	21.63	10.69	24.17	3.97	27	36449.9	99.6	M
Boston_b	USA	42.32	-71.09	Gosling et al. (2007)	Tmax	26	Df	197506	199808	19400601	1970831	20.04	10.69	24.33	3.99	27	36449.9	99.6	M
Brasilia	BRA	-15.78	-47.92	Gasparrini et al. (2015)	Tmean	22.9	Aw	199701	201112	19620101	19921231	24.29	20.96	4.68	14.86	1081	8987.2	97.6	S
Brescia	ITA	45.55	10.22	Gasparrini et al. (2015)	Tmean	22	Cf	198701	201008	19520101	19821231	22.51	12.4	20.28	8.73	208	27006.4	100	M
Brisbane	AUS	-27.46	153.02	Gasparrini et al. (2015)	Tmean	22.8	Cf	198801	200912	19530101	19831231	24.48	20.16	10.46	13.85	27	26374.7	100	M
Brisbane_a	AUS	-27.46	153.02	Sun et al. (2012)	ATmean	27	Cf	200401	200712	19690101	19991231	26.99	20.11	10.79	13.97	27	26374.7	100	M
Brisbane_b	AUS	-27.46	153.02	Qiao et al. (2015)	Tmean	28.4	Cf	199612	200402	19611201	1991231	31.77	20.15	10.58	13.93	27	26374.7	100	S
Brownsville	USA	25.93	-97.48	Gasparrini et al. (2015)	Tmean	26.9	Cf	198501	200609	19500101	19801231	32.03	22.77	13.84	17.84	8	36449.9	99.6	M
Bucharest	ROU	44.44	26.1	McMichael et al. (2008)	Tmean	22	Cf	199401	199712	19590101	19891231	22.67	10.59	25.6	6.59	73	5873.5	96.6	M
Budapest	HUN	47.5	19.08	Baccini et al. (2008)	ATmax	22.8	Cf	199204	200109	19570101	19871231	17.23	10.38	21.64	5.3	102	11843.5	99.2	M
Budapest_a	HUN	47.5	19.08	Gosling et al. (2007)	Tmax	28	Cf	197006	200008	19350601	1965831	21.84	10.46	20.98	5.35	102	11843.5	99.2	M
Buffalo	USA	42.9	-78.85	Gasparrini et al. (2015)	Tmean	21.1	Df	198501	200608	19500101	19801231	21.89	8.85	27.13	3.65	193	36449.9	99.6	M
Burgos	ESP	42.35	-3.69	Gasparrini et al. (2015)	Tmean	17.8	Cs	199001	201012	19550101	19851231	16.49	10.71	17.53	5	889	21517.3	99.9	M
Busan	KOR	35.1	129.04	Gasparrini et al. (2015)	Tmean	28.7	Cf	199201	201012	19570101	19871231	34.46	13.94	25.39	8.48	94	18083.1	98.1	S
Caceres	ESP	39.47	-6.38	Gasparrini et al. (2015)	Tmean	23.2	Cs	199001	201009	19550101	19851231	22.24	16.19	19.16	6.71	415	21517.3	99.9	M
Cadiz	ESP	36.53	-6.29	Gasparrini et al. (2015)	Tmean	22.8	Cs	199001	201012	19550101	19851231	24.31	17.79	13.71	11.26	12	21517.3	99.9	M
Calgary	CAN	51.07	-114.06	Martin et al. (2012)	Tmean	14.8	Df	198101	200012	19460101	19761231	12.83	4	27.07	-2.87	1081	29185.4	100	M
Calgary_a	CAN	51.07	-114.06	Gasparrini et al. (2015)	Tmean	14.7	Df	198601	200912	19510101	19811231	12.7	4.08	27.89	-3.04	1081	29185.4	100	M
Cantonmassillon	USA	40.8	-81.38	Gasparrini et al. (2015)	Tmean	22.8	Df	198501	200612	19500101	19801231	24.79	9.83	26.47	4.33	335	36449.9	99.6	M
Capetown	ZAF	-33.93	18.42	McMichael et al. (2008)	Tmean	17	Cs	199601	199912	19610101	19911231	16.72	17.16	8.6	12.65	22	7702.5	98.5	M
Capetown_a	ZAF	-33.93	18.42	Wichmann (2017)	ATmean	18.6	Cs	200601	201012	19710101	20011231	18.59	17.1	8.69	12.44	22	7702.5	98.5	M
Castellon	ESP	39.98	-0.03	Gasparrini et al. (2015)	Tmean	23.3	BS	199001	201012	19550101	19851231	23.64	17.98	15.66	11.05	37	21517.3	99.9	S
Castellon_a	ESP	39.98	-0.03	Iniguez et al. (2010)	Tmean	19.9	BS	199001	199612	19550101	19851231	20.36	17.98	15.66	11.05	37	21517.3	99.9	M
Changchun	CHN	43.88	125.32	Yang et al. (2015)	Tmean	20.6	Dw	200701	201312	19720101	20021231	21.24	5.86	38.51	-1.68	1913	2933.3	97.2	S
Changsha	CHN	28.2	112.97	Huang et al. (2017)	Tmean	29	Cf	200801	201112	19730101	20031231	34.67	17.47	24.33	13.69	74	2933.3	97.2	M
Changsha_a	CHN	28.2	112.97	Bao et al. (2016)	Tmean	26.9	Cf	200801	201112	19730101	20031231	31.71	17.47	24.33	13.69	74	2933.3	97.2	M
Changsha_b	CHN	28.2	112.97	Wu et al. (2013)	Tmean	25	Cf	200601	200912	19710101	20011231	28.45	17.45	24.36	13.68	74	2933.3	97.2	M
Changsha_c	CHN	28.2	112.97	Yang et al. (2015)	Tmean	25.1	Cf	200701	201312	19720101	20021231	28.76	17.46	24.29	13.7	74	2933.3	97.2	M
Charleston	USA	32.79	-79.99	Gasparrini et al. (2015)	Tmean	22.8	Cf	198501	200612	19500101	19801231	25.09	12.68	23.73	6.6	258	36449.9	99.6	M

Cities	ISO3	LAT	LON	Citation	Metric	MMT_{ori}	CZ	Start.SP	End.SP	Start30	End30	MMT_{AT}	TMean	Amp	T_{dewp}	Elev	GDP	Water	Set
Charlotte	USA	35.21	-80.83	Gasparrini et al. (2015)	Tmean	26.1	Cf	198501	200609	19500101	19801231	29.32	15.6	21.69	8.83	216	36449.9	99.6	M
Charlotte_a	USA	35.21	-80.83	Curriero et al. (2002)	Tmean	32.43	Cf	197301	199412	19380101	19681231	34.62	15.96	21.35	9.1	216	36449.9	99.6	M
Chattanooga	USA	35.05	-85.27	Gasparrini et al. (2015)	Tmean	25.3	Cf	198501	200612	19500101	19801231	28.67	15.2	22.97	9.37	223	36449.9	99.6	M
Chengdu	CHN	30.67	104.07	Yang et al. (2015)	Tmean	24.1	Cw	200701	201312	19720101	20021231	26.65	16.46	20.17	12.85	21	2933.3	97.2	M
Chiangmai	THA	18.79	98.98	Gasparrini et al. (2015)	Tmean	27.9	Aw	199901	200808	19640101	19941231	31.79	25.57	8.87	18.66	335	7314.5	96.6	M
Chiangmai_a	THA	18.79	98.98	McMichael et al. (2008)	Tmean	28	Aw	199501	199712	19600101	19901231	31.79	25.57	9.01	18.77	335	7314.5	96.6	M
Chicago	USA	41.84	-87.68	Curriero et al. (2002)	Tmean	18.43	Df	197301	199412	19380101	19681231	17.86	10.09	28.5	4.22	180	36449.9	99.6	M
Chicago_a	USA	41.84	-87.68	Gasparrini et al. (2015)	Tmean	24.7	Df	198501	200612	19500101	19801231	26.18	10.11	29.29	4.12	180	36449.9	99.6	M
Chisinau	MDA	47.01	28.86	Corobov et al. (2013)	Tmean	22	Cf	200004	200809	19650101	19951231	22.05	9.74	25.13	4.04	83	1839.7	96.7	M
Chongqing	CHN	29.56	106.55	Li et al. (2014)	Tmax	34	Cf	201109	201209	19760901	2006931	29.35	18.13	21.3	14.17	157	2933.3	97.2	M
Chongqing_a	CHN	29.56	106.55	Yang et al. (2015)	Tmean	29.2	Cf	201101	201312	19760101	20061231	32.38	18.15	21.3	14.16	157	2933.3	97.2	M
Christchurch	NZL	-43.53	172.64	Hales et al. (2000)	Tmax	20.5	Cf	198806	199312	19530101	19831231	12.5	11.42	11.63	6.94	9	21509.8	100	M
Cincinnati	USA	39.14	-84.5	Gasparrini et al. (2015)	Tmean	23.3	Cf	198501	200609	19500101	19801231	25.74	12.25	26.79	6.73	187	36449.9	99.6	M
Ciudadreal	ESP	38.98	-3.94	Montero et al. (2012)	Tmax	35	Cs	197501	200312	19730101	20031231	26.65	15.41	21.67	6.92	628	21517.3	99.9	M
Ciudadreal_a	ESP	38.98	-3.94	Gasparrini et al. (2015)	Tmean	23.6	Cs	199001	201012	19550101	19851231	22.52	14.46	20.86	6.65	628	21517.3	99.9	M
Civitavecchia	ITA	42.1	11.8	Gasparrini et al. (2015)	Tmean	23.1	Cs	198701	201009	19520101	19821231	25.5	18.56	4.76	12.75	102	27006.4	100	M
Cleveland	USA	41.48	-81.67	Gasparrini et al. (2015)	Tmean	21.9	Df	198501	200609	19500101	19801231	23.01	10.7	26.84	5.23	198	36449.9	99.6	M
Columbia	USA	34.02	-81.01	Gasparrini et al. (2015)	Tmean	26.4	Cf	198501	200612	19500101	19801231	29.89	17.33	20.88	10.72	77	36449.9	99.6	M
Columbus	USA	32.49	-84.94	Gasparrini et al. (2015)	Tmean	23.6	Cf	198501	200612	19500101	19801231	25.1	11.35	26.58	5.68	240	36449.9	99.6	M
Cordoba	ESP	37.88	-4.77	Gasparrini et al. (2015)	Tmean	25	Cs	199001	201009	19550101	19851231	25.08	17.82	19.47	10.75	131	21517.3	99.9	M
Cuenca	ESP	40.08	-2.14	Montero et al. (2012)	Tmax	32	Cs	197501	200312	19730101	2004131	23.88	13.68	20.5	4.96	1001	21517.3	99.9	M
Cuenca_a	ESP	40.08	-2.14	Gasparrini et al. (2015)	Tmean	20.6	Cs	199001	201012	19550101	19851231	18.62	13.22	20.52	4.57	1001	21517.3	99.9	M
Cuiaba	BRA	-15.58	-56.08	Gasparrini et al. (2015)	Tmean	28.1	Aw	199701	201112	19620101	19921231	31.6	27.32	5.22	19.84	177	8987.2	97.6	M
Curitiba	BRA	-25.42	-49.25	Gasparrini et al. (2015)	Tmean	21.3	Cf	199701	201112	19620101	19921231	22.89	17.16	9.05	13.59	917	8987.2	97.6	M
Daegu	KOR	35.87	128.6	Gasparrini et al. (2015)	Tmean	26.4	Cw	199201	201009	19570101	19871231	29.96	13.55	28.31	6.85	51	18083.1	98.1	M
Daegu_a	KOR	35.87	128.6	Kim et al. (2006)	Tmean	28.1	Cw	199406	200308	19590101	19891231	32.57	13.59	28.08	6.87	51	18083.1	98.1	M
Daegu_b	KOR	35.87	128.6	Ha et al. (2011)	Tmean	28.2	Cw	199101	200812	19560101	19861231	32.68	13.53	28.4	6.85	51	18083.1	98.1	M
Daegu_c	KOR	35.87	128.6	Kim et al. (2011)	Tmean	24.36	Cw	200106	200809	19660101	19961231	26.73	13.71	27.45	6.7	51	18083.1	98.1	S
Daejeon	KOR	36.32	127.42	Kim et al. (2006)	Tmean	28.1	Df	199406	200308	19590101	19891231	33.9	12.26	29	6.97	86	18083.1	98.1	M
Daejeon_a	KOR	36.32	127.42	Gasparrini et al. (2015)	Tmean	24.1	Df	199201	201012	19570101	19871231	27.3	12.23	29.24	6.98	86	18083.1	98.1	M
Dallas	USA	32.8	-96.79	Gasparrini et al. (2015)	Tmean	27.8	Cf	198501	200612	19500101	19801231	29.76	19.39	23.84	11.18	148	36449.9	99.6	M
Dallas_a	USA	32.8	-96.79	Gosling et al. (2007)	Tmax	34	Cf	197506	199808	19400601	1970831	28.04	19.42	23.63	11.28	148	36449.9	99.6	M
Dayton	USA	39.76	-84.2	Gasparrini et al. (2015)	Tmean	22.5	Cf	198501	200612	19500101	19801231	23.88	11.22	27.17	5.45	240	36449.9	99.6	M
Daytonabeach	USA	29.21	-81.04	Gasparrini et al. (2015)	Tmean	26.9	Cf	198501	200612	19500101	19801231	31.75	21.56	13.67	16.28	5	36449.9	99.6	M
Delhi	IND	28.64	77.21	McMichael et al. (2008)	Tmean	29	Cw	199101	199412	19560101	19861231	33.29	24.83	20	14.17	218	1998.5	92.3	M
Denver	USA	39.73	-104.97	Gasparrini et al. (2015)	Tmean	21.1	BS	198501	200612	19500101	19801231	20.75	11.82	16.67	6.22	1614	36449.9	99.6	M
Desmoines	USA	41.59	-93.62	Gasparrini et al. (2015)	Tmean	22.5	Df	198501	200612	19500101	19801231	24.05	9.97	32.35	3.81	267	36449.9	99.6	M
Detroit	USA	42.39	-83.1	Gasparrini et al. (2015)	Tmean	23.9	Df	198501	200609	19500101	19801231	25.5	10.23	27.94	3.81	197	36449.9	99.6	S
Dhaka	BGD	23.72	90.41	Burkart et al. (2011)	Tmean	29.4	Aw	200301	200712	19680101	19981231	31.4	25.81	10.86	20.42	81	1304.4	83.2	M
Dublin	IRL	53.33	-6.25	Baccini et al. (2008)	ATmax	23.9	Cf	199004	200009	19550101	19851231	18.87	9.63	11.53	6.49	20	30155.3	95.9	M

Cities	ISO3	LAT	LON	Citation	Metric	MMT_{ori}	CZ	Start.SP	End.SP	Start30	End30	MMT_{AT}	TMean	Amp	T_{dewp}	Elev	GDP	Water	Set
Durban	ZAF	-29.85	31.02	Wichmann (2017)	ATmean	24.8	Cf	200601	201012	19710101	20011231	24.8	21.32	7.92	16.54	49	7702.5	98.5	M
Edmonton	CAN	53.55	-113.57	Martin et al. (2012)	Tmean	12.8	Df	198101	200012	19460101	19761231	10.81	2.46	33.09	-2.61	666	29185.4	100	M
Edmonton_a	CAN	53.55	-113.57	Gasparrini et al. (2015)	Tmean	15.6	Df	198601	200909	19510101	19811231	14.09	2.82	32.34	-2.52	666	29185.4	100	M
Elpaso	USA	31.79	-106.42	Gasparrini et al. (2015)	Tmean	27.5	Bw	198501	200612	19500101	19801231	25.36	17.95	22.43	1.52	1174	36449.9	99.6	S
Erie	USA	42.11	-80.08	Gasparrini et al. (2015)	Tmean	23.1	Df	198501	200612	19500101	19801231	25.02	9.24	26.05	4.31	222	36449.9	99.6	M
Flint	USA	43.03	-83.69	Gasparrini et al. (2015)	Tmean	22.5	Df	198501	200609	19500101	19801231	24.09	8.72	27.69	3.45	232	36449.9	99.6	M
Fortaleza	BRA	-3.78	-38.59	Gasparrini et al. (2015)	Tmean	26.9	As	199701	201112	19620101	19921231	31.73	27.24	1.67	23.09	29	8987.2	97.6	S
Fortlauderdale	USA	26.14	-80.14	Gasparrini et al. (2015)	Tmean	26.1	Am	198501	200612	19500101	19801231	29.75	24.48	9.71	18.71	3	36449.9	99.6	M
Fortmyers	USA	26.63	-81.86	Gasparrini et al. (2015)	Tmean	24.2	Cf	198501	200609	19500101	19801231	27.39	22.9	10.75	17.81	3	36449.9	99.6	M
Fortpiercenorth	USA	27.44	-80.34	Gasparrini et al. (2015)	Tmean	23.9	Cf	198501	200609	19850101	20051231	27.31	22.8	10.26	18.03	3	36449.9	99.6	M
Fortworth	USA	32.74	-97.33	Gasparrini et al. (2015)	Tmean	27.8	Cf	198501	200612	19500101	19801231	31.06	18.67	23.85	10.14	180	36449.9	99.6	M
Fresno	USA	36.78	-119.79	Gasparrini et al. (2015)	Tmean	26.9	BS	198501	200612	19500101	19801231	26.08	16.86	21.39	8.13	95	36449.9	99.6	M
Frosinone	ITA	41.65	13.35	Gasparrini et al. (2015)	Tmean	22.1	Cf	198701	201012	19520101	19821231	22.81	14.9	19.38	9.14	211	27006.4	100	M
Fuzhou	CHN	26.06	119.31	Gasparrini et al. (2015)	Tmean	27.6	Cf	199601	200812	19610101	19911231	32.87	19.81	18.95	15.12	20	2933.3	97.2	M
Galveston	USA	29.28	-94.83	Gasparrini et al. (2015)	Tmean	28.3	Cf	198501	200609	19500101	19801231	33.17	20.92	17.5	16.15	2	36449.9	99.6	M
Gary	USA	41.58	-87.35	Gasparrini et al. (2015)	Tmean	23.9	Df	198501	200608	19850101	20051231	25.41	11.56	27.98	5.59	183	36449.9	99.6	S
Genoa	ITA	44.42	8.93	Gasparrini et al. (2015)	Tmean	22.4	Cs	198701	201012	19520101	19821231	23.87	15.22	16.12	9.2	144	27006.4	100	M
Gijon	ESP	43.53	-5.67	Iniguez et al. (2010)	Tmean	15.9	Cf	199001	199612	19550101	19851231	15.47	13.99	11.1	10.06	36	21517.3	99.9	M
Girona	ESP	41.98	2.81	Gasparrini et al. (2015)	Tmean	21	Cf	199001	201008	19550101	19851231	21.69	13.87	16.9	8.91	115	21517.3	99.9	M
Goiania	BRA	-16.67	-49.27	Gasparrini et al. (2015)	Tmean	24.2	Aw	199701	201109	19620101	19921231	26.3	23.29	4.53	16.5	792	8987.2	97.6	M
Granada	ESP	37.17	-3.59	Gasparrini et al. (2015)	Tmean	23	Cs	199001	201012	19550101	19851231	22.39	15.74	19.94	6.6	733	21517.3	99.9	M
Grandrapids	USA	42.96	-85.66	Gasparrini et al. (2015)	Tmean	22.5	Df	198501	200612	19500101	19801231	23.95	8.61	28.87	3.69	210	36449.9	99.6	M
Greensboro	USA	36.08	-79.82	Gasparrini et al. (2015)	Tmean	26.1	Cf	198501	200612	19500101	19801231	29.43	14.26	22.6	8.04	257	36449.9	99.6	M
Greenville	USA	34.84	-82.39	Gasparrini et al. (2015)	Tmean	24.7	Cf	198501	200612	19500101	19801231	26.85	16.12	20.1	9.04	299	36449.9	99.6	M
Guadalajara	ESP	40.64	-3.17	Gasparrini et al. (2015)	Tmean	20.4	Cs	199001	201009	19550101	19851231	18.83	14.13	9	6.4	688	21517.3	99.9	M
Guadalajara_a	ESP	40.64	-3.17	Montero et al. (2012)	Tmax	35	Cs	197501	200312	19750201	2006231	25.49	14.92	14.64	6.46	688	21517.3	99.9	M
Guangzhou	CHN	23.12	113.25	Gasparrini et al. (2015)	Tmean	28.7	Cw	199601	200809	19610101	19911231	34.27	22.1	15.97	17.31	14	2933.3	97.2	S
Guangzhou_a	CHN	23.12	113.25	Wu et al. (2013)	Tmean	26	Cw	200601	201012	19710101	20011231	29.96	22.28	15.72	17.31	14	2933.3	97.2	M
Guangzhou_b	CHN	23.12	113.25	Yang et al. (2015)	Tmean	29	Cw	201101	201312	19760101	20061231	34.98	22.42	15.64	17.18	14	2933.3	97.2	M
Guilin	CHN	25.28	110.29	Bao et al. (2016)	Tmean	24.5	Cf	200801	201112	19730101	20031231	27.55	19.1	20.65	14.1	9	2933.3	97.2	M
Haikou	CHN	20.05	110.34	Huang et al. (2017)	Tmean	30	Cw	200801	201112	19730101	20031231	36.42	24.21	11.42	21.11	248	2933.3	97.2	M
Haikou_a	CHN	20.05	110.34	Bao et al. (2016)	Tmean	15	Cw	200801	201112	19730101	20031231	14.88	24.21	11.42	21.11	248	2933.3	97.2	M
Halifax	CAN	44.62	-63.69	Gasparrini et al. (2015)	Tmean	16.4	Df	198601	200912	19510101	19811231	16.07	5.47	20.94	2.03	90	29185.4	100	M
Hamilton_CA	CAN	43.27	-79.92	Gasparrini et al. (2015)	Tmean	18.2	Df	198601	200909	19510101	19811231	18.07	8.8	28.44	3.19	144	29185.4	100	M
Hamilton_CA_a	CAN	43.27	-79.92	Martin et al. (2012)	Tmean	17.5	Df	198101	200012	19460101	19761231	17.31	9.16	28.06	3.67	144	29185.4	100	M
Hamilton_US	USA	39.4	-84.56	Gasparrini et al. (2015)	Tmean	23.6	Cf	198501	200609	19990101	20101231	25.75	12.25	26.21	6.54	208	36449.9	99.6	M
Hangzhou	CHN	30.26	120.17	Gasparrini et al. (2015)	Tmean	27	Cf	199601	200809	19610101	19911231	32.12	16.55	24.91	12.19	18	2933.3	97.2	M
Harbin	CHN	45.75	126.65	Li et al. (2014)	Tmax	29	Dw	200806	201008	19730601	2003831	24.03	4.64	41.52	-2.37	29	2933.3	97.2	M
Harbin_a	CHN	45.75	126.65	Yang et al. (2015)	Tmean	20.6	Dw	200701	201312	19720101	20021231	21.14	4.47	41.65	-2.52	29	2933.3	97.2	M
Harrisburg	USA	40.27	-76.88	Gasparrini et al. (2015)	Tmean	23.9	Cf	198501	200609	19500101	19801231	25.52	11.85	26.3	5.07	114	36449.9	99.6	M

Cities	ISO3	LAT	LON	Citation	Metric	MMT_{ori}	CZ	Start.SP	End.SP	Start30	End30	MMT_{AT}	TMean	Amp	T_{dewp}	Elev	GDP	Water	Set
Hartford	USA	41.76	-72.69	Gasparrini et al. (2015)	Tmean	21.4	Df	198501	200612	19500101	19801231	21.59	10.65	24.98	4.51	27	36449.9	99.6	M
Hefei	CHN	31.86	117.28	Huang et al. (2017)	Tmean	29	Cf	200801	201112	19730101	20031231	35.61	16.17	25.73	10.98	47	2933.3	97.2	S
Helsinki	FIN	60.17	24.94	Baccini et al. (2008)	ATmax	23.6	Df	199004	200009	19550101	19851231	18.18	4.78	25.23	1.31	18	26732.3	100	M
Hongkong	HKG	22.28	114.15	Gasparrini et al. (2015)	Tmean	28.6	Cw	199601	200812	19610101	19911231	34.73	23.18	13.47	18.43	3	26962.7	98	M
Honolulu	USA	21.31	-157.83	Gasparrini et al. (2015)	Tmean	29.2	As	198501	200609	19500101	19801231	33.31	24.62	4.49	18.34	141	36449.9	99.6	M
Houston	USA	29.76	-95.38	Gasparrini et al. (2015)	Tmean	25.3	Cf	198501	200609	19500101	19801231	29	19.79	15.99	13.99	15	36449.9	99.6	M
Huelva	ESP	37.25	-6.94	Iniguez et al. (2010)	Tmean	21.8	Cs	199001	199612	19550101	19851231	21.61	18.59	15.38	10.61	13	21517.3	99.9	M
Huelva	ESP	37.25	-6.94	Gasparrini et al. (2015)	Tmean	23.6	Cs	199001	201012	19550101	19851231	23.24	18.59	15.38	10.61	13	21517.3	99.9	M
Huesca	ESP	42.14	-0.41	Gasparrini et al. (2015)	Tmean	21.2	Cf	199001	201009	19550101	19851231	20.14	13.84	19.02	5.57	470	21517.3	99.9	M
Incheon	KOR	37.45	126.73	Gasparrini et al. (2015)	Tmean	24.1	Cw	199201	201009	19570101	19871231	27.49	11.72	28.69	6.2	34	18083.1	98.1	M
Incheon_a	KOR	37.45	126.73	Kim et al. (2006)	Tmean	26.6	Cw	199406	200308	19590101	19891231	31.53	11.76	28.47	6.19	34	18083.1	98.1	M
Incheon_b	KOR	37.45	126.73	Ha et al. (2011)	Tmean	27.1	Cw	199101	200812	19560101	19861231	32.52	11.72	28.78	6.2	34	18083.1	98.1	M
Indianapolis	USA	39.79	-86.15	Gasparrini et al. (2015)	Tmean	23.6	Df	198501	200612	19500101	19801231	25.8	11.46	27.77	6.04	222	36449.9	99.6	M
Istanbul	TUR	41.02	28.96	Leone et al. (2013)	ATmax	30.7	Cs	199204	199509	19570101	19871231	26.29	14.18	19.17	8.91	270	9351.5	96.8	M
Jacksonville	USA	30.32	-81.66	Gasparrini et al. (2015)	Tmean	26.7	Cf	198501	200612	19500101	19801231	31.3	20.25	16.25	14.76	9	36449.9	99.6	M
Jacksonville_a	USA	30.32	-81.66	Curriero et al. (2002)	Tmean	24.86	Cf	197301	199412	19380101	19681231	28.67	20.57	15.91	15.01	9	36449.9	99.6	M
Jaen	ESP	37.77	-3.8	Gasparrini et al. (2015)	Tmean	24	Cs	199001	201012	19550101	19851231	23.35	24.18	0.94	10.74	612	21517.3	99.9	M
Jersey	USA	40.72	-74.07	Gasparrini et al. (2015)	Tmean	24.2	Cf	198501	200612	19500101	19801231	26.15	12.41	25.94	5.53	11	36449.9	99.6	M
Jinan	CHN	36.67	117	Yang et al. (2015)	Tmean	24.9	Cw	201101	201312	19760101	20061231	27.3	14.92	28.01	5.07	43	2933.3	97.2	M
Joaopessoa	BRA	-7.12	-34.87	Gasparrini et al. (2015)	Tmean	27.1	Am	199701	201112	19620101	19921231	31.43	26.36	3.16	22.19	4	8987.2	97.6	M
Johannesburg	ZAF	-26.2	28.08	Wichmann (2017)	ATmean	18.7	Cw	200601	201012	19710101	20011231	18.69	15.94	10.4	6.7	1691	7702.5	98.5	M
Kansas	USA	39.08	-94.56	Gasparrini et al. (2015)	Tmean	23.9	Cf	198501	200612	19500101	19801231	25.47	13.49	30.08	5.94	265	36449.9	99.6	M
Kingston	CAN	44.29	-76.51	Gasparrini et al. (2015)	Tmean	18	Df	198601	200909	19850101	20051231	17.98	7.9	29.3	3.3	108	29185.4	100	M
Kitchener	CAN	43.44	-80.51	Gasparrini et al. (2015)	Tmean	18.1	Df	198601	200903	19510101	19811231	18.07	8.04	30.65	3.35	344	29185.4	100	M
Knoxville	USA	35.97	-83.94	Gasparrini et al. (2015)	Tmean	24.4	Cf	198501	200612	19500101	19801231	27.38	14.82	22.79	8.81	302	36449.9	99.6	M
Kunming	CHN	25.04	102.72	Wu et al. (2013)	Tmean	19	Cw	200601	200912	19710101	20011231	18.7	15.32	12.29	9.27	69	2933.3	97.2	M
Kunming_a	CHN	25.04	102.72	Yang et al. (2015)	Tmean	23.3	Cw	200701	201312	19720101	20021231	23.6	15.33	12.28	9.27	69	2933.3	97.2	M
Kwangju	KOR	35.15	126.92	Gasparrini et al. (2015)	Tmean	25.9	Cf	199201	201009	19570101	19871231	29.79	11.58	29.98	6.16	93	18083.1	98.1	M
Lacoruna	ESP	43.33	-8.42	Gasparrini et al. (2015)	Tmean	18.7	Cs	199001	201009	19550101	19851231	18.99	14.14	10.18	10.02	76	21517.3	99.9	M
Lakeland	USA	28.04	-81.96	Gasparrini et al. (2015)	Tmean	26.1	Cf	198501	200612	19850101	20051231	29.51	23.35	12.17	16.42	46	36449.9	99.6	S
Lancaster	USA	34.69	-118.15	Gasparrini et al. (2015)	Tmean	24.4	Cf	198501	200612	19500101	19801231	26.86	11.99	27.37	5.22	103	36449.9	99.6	M
Lansing	USA	42.72	-84.55	Gasparrini et al. (2015)	Tmean	22.2	Df	198501	200612	19500101	19801231	23.69	8.73	26.83	3.86	262	36449.9	99.6	M
Lanzhou	CHN	36.06	103.79	Gasparrini et al. (2015)	Tmean	20	BS	199601	200809	19610101	19911231	18.79	9.03	28.33	-0.32	1628	2933.3	97.2	M
Lasvegas	USA	36.19	-115.22	Gasparrini et al. (2015)	Tmean	30	Bw	198501	200612	19500101	19801231	27.96	19.77	26.9	-1.02	692	36449.9	99.6	M
Latina	ITA	41.47	12.89	Gasparrini et al. (2015)	Tmean	22.6	Cs	198701	201009	19520101	19821231	24.45	14.86	16.77	10.31	18	27006.4	100	M
Leon	ESP	42.59	-5.57	Gasparrini et al. (2015)	Tmean	17.7	Cs	199001	201009	19550101	19851231	16.11	11.43	17.9	4.84	839	21517.3	99.9	M
Lisbon	PRT	38.72	-9.14	Leone et al. (2013)	ATmax	28.4	Cs	200004	200409	19650101	19951231	22.15	16.23	12.68	10.7	78	18872.4	98.7	S
Lisbon_a	PRT	38.72	-9.14	Gosling et al. (2007)	Tmax	28	Cs	198006	199808	19450601	1975831	21.81	15.34	13.15	9.86	78	18872.4	98.7	M
Littlerock	USA	34.74	-92.33	Gasparrini et al. (2015)	Tmean	26.1	Cf	198501	200612	19500101	19801231	29.26	16.47	23.79	9.98	108	36449.9	99.6	M
Ljubljana	SVN	46.06	14.51	Baccini et al. (2008)	ATmax	21.5	Cf	199204	199909	19570101	19871231	15.28	9.13	21.83	5.24	295	18036.5	99.8	M

Cities	ISO3	LAT	LON	Citation	Metric	MMT_{ori}	CZ	Start.SP	End.SP	Start30	End30	MMT_{AT}	TMean	Amp	T_{dewp}	Elev	GDP	Water	Set
Ljubljana_a	SVN	46.06	14.51	McMichael et al. (2008)	Tmean	17	Cf	198901	199212	19540101	19841231	16.27	9.2	21.63	5.3	295	18036.5	99.8	S
Lleida	ESP	41.62	0.63	Gasparrini et al. (2015)	Tmean	22.4	Cf	199001	201012	19550101	19851231	21.71	15.57	21.44	7.35	157	21517.3	99.9	M
Logrono	ESP	42.47	-2.44	Gasparrini et al. (2015)	Tmean	20.7	Cf	199001	201012	19550101	19851231	20.59	13.57	17.3	6.39	405	21517.3	99.9	M
London_CA	CAN	43.01	-81.29	Gasparrini et al. (2015)	Tmean	18.5	Df	198601	200912	19850101	20051231	18.53	8.22	27.32	3.69	262	29185.4	100	M
London_CA_a	CAN	43.01	-81.29	Martin et al. (2012)	Tmean	15.8	Df	198101	200012	19820101	2014431	14.89	8.16	27.3	3.57	262	29185.4	100	M
London_UK	GBR	51.5	-0.12	Gasparrini et al. (2015)	Tmean	19.5	Cf	199301	200612	19580101	19881231	19.14	11.16	14.65	6.7	24	26030.7	100	M
London_UK_a	GBR	51.5	-0.12	Baccini et al. (2008)	ATmax	23.9	Cf	199204	200009	19570101	19871231	18.4	11.14	14.76	6.7	24	26030.7	100	M
London_UK_b	GBR	51.5	-0.12	Gosling et al. (2007)	Tmax	24	Cf	197606	200308	19410601	1971831	18.44	10.64	13.16	6.57	24	26030.7	100	S
Losangeles	USA	34.09	-118.38	Gasparrini et al. (2015)	Tmean	22.8	Cs	198501	200612	19500101	19801231	22.64	17.76	10.52	9.73	163	36449.9	99.6	M
Louisville	USA	38.23	-85.75	Gasparrini et al. (2015)	Tmean	24.2	Cf	198501	200609	19500101	19801231	26.66	13.6	25.58	7.45	140	36449.9	99.6	S
Lubbock	USA	33.56	-101.88	Gasparrini et al. (2015)	Tmean	26.1	BS	198501	200612	19500101	19801231	26.75	15.6	23.92	4.56	987	36449.9	99.6	M
Lugo	ESP	43.02	-7.56	Gasparrini et al. (2015)	Tmean	17.2	Cs	199001	201012	19550101	19851231	16.73	10.76	12.29	7.53	451	21517.3	99.9	M
Maceio	BRA	-9.67	-35.72	Gasparrini et al. (2015)	Tmean	25.6	Am	199701	201112	19620101	19921231	30.23	24.89	3.46	21.36	1	8987.2	97.6	S
Madison	USA	43.07	-89.39	Gasparrini et al. (2015)	Tmean	22.5	Df	198501	200612	19500101	19801231	24.15	7.88	31.18	2.55	265	36449.9	99.6	M
Madrid	ESP	40.42	-3.71	Gasparrini et al. (2015)	Tmean	21.9	Cs	199001	201012	19550101	19851231	20.33	14.35	20.34	6.12	633	21517.3	99.9	M
Madrid_a	ESP	40.42	-3.71	Iniguez et al. (2010)	Tmean	17.6	Cs	199001	199612	19550101	19851231	15.77	14.35	20.34	6.12	633	21517.3	99.9	M
Malaga	ESP	36.72	-4.42	Gasparrini et al. (2015)	Tmean	23.1	Cs	199001	201012	19550101	19851231	24.09	17.48	13.54	11.11	117	21517.3	99.9	M
Manaus	BRA	-3.13	-60.02	Gasparrini et al. (2015)	Tmean	27.4	Am	199701	201109	19620101	19921231	33.51	26.8	2.37	23.98	33	8987.2	97.6	M
Manila	PHL	14.63	121.03	Seposo et al. (2015)	Tmean	30	Af	200601	201012	19710101	20011231	35.59	27.65	4.03	22.87	25	3350.7	92	M
Mcallen	USA	26.22	-98.24	Gasparrini et al. (2015)	Tmean	29.2	BS	198501	200612	19500101	19801231	34.16	22.66	15.89	16.77	35	36449.9	99.6	M
Melbourne	AUS	-37.81	144.96	Gasparrini et al. (2015)	Tmean	22.4	Cf	198801	200912	19530101	19831231	21.89	14.47	11.43	8.33	68	26374.7	100	M
Melbourne_US	USA	28.11	-80.63	Gasparrini et al. (2015)	Tmean	26.7	Cf	198501	200612	19500101	19801231	30.47	23	12.28	17.87	7	36449.9	99.6	M
Melilla	ESP	35.3	-2.95	Gasparrini et al. (2015)	Tmean	23.7	Cs	199001	201008	19550101	19851231	25.46	18.95	12.07	12.77	106	21517.3	99.9	M
Memphis	USA	35.12	-89.97	Gasparrini et al. (2015)	Tmean	26.4	Cf	198501	200612	19500101	19801231	29.83	16.8	24.02	9.95	87	36449.9	99.6	S
Mexicocity	MEX	19.5	-99.12	McMichael et al. (2008)	Tmean	18	Cw	199401	199812	19590101	19891231	16.57	16.39	6.17	6.66	2266	10318.5	93.8	M
Miami	USA	25.79	-80.22	Curriero et al. (2002)	Tmean	27.18	Am	197301	199412	19380101	19681231	32.14	24.32	9.36	18.87	5	36449.9	99.6	M
Miami_a	USA	25.79	-80.22	Gasparrini et al. (2015)	Tmean	24.7	Am	198501	200609	19500101	19801231	27.91	24.11	9.43	18.83	5	36449.9	99.6	M
Milan	ITA	45.48	9.19	Baccini et al. (2008)	ATmax	31.8	Cf	199104	200009	19560101	19861231	25.74	12.19	21.66	8.14	125	27006.4	100	M
Milwaukee	USA	43.05	-87.96	Gasparrini et al. (2015)	Tmean	20.8	Df	198501	200608	19500101	19801231	21.53	8.45	29.42	3.05	205	36449.9	99.6	S
Minneapolisstpaul	USA	44.96	-93.27	Gasparrini et al. (2015)	Tmean	22.2	Df	198501	200612	19500101	19801231	23.04	7.33	34.94	1.18	269	36449.9	99.6	S
Mobile	USA	30.68	-88.1	Gasparrini et al. (2015)	Tmean	26.7	Cf	198501	200612	19500101	19801231	31.29	19.41	18.02	13.91	15	36449.9	99.6	M
Monterrey	MEX	25.66	-100.31	McMichael et al. (2008)	Tmean	31	BS	199601	199912	19610101	19911231	34.56	22.38	15.86	15.26	581	10318.5	93.8	M
Montreal	CAN	45.57	-73.66	Martin et al. (2012)	Tmean	15.2	Df	198101	200012	19460101	19761231	13.85	5.26	26.9	0.36	37	29185.4	100	S
Montreal_a	CAN	45.57	-73.66	Gasparrini et al. (2015)	Tmean	18.9	Df	198601	200909	19510101	19811231	18.59	5.74	29.75	0.5	37	29185.4	100	M
Moscow	RUS	55.75	37.62	Revich and Shaposhnikov (2008)	Tmean	18	Df	200001	200612	19650101	19951231	17.74	4.96	28.99	0.75	145	6825.4	98.2	M
Murcia	ESP	37.98	-1.13	Gasparrini et al. (2015)	Tmean	23.3	BS	199001	201012	19550101	19851231	23.17	19.01	17.49	9.04	34	21517.3	99.9	M
Myrtlebeach	USA	33.7	-78.88	Gasparrini et al. (2015)	Tmean	25.8	Cf	198501	200612	19500101	19801231	29.54	17.78	20.13	12.49	7	36449.9	99.6	M
Nanjing	CHN	32.06	118.77	Li et al. (2014)	Tmax	35	Cf	200405	201009	19690501	1999931	30.16	15.62	25.51	10.82	10	2933.3	97.2	M
Nanjing_a	CHN	32.06	118.77	Yang et al. (2015)	Tmean	27.9	Cf	200701	201312	19720101	20021231	32.97	15.69	25.5	10.87	10	2933.3	97.2	M

Cities	ISO3	LAT	LON	Citation	Metric	MMT_{ori}	CZ	Start.SP	End.SP	Start30	End30	MMT_{AT}	TMean	Amp	T_{dewp}	Elev	GDP	Water	Set
Nanning	CHN	22.82	108.32	Huang et al. (2017)	Tmean	29	Cf	200801	201112	19730101	20031231	34.71	22.06	16.3	17.63	155	2933.3	97.2	M
Naples	USA	26.15	-81.8	Gasparrini et al. (2015)	Tmean	24.7	Aw	198501	200612	19850101	20051231	27.59	23.48	10.21	18.15	2	36449.9	99.6	M
Nashua	USA	42.75	-71.48	Gasparrini et al. (2015)	Tmean	22.2	Df	198501	200612	19850101	20051231	22.66	10.79	25.95	3.36	60	36449.9	99.6	M
Nashvilledavidson	USA	36.15	-86.76	Gasparrini et al. (2015)	Tmean	25	Cf	198501	200612	19500101	19801231	28.01	15.1	23.9	8.97	147	36449.9	99.6	M
Natal	BRA	-5.8	-35.2	Gasparrini et al. (2015)	Tmean	24.5	As	199701	201109	19620101	19921231	29.03	26.28	2.92	22.17	3	8987.2	97.6	M
Newark	USA	40.74	-74.18	Gasparrini et al. (2015)	Tmean	23.9	Cf	198501	200612	19500101	19801231	25.32	12.19	26.59	5.72	33	36449.9	99.6	M
Newburgh	USA	41.5	-74.02	Gasparrini et al. (2015)	Tmean	23.3	Df	198501	200608	19500101	19801231	23.71	9.89	26.29	3.84	64	36449.9	99.6	M
Newhaven	USA	41.31	-72.92	Gasparrini et al. (2015)	Tmean	21.7	Cf	198501	200612	19500101	19801231	23.77	11.6	24.15	5.1	23	36449.9	99.6	S
Newlondon	USA	41.35	-72.1	Gasparrini et al. (2015)	Tmean	23.3	Cf	198501	200609	19500101	19801231	26.14	11.72	20.29	6.29	33	36449.9	99.6	S
Newyorkcity	USA	40.7	-73.92	Gasparrini et al. (2015)	Tmean	23.1	Cf	198501	200612	19500101	19801231	24.81	12.22	25.19	5.25	18	36449.9	99.6	M
Newyorkcity_a	USA	40.7	-73.92	Curriero et al. (2002)	Tmean	19.12	Cf	197301	199412	19380101	19681231	18.93	12.3	23.19	5.3	18	36449.9	99.6	M
Oakland	USA	37.8	-122.23	Gasparrini et al. (2015)	Tmean	20.8	Cs	198501	200609	19500101	19801231	20.34	14.28	9.17	9.56	67	36449.9	99.6	M
Ocala	USA	29.19	-82.13	Gasparrini et al. (2015)	Tmean	26.7	Cf	198501	200609	19500101	19801231	30.64	21.56	12.87	16.1	22	36449.9	99.6	M
Oklahoma	USA	35.48	-97.53	Gasparrini et al. (2015)	Tmean	28.1	Cf	198501	200612	19500101	19801231	31.21	15.54	26.28	7.74	367	36449.9	99.6	M
Omaha	USA	41.26	-96.01	Gasparrini et al. (2015)	Tmean	23.3	Df	198501	200612	19500101	19801231	24.85	10.57	31.81	4.07	350	36449.9	99.6	M
Orange	USA	33.8	-117.83	Gasparrini et al. (2015)	Tmean	25.6	Cs	198501	200609	19500101	19801231	25.34	17.61	10.62	10.26	86	36449.9	99.6	M
Orlando	USA	28.53	-81.38	Gasparrini et al. (2015)	Tmean	27.2	Cf	198501	200612	19500101	19801231	31.97	21.78	12.94	16.42	31	36449.9	99.6	M
Ottawa	CAN	45.4	-75.73	Gasparrini et al. (2015)	Tmean	18.3	Df	198601	200912	19510101	19811231	17.92	5.46	31.66	0	64	29185.4	100	M
Ottawa_a	CAN	45.4	-75.73	Martin et al. (2012)	Tmean	15.8	Df	198101	200012	19460101	19761231	14.69	5.73	30.63	0.34	64	29185.4	100	M
Ourense	ESP	42.33	-7.87	Gasparrini et al. (2015)	Tmean	20.5	Cs	199001	201012	19550101	19851231	20.15	11.33	3.64	6.32	242	21517.3	99.9	M
Oviedo	ESP	43.35	-5.83	Iniguez et al. (2010)	Tmean	24.7	Cs	199001	199612	19550101	19851231	25.95	12.03	11.55	8.59	271	21517.3	99.9	M
Oviedo	ESP	43.35	-5.83	Gasparrini et al. (2015)	Tmean	18	Cs	199001	201009	19550101	19851231	18.43	12.03	11.55	8.59	271	21517.3	99.9	M
Palermo	ITA	38.12	13.36	Leone et al. (2013)	ATmax	31.8	Cs	200104	200509	19660101	19961231	29.13	18.67	14.67	10.43	59	27006.4	100	M
Palermo_a	ITA	38.12	13.36	Gasparrini et al. (2015)	Tmean	24.5	Cs	198701	201012	19520101	19821231	25.38	18.03	12.16	9.82	59	27006.4	100	M
Palmademallorca	ESP	39.57	2.65	Gasparrini et al. (2015)	Tmean	22.6	Cs	199001	201012	19550101	19851231	24.39	15.78	15.75	11.54	49	21517.3	99.9	S
Pamplona	ESP	42.82	-1.63	Gasparrini et al. (2015)	Tmean	19.7	Cf	199001	201012	19550101	19851231	19.05	12.9	17.77	6.19	466	21517.3	99.9	M
Paris	FRA	48.87	2.33	Baccini et al. (2008)	ATmax	24.1	Cf	199204	200009	19570101	19871231	18.76	10.88	17.56	6.62	47	26192.7	100	S
Pensacola	USA	30.44	-87.21	Gasparrini et al. (2015)	Tmean	26.9	Cf	198501	200612	19500101	19801231	31.85	19.96	16.92	14.83	22	36449.9	99.6	M
Philadelphia	USA	40	-75.14	Gasparrini et al. (2015)	Tmean	23.3	Cf	198501	200612	19500101	19801231	24.89	12.81	25.68	5.95	36	36449.9	99.6	M
Philadelphia_a	USA	40	-75.14	Curriero et al. (2002)	Tmean	21.43	Cf	197301	199412	19380101	19681231	22.19	12.94	25.18	6.2	36	36449.9	99.6	M
Phoenix	USA	33.53	-112.08	Harlan et al. (2013)	ATmax	41.7	BS	200001	200812	19650101	19951231	34.5	22.79	23.18	5.27	356	36449.9	99.6	M
Phoenix_a	USA	33.53	-112.08	Gasparrini et al. (2015)	Tmean	29.2	BS	198501	200612	19500101	19801231	28.06	22.8	23.4	5.32	356	36449.9	99.6	M
Pittsburgh	USA	40.44	-79.98	Gasparrini et al. (2015)	Tmean	23.3	Cf	198501	200609	19500101	19801231	22.12	10.91	25.49	4.55	280	36449.9	99.6	M
Pontevedra	ESP	42.42	-8.66	Gasparrini et al. (2015)	Tmean	19	Cs	199001	201009	19550101	19851231	19.2	15.35	9.41	9.13	94	21517.3	99.9	M
Portland_US_ME	USA	43.67	-70.27	Gasparrini et al. (2015)	Tmean	20.6	Df	198501	200612	19500101	19801231	21.6	7.7	26.6	2.43	17	36449.9	99.6	S
Portland_US_OR	USA	43.67	-70.27	Gasparrini et al. (2015)	Tmean	21.4	Df	198501	200612	19500101	19801231	21.05	11.82	16.67	6.22	17	36449.9	99.6	M
Portoalegre	BRA	-30.03	-51.2	Gasparrini et al. (2015)	Tmean	24.2	Cf	199701	201109	19620101	19921231	26.22	20.01	11.9	15.45	22	8987.2	97.6	S
Prague	CZE	50.08	14.43	Baccini et al. (2008)	ATmax	22	Cf	199204	200009	19570101	19871231	15.85	8.28	21.47	3.92	226	16132.4	99.9	M
Providence	USA	41.82	-71.42	Gasparrini et al. (2015)	Tmean	23.3	Cf	198501	200612	19500101	19801231	25.41	10.16	26.39	3.78	28	36449.9	99.6	M
Puntagorda	USA	26.92	-82.05	Gasparrini et al. (2015)	Tmean	25.8	Cf	198501	200612	19990101	20101231	30.06	22.52	11.98	17.17	2	36449.9	99.6	M

Cities	ISO3	LAT	LON	Citation	Metric	MMT_{ori}	CZ	Start.SP	End.SP	Start30	End30	MMT_{AT}	TMean	Amp	T_{dewp}	Elev	GDP	Water	Set
Quebeccity	CAN	46.89	-71.34	Martin et al. (2012)	Tmean	15.7	Df	198101	200012	19460101	19761231	14.62	3.45	24.13	-0.74	173	29185.4	100	M
Raleigh	USA	35.82	-78.64	Gasparrini et al. (2015)	Tmean	25.3	Cf	198501	200609	19500101	19801231	28.87	14.84	21.84	8.74	95	36449.9	99.6	M
Reading	USA	40.34	-75.93	Gasparrini et al. (2015)	Tmean	24.4	Cf	198501	200609	19500101	19801231	23.92	11.07	25.09	4.92	121	36449.9	99.6	M
Recife	BRA	-8.05	-34.9	Gasparrini et al. (2015)	Tmean	25.7	Am	199701	201112	19620101	19921231	30.57	26.76	3.36	22.22	2	8987.2	97.6	M
Regina	CAN	50.48	-104.65	Martin et al. (2012)	Tmean	15	Df	198101	200012	19460101	19761231	13.3	1.93	29.91	-3.13	574	29185.4	100	M
Regina_a	CAN	50.48	-104.65	Gasparrini et al. (2015)	Tmean	16.6	Df	198601	200912	19510101	19811231	15.22	2.7	34.74	-3.01	574	29185.4	100	M
Riverside	USA	33.95	-117.4	Gasparrini et al. (2015)	Tmean	28.3	Cs	198501	200612	19500101	19801231	27.95	16.83	16.05	6.35	40	36449.9	99.6	M
Rochester	USA	43.17	-77.61	Gasparrini et al. (2015)	Tmean	21.7	Df	198501	200612	19500101	19801231	23.14	9.05	27.4	3.95	156	36449.9	99.6	M
Rockford	USA	42.27	-89.07	Gasparrini et al. (2015)	Tmean	21.9	Df	198501	200609	19500101	19801231	23.28	8.49	29.57	3.05	231	36449.9	99.6	M
Rome	ITA	41.89	12.5	Gasparrini et al. (2015)	Tmean	22.1	Cs	198701	201008	19520101	19821231	22.96	15.49	17.11	9.7	35	27006.4	100	M
Rome_a	ITA	41.89	12.5	Leone et al. (2013)	ATmax	31.4	Cs	199204	200609	19570101	19871231	26.49	15.49	17.35	9.97	35	27006.4	100	M
Rome_b	ITA	41.89	12.5	Baccini et al. (2008)	ATmax	30.3	Cs	199204	200009	19570101	19871231	25.53	15.49	17.35	9.97	35	27006.4	100	M
Sacramento	USA	38.56	-121.47	Gasparrini et al. (2015)	Tmean	25.3	Cs	198501	200612	19500101	19801231	24.1	15.79	17.9	7.96	12	36449.9	99.6	M
Saginaw	USA	43.42	-83.95	Gasparrini et al. (2015)	Tmean	21.4	Df	198501	200608	19500101	19801231	22.47	8.48	25.36	3.49	183	36449.9	99.6	M
Saintjohn	CAN	45.3	-66.08	Gasparrini et al. (2015)	Tmean	15.6	Df	198601	200909	19510101	19811231	15.04	6.6	19.21	1.33	28	29185.4	100	M
Salamanca	ESP	40.97	-5.67	Gasparrini et al. (2015)	Tmean	19.2	Cs	199001	201012	19550101	19851231	17.94	12.25	19.4	5.69	792	21517.3	99.9	M
Salinas	USA	36.68	-121.64	Gasparrini et al. (2015)	Tmean	20.6	Cs	198501	200612	19500101	19801231	19.87	13.53	8.25	8.24	21	36449.9	99.6	M
Saltlakecity	USA	40.75	-111.89	Gasparrini et al. (2015)	Tmean	24.7	Df	198501	200612	19500101	19801231	22.31	10.92	28.67	0.28	1321	36449.9	99.6	M
Salvador	BRA	-12.97	-38.5	McMichael et al. (2008)	Tmean	23	Af	199601	199912	19610101	19911231	27.63	26.22	3.2	21.94	3	8987.2	97.6	S
Salvador_a	BRA	-12.97	-38.5	Gasparrini et al. (2015)	Tmean	27	Af	199701	201112	19620101	19921231	32.23	26.26	3.2	22	3	8987.2	97.6	M
Sanantonio	USA	29.45	-98.51	Gasparrini et al. (2015)	Tmean	30	Cf	198501	200609	19500101	19801231	33.91	20.43	19.26	12.95	222	36449.9	99.6	M
Sandiego	USA	32.78	-117.15	Gasparrini et al. (2015)	Tmean	23.3	BS	198501	200609	19500101	19801231	24.45	17.22	9.36	10.84	80	36449.9	99.6	M
Sanfrancisco	USA	37.76	-122.44	Gasparrini et al. (2015)	Tmean	20.8	Cs	198501	200612	19500101	19801231	19.8	13.22	8.3	8.55	71	36449.9	99.6	M
Sanjose	USA	37.3	-121.87	Gasparrini et al. (2015)	Tmean	23.3	Cs	198501	200609	19500101	19801231	22.61	16.07	10.25	8.79	39	36449.9	99.6	M
Sansebastian	ESP	40.55	-3.62	Gasparrini et al. (2015)	Tmean	18.5	Cs	199001	201009	19550101	19851231	16.82	13.55	20.19	5.45	655	21517.3	99.9	M
Santander	ESP	43.47	-3.8	Gasparrini et al. (2015)	Tmean	18.8	Cf	199001	201009	19550101	19851231	19.6	14.04	10.97	9.72	23	21517.3	99.9	M
Santiago_CL	CHL	-33.45	-70.67	McMichael et al. (2008)	Tmean	16	Cs	198801	199112	19530101	19831231	15.4	15.06	12.4	7.84	516	9848.9	99.2	M
Saoluis	BRA	-2.52	-44.27	Gasparrini et al. (2015)	Tmean	26.9	Aw	199701	201109	19620101	19921231	32.52	27.16	1.97	23.46	3	8987.2	97.6	M
Saopaulo	BRA	-23.53	-46.62	Gasparrini et al. (2015)	Tmean	21.5	Cf	199701	201112	19620101	19921231	22.91	19.86	7.8	15.26	646	8987.2	97.6	M
Saopaulo_a	BRA	-23.53	-46.62	Gouveia et al. (2003)	Tmean	20	Cf	199101	199412	19560101	19861231	21.02	19.83	7.58	15.2	646	8987.2	97.6	M
Sarasota	USA	27.34	-82.54	Gasparrini et al. (2015)	Tmean	23.9	Cf	198501	200612	19500101	19801231	26.84	23.14	13.13	18.09	5	36449.9	99.6	M
Saskatoon	CAN	52.16	-106.65	Gasparrini et al. (2015)	Tmean	16.1	Df	198601	200909	19510101	19811231	15.17	- 0.59	36.64	-6.38	465	29185.4	100	M
Scranton	USA	41.41	-75.67	Gasparrini et al. (2015)	Tmean	20.8	Df	198501	200609	19500101	19801231	21.57	9.68	26.64	3.7	314	36449.9	99.6	M
Seattle	USA	47.63	-122.33	Gasparrini et al. (2015)	Tmean	19.4	Cs	198501	200612	19500101	19801231	17.92	10.52	15.04	5.75	48	36449.9	99.6	M
Segovia	ESP	40.94	-4.11	Gasparrini et al. (2015)	Tmean	19.8	Cs	199001	201009	19550101	19851231	17.73	9.47	19.34	2.47	1013	21517.3	99.9	M
Seoul	KOR	37.57	127	Chung et al. (2009**)	ATmean	33.1	Dw	199104	200609	19560101	19861231	33.07	11.86	30.1	6.36	61	18083.1	98.1	M
Seoul_a	KOR	37.57	127	Ha and Kim (2012)	Tmean	27.2	Dw	199306	200908	19580101	19881231	31.81	11.88	29.98	6.27	61	18083.1	98.1	M
Seoul_b	KOR	37.57	127	Ha et al. (2011)	Tmean	28.4	Dw	199101	200812	19560101	19861231	33.47	11.86	30.1	6.36	61	18083.1	98.1	M
Seoul_c	KOR	37.57	127	Kim et al. (2006)	Tmean	28.1	Dw	199406	200308	19590101	19891231	33.08	11.91	29.72	6.28	61	18083.1	98.1	M

Cities	ISO3	LAT	LON	Citation	Metric	MMT_{ori}	CZ	Start.SP	End.SP	Start30	End30	MMT_{AT}	TMean	Amp	T_{dewp}	Elev	GDP	Water	Set
Seoul_d	KOR	37.57	127	Kim et al. (2011)	Tmean	23.58	Dw	200106	200809	19660101	19961231	25.96	12	28.91	6.13	61	18083.1	98.1	M
Seoul_e	KOR	37.57	127	Gasparrini et al. (2015)	Tmean	24.5	Dw	199201	201009	19570101	19871231	27.54	11.87	30	6.35	61	18083.1	98.1	M
Sevilla	ESP	37.4	-5.98	Gasparrini et al. (2015)	Tmean	25.7	Cs	199001	201012	19550101	19851231	26.3	18.52	18.1	10.64	7	21517.3	99.9	M
Sevilla_a	ESP	37.4	-5.98	Iniguez et al. (2010)	Tmean	22.75	Cs	199001	199612	19730101	20031231	22.69	18.89	18.21	10.9	7	21517.3	99.9	M
Shanghai	CHN	31.23	121.47	Kan et al. (2003)	Tmean	26.7	Cf	200006	200112	19650101	19951231	32.56	16.23	24.07	11.76	6	2933.3	97.2	M
Shanghai_a	CHN	31.23	121.47	Gasparrini et al. (2015)	Tmean	29.2	Cf	199601	200812	19610101	19911231	35.49	16.22	24.5	11.78	6	2933.3	97.2	S
Shanghai_b	CHN	31.23	121.47	Yang et al. (2015)	Tmean	24.5	Cf	200701	201312	19720101	20021231	26.98	16.48	23.87	12.04	6	2933.3	97.2	M
Shenyang	CHN	41.79	123.43	Gasparrini et al. (2015)	Tmean	22	Dw	199601	200812	19610101	19911231	23.08	8.48	35.82	0.81	43	2933.3	97.2	M
Shenyang_a	CHN	41.79	123.43	Yang et al. (2015)	Tmean	21.5	Dw	200701	201312	19720101	20021231	22.69	8.63	35.82	0.94	43	2933.3	97.2	M
Shenzhen	CHN	22.54	114.11	Li et al. (2014)	Tmax	33	Cw	200409	201009	19690901	1999931	29.82	22.75	14.41	18.09	53	2933.3	97.2	M
Shijiazhuang	CHN	38.04	114.48	Yang et al. (2015)	Tmean	23.8	Dw	200701	201312	19720101	20021231	25.29	13.94	29.06	4.87	524	2933.3	97.2	S
Shreveport	USA	32.47	-93.77	Gasparrini et al. (2015)	Tmean	26.9	Cf	198501	200612	19500101	19801231	30.99	18.35	21	12.31	64	36449.9	99.6	M
Sofia	BGR	42.68	23.32	McMichael et al. (2008)	Tmean	16	Cf	199601	199912	19610101	19911231	15.1	9.86	22.58	4.11	575	6370.6	99.9	M
Soria	ESP	41.77	-2.46	Gasparrini et al. (2015)	Tmean	18.3	Cf	199001	201012	19550101	19851231	16.65	11.4	19.03	4.57	1053	21517.3	99.9	M
Spokane	USA	47.67	-117.41	Gasparrini et al. (2015)	Tmean	20.8	Cs	198501	200612	19500101	19801231	18.94	8.68	25.78	1.07	602	36449.9	99.6	M
Springfield	USA	37.2	-93.29	Gasparrini et al. (2015)	Tmean	21.4	Df	198501	200612	19500101	19801231	20.91	9.71	27.12	3.1	51	36449.9	99.6	M
Stjohns	CAN	47.58	-52.69	Martin et al. (2012)	Tmean	26	Df	198101	200012	19460101	19761231	31.58	4.67	18.22	2.59	95	29185.4	100	M
Stjohns	CAN	47.58	-52.69	Gasparrini et al. (2015)	Tmean	16.5	Df	198601	200909	19510101	19811231	16.53	5.24	17.63	2.72	95	29185.4	100	M
Stlouis	USA	38.63	-90.24	Gasparrini et al. (2015)	Tmean	27.2	Cf	198501	200603	19500101	19801231	30.41	13.25	28.37	6.93	155	36449.9	99.6	M
Stockholm	SWE	59.33	18.05	Baccini et al. (2008)	ATmax	21.7	Df	199004	200009	19550101	19851231	16.98	6.7	22.37	2.64	20	29258	100	M
Stockholm_a	SWE	59.33	18.05	Gasparrini et al. (2015)	Tmean	18.9	Df	199001	200212	19550101	19851231	18.3	6.7	22.37	2.64	20	29258	100	M
Stockton	USA	37.98	-121.3	Gasparrini et al. (2015)	Tmean	25.6	Cs	198501	200609	19500101	19801231	24.75	16.15	17.84	7.83	2	36449.9	99.6	M
Sudbury	CAN	46.51	-81.02	Gasparrini et al. (2015)	Tmean	16.7	Df	198601	200909	19510101	19811231	15.79	3.8	33.67	-1.39	298	29185.4	100	M
Suzhou	CHN	33.64	116.98	Gasparrini et al. (2015)	Tmean	26.9	Cf	199601	200812	19610101	19911231	31.42	16.33	25.4	11.64	6	2933.3	97.2	M
Sydney	AUS	-33.87	151.21	Gasparrini et al. (2015)	Tmean	22.6	Cf	198801	200912	19530101	19831231	23.8	17.36	11.16	11.28	1	26374.7	100	M
Sydney_a	AUS	-33.87	151.21	Gosling et al. (2007)	Tmax	26	Cf	198812	200302	19531201	1983231	21.4	17.38	11.16	11.3	1	26374.7	100	M
Syracuse	USA	43.05	-76.14	Gasparrini et al. (2015)	Tmean	21.1	Df	198501	200612	19500101	19801231	21.95	8.94	27.74	3.52	144	36449.9	99.6	M
Tacoma	USA	47.24	-122.46	Gasparrini et al. (2015)	Tmean	20	Cs	198501	200609	19500101	19801231	18.93	10.66	15.36	5.91	77	36449.9	99.6	M
Taiyuan	CHN	37.87	112.56	Gasparrini et al. (2015)	Tmean	23.3	Dw	199601	200809	19610101	19911231	24.08	10.12	28.95	1.09	811	2933.3	97.2	M
Tampa	USA	27.97	-82.46	Curriero et al. (2002)	Tmean	27.06	Cf	197301	199412	19380101	19681231	30.94	22.35	12.97	16.91	8	36449.9	99.6	M
Tampa_a	USA	27.97	-82.46	Gasparrini et al. (2015)	Tmean	25	Cf	198501	200612	19500101	19801231	28.1	22.12	13.32	16.77	8	36449.9	99.6	M
Tarragona	ESP	41.12	1.24	Gasparrini et al. (2015)	Tmean	23.8	Cs	199001	201012	19550101	19851231	25.32	16.79	16.11	10.21	58	21517.3	99.9	M
Tehran	IRN	35.67	51.42	Farajzadeh and Darand (2009)	Tmean	28.5	Cs	200204	200509	19670101	19971231	26.3	17.62	28.98	0.63	1157	9436	98.3	S
Telaviv	ISR	32.07	34.76	Perez et al. (2012)	ATmean	29.49	Cs	200004	200409	19650101	19951231	29.48	19.98	14.13	13.5	28	24941.9	100	S
Telaviv_a	ISR	32.07	34.76	Leone et al. (2013)	ATmax	32.8	Cs	199104	199609	19560101	19861231	28.15	20.1	13.35	13.45	28	24941.9	100	M
Tenerife	ESP	28.47	-16.25	Gasparrini et al. (2015)	Tmean	23.7	Cs	199001	201012	19550101	19851231	24.37	17.98	8.02	11.79	320	21517.3	99.9	M
Teresina	BRA	-5.08	-42.82	Gasparrini et al. (2015)	Tmean	28	Aw	199701	201112	19620101	19921231	33.32	28.34	3.16	22.03	67	8987.2	97.6	M
Teruel	ESP	40.34	-1.11	Gasparrini et al. (2015)	Tmean	19.3	Cf	199001	201012	19550101	19851231	18.12	13.6	11.98	4.41	939	21517.3	99.9	M
Thunderbay	CAN	48.45	-89.32	Gasparrini et al. (2015)	Tmean	15.4	Df	198601	200912	19510101	19811231	17.01	-6.5	33.3	-6.64	289	29185.4	100	M

Cities	ISO3	LAT	LON	Citation	Metric	MMT_{ori}	CZ	Start.SP	End.SP	Start30	End30	MMT_{AT}	TMean	Amp	T_{dewp}	Elev	GDP	Water	Set
Tianjin	CHN	39.13	117.19	Gasparrini et al. (2015)	Tmean	25.6	Dw	199601	200809	19610101	19911231	28.63	13	29.81	4.14	4	2933.3	97.2	M
Tianjin_a	CHN	39.13	117.19	Yang et al. (2015)	Tmean	24.5	Dw	200701	201312	19720101	20021231	26.41	13.12	29.98	4.46	4	2933.3	97.2	M
Tokyo	JPN	35.69	139.75	Gasparrini et al. (2015)	Tmean	26.5	Cf	198501	201212	19500101	19801231	30.39	16.05	22.17	9.11	14	26795.2	100	M
Tokyo_a	JPN	35.69	139.75	Chung et al. (2009**)	ATmean	31.5	Cf	197204	199409	19370101	19671231	31.49	15.95	22.38	9.67	14	26795.2	100	M
Toledo_ES	ESP	39.86	-4.03	Montero et al. (2012)	Tmax	38	Cs	197501	200312	19730101	20031231	30.07	16.24	21.37	8.28	528	21517.3	99.9	M
Toledo_ES_a	ESP	39.86	-4.03	Gasparrini et al. (2015)	Tmean	23.4	Cs	199001	201012	19550101	19851231	22.25	15.76	20.79	8.62	528	21517.3	99.9	M
Toledo_US	USA	41.67	-83.58	Gasparrini et al. (2015)	Tmean	21.7	Df	198501	200612	19500101	19801231	22.71	10.04	27.71	4.45	186	36449.9	99.6	M
Toronto	CAN	43.67	-79.42	Gasparrini et al. (2015)	Tmean	18.9	Df	198601	200912	19510101	19811231	18.95	8.6	25.96	3.79	129	29185.4	100	M
Toronto_a	CAN	43.67	-79.42	Martin et al. (2012)	Tmean	18.1	Df	198101	200012	19460101	19761231	17.82	8.58	25.78	3.89	129	29185.4	100	M
Trenton	USA	40.22	-74.76	Gasparrini et al. (2015)	Tmean	24.2	Cf	198501	200612	19500101	19801231	25.97	12.34	26.29	5.65	24	36449.9	99.6	M
Tucson	USA	32.21	-110.92	Gasparrini et al. (2015)	Tmean	28.9	BS	198501	200612	19500101	19801231	28.43	20.29	20.53	2.63	760	36449.9	99.6	M
Tulsa	USA	36.13	-95.94	Gasparrini et al. (2015)	Tmean	26.9	Cf	198501	200609	19500101	19801231	30.23	15.51	27.18	8.3	218	36449.9	99.6	M
Tunis	TUN	36.8	10.18	Leone et al. (2013)	ATmax	35.5	Cs	200504	200709	19700101	20001231	29.39	18.48	16.29	12.68	27	6003.3	97.6	M
Turin	ITA	45.08	7.68	Baccini et al. (2008)	ATmax	27	Cf	199104	199909	19560101	19861231	21.44	11.45	20.81	7.23	250	27006.4	100	M
Turin_a	ITA	45.08	7.68	Gasparrini et al. (2015)	Tmean	19.8	Cf	198701	201012	19520101	19821231	19.97	11	19.57	6.46	250	27006.4	100	M
Ulsan	KOR	35.53	129.35	Gasparrini et al. (2015)	Tmean	25.9	Cf	199201	201012	19570101	19871231	29.87	13.6	25.35	7.58	24	18083.1	98.1	S
Utica	USA	43.1	-75.23	Gasparrini et al. (2015)	Tmean	21.7	Df	198501	200612	19500101	19801231	23.25	7.93	24.27	2.68	166	36449.9	99.6	M
Valencia	ESP	39.48	-0.39	Gasparrini et al. (2015)	Tmean	24	Cs	199001	201008	19550101	19851231	25.63	16.57	15.65	10.57	22	21517.3	99.9	M
Valencia_a	ESP	39.48	-0.39	Iniguez et al. (2010)	Tmean	20	Cs	199001	199612	19550101	19851231	20.15	16.57	15.65	10.57	22	21517.3	99.9	M
Valencia_b	ESP	39.48	-0.39	Leone et al. (2013)	ATmax	32	Cs	199404	200309	19590101	19891231	26.44	16.74	15.84	10.74	22	21517.3	99.9	M
Valencia_c	ESP	39.48	-0.39	Baccini et al. (2008)	ATmax	28.2	Cs	199504	200009	19600101	19901231	22.74	16.78	15.89	10.79	22	21517.3	99.9	M
Valladolid	ESP	41.65	-4.74	Gasparrini et al. (2015)	Tmean	20	Cs	199001	201012	19550101	19851231	18.63	11.92	19.34	4.8	713	21517.3	99.9	M
Vancouver	CAN	49.27	-123.15	Gasparrini et al. (2015)	Tmean	16.7	Cf	198601	200909	19510101	19811231	16.05	9.91	14.17	6.72	34	29185.4	100	M
Vancouver_a	CAN	49.27	-123.15	Martin et al. (2012)	Tmean	16	Cf	198101	200012	19460101	19761231	15.36	10.29	11.1	7.24	34	29185.4	100	M
Victoria	CAN	48.46	-123.42	Gasparrini et al. (2015)	Tmean	15.7	Cs	198601	200908	19510101	19811231	14.95	8.27	7.47	4.44	48	29185.4	100	M
Vigo	ESP	42.22	-8.71	Iniguez et al. (2010)	Tmean	13.9	Cs	199001	199612	19550101	19851231	13	13.42	12.66	9.82	131	21517.3	99.9	M
Virginiabeach	USA	36.83	-76.09	Gasparrini et al. (2015)	Tmean	25.3	Cf	198501	200612	19500101	19801231	29.02	15.42	22.15	9.33	4	36449.9	99.6	M
Viterbo	ITA	42.42	12.09	Gasparrini et al. (2015)	Tmean	21.5	Cs	198701	201012	19520101	19821231	21.74	13.02	18.45	6.95	335	27006.4	100	S
Vitoria_BR	BRA	-20.32	-40.35	Gasparrini et al. (2015)	Tmean	26.8	Aw	199701	201109	19620101	19921231	31.16	24.46	5.68	20.54	29	8987.2	97.6	M
Vitoria_ES	ESP	42.85	-2.67	Gasparrini et al. (2015)	Tmean	17.8	Cf	199001	201012	19550101	19851231	17.27	11.87	15.71	6.75	523	21517.3	99.9	M
Vitoria_ES_a	ESP	42.85	-2.67	Iniguez et al. (2010)	Tmean	18.4	Cf	199001	199612	19550101	19851231	17.64	11.83	15.73	6.69	523	21517.3	99.9	M
WashingtonDC	USA	38.91	-77.01	Gasparrini et al. (2015)	Tmean	25.8	Cf	198501	200612	19500101	19801231	28.75	14.13	24.78	6.87	41	36449.9	99.6	M
WashingtonDC_a	USA	38.91	-77.01	Curriero et al. (2002)	Tmean	21.42	Cf	197301	199412	19380101	19681231	22.09	13.9	24.5	6.9	41	36449.9	99.6	M
Westpalmbeach	USA	26.71	-80.06	Gasparrini et al. (2015)	Tmean	24.2	Af	198501	200612	19500101	19801231	26.58	23.57	10.4	18.44	5	36449.9	99.6	M
Wichita	USA	37.69	-97.34	Gasparrini et al. (2015)	Tmean	25	Cf	198501	200612	19500101	19801231	27.24	13.6	28.81	6.23	398	36449.9	99.6	M
Wilmington	USA	34.22	-77.91	Gasparrini et al. (2015)	Tmean	23.6	Cf	198501	200612	19500101	19801231	25.98	12.47	25.5	6.1	38	36449.9	99.6	M
Windsor_CA	CAN	42.3	-83.02	Gasparrini et al. (2015)	Tmean	20.2	Df	198601	200909	19510101	19811231	20.64	9.45	28.92	4.31	186	29185.4	100	M
Windsor_CA_b	CAN	42.3	-83.02	Martin et al. (2012)	Tmean	19.2	Df	198101	200012	19460101	19761231	19.2	10.1	26.95	4.71	186	29185.4	100	M
Winnipeg	CAN	49.91	-97.25	Martin et al. (2012)	Tmean	29	Df	198101	200012	19460101	19761231	31.32	3.29	36.45	-2.33	235	29185.4	100	M
Winnipeg	CAN	49.91	-97.25	Gasparrini et al. (2015)	Tmean	17.2	Df	198601	200912	19510101	19811231	16.38	3.26	36.45	-2.27	235	29185.4	100	M

Cities	ISO3	LAT	LON	Citation	Metric	MMT_{ori}	CZ	Start.SP	End.SP	Start30	End30	MMT_{AT}	TMean	Amp	T_{dewp}	Elev	GDP	Water	Set
Worcester	USA	42.27	-71.8	Gasparrini et al. (2015)	Tmean	20	Df	198501	200608	19500101	19801231	20.43	8.29	26.08	2.25	180	36449.9	99.6	M
Wuhan	CHN	30.58	114.27	Bao et al. (2016)	Tmean	22.9	Cf	200801	201112	19730101	20031231	25.46	16.95	25.16	12.26	112	2933.3	97.2	M
Wulumqi	CHN	43.8	87.58	Gasparrini et al. (2015)	Tmean	23.3	BS	199601	200812	19610101	19911231	21.62	7.64	39.22	-2	888	2933.3	97.2	M
Xian	CHN	34.26	108.94	Gasparrini et al. (2015)	Tmean	24	Cw	199601	200809	19610101	19911231	25.95	13.62	26.88	7.56	421	2933.3	97.2	M
York	USA	39.96	-76.73	Gasparrini et al. (2015)	Tmean	22.5	Cf	198501	200612	19990101	20101231	24.35	11.45	25.44	5.33	141	36449.9	99.6	M
Youngstownwarren	USA	41.1	-80.65	Gasparrini et al. (2015)	Tmean	20.8	Df	198501	200609	19500101	19801231	21.82	9.2	26.34	3.96	299	36449.9	99.6	M
Zamora	ESP	41.52	-5.75	Gasparrini et al. (2015)	Tmean	20.3	Cs	199001	201009	19550101	19851231	18.83	13.27	19.47	5.4	653	21517.3	99.9	M
Zaragoza	ESP	41.65	-0.89	Gasparrini et al. (2015)	Tmean	22.6	BS	199001	201012	19550101	19851231	22.22	14.58	18.83	6.9	198	21517.3	99.9	M
Zaragoza_a	ESP	41.65	-0.89	Iniguez et al. (2010)	Tmean	18.8	BS	199001	199612	19550101	19851231	17.58	14.58	18.83	6.9	198	21517.3	99.9	M
Zhengzhou	CHN	34.76	113.65	Yang et al. (2015)	Tmean	25.9	Cw	201101	201312	19760101	20061231	27.89	14.74	26.63	7.13	215	2933.3	97.2	M
Zhuhai	CHN	22.28	113.57	Wu et al. (2013)	Tmean	26	Cw	200601	201012	19710101	20011231	31.12	22.57	14.55	18.89	21	2933.3	97.2	M
Zurich	CHE	47.37	8.55	Baccini et al. (2008)	ATmax	21.8	Cf	199004	199609	19550101	19851231	16.04	8.66	20.23	4.87	488	35675.1	100	M

Tab. B.6.: **List of climate stations used to obtain GSOD climate data per city.** Stn.no = Station number, Stn. = Station name. Station information recorded row-wise (for Stations 1 to 4, 5 to 8 and 9 to 11) for the number of stations used per city, “0" indicates no additional stations.

Cities	ISO3	LAT	LON	Stn.no 1,5,9	Stn.no 2,6,10	Stn.no 3,7,11	Stn.no 4,8	Stn. 1,5,9	Stn. 2,6,10	Stn. 3,7,11	Stn. 4,8
Abbotsford	CAN	49.05	-122.33	71108099999	0	0	0	ABBOTSFORD ARPT	0	0	0
Adelaide	AUS	-34.93	138.6	94672099999	94675099999	94808099999	95677099999	ADELAIDE AIRPORT	KENT TOWN	NOARLUNGA	PARAFIELD AIRPORT
Akron	USA	41.07	-81.52	72430314813	72521014895	0	0	AKRON FULTON INTL	AKRON/AKRON-CANTON	0	0
Albacete	ESP	39	-1.87	8280099999	0	0	0	ALBACETE/LOS LLANOS	0	0	0
Albacete_a	ESP	39	-1.87	8280099999	0	0	0	ALBACETE/LOS LLANOS	0	0	0
Albuquerque	USA	35.11	-106.61	7236473034	72365023050	0	0	DOUBLE EAGLE II	ALBUQUERQUE INTL	0	0
Alicante	ESP	38.35	-0.48	8360099999	0	0	0	ALICANTE/EL ALTET	0	0	0
Allentown	USA	40.6	-75.48	72517014737	0	0	0	ALLENTOWN/A.-BETHLE	0	0	0
Almeria	ESP	36.83	-2.43	8487099999	0	0	0	ALMERIA/AEROPUERTO	0	0	0
Anshan	CHN	41.12	122.99	54339099999	0	0	0	ANSHAN	0	0	0
Athens	GRC	37.98	23.73	16716099999	16718099999	0	0	ATHINAI AP HELLINIKO	ELEFSIS (AIRPORT)	0	0
Athens_a	GRC	37.98	23.73	16716099999	16718099999	0	0	ATHINAI AP HELLINIKO	ELEFSIS (AIRPORT)	0	0
Atlanta	USA	33.76	-84.4	72219013874	72219599999	0	0	ATLANTA MUNICICPAL	FULTON CO ARPT BROW	0	0
Atlanta_a	USA	33.76	-84.4	72219013874	7221953888	72219599999	0	ATLANTA MUNICICPAL	FULTON CO ARPT BROW	FULTON CO ARPT BROW	0
Atlantic	USA	39.36	-74.44	72407093730	72407613724	0	0	ATLANTIC CITY INTL	ATLANTIC CITY (CGS)	0	0
Austin	USA	30.3	-97.75	72254013904	72254413958	72254513904	72254599999	AUSTIN/MUELLER MUNI	AUSTIN CAMP MABRY	BERGSTROM AFB/AUSTI	BERGSTROM AFB/AUSTI
Avila	ESP	40.67	-4.7	8210099999	0	0	0	AVILA	0	0	0
Badajoz	ESP	38.88	-6.97	8330099999	0	0	0	BADAJOZ/TALAVERA LA	0	0	0
Bakersfield	USA	35.36	-119.03	72384023155	0	0	0	BAKERSFIELD/MEADOWS	0	0	0
Baltimore	USA	39.31	-76.62	72406093721	0	0	0	BALTIMORE-WASHINGTO	0	0	0
Baltimore_a	USA	39.31	-76.62	72406093721	74594493784	0	0	BALTIMORE-WASHINGTO	BALTIMORE	0	0
Bangkok	THA	13.75	100.52	48453099999	48455099999	48456099999	0	BANG NA AGROMET	BANGKOK METROPOLIS	DON MUANG	0
Bangkok_a	THA	13.75	100.52	48455099999	48456099999	0	0	BANGKOK METROPOLIS	DON MUANG	0	0
Barcelona	ESP	41.4	2.17	8181099999	0	0	0	BARCELONA/AEROPUERT	0	0	0
Barcelona_a	ESP	41.4	2.17	8181099999	0	0	0	BARCELONA/AEROPUERT	0	0	0
Barcelona_b	ESP	41.4	2.17	8181099999	0	0	0	BARCELONA/AEROPUERT	0	0	0
Barcelona_c	ESP	41.4	2.17	8181099999	0	0	0	BARCELONA/AEROPUERT	0	0	0
Bari	ITA	41.12	16.87	16270099999	16271099999	0	0	BARI/PALESE MACCHIE	BARI	0	0
Bari_a	ITA	41.12	16.87	16270099999	0	0	0	BARI/PALESE MACCHIE	0	0	0
Barnstable	USA	41.66	-70.35	72506794720	72506799999	0	0	BARNSTABLE MUNI BOA	BARNSTABLE MUNI BOA	0	0
Batonrouge	USA	30.46	-91.14	72231713970	0	0	0	BATON ROUGE METRO R	0	0	0
Beijing	CHN	39.91	116.39	54511099999	0	0	0	BEIJING	0	0	0
Beijing_a	CHN	39.91	116.39	54511099999	0	0	0	BEIJING	0	0	0
Beijing_b	CHN	39.91	116.39	54511099999	0	0	0	BEIJING	0	0	0
Beirut	LBN	33.87	35.51	40100099999	0	0	0	RAFIC HARIRI INTL	0	0	0
Belem	BRA	-1.45	-48.48	82193099999	0	0	0	BELEM (AEROPORTO)	0	0	0
Belohorizonte	BRA	-19.92	-43.93	83583099999	83587099999	83672499999	0	BELO HORIZONTE /AER	BELO HORIZONTE	CARLOS PRATES	0
Bilbao	ESP	43.25	-2.93	8025099999	0	0	0	BILBAO/SONDICA	0	0	0
Bilbao_a	ESP	43.25	-2.93	8025099999	0	0	0	BILBAO/SONDICA	0	0	0
Birmingham	USA	33.52	-86.81	72228013876	0	0	0	BIRMINGHAM MUNI	0	0	0
Bologna	ITA	44.5	11.34	16132099999	16140099999	0	0	BOLOGNA	BOLOGNA/BORGO PANIG	0	0
Boston	USA	42.32	-71.09	72509014739	0	0	0	BOSTON/LOGAN INTL	0	0	0
Boston_a	USA	42.32	-71.09	72509014739	0	0	0	BOSTON/LOGAN INTL	0	0	0
Boston_b	USA	42.32	-71.09	72509014739	0	0	0	BOSTON/LOGAN INTL	0	0	0
Brasilia	BRA	-15.78	-47.92	83377099999	83378099999	0	0	BRASILIA	BRASILIA /AEROPORTO	0	0
Brescia	ITA	45.55	10.22	16088099999	16259399999	0	0	BRESCIA/GHEDI	MONTICHIARI	0	0
Brisbane	AUS	-27.46	153.02	94575099999	94576099999	94578099999	94578599999	ARCHERFIELD AIRPORT	BRISBANE	BRISBANE AERO	BRISBANE INTL ARPT
				94579099999	0	0	0	BRISBANE ARPT02 AWS	0	0	0

Cities	ISO3	LAT	LON	Stn.no 1,5,9	Stn.no 2,6,10	Stn.no 3,7,11	Stn.no 4,8	Stn. 1,5,9	Stn. 2,6,10	Stn. 3,7,11	Stn. 4,8
Brisbane_a	AUS	-27.46	153.02	94575099999	94576099999	94578099999	0	ARCHERFIELD AIRPORT	BRISBANE	BRISBANE AERO	0
Brisbane_b	AUS	-27.46	153.02	94575099999	94576099999	94578099999	94579099999	ARCHERFIELD AIRPORT	BRISBANE	BRISBANE AERO	BRISBANE ARPT02 AWS
Brownsville	USA	25.93	-97.48	72250012919	0	0	0	BROWNSVILLE INTL	0	0	0
Bucharest	ROU	44.44	26.1	15420099999	15421099999	15422099999	0	BUCURESTI INMH-BANE	BUCURESTI AFUMATI	BUCARESTI FILARET	0
Budapest	HUN	47.5	19.08	12830599999	12839099999	12840099999	12843099999	TOKOL	BUDAPEST/FERIHEGY I	BUDAPEST MET CENTER	BUDAPEST/PESTSZENTL
Budapest_a	HUN	47.5	19.08	12830599999	12838099999	12839099999	12840099999	TOKOL	BUDAORS	BUDAPEST/FERIHEGY I	BUDAPEST MET CENTER
				12843099999	0	0	0	BUDAPEST/PESTSZENTL	0	0	0
Buffalo	USA	42.9	-78.85	72528014733	72528599999	0	0	GREATER BUFFALO INT	BUFFALO (CGS)	0	0
Burgos	ESP	42.35	-3.69	8075099999	0	0	0	BURGOS/VILLAFRIA	0	0	0
Busan	KOR	35.1	129.04	47153099999	47159099999	0	0	GIMHAE INTL AIRPORT	BUSAN	0	0
Caceres	ESP	39.47	-6.38	8261099999	0	0	0	CACERES	0	0	0
Cadiz	ESP	36.53	-6.29	8449013025	0	0	0	ROTA	0	0	0
Calgary	CAN	51.07	-114.06	71235099999	71877099999	71877899999	0	COP UPPER	CALGARY INTL	COP UPPER	0
Calgary_a	CAN	51.07	-114.06	71235099999	71393099999	71877099999	71877899999	COP UPPER	CALGARY INTL CS	CALGARY INTL	COP UPPER
Cantonmassillon	USA	40.8	-81.38	72521014895	0	0	0	AKRON/AKRON-CANTON	0	0	0
Capetown	ZAF	-33.93	18.42	68816099999	68920099999	0	0	CAPE TOWN INTNL. AI	CAPE AGULHAS	0	0
Capetown_a	ZAF	-33.93	18.42	68816099999	68920099999	0	0	CAPE TOWN INTNL. AI	CAPE AGULHAS	0	0
Castellon	ESP	39.98	-0.03	8286099999	0	0	0	CASTELLON	0	0	0
Castellon_a	ESP	39.98	-0.03	8286099999	0	0	0	CASTELLON	0	0	0
Changchun	CHN	43.88	125.32	54161099999	0	0	0	CHANGCHUN	0	0	0
Changsha	CHN	28.2	112.97	59287199999	57687099999	0	0	CHANGSHA HUANGHUA	CHANGSHA	0	0
Changsha_a	CHN	28.2	112.97	59287199999	57687099999	0	0	CHANGSHA HUANGHUA	CHANGSHA	0	0
Changsha_b	CHN	28.2	112.97	59287199999	57687099999	0	0	CHANGSHA HUANGHUA	CHANGSHA	0	0
Changsha_c	CHN	28.2	112.97	59287199999	57687099999	0	0	CHANGSHA HUANGHUA	CHANGSHA	0	0
Charleston	USA	32.79	-79.99	72414013866	0	0	0	YEAGER	0	0	0
Charlotte	USA	35.21	-80.83	72314013881	0	0	0	CHARLOTTE/DOUGLAS	0	0	0
Charlotte_a	USA	35.21	-80.83	72314013881	0	0	0	CHARLOTTE/DOUGLAS	0	0	0
Chattanooga	USA	35.05	-85.27	72324013882	0	0	0	CHATTANOOGA/LOVELL	0	0	0
Chengdu	CHN	30.67	104.07	56294099999	0	0	0	CHENGDU	0	0	0
Chiangmai	THA	18.79	98.98	48327099999	0	0	0	CHIANG MAI	0	0	0
Chiangmai_a	THA	18.79	98.98	48327099999	0	0	0	CHIANG MAI	0	0	0
Chicago	USA	41.84	-87.68	72530094846	72530799999	72534014819	72534694866	CHICAGO/O HARE ARPT	WILMETTE (MARINES)	CHICAGO/MIDWAY	CHICAGO/MEIGS
Chicago_a	USA	41.84	-87.68	72530094846	72530799999	72534014819	72534099999	CHICAGO/O HARE ARPT	WILMETTE (MARINES)	CHICAGO/MIDWAY	CHICAGO/MIDWAY
				72534694866	72534699999	99725599999	99733899999	CHICAGO/MEIGS	CHICAGO/MEIGS	CALUMET II	CHICAGO
Chisinau	MDA	47.01	28.86	33815099999	33838799999	0	0	KISINEV	CHISINAU	0	0
Chongqing	CHN	29.56	106.55	57516099999	0	0	0	CHONGQING	0	0	0
Chongqing_a	CHN	29.56	106.55	57516099999	0	0	0	CHONGQING	0	0	0
Christchurch	NZL	-43.53	172.64	93780099999	0	0	0	CHRISTCHURCH	0	0	0
Cincinnati	USA	39.14	-84.5	72429793812	0	0	0	CINCINNATI MUNI LUN	0	0	0
Ciudadreal	ESP	38.98	-3.94	8348099999	0	0	0	CIUDAD REAL	0	0	0
Ciudadreal_a	ESP	38.98	-3.94	8014199999	8348099999	0	0	CIUDAD REAL	CIUDAD REAL	0	0
Civitavecchia	ITA	42.1	11.8	16214099999	0	0	0	CIVITAVECCHIA	0	0	0
Cleveland	USA	41.48	-81.67	72524014820	7252454853	72524599999	7252474805	CLEVELAND	BURKE LAKEFRONT	BURKE LAKEFRONT	CUYAHOGA CO
				72524799999	99769299999	0	0	CUYAHOGA CO	CLEVELAND	0	0
Columbia	USA	34.02	-81.01	72310013883	72310453867	72310499999	99999953867	COLUMBIA METRO	COLUMBIA OWENS APT	COLUMBIA OWENS APT	COLUMBIA OWENS DOWN-TOWN AP
Columbus	USA	32.49	-84.94	72428014821	72428463825	72428499999	72428513812	COLUMBUS/PORT COLUM	BOLTON FLD	BOLTON FLD	RICKENBACKER INTL
				7242884804	72428899999	0	0	OHIO STATE UNIVERSI	OHIO STATE UNIVERSI	0	0
Cordoba	ESP	37.88	-4.77	8410099999	0	0	0	CORDOBA/AEROPUERTO	0	0	0
Cuenca	ESP	40.08	-2.14	8231099999	0	0	0	CUENCA	0	0	0
Cuenca_a	ESP	40.08	-2.14	8231099999	0	0	0	CUENCA	0	0	0

Cities	ISO3	LAT	LON	Stn.no 1,5,9	Stn.no 2,6,10	Stn.no 3,7,11	Stn.no 4,8	Stn. 1,5,9	Stn. 2,6,10	Stn. 3,7,11	Stn. 4,8
Cuiaba	BRA	-15.58	-56.08	83361099999	83362099999	0	0	CUIABA	CUIABA (AEROPORTO)	0	0
Curitiba	BRA	-25.42	-49.25	83840099999	83842099999	0	0	CURITIBA /AEROPORTO	CURITIBA	0	0
Daegu	KOR	35.87	128.6	47142099999	47142599999	47143099999	69358499999	DAEGU AB	CAMP WALKER (H-805)	DAEGU	USAG WALKER TMQ-53P
Daegu_a	KOR	35.87	128.6	47142099999	47142599999	47143099999	69358499999	DAEGU AB	CAMP WALKER (H-805)	DAEGU	USAG WALKER TMQ-53P
Daegu_b	KOR	35.87	128.6	47142099999	47142599999	47143099999	69358499999	DAEGU AB	CAMP WALKER (H-805)	DAEGU	USAG WALKER TMQ-53P
Daegu_c	KOR	35.87	128.6	47142099999	47143099999	69358499999	0	DAEGU AB	DAEGU	USAG WALKER TMQ-53P	0
Daejeon	KOR	36.32	127.42	47133099999	0	0	0	DAEJEON	0	0	0
Daejeon_a	KOR	36.32	127.42	47133099999	0	0	0	DAEJEON	0	0	0
Dallas	USA	32.8	-96.79	72258013960	72258113960	72258313960	7225983970	DALLAS LOVE FIELD	DALLAS LOVE FIELD	DALLAS LOVE FLD	ADDISON
				72259899999	7225993971	72259999999	0	ADDISON	DALLAS EXECUTIVE	DALLAS EXECUTIVE	0
Dallas_a	USA	32.8	-96.79	72258013960	72258113960	72258313960	72259899999	DALLAS LOVE FIELD	DALLAS LOVE FIELD	DALLAS LOVE FLD	ADDISON
				72259999999	0	0	0	DALLAS EXECUTIVE	0	0	0
Dayton	USA	39.76	-84.2	72427653859	72427699999	72429093815	0	DAYTON WRIGHT BROTHE	DAYTON WRIGHT BROTHE	DAYTON/JAMES M COX	0
Daytonabeach	USA	29.21	-81.04	72205612834	72234192822	72234199999	72236192808	DAYTONA BEACH INTL	ORMOND BEACH MUNI	ORMOND BEACH MUNI	NEW SMYRNA BEACH MUN
				72236199999	0	0	0	NEW SMYRNA BEACH MUN	0	0	0
Delhi	IND	28.64	77.21	42182099999	0	0	0	NEW DELHI/SAFDARJUN	0	0	0
Denver	USA	39.73	-104.97	72698024229	72698524242	72698599999	0	PORTLAND INTL ARPT	PORTLAND TROUTDALE	PORTLAND TROUTDALE	0
Desmoines	USA	41.59	-93.62	72546014933	0	0	0	DES MOINES INTL	0	0	0
Detroit	USA	42.39	-83.1	72537514822	0	0	0	DETROIT CITY	0	0	0
Dhaka	BGD	23.72	90.41	41923099999	0	0	0	DHAKA	0	0	0
Dublin	IRL	53.33	-6.25	3969099999	0	0	0	DUBLIN AIRPORT	0	0	0
Durban	ZAF	-29.85	31.02	68588099999	0	0	0	DURBAN INTNL. AIRPO	0	0	0
Edmonton	CAN	53.55	-113.57	71123099999	71879099999	0	0	EDMONTON INTL ARPT	EDMONTON MUNICIPAL	0	0
Edmonton_a	CAN	53.55	-113.57	71123099999	71155099999	71157099999	71879099999	EDMONTON INTL ARPT	EDMONTON INTERNATIO	EDMONTON MUNICIPAL	EDMONTON MUNICIPAL
Elpaso	USA	31.79	-106.42	72270023044	0	0	0	EL PASO INTL ARPT	0	0	0
Erie	USA	42.11	-80.08	72526014860	0	0	0	ERIE INTL AIRPORT	0	0	0
Flint	USA	43.03	-83.69	72637014826	0	0	0	FLINT/BISHOP INTL	0	0	0
Fortaleza	BRA	-3.78	-38.59	82397099999	82398099999	0	0	FORTALEZA	FORTALEZA /AEROPORT	0	0
Fortlauderdale	USA	26.14	-80.14	72202512849	72203792809	72203799999	72203912885	FORT LAUDERDALE HOL	NORTH PERRY	NORTH PERRY	FORT LAUDER-DALE EXEC
				72203999999	72204992805	72204999999	0	FORT LAUDERDALE EXEC	POMPANO BEACH AIRPAR	POMPANO BEACH AIRPAR	0
Fortmyers	USA	26.63	-81.86	72210612835	72210812894	72210899999	0	FORT MYERS/PAGE FLD	SOUTHWEST FLORIDA I	SOUTHWEST FLORIDA I	0
Fortpiercenorth	USA	27.44	-80.34	72210312895	72210399999	0	0	ST LUCIE CO INTL	ST LUCIE CO INTL	0	0
Fortworth	USA	32.74	-97.33	7225933985	72259513911	72259613961	0	FORT WORTH SPINKS	FORT WORTH NAS JRB	FORT WORTH MEACHAM	0
Fresno	USA	36.78	-119.79	72389093193	72389723167	0	0	FRESNO AIR TERMINAL	FRESNO CHANDLER EXEC	0	0
Frosinone	ITA	41.65	13.35	16244099999	0	0	0	FROSINONE	0	0	0
Fuzhou	CHN	26.06	119.31	58847099999	0	0	0	FUZHOU	0	0	0
Galveston	USA	29.28	-94.83	72242012923	72242099999	72242212923	99736399999	GALVESTON	GALVESTON	SCHOLES INTL AT GLSTON APT	GALVESTON PLEASURE
Gary	USA	41.58	-87.35	7253374807	72533799999	0	0	GARY CHICAGO	GARY CHICAGO	0	0
Genoa	ITA	44.42	8.93	16120099999	16121099999	0	0	GENOVA/SESTRI	GENOVA/SESTRI	0	0
Gijon	ESP	43.53	-5.67	8014099999	0	0	0	GIJON-MUSEL	0	0	0
Girona	ESP	41.98	2.81	8184099999	0	0	0	GERONA/COSTA BRAVA	0	0	0
Goiania	BRA	-16.67	-49.27	83423099999	83424099999	0	0	GOIANIA	GOIANIA (AEROPORTO)	0	0
Granada	ESP	37.17	-3.59	8014499999	8419099999	0	0	ARMILLA	GRANADA/AEROPUERTO	0	0
Grandrapids	USA	42.96	-85.66	72635094860	0	0	0	GRAND RAPIDS/KENT C	0	0	0
Greensboro	USA	36.08	-79.82	72317013723	0	0	0	GREENSBORO/G.-HIGH	0	0	0
Greenville	USA	34.84	-82.39	72311913886	72312263889	0	0	GREENVILLE DOWNTOWN	GREENVILLE	0	0
Guadalajara	ESP	40.64	-3.17	8226099999	0	0	0	GUADALAJARA	0	0	0
Guadalajara_a	ESP	40.64	-3.17	8226099999	0	0	0	GUADALAJARA	0	0	0

Cities	ISO3	LAT	LON	Stn.no 1,5,9	Stn.no 2,6,10	Stn.no 3,7,11	Stn.no 4,8	Stn. 1,5,9	Stn. 2,6,10	Stn. 3,7,11	Stn. 4,8
Guangzhou	CHN	23.12	113.25	59287099999	0	0	0	GUANGZHOU	0	0	0
Guangzhou_a	CHN	23.12	113.25	59287099999	0	0	0	GUANGZHOU	0	0	0
Guangzhou_b	CHN	23.12	113.25	59287099999	0	0	0	GUANGZHOU	0	0	0
Guilin	CHN	25.28	110.29	57957099999	0	0	0	GUILIN	0	0	0
Haikou	CHN	20.05	110.34	47031199999	59758099999	0	0	MEILAN	HAIKOU	0	0
Haikou_a	CHN	20.05	110.34	47031199999	59758099999	0	0	MEILAN	HAIKOU	0	0
Halifax	CAN	44.62	-63.69	71327099999	71601099999	71601599999	0	HALIFAX WINDSOR PAR	SHEARWATER	SHEARWATER JETTY	0
Hamilton_CA	CAN	43.27	-79.92	71263099999	71437099999	71437599999	0	HAMILTON AIRPORT	BURLINGTON PIERS	BURLINGTON PIERS \	0
Hamilton_CA_a	CAN	43.27	-79.92	71263099999	71437099999	71437599999	71624699999	HAMILTON AIRPORT	BURLINGTON PIERS	BURLINGTON PIERS \	HAMILTON AIRPORT
Hamilton_US	USA	39.4	-84.56	72521753855	72521799999	0	0	BUTLER CO RGNL	BUTLER CO RGNL	0	0
Hangzhou	CHN	30.26	120.17	58457099999	0	0	0	HANGZHOU	0	0	0
Harbin	CHN	45.75	126.65	50953099999	0	0	0	HARBIN	0	0	0
Harbin_a	CHN	45.75	126.65	50953099999	0	0	0	HARBIN	0	0	0
Harrisburg	USA	40.27	-76.88	72511014751	72511114751	72511514711	72511814751	HARRISBURG CAPITAL CITY ARPT	HARRISBURG CAPITAL CITY ARPT	HARRISBURG INTL	HARRISBURG/CAPITAL
Hartford	USA	41.76	-72.69	72508714752	72508799999	0	0	HARTFORD BRAINARD	HARTFORD BRAINARD	0	0
Hefei	CHN	31.86	117.28	58321099999	0	0	0	HEFEI	0	0	0
Helsinki	FIN	60.17	24.94	2974099999	2975099999	0	0	HELSINKI-VANTAA	HELSINKI-MALMI	0	0
Hongkong	HKG	22.28	114.15	45004099999	45007099999	0	0	KOWLOON	HONG KONG INTERNATI	0	0
Honolulu	USA	21.31	-157.83	91182022521	0	0	0	HONOLULU INTL	0	0	0
Houston	USA	29.76	-95.38	72243512918	0	0	0	WILLIAM P HOBBY	0	0	0
Huelva	ESP	37.25	-6.94	8383099999	0	0	0	HUELVA	0	0	0
Huelva	ESP	37.25	-6.94	8383099999	0	0	0	HUELVA	0	0	0
Huesca	ESP	42.14	-0.41	8094099999	0	0	0	HUESCA-PIRINEOS	0	0	0
Incheon	KOR	37.45	126.73	47112099999	47113199999	0	0	INCHEON	INCHEON INTL	0	0
Incheon_a	KOR	37.45	126.73	47112099999	0	0	0	INCHEON	0	0	0
Incheon_b	KOR	37.45	126.73	47112099999	47113199999	0	0	INCHEON	INCHEON INTL	0	0
Indianapolis	USA	39.79	-86.15	72438093819	72438453842	72438499999	0	INDIANAPOLIS/I.-MUN	EAGLE CREEK AIRPARK	EAGLE CREEK AIRPARK	0
Istanbul	TUR	41.02	28.96	17060099999	0	0	0	ISTANBUL/ATATURK	0	0	0
Jacksonville	USA	30.32	-81.66	72206013889	72206593837	72206763823	72206793832	JACKSONVILLE/INTNL.	JACKSONVILLE NAS	CECIL FLD	CECIL FLD
				72206799999	72206853860	72206899999	0	CECIL FLD	JACKSONVILLE/CRAIG	JACKSONVILLE/CRAIG	0
Jacksonville_a	USA	30.32	-81.66	72206013889	72206593837	72206793832	72206899999	JACKSONVILLE/INTNL.	JACKSONVILLE NAS	CECIL FLD	JACKSONVILLE/CRAIG
Jaen	ESP	37.77	-3.8	8417099999	0	0	0	JAEN	0	0	0
Jersey	USA	40.72	-74.07	72502014734	72502594741	99774399999	0	NEWARK INTL AIRPORT	TETERBORO	ROBINS REEF	0
Jinan	CHN	36.67	117	54823099999	0	0	0	JINAN	0	0	0
Joaopessoa	BRA	-7.12	-34.87	82798099999	0	0	0	JOAO PESSOA	0	0	0
Johannesburg	ZAF	-26.2	28.08	68267199999	68267299999	68346399999	68368099999	GRAND CENTRAL	JOHANNESBURG B/G	RAND	JOHANNESBURG INTNL.
Kansas	USA	39.08	-94.56	72446113988	72446399999	0	0	KANSAS CITY DOWNTOWN AP	CHARLES B WHEELER D	0	0
Kingston	CAN	44.29	-76.51	71620099999	71620499999	0	0	KINGSTON	KINGSTON (MARS)	0	0
Kitchener	CAN	43.44	-80.51	71368099999	71368199999	71368399999	0	KITCHENER/WATERLOO	WATERLOO WELL	WATERLOO WELL	0
Knoxville	USA	35.97	-83.94	72326013891	0	0	0	KNOXVILLE MUNICIPAL	0	0	0
Kunming	CHN	25.04	102.72	56778099999	0	0	0	KUNMING	0	0	0
Kunming_a	CHN	25.04	102.72	56778099999	0	0	0	KUNMING	0	0	0
Kwangju	KOR	35.15	126.92	47111099999	47120599999	69215499999	0	SEOUL AB	MAESANRI	GWANGJUUP (TMQ-53P)	0
Lacoruna	ESP	43.33	-8.42	8001099999	8002099999	0	0	LA CORUNA	LA CORUNA/ALVEDRO	0	0
Lakeland	USA	28.04	-81.96	72211912883	72211999999	72212312809	72212399999	LAKELAND LINDER RGN	LAKELAND LINDER RGN	BARTOW MUNI	BARTOW MUNI
Lancaster	USA	34.69	-118.15	72511654737	72511699999	0	0	LANCASTER	LANCASTER	0	0
Lansing	USA	42.72	-84.55	72539014836	72541754822	0	0	LANSING/CAPITAL CIT	MASON JEWETT FLD	0	0
Lanzhou	CHN	36.06	103.79	52533199999	52889099999	0	0	ZHONGCHUAN	LANZHOU	0	0
Lasvegas	USA	36.19	-115.22	72386023169	72386523112	72484653123	72484699999	LAS VEGAS/MCCARRAN	NELLIS AFB	NORTH LAS VEGAS	NORTH LAS VEGAS
Latina	ITA	41.47	12.89	16243099999	0	0	0	LATINA	0	0	0
Leon	ESP	42.59	-5.57	8055099999	0	0	0	LEON/VIRGEN DEL CAM	0	0	0
Lisbon	PRT	38.72	-9.14	8535099999	8536099999	8579099999	0	LISBOA/GEOF	LISBOA/PORTELA	LISBOA/GAGO COUTINH	0

Cities	ISO3	LAT	LON	Stn.no 1,5,9	Stn.no 2,6,10	Stn.no 3,7,11	Stn.no 4,8	Stn. 1,5,9	Stn. 2,6,10	Stn. 3,7,11	Stn. 4,8
Lisbon_a	PRT	38.72	-9.14	8536099999	8579099999	0	0	LISBOA/PORTELA	LISBOA/GAGO COUTINH	0	0
Littlerock	USA	34.74	-92.33	7234003952	72340099999	72340113963	72340313963	LITTLE ROCK WSFO	LITTLE ROCK WSFO	LITTLE ROCK ADAMS FIELD	ADAMS FLD
Ljubljana	SVN	46.06	14.51	13014099999	13015099999	14014099999	14015099999	LJUBLJANA/BRNIK	LJUBLJANA/BEZIGRAD	LJUBLJANA/BRNIK	LJUBLJANA/BEZIGRAD
Ljubljana_a	SVN	46.06	14.51	13014099999	13015099999	0	0	LJUBLJANA/BRNIK	LJUBLJANA/BEZIGRAD	0	0
Lleida	ESP	41.62	0.63	8171099999	0	0	0	LERIDA	0	0	0
Logrono	ESP	42.47	-2.44	8084099999	0	0	0	LOGRONO/AGONCILLO	0	0	0
London_CA	CAN	43.01	-81.29	71622099999	71623099999	0	0	LONDON CS	LONDON	0	0
London_CA_a	CAN	43.01	-81.29	71623099999	0	0	0	LONDON	0	0	0
London_UK	GBR	51.5	-0.12	3768399999	3772099999	3779099999	0	LONDON/CITY	LONDON/HEATHROW AIR	LONDON WEATHER CENT	0
London_UK_a	GBR	51.5	-0.12	3768399999	3772099999	3779099999	0	LONDON/CITY	LONDON/HEATHROW AIR	LONDON WEATHER CENT	0
London_UK_b	GBR	51.5	-0.12	3768399999	3772099999	3775099999	3778099999	LONDON/CITY	LONDON/HEATHROW AIR	KEW-IN-LONDON	LONDON WEA CENTER
				3779099999	3782099999	0	0	LONDON WEATHER CENT	BLACKWALL	0	0
Losangeles	USA	34.09	-118.38	72287493134	72288023152	72288593197	72288599999	LA USC DOWNTOWN CAM	BURBANK/GLENDALE	SANTA MONICA MUNI	SANTA MONICA MUNI
				72288623130	72291399999	72295023174	7229563167	VAN NUYS	MARINA DEL REY	LOS ANGELES INTL	JACK NORTHROP FLD H
				72295699999	74505753130	0	0	JACK NORTHROP FLD H	WHITEMAN	0	0
Louisville	USA	38.23	-85.75	72423093821	72423513810	0	0	LOUISVILLE/STANDIFO	BOWMAN FLD	0	0
Lubbock	USA	33.56	-101.88	72267023042	72267523021	0	0	LUBBOCK/LUBBOCK INT	REESE AFB/LUBBOCK	0	0
Lugo	ESP	43.02	-7.56	8008099999	0	0	0	LUGO/ROZAS	0	0	0
Maceio	BRA	-9.67	-35.72	82993099999	0	0	0	MACEIO (AEROPORTO)	0	0	0
Madison	USA	43.07	-89.39	72641014837	0	0	0	MADISON/DANE COUNTY	0	0	0
Madrid	ESP	40.42	-3.71	8220099999	8221099999	8223099999	0	MADRID/C. UNIVERSIT	MADRID/BARAJAS RS	MADRID/CUATRO VIENT	0
Madrid_a	ESP	40.42	-3.71	8220099999	8221099999	8223099999	0	MADRID/C. UNIVERSIT	MADRID/BARAJAS RS	MADRID/CUATRO VIENT	0
Malaga	ESP	36.72	-4.42	8482099999	0	0	0	MALAGA/AEROPUERTO	0	0	0
Manaus	BRA	-3.13	-60.02	82111099999	82332099999	0	0	EDUARDO GOMES INTL	MANAUS (AEROPORTO)	0	0
Manila	PHL	14.63	121.03	98425099999	98429099999	98430099999	0	MANILA	NINOY AQUINO INTERN	SCIENCE GARDEN	0
Mcallen	USA	26.22	-98.24	72250612959	0	0	0	MC ALLEN MILLER INT	0	0	0
Melbourne	AUS	-37.81	144.96	94868099999	95866099999	0	0	MELBOURNE	ESSENDON AIRPORT	0	0
Melbourne_US	USA	28.11	-80.63	72204012838	74795012867	74795099999	0	MELBOURNE REGIONAL	PATRICK AFB/COCOA B	PATRICK AFB/COCOA B	0
Melilla	ESP	35.3	-2.95	60338099999	0	0	0	MELILLA	0	0	0
Memphis	USA	35.12	-89.97	72334013893	0	0	0	MEMPHIS INTL ARPT	0	0	0
Mexicocity	MEX	19.5	-99.12	76679099999	76679399999	76680099999	0	AEROP. INTERNACIONA	LICENCIADO BENITO J	MEXICO CITY	0
Miami	USA	25.79	-80.22	72202012839	72202499999	0	0	MIAMI	OPA LOCKA	0	0
Miami_a	USA	25.79	-80.22	72202012839	72202412882	72202499999	0	MIAMI	OPA LOCKA	OPA LOCKA	0
Milan	ITA	45.48	9.19	16080099999	0	0	0	MILANO/LINATE	0	0	0
Milwaukee	USA	43.05	-87.96	72640014839	72640594869	99734299999	0	MILWAUKEE/GEN. MITC	LAWRENCE J TIMMERMAN	MILWAUKEE	0
Minneapolisstpaul	USA	44.96	-93.27	72658014922	0	0	0	MINNEAPOLIS/ST.PAUL	0	0	0
Mobile	USA	30.68	-88.1	72223013894	72223513838	0	0	MOBILE/BATES FIELD	MOBILE DOWNTOWN	0	0
Monterrey	MEX	25.66	-100.31	76393099999	76394099999	76394399999	0	MONTERREY (CITY)	AEROP.INTERNACIONAL	GENERAL MARIANO ESC	0
Montreal	CAN	45.57	-73.66	71183099999	71612099999	71627094792	71627099999	PIERRE TRUDEAU INTL	MCTAVISH	MONTREAL/TRUDEAU INT	MONTREAL/TRUDEAU INT
Montreal_a	CAN	45.57	-73.66	71183099999	71612099999	71627094792	71627099999	PIERRE TRUDEAU INTL	MCTAVISH	MONTREAL/TRUDEAU INT	MONTREAL/TRUDEAU INT
Moscow	RUS	55.75	37.62	27515599999	27612099999	0	0	SHEREMETYEVO	MOSKVA	0	0
Murcia	ESP	37.98	-1.13	8429099999	8430099999	0	0	MURCIA/ALCANTARILLA	MURCIA	0	0
Myrtlebeach	USA	33.7	-78.88	74791013717	74791593718	0	0	MYRTLE BEACH CIV	NORTH MYRTLE BEACH	0	0
Nanjing	CHN	32.06	118.77	58238099999	0	0	0	NANJING	0	0	0
Nanjing_a	CHN	32.06	118.77	58238099999	0	0	0	NANJING	0	0	0
Nanning	CHN	22.82	108.32	59431099999	0	0	0	NANNING	0	0	0
Naples	USA	26.15	-81.8	72203812897	72203899999	99735199999	0	NAPLES MUNI	NAPLES MUNI	NAPLES	0
Nashua	USA	42.75	-71.48	74394654754	74394699999	0	0	BOIRE FLD	BOIRE FLD	0	0
Nashvilledavidson	USA	36.15	-86.76	72327013897	0	0	0	NASHVILLE/METROPOLI	0	0	0

Cities	ISO3	LAT	LON	Stn.no 1,5,9	Stn.no 2,6,10	Stn.no 3,7,11	Stn.no 4,8	Stn. 1,5,9	Stn. 2,6,10	Stn. 3,7,11	Stn. 4,8
Natal	BRA	-5.8	-35.2	82599099999	0	0	0	NATAL AEROPORTO	0	0	0
Newark	USA	40.74	-74.18	72409454743	72409499999	72502014734	72502594741	ESSEX CO	ESSEX CO	NEWARK INTL AIRPORT	TETERBORO
				99774399999	0	0	0	ROBINS REEF	0	0	0
Newburgh	USA	41.5	-74.02	72503614757	72503814714	0	0	DUTCHESS CO	STEWART INTL	0	0
Newhaven	USA	41.31	-72.92	72504514758	99728499999	0	0	TWEED NEW HAVEN	NEW HAVEN	0	0
Newlondon	USA	41.35	-72.1	72504614707	0	0	0	GROTON NEW LONDON	0	0	0
Newyorkcity	USA	40.7	-73.92	72503014732	72503394728	74486094789	99727299999	NEW YORK/LA GUARDIA	NYC CENTRAL PARK	NEW YORK/JOHN F. KE	BERGEN POINT
				99999994728	0	0	0	NEW YORK CENTRAL PARK ARSNL B	0	0	0
Newyorkcity_a	USA	40.7	-73.92	72503014732	72503394728	74486094789	99999994728	NEW YORK/LA GUARDIA	NYC CENTRAL PARK	NEW YORK/JOHN F. KE	NEW YORK CENTRAL PARK ARSNL B
Oakland	USA	37.8	-122.23	72493023230	72493099999	72493593228	72493599999	OAKLAND/METROP. OAK	OAKLAND/METROP. OAK	HAYWARD AIR TERM	HAYWARD AIR TERM
Ocala	USA	29.19	-82.13	72205512861	72205599999	0	0	OCALA INTL J TAYLOR	OCALA INTL J TAYLOR	0	0
Oklahoma	USA	35.48	-97.53	72353013967	72354013919	7235443954	72354499999	OKLAHOMA CITY/W. RO	TINKER AFB	OKLAHOMA CITY/WILEY	OKLAHOMA CITY/WILEY
Omaha	USA	41.26	-96.01	7203084992	72030899999	72550014942	72553094918	MILLARD	MILLARD	OMAHA/EPPLEY FIELD	OMAHA
				72554014949	0	0	0	OFFUTT AFB	0	0	0
Orange	USA	33.8	-117.83	69014093101	72290899999	72291593114	7229763166	EL TORO MCAS	EL TORO(USMC)	TUSTIN MCAF	FULLERTON MUNICIPAL
				72297699999	72297793184	99999993101	0	FULLERTON MUNICIPAL	JOHN WAYNE ARPT ORA	EL TORO MCAS	0
Orlando	USA	28.53	-81.38	72205012815	72205312841	0	0	ORLANDO/JETPORT	EXECUTIVE	0	0
Ottawa	CAN	45.4	-75.73	71063099999	71628099999	0	0	OTTAWA RECREATION C	OTTAWA INTL. ONT	0	0
Ottawa_a	CAN	45.4	-75.73	71063099999	71628099999	0	0	OTTAWA RECREATION C	OTTAWA INTL. ONT	0	0
Ourense	ESP	42.33	-7.87	8048099999	0	0	0	ORENSE	0	0	0
Oviedo	ESP	43.35	-5.83	8015099999	0	0	0	OVIEDO	0	0	0
Oviedo	ESP	43.35	-5.83	8015099999	0	0	0	OVIEDO	0	0	0
Palermo	ITA	38.12	13.36	16410099999	0	0	0	PALERMO BOCCADIFALC	0	0	0
Palermo_a	ITA	38.12	13.36	16409099999	16410099999	0	0	PALERMO BOCCADIFALC	PALERMO BOCCADIFALC	0	0
Palmademallorca	ESP	39.57	2.65	8306099999	0	0	0	PALMA DE MALLORCA/S	0	0	0
Pamplona	ESP	42.82	-1.63	8085099999	0	0	0	PAMPLONA/NOAIN	0	0	0
Paris	FRA	48.87	2.33	7149099999	7150099999	7156099999	7157099999	ORLY	LE BOURGET	PARIS-MONTSOURIS	ROISSY
Pensacola	USA	30.44	-87.21	72222013899	72222113899	72222313899	7222253855	PENSACOLA	PENSACOLA REGIONAL AP	PENSACOLA RGNL	PENSACOLA NAS
Philadelphia	USA	40	-75.14	72408013739	72408594732	72408599999	99728699999	PHILADELPHIA INTL	NORTHEAST PHILADELPH	NORTHEAST PHILADELPH	PHILADELPHIA
Philadelphia_a	USA	40	-75.14	72408013739	72408594732	0	0	PHILADELPHIA INTL	NORTHEAST PHILADELPH	0	0
Phoenix	USA	33.53	-112.08	72278023183	0	0	0	PHOENIX/SKY HARBOR	0	0	0
Phoenix_a	USA	33.53	-112.08	72278023183	0	0	0	PHOENIX/SKY HARBOR	0	0	0
Pittsburgh	USA	40.44	-79.98	72520514762	72520599999	0	0	ALLEGHENY CO	ALLEGHENY CO	0	0
Pontevedra	ESP	42.42	-8.66	8044099999	0	0	0	PONTEVEDRA	0	0	0
Portland_US_ME	USA	43.67	-70.27	72606014764	0	0	0	PORTLAND/INTNL. JET	0	0	0
Portland_US_OR	USA	43.67	-70.27	72698024229	72698524242	72698599999	0	PORTLAND INTL ARPT	PORTLAND TROUTDALE	PORTLAND TROUTDALE	0
Portoalegre	BRA	-30.03	-51.2	83967099999	83971099999	0	0	PORTO ALEGRE	PORTO ALEGRE /AEROP	0	0
Prague	CZE	50.08	14.43	11518099999	11520099999	11567099999	0	PRAHA/RUZYNE	PRAHA-LIBUS	PRAHA-KBELY	0
Providence	USA	41.82	-71.42	72505464710	72507014765	0	0	NORTH CENTRAL STATE	PROVIDENCE/GREEN ST	0	0
Puntagorda	USA	26.92	-82.05	72203412812	72203499999	0	0	CHARLOTTE CO	CHARLOTTE CO	0	0
Quebeccity	CAN	46.89	-71.34	71392099999	71714099999	0	0	STE FOY (U. LAVAL)	JEAN LESAGE INTL	0	0
Raleigh	USA	35.82	-78.64	72306013722	0	0	0	RALEIGH/RALEIGH-DUR	0	0	0
Reading	USA	40.34	-75.93	72510114712	72510314712	0	0	READING SPAATZ FIELD	READING RGNL CARL A	0	0
Recife	BRA	-8.05	-34.9	82899099999	82900099999	0	0	RECIFE (AEROPORTO)	RECIFE	0	0
Regina	CAN	50.48	-104.65	71514099999	71863099999	0	0	REGINA UNIVERSITY	REGINA INTL	0	0
Regina_a	CAN	50.48	-104.65	71514099999	71863099999	0	0	REGINA UNIVERSITY	REGINA INTL	0	0
Riverside	USA	33.95	-117.4	72033399999	72286023119	7228693171	72286999999	CORONA MUNI	RIVERSIDE/MARCH AFB	RIVERSIDE MUNI	RIVERSIDE MUNI
				7470403102	0	0	0	ONTARIO INTL ARPT	0	0	0

Cities	ISO3	LAT	LON	Stn.no 1,5,9	Stn.no 2,6,10	Stn.no 3,7,11	Stn.no 4,8	Stn. 1,5,9	Stn. 2,6,10	Stn. 3,7,11	Stn. 4,8
Rochester	USA	43.17	-77.61	72529014768	0	0	0	ROCHESTER-MONROE CO	0	0	0
Rockford	USA	42.27	-89.07	72543094822	0	0	0	GREATER ROCKFORD	0	0	0
Rome	ITA	41.89	12.5	16235099999	16238099999	16239099999	16240099999	ROMA/URBE	ROME CENTOCELLE	ROMA/CIAMPINO	ROME
				16247099999	0	0	0	TEVERE A RIPETTA	0	0	0
Rome_a	ITA	41.89	12.5	16235099999	16238099999	16239099999	16240099999	ROMA/URBE	ROME CENTOCELLE	ROMA/CIAMPINO	ROME
				16247099999	0	0	0	TEVERE A RIPETTA	0	0	0
Rome_b	ITA	41.89	12.5	16235099999	16239099999	16240099999	0	ROMA/URBE	ROMA/CIAMPINO	ROME	0
Sacramento	USA	38.56	-121.47	72483023232	72483323206	72483399999	72483623208	SACRAMENTO/EXECUTIV	SACRAMENTO MATHER FL	SACRAMENTO MATHER FL	MC CLELLAN AFLD
				72483993225	0	0	0	SACRAMENTO INTL	0	0	0
Saginaw	USA	43.42	-83.95	7221254829	72212599999	72637914845	0	SAGINAW CO H W BROWN	SAGINAW CO H W BROWN	MBS INTL	0
Saintjohn	CAN	45.3	-66.08	71609099999	0	0	0	SAINT JOHN ARPT	0	0	0
Salamanca	ESP	40.97	-5.67	8202099999	0	0	0	SALAMANCA/MATACAN	0	0	0
Salinas	USA	36.68	-121.64	72491723233	0	0	0	SALINAS MUNI	0	0	0
Saltlakecity	USA	40.75	-111.89	72572024127	0	0	0	SALT LAKE CITY INTL	0	0	0
Salvador	BRA	-12.97	-38.5	83229099999	83248099999	0	0	SALVADOR	SALVADOR /AEROPORTO	0	0
Salvador_a	BRA	-12.97	-38.5	83248099999	0	0	0	SALVADOR /AEROPORTO	0	0	0
Sanantonio	USA	29.45	-98.51	72253012921	72253512909	72253599999	0	SAN ANTONIO INTL	LACKLAND AFB KELLY	LACKLAND AFB KELLY	0
Sandiego	USA	32.78	-117.15	72290023188	72290199999	7229033131	72290399999	SAN DIEGO/LINDBERGH	SAN DIEGO/MONTGOMER	MONTGOMERY FLD	MONTGOMERY FLD
				72290693112	72290753143	72290799999	72291499999	NORTH ISLAND NAS	GILLESPIE FLD	GILLESPIE FLD	MISSION BEACH
				72293093107	99729299999	99999993107	0	SAN DIEGO/MIRAMAR N	LA JOLLA	SAN DIEGO MIRAMAR NAS	0
Sanfrancisco	USA	37.76	-122.44	72494023234	99401699999	0	0	SAN FRANCISCO INTL	SAN FRANCISCO	0	0
Sanjose	USA	37.3	-121.87	72494523293	72494693232	72494699999	74509023244	NORMAN Y MINETA SAN	REID HILLVIEW OF SAN	REID HILLVIEW OF SAN	MOUNTAIN VIEW /SUNN
Sansebastiandelosrey	ESP	40.55	-3.62	8220099999	8221099999	8227099999	0	MADRID/C. UNIVERSIT	MADRID/BARAJAS RS	MADRID/TORREJON	0
Santander	ESP	43.47	-3.8	8023099999	0	0	0	SANTANDER	0	0	0
Santiago_CL	CHL	-33.45	-70.67	85579099999	85580099999	85581099999	0	LOS CERRILLOS	SANTIAGO/EULOGIO SA	EL BOSQUE(CAFB)	0
Saoluis	BRA	-2.52	-44.27	82281099999	0	0	0	SAO LUIZ /AEROPORTO	0	0	0
Saopaulo	BRA	-23.53	-46.62	83075099999	83775399999	83779099999	83780099999	GUARULHOS	GUARULHOS	MARTE	SAO PAULO /AEROPORT
Saopaulo_a	BRA	-23.53	-46.62	83775399999	83779099999	83780099999	83781099999	GUARULHOS	MARTE	SAO PAULO /AEROPORT	SAO PAULO
Sarasota	USA	27.34	-82.54	72211512871	72211599999	0	0	SARASOTA BRADENTON	SARASOTA BRADENTON	0	0
Saskatoon	CAN	52.16	-106.65	71496099999	71866099999	0	0	SASKATOON RCS	SASKATOON DIEFENBAKE	0	0
Scranton	USA	41.41	-75.67	72513014777	0	0	0	WILKES-BARRE-SCRANT	0	0	0
Seattle	USA	47.63	-122.33	72793024233	0	0	0	SEATTLE-TACOMA INTL	0	0	0
Segovia	ESP	40.94	-4.11	8213099999	8215099999	0	0	SEGOVIA	NAVACERRADA	0	0
Seoul	KOR	37.57	127	47108099999	47110099999	47110599999	47111099999	SEOUL	GIMPO INTL AIRPORT	H 208 HELIPORT	SEOUL AB
				47112599999	47117099999	0	0	COMMAND POST TANGO	SEOUL (KOR-AF HQ)	0	0
Seoul_a	KOR	37.57	127	47108099999	47110099999	47110599999	47111099999	SEOUL	GIMPO INTL AIRPORT	H 208 HELIPORT	SEOUL AB
				47112599999	47117099999	0	0	COMMAND POST TANGO	SEOUL (KOR-AF HQ)	0	0
Seoul_b	KOR	37.57	127	47108099999	47110099999	47110599999	47111099999	SEOUL	GIMPO INTL AIRPORT	H 208 HELIPORT	SEOUL AB
				47112599999	47117099999	0	0	COMMAND POST TANGO	SEOUL (KOR-AF HQ)	0	0
Seoul_c	KOR	37.57	127	47108099999	47110099999	47110599999	47111099999	SEOUL	GIMPO INTL AIRPORT	H 208 HELIPORT	SEOUL AB
				47112599999	47117099999	0	0	COMMAND POST TANGO	SEOUL (KOR-AF HQ)	0	0
Seoul_d	KOR	37.57	127	47108099999	47110099999	47110599999	47111099999	SEOUL	GIMPO INTL AIRPORT	H 208 HELIPORT	SEOUL AB
				47117099999	0	0	0	SEOUL (KOR-AF HQ)	0	0	0
Seoul_e	KOR	37.57	127	47108099999	47110099999	47110599999	47111099999	SEOUL	GIMPO INTL AIRPORT	H 208 HELIPORT	SEOUL AB
				47112599999	47117099999	0	0	COMMAND POST TANGO	SEOUL (KOR-AF HQ)	0	0
Sevilla	ESP	37.4	-5.98	8390099999	8391099999	0	0	SEVILLA/TABLADA	SEVILLA/SAN PABLO	0	0
Sevilla_a	ESP	37.4	-5.98	8390099999	8391099999	0	0	SEVILLA/TABLADA	SEVILLA/SAN PABLO	0	0
Shanghai	CHN	31.23	121.47	58362099999	58367099999	0	0	SHANGHAI	SHANGHAI/HONGQIAO	0	0
Shanghai_a	CHN	31.23	121.47	58362099999	58367099999	0	0	SHANGHAI	SHANGHAI/HONGQIAO	0	0
Shanghai_b	CHN	31.23	121.47	58362099999	58367099999	0	0	SHANGHAI	SHANGHAI/HONGQIAO	0	0

Cities	ISO3	LAT	LON	Stn.no 1,5,9	Stn.no 2,6,10	Stn.no 3,7,11	Stn.no 4,8	Stn. 1,5,9	Stn. 2,6,10	Stn. 3,7,11	Stn. 4,8
Shenyang	CHN	41.79	123.43	54342099999	0	0	0	SHENYANG	0	0	0
Shenyang_a	CHN	41.79	123.43	54342099999	0	0	0	SHENYANG	0	0	0
Shenzhen	CHN	22.54	114.11	45032099999	59493099999	0	0	TA KWU LING	SHENZHEN	0	0
Shijiazhuang	CHN	38.04	114.48	53698099999	0	0	0	SHIJIAZHUANG	0	0	0
Shreveport	USA	32.47	-93.77	72248013957	72248453905	72248499999	0	SHREVEPORT REGIONAL	SHREVEPORT DOWNTOWN	SHREVEPORT DOWNTOWN	0
Sofia	BGR	42.68	23.32	15614099999	0	0	0	SOFIA (OBSERV.)	0	0	0
Soria	ESP	41.77	-2.46	8148099999	0	0	0	SORIA	0	0	0
Spokane	USA	47.67	-117.41	72785024157	72785524114	72785694176	72785699999	SPOKANE INTL ARPT	FAIRCHILD AFB	FELTS FLD	FELTS FLD
				99999994176	0	0	0	SPOKANE FELTS FIELD	0	0	0
Springfield	USA	37.2	-93.29	74491014703	74491514775	0	0	CHICOPEE FALLS/WEST	BARNES MUNI	0	0
Stjohns	CAN	47.58	-52.69	71250099999	71801099999	71802099999	0	ST JOHNS WEST CLIMAT	ST JOHNS ARPT	ST JOHNS WEST UA	0
Stjohns	CAN	47.58	-52.69	71250099999	71801099999	71802099999	0	ST JOHNS WEST CLIMAT	ST JOHNS ARPT	ST JOHNS WEST UA	0
Stlouis	USA	38.63	-90.24	72434013994	0	0	0	ST. LOUIS/LAMBERT	0	0	0
Stockholm	SWE	59.33	18.05	2464099999	2485099999	0	0	STOCKHOLM/BROMMA	STOCKHOLM	0	0
Stockholm_a	SWE	59.33	18.05	2464099999	2484099999	2485099999	0	STOCKHOLM/BROMMA	STOCKHOLM/OBSERVATO	STOCKHOLM	0
Stockton	USA	37.98	-121.3	72492023237	0	0	0	STOCKTON/METROPOLIT	0	0	0
Sudbury	CAN	46.51	-81.02	71730099999	0	0	0	SUDBURY	0	0	0
Suzhou	CHN	33.64	116.98	58358099999	0	0	0	SUZHOU	0	0	0
Sydney	AUS	-33.87	151.21	94766099999	94767099999	94767599999	95765099999	CANTERBURY RACECOUR	SYDNEY AIRPORT AMO	SYDNEY INTL AIRPORT	SYDNEY OLYMPIC PARK
Sydney_a	AUS	-33.87	151.21	94766099999	94767099999	94767599999	95765099999	CANTERBURY RACECOUR	SYDNEY AIRPORT AMO	SYDNEY INTL AIRPORT	SYDNEY OLYMPIC PARK
Syracuse	USA	43.05	-76.14	72519014771	0	0	0	SYRACUSE/HANCOCK	0	0	0
Tacoma	USA	47.24	-122.46	72793894274	72793899999	74206024207	74207024201	TACOMA NARROWS	TACOMA NARROWS	MC CHORD FIELD	GRAY AAF
				74207199999	0	0	0	FORT LEWIS/GRAY AAF	0	0	0
Taiyuan	CHN	37.87	112.56	53772099999	0	0	0	TAIYUAN	0	0	0
Tampa	USA	27.97	-82.46	72211012842	74788012810	0	0	TAMPA INTL AIRPORT	MACDILL AFB/TAMPA	0	0
Tampa_a	USA	27.97	-82.46	72037492825	72211012842	74788012810	74788099999	PETER O KNIGHT	TAMPA INTL AIRPORT	MACDILL AFB/TAMPA	MACDILL AFB/TAMPA
Tarragona	ESP	41.12	1.24	8175099999	0	0	0	REUS/AEROPUERTO	0	0	0
Tehran	IRN	35.67	51.42	40754099999	0	0	0	TEHRAN-MEHRABAD	0	0	0
Telaviv	ISR	32.07	34.76	40176099999	40176299999	40180099999	0	SDE-DOV (TEL-AVIV)	SDE DOV	BEN-GURION INT. AIR	0
Telaviv_a	ISR	32.07	34.76	40176099999	40180099999	0	0	SDE-DOV (TEL-AVIV)	BEN-GURION INT. AIR	0	0
Tenerife	ESP	28.47	-16.25	60015099999	60020099999	0	0	TENERIFE/LOS RODEOS	STA. CRUZ DE TENERI	0	0
Teresina	BRA	-5.08	-42.82	82579099999	0	0	0	TERESINA /AEROPORTO	0	0	0
Teruel	ESP	40.34	-1.11	8235099999	0	0	0	TERUEL	0	0	0
Thunderbay	CAN	48.45	-89.32	71072099999	71667099999	71749099999	0	THUNDER BAY	THUNDER BAY CS	THUNDER BAY AIRPORT	0
Tianjin	CHN	39.13	117.19	54527099999	54527399999	0	0	TIANJIN	BINHAI	0	0
Tianjin_a	CHN	39.13	117.19	54527099999	54527399999	0	0	TIANJIN	BINHAI	0	0
Tokyo	JPN	35.69	139.75	47662099999	47671099999	47671399999	47683099999	TOKYO	TOKYO INTERNATIONAL	ICHIGAYA	CHOFU AIRPORT
				47687099999	47999599999	0	0	TOKYO HELIPORT	ICHIKAWA \	0	0
Tokyo_a	JPN	35.69	139.75	47662099999	47671099999	47671399999	47683099999	TOKYO	TOKYO INTERNATIONAL	ICHIGAYA	CHOFU AIRPORT
				47687099999	47999599999	0	0	TOKYO HELIPORT	ICHIKAWA	0	0
Toledo_ES	ESP	39.86	-4.03	8272099999	0	0	0	TOLEDO	0	0	0
Toledo_ES_a	ESP	39.86	-4.03	8272099999	0	0	0	TOLEDO	0	0	0
Toledo_US	USA	41.67	-83.58	7242874848	72428799999	72428999999	72536094830	METCALF FLD	METCALF FLD	TOLEDO (CGS)	TOLEDO EXPRESS
Toronto	CAN	43.67	-79.42	71265099999	71508099999	71624099999	0	TORONTO CITY CENTRE	TORONTO CITY	TORONTO PEARSON INT	0
Toronto_a	CAN	43.67	-79.42	71265099999	71624099999	0	0	TORONTO CITY CENTRE	TORONTO PEARSON INT	0	0
Trenton	USA	40.22	-74.76	72409514792	99768799999	0	0	TRENTON MERCER	BURLINGTON DEL RIVE	0	0
Tucson	USA	32.21	-110.92	72274023160	72274523109	0	0	TUCSON INTL	DAVIS MONTHAN AFB	0	0
Tulsa	USA	36.13	-95.94	72356013968	0	0	0	TULSA INTL ARPT(AW)	0	0	0
Tunis	TUN	36.8	10.18	60715099999	0	0	0	TUNIS-CARTHAGE	0	0	0

Cities	ISO3	LAT	LON	Stn.no 1,5,9	Stn.no 2,6,10	Stn.no 3,7,11	Stn.no 4,8	Stn. 1,5,9	Stn. 2,6,10	Stn. 3,7,11	Stn. 4,8
Turin	ITA	45.08	7.68	16059099999	0	0	0	TORINO/CASELLE	0	0	0
Turin_a	ITA	45.08	7.68	16059099999	16060099999	16061099999	0	TORINO/CASELLE	TORINO	TORINO/BRIC DELLA C	0
Ulsan	KOR	35.53	129.35	47152099999	0	0	0	ULSAN	0	0	0
Utica	USA	43.1	-75.23	72519794794	0	0	0	ONEIDA CO	0	0	0
Valencia	ESP	39.48	-0.39	8284099999	0	0	0	VALENCIA/AEROPUERTO	0	0	0
Valencia_a	ESP	39.48	-0.39	8284099999	0	0	0	VALENCIA/AEROPUERTO	0	0	0
Valencia_b	ESP	39.48	-0.39	8284099999	0	0	0	VALENCIA/AEROPUERTO	0	0	0
Valencia_c	ESP	39.48	-0.39	8284099999	0	0	0	VALENCIA/AEROPUERTO	0	0	0
Valladolid	ESP	41.65	-4.74	8140099999	8141099999	0	0	VALLADOLID/VILLANUB	VALLADOLID	0	0
Vancouver	CAN	49.27	-123.15	71202599999	71784099999	71892099999	0	WEST VAN CYPRESS	WEST VANCOUVER AUT	VANCOUVER INT. AIRP	0
Vancouver_a	CAN	49.27	-123.15	71202599999	71784099999	71892099999	0	WEST VAN CYPRESS	WEST VANCOUVER AUT	VANCOUVER INT. AIRP	0
Victoria	CAN	48.46	-123.42	71200099999	71200399999	71473599999	71783099999	VICTORIA GONZALES C	VICTORIA (AUTO8)	VICTORIA HARBOUR	VICTORIA UNIV CS
				71798099999	71799499999	0	0	ESQUIMALT MARITIME	VICTORIA UNIV	0	0
Vigo	ESP	42.22	-8.71	8045099999	0	0	0	VIGO/PEINADOR	0	0	0
Virginiabeach	USA	36.83	-76.09	72307513769	72308013737	0	0	OCEANA NAS	NORFOLK INTL ARPT	0	0
Viterbo	ITA	42.42	12.09	16216099999	16218099999	0	0	VITERBO	VITERBO	0	0
Vitoria_BR	BRA	-20.32	-40.35	83649099999	0	0	0	VITORIA (AEROPORTO)	0	0	0
Vitoria_ES	ESP	42.85	-2.67	8080099999	0	0	0	VITORIA	0	0	0
Vitoria_ES_a	ESP	42.85	-2.67	8080099999	0	0	0	VITORIA	0	0	0
WashingtonDC	USA	38.91	-77.01	72405013743	0	0	0	WASHINGTON/NATIONAL	0	0	0
WashingtonDC_a	USA	38.91	-77.01	72405013743	0	0	0	WASHINGTON/NATIONAL	0	0	0
Westpalmbeach	USA	26.71	-80.06	72203012844	0	0	0	WEST PALM BEACH/IN	0	0	0
Wichita	USA	37.69	-97.34	7245003928	7245053923	0	0	WICHITA/MID-CONTINE	MC CONNELL AFB	0	0
Wilmington	USA	34.22	-77.91	72408913781	0	0	0	WILMINGTON NEW CAST	0	0	0
Windsor_CA	CAN	42.3	-83.02	71538099999	0	0	0	WINDSOR	0	0	0
Windsor_CA_b	CAN	42.3	-83.02	71538099999	0	0	0	WINDSOR	0	0	0
Winnipeg	CAN	49.91	-97.25	71852099999	0	0	0	WINNIPEG INT.AIRPOR	0	0	0
Winnipeg	CAN	49.91	-97.25	71579099999	71843099999	71849099999	71852099999	WINNIPEG THE FORKS	WINNIPEG UA	WINNIPEG ARPT CS	WINNIPEG INT.AIRPOR
Worcester	USA	42.27	-71.8	72509594746	0	0	0	WORCESTER RGNL	0	0	0
Wuhan	CHN	30.58	114.27	57494099999	0	0	0	WUHAN	0	0	0
Wulumqi	CHN	43.8	87.58	51463099999	51463599999	0	0	WU LU MU QI	DIWOPU	0	0
Xian	CHN	34.26	108.94	57036099999	0	0	0	XIAN	0	0	0
York	USA	39.96	-76.73	72511493778	72511499999	0	0	YORK	YORK	0	0
Youngstownwarren	USA	41.1	-80.65	72525014852	0	0	0	YOUNGSTOWN MUNI	0	0	0
Zamora	ESP	41.52	-5.75	8130099999	0	0	0	ZAMORA	0	0	0
Zaragoza	ESP	41.65	-0.89	8160099999	8160599999	0	0	ZARAGOZA/AEROPUERTO	ZARAGOZA (USAFB)	0	0
Zaragoza_a	ESP	41.65	-0.89	8160099999	8160599999	0	0	ZARAGOZA/AEROPUERTO	ZARAGOZA (USAFB)	0	0
Zhengzhou	CHN	34.76	113.65	57083099999	0	0	0	ZHENGZHOU	0	0	0
Zhuhai	CHN	22.28	113.57	45011099999	0	0	0	TAIPA GRANDE	0	0	0
Zurich	CHE	47.37	8.55	6660099999	6670099999	0	0	ZUERICH-FLUNTER	ZURICH-KLOTEN	0	0

Tab. B.7.: MMTs for 599 European cities (> 100 000 inhabitants) (> 100 000 inhabitants) estimated by the sigmoid model. POP2000 = Population as of 2000, MMT.EST = MMT estimate in AT [°C]

City	Country	ISO3	Region	LAT	LON	LATLON	POP2000	MMT.EST
IRANE	ALBANIA	ALB	SOUTH	41.33	19.82	100.00	342761	18.23
GRAZ	AUSTRIA	AUT	WEST	47.08	15.42	174.00	227374	18.15
INNSBRUCK	AUSTRIA	AUT	WEST	47.28	11.41	234.00	113855	16.04
LINZ	AUSTRIA	AUT	WEST	48.31	14.29	310.00	185370	17.26
SALZBURG	AUSTRIA	AUT	WEST	47.81	13.04	430.00	142793	17.50
WIEN	AUSTRIA	AUT	WEST	48.22	16.37	564.00	1549092	20.47
BARANAVICI	BELARUS	BLR	EAST	53.14	26.02	5.00	167928	17.07
BOBRUISK	BELARUS	BLR	EAST	53.15	29.23	10.00	221000	17.23
BORISOV	BELARUS	BLR	EAST	54.23	28.49	13.00	151931	17.02
BREST	BELARUS	BLR	EAST	52.10	23.70	16.00	289187	17.29
GOMEL	BELARUS	BLR	EAST	52.44	30.98	22.00	483853	17.60
GRODNO	BELARUS	BLR	EAST	53.68	23.81	25.00	305402	16.93
LIDA	BELARUS	BLR	EAST	53.88	25.30	36.00	102059	17.04
MINSK	BELARUS	BLR	EAST	53.90	27.57	41.00	1688585	16.97
MOGILEV	BELARUS	BLR	EAST	53.91	30.34	44.00	355900	17.02
MOZYR	BELARUS	BLR	EAST	52.05	29.27	50.00	110943	17.49
NOVOPOLOTSK	BELARUS	BLR	EAST	55.53	28.65	55.00	107396	16.92
ORSA	BELARUS	BLR	EAST	54.51	30.41	58.00	136100	16.91
PINSK	BELARUS	BLR	EAST	52.12	26.07	62.00	131265	17.38
SOLIGORSK	BELARUS	BLR	EAST	52.80	27.53	80.00	101837	17.29
VITEBSK	BELARUS	BLR	EAST	55.19	30.19	88.00	347308	17.00
ANTWERPEN	BELGIUM	BEL	WEST	51.22	4.42	23.00	452301	18.55
BRUGGE	BELGIUM	BEL	WEST	51.22	3.23	100.00	116844	18.19
BRUSSEL	BELGIUM	BEL	WEST	50.83	4.33	102.00	970683	18.51
BRUXELLES	BELGIUM	BEL	WEST	50.83	4.33	103.00	135651	18.51
CHARLEROI	BELGIUM	BEL	WEST	50.42	4.43	115.00	201997	17.64
GENT	BELGIUM	BEL	WEST	51.05	3.72	225.00	227015	18.31
LIEGE	BELGIUM	BEL	WEST	50.64	5.57	383.00	187627	18.05
NAMUR	BELGIUM	BEL	WEST	50.47	4.87	457.00	105165	17.75
SCHAERBEEK	BELGIUM	BEL	WEST	50.85	4.38	548.00	106886	18.51
BANJALUKA	BOSNIA-HER	BIH	SOUTH	44.78	17.19	4.00	162828	18.77
SARAJEVO	BOSNIA-HER	BIH	SOUTH	43.85	18.38	56.00	388812	17.02
BURGAS	BULGARIA	BGR	EAST	42.50	27.47	10.00	193577	20.38
DOBRIC	BULGARIA	BGR	EAST	43.57	27.83	16.00	100828	18.53
PLEVEN	BULGARIA	BGR	EAST	43.42	24.62	67.00	123082	19.82
PLOVDIV	BULGARIA	BGR	EAST	42.15	24.75	70.00	340684	19.88
RUSE	BULGARIA	BGR	EAST	43.86	25.97	76.00	162988	26.46
SLIVEN	BULGARIA	BGR	EAST	42.69	26.33	90.00	101293	19.66
SOFIJA	BULGARIA	BGR	EAST	42.68	23.32	96.00	1098433	16.79
STARAZAGORA	BULGARIA	BGR	EAST	42.43	25.64	99.00	144700	19.51
RIJEKA	CROATIA	HRV	SOUTH	45.34	14.41	141.00	146051	16.98
SPLIT	CROATIA	HRV	SOUTH	43.51	16.46	166.00	176515	20.19
ZAGREB	CROATIA	HRV	SOUTH	45.80	16.00	204.00	693214	18.73
BRNO	CZECH REP	CZE	EAST	49.20	16.61	14.00	380056	17.98
LIBEREC	CZECH REP	CZE	EAST	50.78	15.06	84.00	100040	16.53
OLOMOUC	CZECH REP	CZE	EAST	49.61	17.25	108.00	103530	17.51
OSTRAVA	CZECH REP	CZE	EAST	49.83	18.27	114.00	320109	17.59
PLZEN	CZECH REP	CZE	EAST	49.75	13.37	123.00	166947	17.15
PRAHA	CZECH REP	CZE	EAST	50.08	14.43	127.00	1181877	17.73
AALBORG	DENMARK	DNK	NORTH	57.05	9.92	8.00	119617	17.45
ARHUS	DENMARK	DNK	NORTH	56.16	10.21	42.00	217260	17.78
ODENSE	DENMARK	DNK	NORTH	55.40	10.38	572.00	145062	17.61
TALLINN	ESTONIA	EST	NORTH	59.43	24.73	67.00	400378	16.72
TARTU	ESTONIA	EST	NORTH	58.37	26.74	73.00	101169	16.95
LAHDEN	FINLAND	FIN	NORTH	60.99	25.66	252.00	110160	17.10
OULU	FINLAND	FIN	NORTH	65.01	25.47	365.00	157605	16.76
TAMPERE	FINLAND	FIN	NORTH	61.50	23.75	506.00	270753	16.99
TURKU	FINLAND	FIN	NORTH	60.45	22.25	522.00	239018	17.24
VANTAA	FINLAND	FIN	NORTH	60.29	25.04	572.00	178471	17.26
SKOPJE	MACEDONIA	MKD	SOUTH	42.00	21.47	66.00	461409	17.06
AMIENS	FRANCE	FRA	WEST	49.90	2.30	27.00	277159	18.06
ANGERS	FRANCE	FRA	WEST	47.47	-0.55	31.00	335300	19.32
ANGOULEME	FRANCE	FRA	WEST	45.65	0.15	33.00	154799	20.15
ANNECY	FRANCE	FRA	WEST	45.90	6.12	35.00	190819	17.35
ARRAS	FRANCE	FRA	WEST	50.28	2.78	49.00	125800	18.13
AVIGNON	FRANCE	FRA	WEST	43.95	4.82	67.00	294343	23.88

City	Country	ISO3	Region	LAT	LON	LATLON	POP2000	MMT.EST
BAYONNE	FRANCE	FRA	WEST	43.48	-1.48	85.00	214777	19.83
BEAUVAIS	FRANCE	FRA	WEST	49.43	2.08	91.00	101594	18.19
BELFORT	FRANCE	FRA	WEST	47.63	6.87	93.00	105769	17.98
BESANCON	FRANCE	FRA	WEST	47.25	6.03	103.00	223466	18.66
BETHUNE	FRANCE	FRA	WEST	50.53	2.63	105.00	268610	18.22
BEZIERS	FRANCE	FRA	WEST	43.35	3.25	107.00	126060	22.93
BLOIS	FRANCE	FRA	WEST	47.58	1.33	110.00	117125	19.12
BORDEAUX	FRANCE	FRA	WEST	44.83	-0.57	115.00	930153	20.89
BOULOGNESURMER	FRANCE	FRA	WEST	50.72	1.62	117.00	136095	17.92
BOURGENBRESSE	FRANCE	FRA	WEST	46.20	5.22	119.00	102268	19.53
BOURGES	FRANCE	FRA	WEST	47.08	2.40	121.00	123650	19.09
BREST	FRANCE	FRA	WEST	48.40	-4.48	128.00	306874	17.63
CAEN	FRANCE	FRA	WEST	49.18	-0.35	136.00	373745	18.08
CALAIS	FRANCE	FRA	WEST	50.95	1.83	140.00	126753	17.97
CHALONSURSAONE	FRANCE	FRA	WEST	46.78	4.85	159.00	132307	19.20
CHAMBERY	FRANCE	FRA	WEST	45.57	5.93	161.00	131567	18.00
CHARLEVILLEMEZIERES	FRANCE	FRA	WEST	49.77	4.72	167.00	109524	17.35
CHARTRES	FRANCE	FRA	WEST	48.45	1.50	169.00	132344	18.39
CHERBOURG	FRANCE	FRA	WEST	49.65	-1.65	187.00	118406	17.49
CLERMONTFERRAND	FRANCE	FRA	WEST	45.78	3.08	194.00	416519	17.88
COLMAR	FRANCE	FRA	WEST	48.08	7.37	202.00	116271	18.64
COMPIEGNE	FRANCE	FRA	WEST	49.42	2.83	204.00	110442	18.57
DIJON	FRANCE	FRA	WEST	47.32	5.02	226.00	328246	18.60
DOUAILENS	FRANCE	FRA	WEST	50.37	3.08	234.00	554756	18.11
FORBACH	FRANCE	FRA	WEST	49.18	6.90	274.00	103436	18.29
GRENOBLE	FRANCE	FRA	WEST	45.17	5.72	297.00	515648	17.10
HAGONDANGEBRIEY	FRANCE	FRA	WEST	49.25	6.17	304.00	121406	18.39
LAVAL	FRANCE	FRA	WEST	48.07	-0.77	347.00	103573	18.41
LEMANS	FRANCE	FRA	WEST	48.00	0.20	353.00	296041	18.84
LILLE	FRANCE	FRA	WEST	50.63	3.07	363.00	1147070	18.15
LIMOGES	FRANCE	FRA	WEST	45.85	1.25	367.00	249850	18.47
LORIENT	FRANCE	FRA	WEST	47.75	-3.37	377.00	186137	18.10
LYON	FRANCE	FRA	WEST	45.75	4.85	394.00	1653987	19.59
MAUBEUGE	FRANCE	FRA	WEST	50.28	3.97	404.00	117526	17.49
METZ	FRANCE	FRA	WEST	49.13	6.17	438.00	323350	18.39
MONTBELIARD	FRANCE	FRA	WEST	47.52	6.80	451.00	180202	17.98
MONTPELLIER	FRANCE	FRA	WEST	43.60	3.88	465.00	461516	22.98
MULHOUSE	FRANCE	FRA	WEST	47.75	7.33	471.00	270618	18.87
NANCY	FRANCE	FRA	WEST	48.68	6.20	473.00	412129	18.19
NANTES	FRANCE	FRA	WEST	47.22	-1.55	475.00	715342	19.42
NEVERS	FRANCE	FRA	WEST	46.98	3.17	481.00	101613	18.99
NIMES	FRANCE	FRA	WEST	43.83	4.35	487.00	222860	23.50
NIORT	FRANCE	FRA	WEST	46.32	-0.47	489.00	126906	19.57
ORLEANS	FRANCE	FRA	WEST	47.92	1.90	503.00	359472	18.95
PARIS	FRANCE	FRA	WEST	48.87	2.33	512.00	11245118	19.66
PAU	FRANCE	FRA	WEST	43.30	-0.37	516.00	219462	19.81
PERPIGNAN	FRANCE	FRA	WEST	42.68	2.88	524.00	254509	22.70
POITIERS	FRANCE	FRA	WEST	46.58	0.33	533.00	211743	19.16
QUIMPER	FRANCE	FRA	WEST	48.00	-4.10	547.00	123654	17.64
REIMS	FRANCE	FRA	WEST	49.25	4.03	553.00	293946	18.48
RENNES	FRANCE	FRA	WEST	48.08	-1.68	557.00	525520	18.68
ROANNE	FRANCE	FRA	WEST	46.05	4.07	416.00	105354	18.57
ROUEN	FRANCE	FRA	WEST	49.43	1.08	428.00	523956	18.29
SAINTBRIEUC	FRANCE	FRA	WEST	48.52	-2.78	570.00	122134	17.77
SAINTETIENNE	FRANCE	FRA	WEST	45.43	4.40	584.00	323270	17.04
SAINTNAZAIRE	FRANCE	FRA	WEST	47.28	-2.20	603.00	173710	19.16
SAINTQUENTIN	FRANCE	FRA	WEST	49.85	3.28	609.00	104113	17.92
STRASBOURG	FRANCE	FRA	WEST	48.58	7.75	640.00	618554	19.09
TARBES	FRANCE	FRA	WEST	43.23	0.08	644.00	110563	18.19
THIONVILLE	FRANCE	FRA	WEST	49.37	6.17	652.00	154405	18.14
TOULON	FRANCE	FRA	WEST	43.12	5.93	660.00	575380	21.97
TOULOUSE	FRANCE	FRA	WEST	43.60	1.43	662.00	970212	21.10
TOURS	FRANCE	FRA	WEST	47.38	0.68	666.00	377299	19.24
TROYES	FRANCE	FRA	WEST	48.30	4.08	670.00	172992	19.16
VALENCE	FRANCE	FRA	WEST	44.93	4.90	676.00	168035	21.02
VALENCIENNES	FRANCE	FRA	WEST	50.35	3.53	678.00	403338	17.66
VANNES	FRANCE	FRA	WEST	47.67	-2.75	680.00	118966	18.65
AACHEN	GERMANY	DEU	WEST	50.77	6.09	3.00	246491	18.14
AUGSBURG	GERMANY	DEU	WEST	48.36	10.89	105.00	258456	17.40
BERGISCHGLADBACH	GERMANY	DEU	WEST	50.98	7.15	292.00	105539	18.59

City	Country	ISO3	Region	LAT	LON	LATLON	POP2000	MMT.EST
BERLIN	GERMANY	DEU	WEST	52.52	13.38	301.00	3415873	19.01
BIELEFELD	GERMANY	DEU	WEST	52.03	8.53	320.00	323604	18.15
BOCHUM	GERMANY	DEU	WEST	51.48	7.20	351.00	393493	18.16
BONN	GERMANY	DEU	WEST	50.73	7.10	358.00	301075	18.16
BOTTROP	GERMANY	DEU	WEST	51.53	6.93	375.00	120734	18.56
BRAUNSCHWEIG	GERMANY	DEU	WEST	52.27	10.51	390.00	247837	18.40
BREMEN	GERMANY	DEU	WEST	53.08	8.81	393.00	543738	17.98
BREMERHAVEN	GERMANY	DEU	WEST	53.55	8.58	396.00	122479	18.01
CHEMNITZ	GERMANY	DEU	WEST	50.83	12.92	488.00	259394	17.73
COTTBUS	GERMANY	DEU	WEST	51.77	14.33	506.00	111420	18.71
DARMSTADT	GERMANY	DEU	WEST	49.87	8.64	524.00	138631	18.88
DORTMUND	GERMANY	DEU	WEST	51.51	7.48	594.00	592423	18.40
DRESDEN	GERMANY	DEU	WEST	51.05	13.74	601.00	475436	18.47
DUISBURG	GERMANY	DEU	WEST	51.43	6.75	608.00	519656	18.63
DUSSELDORF	GERMANY	DEU	WEST	51.24	6.79	617.00	570853	18.78
ERFURT	GERMANY	DEU	WEST	50.99	11.03	717.00	203722	17.42
ERLANGEN	GERMANY	DEU	WEST	49.60	11.01	727.00	101743	17.75
ESSEN	GERMANY	DEU	WEST	51.47	7.00	746.00	599449	18.63
FRANKFURT	GERMANY	DEU	WEST	50.12	8.68	803.00	644055	19.13
FREIBURG	GERMANY	DEU	WEST	47.99	7.85	815.00	205243	16.83
FURTH	GERMANY	DEU	WEST	49.48	10.98	860.00	110303	17.71
GELSENKIRCHEN	GERMANY	DEU	WEST	51.51	7.11	900.00	281467	18.50
GERA	GERMANY	DEU	WEST	50.88	12.08	907.00	114293	17.74
GOTTINGEN	GERMANY	DEU	WEST	51.53	9.92	974.00	124627	17.50
HAGEN	GERMANY	DEU	WEST	51.37	7.46	1044.00	205321	17.73
HALLE	GERMANY	DEU	WEST	51.48	11.96	1062.00	255629	18.48
HAMBURG	GERMANY	DEU	WEST	53.55	10.00	1074.00	1720187	17.99
HAMM	GERMANY	DEU	WEST	51.67	7.80	1080.00	183673	18.17
HANNOVER	GERMANY	DEU	WEST	52.40	9.73	1090.00	518649	18.28
HEIDELBERG	GERMANY	DEU	WEST	49.42	8.69	1118.00	140594	19.17
HEILBRONN	GERMANY	DEU	WEST	49.14	9.22	1130.00	120610	18.55
HERNE	GERMANY	DEU	WEST	51.54	7.21	1170.00	175956	18.50
HILDESHEIM	GERMANY	DEU	WEST	52.16	9.95	1213.00	104506	17.99
INGOLSTADT	GERMANY	DEU	WEST	48.77	11.43	1314.00	115506	17.50
JENA	GERMANY	DEU	WEST	50.93	11.58	1328.00	101125	17.80
KAISERSLAUTERN	GERMANY	DEU	WEST	49.45	7.75	1340.00	100525	17.68
KARLSRUHE	GERMANY	DEU	WEST	49.00	8.40	1368.00	278276	19.62
KASSEL	GERMANY	DEU	WEST	51.32	9.48	1374.00	196997	17.44
KIEL	GERMANY	DEU	WEST	54.32	10.12	1399.00	236751	17.60
KOBLENZ	GERMANY	DEU	WEST	50.35	7.60	1427.00	108224	17.88
KOLN	GERMANY	DEU	WEST	50.95	6.97	1433.00	967192	18.87
KREFELD	GERMANY	DEU	WEST	51.33	6.55	1472.00	242862	19.06
LEIPZIG	GERMANY	DEU	WEST	51.35	12.40	1572.00	485513	18.66
LEVERKUSEN	GERMANY	DEU	WEST	51.04	6.99	1594.00	161302	18.78
LUBECK	GERMANY	DEU	WEST	53.87	10.66	1656.00	214653	17.76
LUDWIGSHAFEN	GERMANY	DEU	WEST	49.48	8.44	1674.00	164079	19.53
MAGDEBURG	GERMANY	DEU	WEST	52.13	11.62	1684.00	238702	18.56
MAINZ	GERMANY	DEU	WEST	50.00	8.26	1691.00	184767	18.10
MANNHEIM	GERMANY	DEU	WEST	49.50	8.47	1696.00	309351	19.31
MOERS	GERMANY	DEU	WEST	51.45	6.65	1787.00	107312	19.06
MONCHENGLADBACH	GERMANY	DEU	WEST	51.20	6.42	1795.00	264203	18.39
MULHEIM	GERMANY	DEU	WEST	51.43	6.86	1831.00	173720	18.63
MUNCHEN	GERMANY	DEU	WEST	48.14	11.58	1838.00	1230756	17.72
MUNSTER	GERMANY	DEU	WEST	51.96	7.62	1847.00	266483	18.23
NURNBERG	GERMANY	DEU	WEST	49.45	11.05	1979.00	491679	17.88
OBERHAUSEN	GERMANY	DEU	WEST	51.47	6.86	1989.00	222541	18.63
OFFENBACH	GERMANY	DEU	WEST	50.10	8.77	2022.00	117794	19.11
OLDENBURG	GERMANY	DEU	WEST	53.15	8.21	2034.00	154384	17.97
OSNABRUCK	GERMANY	DEU	WEST	52.28	8.05	2053.00	165656	18.09
PADERBORN	GERMANY	DEU	WEST	51.72	8.74	2077.00	138443	17.67
PFORZHEIM	GERMANY	DEU	WEST	48.89	8.69	2108.00	118255	17.49
POTSDAM	GERMANY	DEU	WEST	52.40	13.07	2142.00	132465	18.74
RECKLINGHAUSEN	GERMANY	DEU	WEST	51.61	7.19	2204.00	125457	18.50
REGENSBURG	GERMANY	DEU	WEST	49.02	12.11	2211.00	126742	17.71
REMSCHEID	GERMANY	DEU	WEST	51.18	7.19	2235.00	119911	17.75
REUTLINGEN	GERMANY	DEU	WEST	48.49	9.21	2247.00	110406	16.94
ROSTOCK	GERMANY	DEU	WEST	54.09	12.10	2311.00	208065	17.79
SAARBRUCKEN	GERMANY	DEU	WEST	49.25	6.97	2338.00	184239	18.29
SALZGITTER	GERMANY	DEU	WEST	52.17	10.33	2347.00	113667	18.14
SCHWERIN	GERMANY	DEU	WEST	53.63	11.40	2466.00	104659	17.99

City	Country	ISO3	Region	LAT	LON	LATLON	POP2000	MMT.EST
SIEGEN	GERMANY	DEU	WEST	50.87	8.01	2512.00	109388	16.98
SOLINGEN	GERMANY	DEU	WEST	51.18	7.06	2537.00	165266	17.75
STUTTGART	GERMANY	DEU	WEST	48.79	9.19	2625.00	586636	18.37
ULM	GERMANY	DEU	WEST	48.40	9.97	2709.00	117465	17.21
WIESBADEN	GERMANY	DEU	WEST	50.08	8.23	2957.00	269752	17.85
WITTEN	GERMANY	DEU	WEST	51.44	7.34	2991.00	103687	17.73
WOLFSBURG	GERMANY	DEU	WEST	52.43	10.78	3018.00	123351	18.37
WUPPERTAL	GERMANY	DEU	WEST	51.26	7.18	3036.00	370397	18.16
WURZBURG	GERMANY	DEU	WEST	49.80	9.94	3042.00	129036	17.96
ZWICKAU	GERMANY	DEU	WEST	50.72	12.50	3067.00	102004	17.09
LARISA	GREECE	GRC	SOUTH	39.64	22.42	1339.00	123564	25.82
PATRAI	GREECE	GRC	SOUTH	38.24	21.73	2022.00	160320	23.85
PERISTERION	GREECE	GRC	SOUTH	38.02	23.70	2071.00	137855	23.14
THESSALONIKI	GREECE	GRC	SOUTH	40.64	22.95	2511.00	365937	25.48
BUDAPEST	HUNGARY	HUN	EAST	47.50	19.08	193.00	1763110	20.92
DEBRECEN	HUNGARY	HUN	EAST	47.53	21.63	274.00	207073	19.91
GYOR	HUNGARY	HUN	EAST	47.68	17.63	463.00	129292	19.84
KECSKEMET	HUNGARY	HUN	EAST	46.90	19.78	644.00	106826	20.38
MISKOLC	HUNGARY	HUN	EAST	48.10	20.78	860.00	183641	19.85
NYIREGYHAZA	HUNGARY	HUN	EAST	47.95	21.72	972.00	116740	19.92
PECS	HUNGARY	HUN	EAST	46.08	18.23	1058.00	160699	19.96
SZEGED	HUNGARY	HUN	EAST	46.25	20.17	1255.00	164256	20.67
SZEKESFEHERVAR	HUNGARY	HUN	EAST	47.20	18.42	1261.00	104495	20.37
REYKJAVIK	ICELAND	ISL	NORTH	64.14	-21.92	220.00	110978	16.14
CORK	IRELAND	IRL	NORTH	51.90	-8.50	127.00	124422	21.27
BERGAMO	ITALY	ITA	SOUTH	45.70	9.67	283.00	113321	22.63
BOLOGNA	ITALY	ITA	SOUTH	44.50	11.34	320.00	374407	25.18
BRESCIA	ITALY	ITA	SOUTH	45.55	10.22	360.00	188249	21.41
FERRARA	ITALY	ITA	SOUTH	44.84	11.61	1035.00	131678	24.63
FIRENZE	ITALY	ITA	SOUTH	43.78	11.24	1059.00	360576	22.79
FOGGIA	ITALY	ITA	SOUTH	41.47	15.55	1075.00	155309	24.94
FORLI	ITALY	ITA	SOUTH	44.22	12.03	1094.00	108455	23.44
LIVORNO	ITALY	ITA	SOUTH	43.55	10.30	1403.00	157363	23.78
MILANO	ITALY	ITA	SOUTH	45.48	9.19	1597.00	1267080	24.47
MODENA	ITALY	ITA	SOUTH	44.65	10.92	1627.00	175650	24.11
MONZA	ITALY	ITA	SOUTH	45.58	9.27	1747.00	120249	22.86
NAPOLI	ITALY	ITA	SOUTH	40.85	14.27	1776.00	1010616	25.27
NOVARA	ITALY	ITA	SOUTH	45.45	8.62	1834.00	100930	23.30
PADOVA	ITALY	ITA	SOUTH	45.41	11.87	1919.00	205874	23.95
PARMA	ITALY	ITA	SOUTH	44.81	10.32	1960.00	164150	23.88
PERUGIA	ITALY	ITA	SOUTH	43.11	12.39	1991.00	148680	21.31
PESCARA	ITALY	ITA	SOUTH	42.46	14.21	1999.00	116868	23.15
PRATO	ITALY	ITA	SOUTH	43.89	11.09	2153.00	171807	22.79
RAVENNA	ITALY	ITA	SOUTH	44.42	12.21	2206.00	134752	24.31
REGGIONELLEMILIA	ITALY	ITA	SOUTH	44.71	10.63	2220.00	140860	23.05
ROMA	ITALY	ITA	SOUTH	41.89	12.50	2270.00	2568776	24.07
SALERNO	ITALY	ITA	SOUTH	40.68	14.77	2330.00	139227	24.60
SASSARI	ITALY	ITA	SOUTH	40.73	8.56	2547.00	120889	21.50
TERNI	ITALY	ITA	SOUTH	42.57	12.65	2772.00	105337	20.24
TORINO	ITALY	ITA	SOUTH	45.08	7.68	2802.00	874528	20.96
TRENTO	ITALY	ITA	SOUTH	46.08	11.12	2847.00	104601	17.85
TRIESTE	ITALY	ITA	SOUTH	45.65	13.77	2868.00	213096	19.49
VERONA	ITALY	ITA	SOUTH	45.44	10.99	2958.00	253468	23.77
VICENZA	ITALY	ITA	SOUTH	45.55	11.54	2972.00	107246	23.49
DAUGAVPILS	LATVIA	LVA	NORTH	55.88	26.53	34.00	115265	16.93
RIGA	LATVIA	LVA	NORTH	56.95	24.10	170.00	764329	17.17
KAUNAS	LITHUANIA	LTU	NORTH	54.87	23.92	41.00	382060	19.78
PANEVEZYS	LITHUANIA	LTU	NORTH	55.73	24.35	80.00	120298	19.85
SIAULIAI	LITHUANIA	LTU	NORTH	55.93	23.32	102.00	134825	19.33
VILNIUS	LITHUANIA	LTU	NORTH	54.67	25.32	139.00	545078	19.33
AMERSFOORT	NETHERL	NLD	WEST	52.16	5.38	19.00	126143	18.33
AMSTERDAM	NETHERL	NLD	WEST	52.37	4.89	23.00	731288	18.24
APELDOORN	NETHERL	NLD	WEST	52.22	5.96	25.00	153261	18.15
ARNHEM	NETHERL	NLD	WEST	51.99	5.91	1.00	138154	18.45
BREDA	NETHERL	NLD	WEST	51.58	4.77	58.00	160615	18.48
DORDRECHT	NETHERL	NLD	WEST	51.80	4.67	104.00	119821	18.40
EDE	NETHERL	NLD	WEST	52.04	5.65	116.00	101700	18.26
EINDHOVEN	NETHERL	NLD	WEST	51.44	5.47	118.00	201728	18.62
EMMEN	NETHERL	NLD	WEST	52.79	6.90	122.00	105972	18.03
ENSCHEDE	NETHERL	NLD	WEST	52.22	6.89	124.00	149505	18.25

City	Country	ISO3	Region	LAT	LON	LATLON	POP2000	MMT.EST
GRONINGEN	NETHERL	NLD	WEST	53.23	6.57	160.00	173139	17.95
HAARLEM	NETHERL	NLD	WEST	52.39	4.62	164.00	148484	18.21
HAARLEMMERMEER	NETHERL	NLD	WEST	52.30	4.70	166.00	111155	18.21
LEIDEN	NETHERL	NLD	WEST	52.17	4.49	242.00	117191	18.24
MAASTRICHT	NETHERL	NLD	WEST	50.85	5.69	262.00	122070	18.75
NIJMEGEN	NETHERL	NLD	WEST	51.84	5.85	284.00	152200	18.45
ROTTERDAM	NETHERL	NLD	WEST	51.93	4.48	340.00	592673	18.42
SGRAVENHAGE	NETHERL	NLD	WEST	52.08	4.28	350.00	441094	18.24
SHERTOGENBOSCH	NETHERL	NLD	WEST	51.70	5.31	352.00	129034	18.48
TILBURG	NETHERL	NLD	WEST	51.57	5.07	382.00	193116	18.46
UTRECHT	NETHERL	NLD	WEST	52.10	5.11	392.00	253825	18.35
ZAANSTAD	NETHERL	NLD	WEST	52.45	4.82	453.00	135762	18.24
ZOETERMEER	NETHERL	NLD	WEST	52.07	4.49	461.00	109941	18.24
ZWOLLE	NETHERL	NLD	WEST	52.52	6.09	471.00	105801	18.07
BERGEN	NORWAY	NOR	NORTH	60.38	5.34	76.00	205538	16.62
OSLO	NORWAY	NOR	NORTH	59.91	10.75	624.00	766518	17.20
STAVANGER	NORWAY	NOR	NORTH	58.97	5.75	806.00	159267	16.86
TRONDHEIM	NORWAY	NOR	NORTH	63.44	10.40	895.00	140751	16.57
BIALYSTOK	POLAND	POL	EAST	53.14	23.16	17.00	287840	17.47
BIELSKOBIALA	POLAND	POL	EAST	49.82	19.05	21.00	178359	17.61
BYDGOSZCZ	POLAND	POL	EAST	53.12	18.01	37.00	375737	17.97
BYTOM	POLAND	POL	EAST	50.35	18.91	39.00	200210	17.70
CHORZOW	POLAND	POL	EAST	50.30	19.03	48.00	130750	17.60
CZESTOCHOWA	POLAND	POL	EAST	50.81	19.13	62.00	253039	17.65
DABROWAGORNICZA	POLAND	POL	EAST	50.33	19.18	64.00	132099	17.60
ELBLAG	POLAND	POL	EAST	54.18	19.40	72.00	127972	17.79
GDANSK	POLAND	POL	EAST	54.36	18.64	76.00	461403	17.31
GLIWICE	POLAND	POL	EAST	50.31	18.67	82.00	205886	17.82
GORZOWWIELKOPOLSKI	POLAND	POL	EAST	52.74	15.23	92.00	125640	18.23
GRUDZIADZ	POLAND	POL	EAST	53.49	18.75	102.00	100981	17.79
KALISZ	POLAND	POL	EAST	51.77	18.10	126.00	108902	18.05
KATOWICE	POLAND	POL	EAST	50.26	19.02	130.00	333509	17.60
KIELCE	POLAND	POL	EAST	50.89	20.65	136.00	212673	17.36
KOSZALIN	POLAND	POL	EAST	54.19	16.18	156.00	109123	17.51
KRAKOW	POLAND	POL	EAST	50.06	19.96	160.00	755619	17.56
LEGNICA	POLAND	POL	EAST	51.21	16.16	182.00	106996	17.78
LODZ	POLAND	POL	EAST	51.77	19.46	186.00	798893	17.85
LUBLIN	POLAND	POL	EAST	51.24	22.57	198.00	355753	17.70
OLSZTYN	POLAND	POL	EAST	53.78	20.49	242.00	171426	17.50
OPOLE	POLAND	POL	EAST	50.68	17.94	246.00	129868	18.08
PLOCK	POLAND	POL	EAST	52.55	19.70	278.00	127683	18.04
POZNAN	POLAND	POL	EAST	52.40	16.90	286.00	579690	18.21
RADOM	POLAND	POL	EAST	51.40	21.16	304.00	229834	17.82
RUDASLASKA	POLAND	POL	EAST	50.30	18.88	310.00	153868	17.70
RYBNIK	POLAND	POL	EAST	50.10	18.55	314.00	142810	17.78
RZESZOW	POLAND	POL	EAST	50.05	22.00	318.00	159642	17.83
SLUPSK	POLAND	POL	EAST	54.47	17.02	336.00	100358	17.22
SOSNOWIEC	POLAND	POL	EAST	50.28	19.12	342.00	236239	17.60
SZCZECIN	POLAND	POL	EAST	53.43	14.53	376.00	415599	17.95
TARNOW	POLAND	POL	EAST	50.01	20.99	384.00	120307	18.01
TORUN	POLAND	POL	EAST	53.02	18.61	394.00	209321	17.89
TYCHY	POLAND	POL	EAST	50.16	19.00	398.00	133573	17.76
WALBRZYCH	POLAND	POL	EAST	50.78	16.28	402.00	132271	17.22
WARSZAWA	POLAND	POL	EAST	52.25	21.00	406.00	1666203	18.18
WLOCLAWEK	POLAND	POL	EAST	52.66	19.06	412.00	121444	18.16
WROCLAW	POLAND	POL	EAST	51.11	17.03	418.00	640426	18.10
ZABRZE	POLAND	POL	EAST	50.30	18.78	424.00	196912	17.70
ZIELONAGORA	POLAND	POL	EAST	51.94	15.49	444.00	117654	18.35
AMADORA	PORTUGAL	PRT	SOUTH	38.75	-9.24	81.00	175487	23.75
BRAGA	PORTUGAL	PRT	SOUTH	41.55	-8.43	179.00	109733	20.85
COIMBRA	PORTUGAL	PRT	SOUTH	40.22	-8.43	267.00	103733	22.90
SETUBAL	PORTUGAL	PRT	SOUTH	38.53	-8.89	789.00	112468	24.99
BALTI	MOLDOVA	MDA	EAST	47.76	27.93	6.00	131541	21.95
CHISINAU	MOLDOVA	MDA	EAST	47.01	28.86	19.00	652131	23.08
TIGHINA	MOLDOVA	MDA	EAST	46.83	29.46	77.00	127905	23.56
TIRASPOL	MOLDOVA	MDA	EAST	46.84	29.64	78.00	179067	23.82
ARAD	ROMANIA	ROU	EAST	46.19	21.32	44.00	176151	23.77
BACAU	ROMANIA	ROU	EAST	46.58	26.92	63.00	181392	22.16
BAIAMARE	ROMANIA	ROU	EAST	47.66	23.58	73.00	140152	20.25
BOTOSANI	ROMANIA	ROU	EAST	47.75	26.67	187.00	117428	22.25

City	Country	ISO3	Region	LAT	LON	LATLON	POP2000	MMT.EST
BRAILA	ROMANIA	ROU	EAST	45.28	27.97	196.00	220261	25.73
BRASOV	ROMANIA	ROU	EAST	45.66	25.61	202.00	291455	17.78
BUCURESTI	ROMANIA	ROU	EAST	44.44	26.10	222.00	1950063	25.17
BUZAU	ROMANIA	ROU	EAST	45.15	26.82	239.00	135984	25.37
CLUJNAPOCA	ROMANIA	ROU	EAST	46.78	23.59	328.00	320114	20.19
CONSTANTA	ROMANIA	ROU	EAST	44.18	28.63	349.00	318153	25.28
CRAIOVA	ROMANIA	ROU	EAST	44.33	23.82	385.00	302889	25.55
DROBETATURNUSEVERIN	ROMANIA	ROU	EAST	44.64	22.66	461.00	106189	26.63
FOCSANI	ROMANIA	ROU	EAST	45.70	27.18	512.00	102839	23.95
GALATI	ROMANIA	ROU	EAST	45.44	28.04	531.00	303903	25.17
IASI	ROMANIA	ROU	EAST	47.17	27.57	612.00	326024	23.11
ORADEA	ROMANIA	ROU	EAST	47.07	21.92	825.00	209673	23.52
PIATRANEAMT	ROMANIA	ROU	EAST	46.94	26.37	884.00	108851	19.38
PITESTI	ROMANIA	ROU	EAST	44.86	24.87	894.00	170821	22.08
PLOIESTI	ROMANIA	ROU	EAST	44.94	26.03	898.00	236370	24.04
RAMNICUVALCEA	ROMANIA	ROU	EAST	45.11	24.38	952.00	108824	21.85
SATUMARE	ROMANIA	ROU	EAST	47.79	22.89	1031.00	118731	23.40
SIBIU	ROMANIA	ROU	EAST	45.79	24.13	1061.00	157863	20.35
SUCEAVA	ROMANIA	ROU	EAST	47.64	26.26	1129.00	107753	20.69
TARGUMURES	ROMANIA	ROU	EAST	46.55	24.56	1168.00	152439	20.14
TIMISOARA	ROMANIA	ROU	EAST	45.76	21.23	1212.00	320878	24.28
ARMAVIR	RUSSIAN FED	RUS	EAST	44.99	41.12	41.00	188432	21.27
BALASIHA	RUSSIAN FED	RUS	EAST	55.83	37.95	68.00	146254	18.13
BATAJSK	RUSSIAN FED	RUS	EAST	47.13	39.75	78.00	105682	23.30
BELGOROD	RUSSIAN FED	RUS	EAST	50.61	36.59	84.00	331523	19.27
BRJANSK	RUSSIAN FED	RUS	EAST	53.24	34.35	135.00	434677	18.25
CEREPOVEC	RUSSIAN FED	RUS	EAST	59.14	37.91	164.00	311861	17.47
CERKESSK	RUSSIAN FED	RUS	EAST	44.29	42.06	167.00	115870	18.69
ELEKTROSTAL	RUSSIAN FED	RUS	EAST	55.79	38.44	212.00	147141	18.12
ELISTA	RUSSIAN FED	RUS	EAST	46.30	44.23	216.00	101068	23.49
GROZNYJ	RUSSIAN FED	RUS	EAST	43.31	45.68	243.00	244068	22.80
HIMKI	RUSSIAN FED	RUS	EAST	55.89	37.44	264.00	139990	18.04
IVANOVO	RUSSIAN FED	RUS	EAST	56.99	40.99	289.00	439372	18.01
JAROSLAVL	RUSSIAN FED	RUS	EAST	57.62	39.87	306.00	616205	17.91
JELEC	RUSSIAN FED	RUS	EAST	52.60	38.51	320.00	117202	18.49
KALININGRAD	RUSSIAN FED	RUS	EAST	54.71	20.50	346.00	425657	18.14
KALUGA	RUSSIAN FED	RUS	EAST	54.54	36.27	352.00	331438	17.76
KISLOVODSK	RUSSIAN FED	RUS	EAST	43.92	42.73	407.00	127234	16.35
KOLOMNA	RUSSIAN FED	RUS	EAST	55.08	38.78	422.00	150844	18.32
KOLPINO	RUSSIAN FED	RUS	EAST	59.75	30.60	425.00	140700	17.85
KOROLYOV	RUSSIAN FED	RUS	EAST	55.91	37.83	438.00	141661	18.13
KOSTROMA	RUSSIAN FED	RUS	EAST	57.77	40.93	443.00	279184	17.96
KOVROV	RUSSIAN FED	RUS	EAST	56.36	41.32	453.00	156269	18.25
KRASNODAR	RUSSIAN FED	RUS	EAST	45.03	38.98	460.00	640921	23.87
KURSK	RUSSIAN FED	RUS	EAST	51.73	36.19	497.00	414334	18.71
LIPECK	RUSSIAN FED	RUS	EAST	52.62	39.62	528.00	496951	18.76
LJUBERCY	RUSSIAN FED	RUS	EAST	55.66	37.95	534.00	158120	18.23
MAHACKALA	RUSSIAN FED	RUS	EAST	42.98	47.51	555.00	436994	23.50
MAJKOP	RUSSIAN FED	RUS	EAST	44.61	40.08	558.00	160263	21.44
MICURINSK	RUSSIAN FED	RUS	EAST	52.90	40.47	579.00	120700	18.89
MOSCOW	RUSSIAN FED	RUS	EAST	55.75	37.62	597.00	9886286	18.13
MURMANSK	RUSSIAN FED	RUS	EAST	68.97	33.08	605.00	350850	16.20
MUROM	RUSSIAN FED	RUS	EAST	55.57	42.04	608.00	126365	18.56
MYTISCI	RUSSIAN FED	RUS	EAST	55.90	37.75	612.00	158389	18.13
NALCIK	RUSSIAN FED	RUS	EAST	43.49	43.61	623.00	267521	18.00
NAZRAN	RUSSIAN FED	RUS	EAST	43.21	44.80	632.00	127276	18.14
NEVINNOMYSSK	RUSSIAN FED	RUS	EAST	44.63	41.95	646.00	130328	20.39
NOGINSK	RUSSIAN FED	RUS	EAST	55.85	38.44	669.00	118756	18.12
NOVOCERKASSK	RUSSIAN FED	RUS	EAST	47.42	40.08	683.00	173426	23.04
NOVOMOSKOVSK	RUSSIAN FED	RUS	EAST	54.09	38.22	695.00	135780	18.02
NOVOSAHTINSK	RUSSIAN FED	RUS	EAST	47.76	39.93	702.00	102218	21.15
OBNINSK	RUSSIAN FED	RUS	EAST	55.10	36.61	719.00	104886	17.92
ODINCOVO	RUSSIAN FED	RUS	EAST	55.67	37.29	722.00	133160	18.02
OREHOVOZUJEVO	RUSSIAN FED	RUS	EAST	55.80	38.97	736.00	123454	18.20
ORJOL	RUSSIAN FED	RUS	EAST	52.97	36.07	742.00	334121	18.27
PETROZAVODSK	RUSSIAN FED	RUS	EAST	61.81	34.33	784.00	266933	17.13
PJATIGORSK	RUSSIAN FED	RUS	EAST	44.05	43.06	788.00	138499	19.71
PODOLSK	RUSSIAN FED	RUS	EAST	55.42	37.54	791.00	185482	18.08
PSKOV	RUSSIAN FED	RUS	EAST	57.83	28.33	809.00	202899	17.89
RJAZAN	RUSSIAN FED	RUS	EAST	54.60	39.70	827.00	520664	18.44

City	Country	ISO3	Region	LAT	LON	LATLON	POP2000	MMT.EST
ROSTOV	RUSSIAN FED	RUS	EAST	47.24	39.71	837.00	1062159	23.30
RYBINSK	RUSSIAN FED	RUS	EAST	58.05	38.83	844.00	226923	17.81
SAHTY	RUSSIAN FED	RUS	EAST	47.69	40.25	853.00	221252	22.24
SANKTPETERBURG	RUSSIAN FED	RUS	EAST	59.89	30.26	868.00	4722279	17.94
SCJOLKOVO	RUSSIAN FED	RUS	EAST	55.90	38.02	890.00	112964	18.11
SERGIJEVPOSAD	RUSSIAN FED	RUS	EAST	56.32	38.13	901.00	113984	17.63
SERPUCHOV	RUSSIAN FED	RUS	EAST	54.92	37.43	906.00	131918	18.06
SMOLENSK	RUSSIAN FED	RUS	EAST	54.78	32.04	929.00	327838	17.56
STARYJOSKOL	RUSSIAN FED	RUS	EAST	51.30	37.84	955.00	208933	18.90
STAVROPOL	RUSSIAN FED	RUS	EAST	45.04	41.97	958.00	348706	20.24
TAMBOV	RUSSIAN FED	RUS	EAST	52.73	41.43	995.00	295921	19.20
TULA	RUSSIAN FED	RUS	EAST	54.20	37.61	1032.00	482134	18.03
TVER	RUSSIAN FED	RUS	EAST	56.86	35.89	1039.00	415541	17.82
VELIKIJELUKI	RUSSIAN FED	RUS	EAST	56.34	30.52	1083.00	106337	17.78
VELIKIJNOVGOROD	RUSSIAN FED	RUS	EAST	58.54	31.26	1086.00	218975	17.84
VLADIKAVKAZ	RUSSIAN FED	RUS	EAST	43.04	44.68	1105.00	312728	19.10
VLADIMIR	RUSSIAN FED	RUS	EAST	56.14	40.40	1108.00	319107	18.14
VOLGODONSK	RUSSIAN FED	RUS	EAST	47.51	42.15	1114.00	167927	23.28
VOLGOGRAD	RUSSIAN FED	RUS	EAST	48.80	44.59	1117.00	1010353	22.91
VOLOGDA	RUSSIAN FED	RUS	EAST	59.22	39.90	1121.00	291271	17.33
VOLZSKIJ	RUSSIAN FED	RUS	EAST	48.82	44.74	1128.00	303887	22.91
VORONEZ	RUSSIAN FED	RUS	EAST	51.67	39.17	1134.00	854483	19.53
ZARSKOJESELO	RUSSIAN FED	RUS	EAST	59.76	30.31	1152.00	101038	17.94
ZELEZNODOROZNYJ	RUSSIAN FED	RUS	EAST	55.75	38.13	1158.00	101348	18.11
ZELJENOGRAD	RUSSIAN FED	RUS	EAST	55.94	37.29	1166.00	205775	18.04
ZUKOVSKIJ	RUSSIAN FED	RUS	EAST	55.55	38.25	1180.00	100835	18.21
BRATISLAVA	SLOVAKIA	SVK	EAST	48.16	17.13	6.00	427958	18.35
KOSICE	SLOVAKIA	SVK	EAST	48.73	21.26	36.00	235961	17.53
LJUBLJANA	SLOVENIA	SVN	SOUTH	46.06	14.51	77.00	261929	18.11
ALBACETE	SPAIN	ESP	SOUTH	39.00	-1.87	18.00	146925	21.48
ALCALADEHENARES	SPAIN	ESP	SOUTH	40.48	-3.37	28.00	174647	21.16
ALCORCON	SPAIN	ESP	SOUTH	40.35	-3.82	42.00	151700	21.90
ALMERIA	SPAIN	ESP	SOUTH	36.83	-2.43	69.00	165172	23.68
BADAJOZ	SPAIN	ESP	SOUTH	38.88	-6.97	129.00	132344	24.84
BILBAO	SPAIN	ESP	SOUTH	43.25	-2.93	174.00	351910	19.30
BURGOS	SPAIN	ESP	SOUTH	42.35	-3.69	191.00	165586	17.10
CARTAGENA	SPAIN	ESP	SOUTH	37.61	-0.98	238.00	182948	24.86
CASTELLO	SPAIN	ESP	SOUTH	42.25	3.08	245.00	146960	21.67
CASTELLONDELAPLANA	SPAIN	ESP	SOUTH	39.98	-0.03	247.00	146263	24.56
CORDOBA	SPAIN	ESP	SOUTH	37.88	-4.77	282.00	307475	25.99
ELCHE	SPAIN	ESP	SOUTH	38.25	-0.70	321.00	194086	23.70
ELX	SPAIN	ESP	SOUTH	38.27	-0.68	337.00	193824	23.70
FUENLABRADA	SPAIN	ESP	SOUTH	40.27	-3.80	361.00	178496	21.90
GETAFE	SPAIN	ESP	SOUTH	40.30	-3.73	375.00	150203	22.01
GRANADA	SPAIN	ESP	SOUTH	37.17	-3.59	389.00	242078	20.40
HUELVA	SPAIN	ESP	SOUTH	37.25	-6.94	408.00	142310	25.26
JAEN	SPAIN	ESP	SOUTH	37.77	-3.80	432.00	111620	25.61
JEREZDELAFRONTERA	SPAIN	ESP	SOUTH	36.68	-6.13	435.00	183277	25.00
LEGANES	SPAIN	ESP	SOUTH	40.33	-3.77	488.00	173383	21.90
LEON	SPAIN	ESP	SOUTH	42.59	-5.57	494.00	132171	17.19
LLEIDA	SPAIN	ESP	SOUTH	41.62	0.63	506.00	112188	23.77
LOGRONO	SPAIN	ESP	SOUTH	42.47	-2.44	513.00	131936	18.48
MADRID	SPAIN	ESP	SOUTH	40.42	-3.71	531.00	2945822	22.01
MATARO	SPAIN	ESP	SOUTH	41.54	2.44	563.00	105863	20.98
MOSTOLES	SPAIN	ESP	SOUTH	40.32	-3.88	614.00	196069	21.90
MURCIA	SPAIN	ESP	SOUTH	37.98	-1.13	621.00	366242	25.34
OURENSE	SPAIN	ESP	SOUTH	42.33	-7.87	664.00	107025	18.84
OVIEDO	SPAIN	ESP	SOUTH	43.35	-5.83	667.00	200638	18.01
PALMA	SPAIN	ESP	SOUTH	39.57	2.65	677.00	332128	22.68
PALMADEMALLORCA	SPAIN	ESP	SOUTH	39.57	2.65	680.00	329897	22.68
PAMPLONA	SPAIN	ESP	SOUTH	42.82	-1.63	682.00	183602	18.11
SABADELL	SPAIN	ESP	SOUTH	41.55	2.10	773.00	184342	21.09
SALAMANCA	SPAIN	ESP	SOUTH	40.97	-5.67	780.00	157008	18.09
SANCRISTOBALDELALAGU	SPAIN	ESP	SOUTH	28.48	-16.32	790.00	128154	18.65
SANTANDER	SPAIN	ESP	SOUTH	43.47	-3.80	829.00	181727	18.89
SEVILLA	SPAIN	ESP	SOUTH	37.40	-5.98	879.00	684472	27.77
TARRAGONA	SPAIN	ESP	SOUTH	41.12	1.24	903.00	112828	22.86
TERRASSA	SPAIN	ESP	SOUTH	41.57	2.00	914.00	172136	20.96
VALENCIA	SPAIN	ESP	SOUTH	39.48	-0.39	972.00	734702	25.51
VALLADOLID	SPAIN	ESP	SOUTH	41.65	-4.74	976.00	317964	18.87

City	Country	ISO3	Region	LAT	LON	LATLON	POP2000	MMT.EST
VIGO	SPAIN	ESP	SOUTH	42.22	-8.71	989.00	279776	19.35
VITORIA	SPAIN	ESP	SOUTH	42.85	-2.67	1027.00	215813	17.36
ZARAGOZA	SPAIN	ESP	SOUTH	41.65	-0.89	1043.00	612822	23.37
MALMO	SWEDEN	SWE	NORTH	55.60	13.00	2091.00	248520	17.82
STOCKHOLM	SWEDEN	SWE	NORTH	59.33	18.05	3186.00	1212196	17.55
UPPSALA	SWEDEN	SWE	NORTH	59.86	17.64	3602.00	124036	17.31
VASTERAS	SWEDEN	SWE	NORTH	59.62	16.55	3719.00	102548	17.39
BASEL	SWITZERLAND	CHE	WEST	47.57	7.60	39.00	166558	18.94
BERN	SWITZERLAND	CHE	WEST	46.92	7.47	46.00	128634	17.48
GENEVE	SWITZERLAND	CHE	WEST	46.21	6.14	149.00	177964	18.18
LAUSANNE	SWITZERLAND	CHE	WEST	46.53	6.67	223.00	124914	18.08
ZURICH	SWITZERLAND	CHE	WEST	47.37	8.55	482.00	363273	18.33
ALCHEVSK	UKRAINE	UKR	EAST	48.47	38.80	3.00	119488	18.16
BERDYANSK	UKRAINE	UKR	EAST	46.75	36.79	12.00	122880	19.38
BILATSERKVA	UKRAINE	UKR	EAST	49.81	30.12	18.00	199916	17.58
CHERKASY	UKRAINE	UKR	EAST	49.44	32.08	31.00	294580	18.15
CHERNIHIV	UKRAINE	UKR	EAST	51.50	31.29	34.00	304239	17.59
CHERNIVTSI	UKRAINE	UKR	EAST	48.29	25.95	37.00	242294	17.42
DNIPRODZERZHYNSK	UKRAINE	UKR	EAST	48.49	34.68	43.00	258071	18.51
DNIPROPETROVSK	UKRAINE	UKR	EAST	48.45	35.04	46.00	1073987	18.67
DONETSK	UKRAINE	UKR	EAST	48.00	37.80	49.00	1023749	18.23
HORLIVKA	UKRAINE	UKR	EAST	48.34	38.05	69.00	295581	18.11
IVANOFRANKIVSK	UKRAINE	UKR	EAST	48.92	24.72	74.00	217663	17.01
KAMYANETSPODILSKYY	UKRAINE	UKR	EAST	48.68	26.58	86.00	100165	17.46
KERCH	UKRAINE	UKR	EAST	45.35	36.46	89.00	158350	19.49
KHARKIV	UKRAINE	UKR	EAST	49.98	36.22	92.00	1481186	17.97
KHERSON	UKRAINE	UKR	EAST	46.65	32.60	98.00	330169	19.49
KHMELNYTSKYY	UKRAINE	UKR	EAST	49.42	27.00	101.00	252537	16.97
KIROVOHRAD	UKRAINE	UKR	EAST	48.51	32.27	104.00	255296	17.92
KRAMATORSK	UKRAINE	UKR	EAST	48.74	37.57	123.00	182359	18.36
KREMENCHUK	UKRAINE	UKR	EAST	49.08	33.42	134.00	234248	18.33
KRYVYYRIH	UKRAINE	UKR	EAST	47.90	33.35	137.00	673574	18.68
KYYIV	UKRAINE	UKR	EAST	50.44	30.52	140.00	2609662	18.00
LUHANSK	UKRAINE	UKR	EAST	48.57	39.31	149.00	465742	18.80
LUTSK	UKRAINE	UKR	EAST	50.75	25.32	152.00	208060	17.14
LVIV	UKRAINE	UKR	EAST	49.84	24.03	155.00	737666	16.98
LYSYCHANSK	UKRAINE	UKR	EAST	48.91	38.43	158.00	115955	18.34
MAKIYIVKA	UKRAINE	UKR	EAST	48.04	37.98	161.00	392803	18.23
MELITOPOL	UKRAINE	UKR	EAST	46.85	35.36	170.00	162045	19.27
MYKOLAYIV	UKRAINE	UKR	EAST	46.96	32.01	176.00	514825	19.31
NIKOPOL	UKRAINE	UKR	EAST	47.57	34.40	179.00	137709	19.05
ODESA	UKRAINE	UKR	EAST	46.49	30.73	195.00	1035905	19.15
PAVLOHRAD	UKRAINE	UKR	EAST	48.54	35.87	203.00	119956	18.65
POLTAVA	UKRAINE	UKR	EAST	49.59	34.55	209.00	317748	18.17
RIVNE	UKRAINE	UKR	EAST	50.63	26.24	215.00	247178	17.11
SEVASTOPOL	UKRAINE	UKR	EAST	44.61	33.54	227.00	343145	18.73
SIMFEROPOL	UKRAINE	UKR	EAST	44.96	34.10	236.00	344083	17.73
SLOVYANSK	UKRAINE	UKR	EAST	48.85	37.58	239.00	125804	18.43
SUMY	UKRAINE	UKR	EAST	50.93	34.79	254.00	292832	17.49
SYEVERODONETSK	UKRAINE	UKR	EAST	48.96	38.49	262.00	120880	18.34
TERNOPIL	UKRAINE	UKR	EAST	49.55	25.60	265.00	226080	16.83
UZHHOROD	UKRAINE	UKR	EAST	48.62	22.31	274.00	117916	17.62
VINNYTSYA	UKRAINE	UKR	EAST	49.24	28.49	277.00	358386	17.20
YENAKIYEVE	UKRAINE	UKR	EAST	48.23	38.23	283.00	105247	18.26
ZAPORIZHZHYA	UKRAINE	UKR	EAST	47.85	35.17	289.00	820305	18.87
ZHYTOMYR	UKRAINE	UKR	EAST	50.26	28.66	295.00	284658	17.17
ABERDEEN	UNITED KINGD	GBR	NORTH	57.13	-2.10	3.00	184521	16.56
BASILDON	UNITED KINGD	GBR	NORTH	51.57	0.47	39.00	103509	17.53
BELFAST	UNITED KINGD	GBR	NORTH	54.58	-5.93	49.00	264761	16.72
BIRMINGHAM	UNITED KINGD	GBR	NORTH	52.47	-1.92	62.00	972380	17.13
BLACKBURN	UNITED KINGD	GBR	NORTH	53.75	-2.48	68.00	106629	16.71
BOLTON	UNITED KINGD	GBR	NORTH	53.58	-2.43	76.00	140261	16.71
BRADFORD	UNITED KINGD	GBR	NORTH	53.78	-1.75	83.00	295331	16.94
BRIGHTON	UNITED KINGD	GBR	NORTH	50.83	-0.15	92.00	134038	17.50
BRISTOL	UNITED KINGD	GBR	NORTH	51.45	-2.58	94.00	412317	17.19
CAMBRIDGE	UNITED KINGD	GBR	NORTH	52.20	0.12	107.00	111401	17.53
CHELMSFORD	UNITED KINGD	GBR	NORTH	51.73	0.48	118.00	100101	17.53
COLCHESTER	UNITED KINGD	GBR	NORTH	51.88	0.90	139.00	103713	17.54
COVENTRY	UNITED KINGD	GBR	NORTH	52.42	-1.55	146.00	305594	17.24
DERBY	UNITED KINGD	GBR	NORTH	52.93	-1.50	163.00	226502	17.28

City	Country	ISO3	Region	LAT	LON	LATLON	POP2000	MMT.EST
DUDLEY	UNITED KINGD	GBR	NORTH	52.50	-2.08	171.00	192287	17.08
DUNDEE	UNITED KINGD	GBR	NORTH	56.50	-2.97	177.00	154985	16.67
EASTBOURNE	UNITED KINGD	GBR	NORTH	50.80	0.25	183.00	103397	17.56
EDINBURGH	UNITED KINGD	GBR	NORTH	55.95	-3.20	191.00	427042	16.47
EXETER	UNITED KINGD	GBR	NORTH	50.70	-3.53	197.00	105881	17.11
GLASGOW	UNITED KINGD	GBR	NORTH	55.83	-4.25	216.00	632331	16.74
GLOUCESTER	UNITED KINGD	GBR	NORTH	51.83	-2.25	220.00	122337	17.37
HUDDERSFIELD	UNITED KINGD	GBR	NORTH	53.65	-1.78	266.00	149092	16.66
IPSWICH	UNITED KINGD	GBR	NORTH	52.08	1.17	276.00	130286	17.47
KINGSTONUPONHULL	UNITED KINGD	GBR	NORTH	53.75	-0.33	292.00	299059	17.27
LEEDS	UNITED KINGD	GBR	NORTH	53.80	-1.58	304.00	443770	16.94
LEICESTER	UNITED KINGD	GBR	NORTH	52.63	-1.13	306.00	328475	17.22
LONDON	UNITED KINGD	GBR	NORTH	51.50	-0.12	327.00	7116815	17.66
LUTON	UNITED KINGD	GBR	NORTH	51.88	-0.42	335.00	183086	17.36
MANCHESTER	UNITED KINGD	GBR	NORTH	53.50	-2.22	341.00	395331	16.70
NEWCASTLEUPONTYNE	UNITED KINGD	GBR	NORTH	54.99	-1.62	364.00	189105	16.76
NEWPORT	UNITED KINGD	GBR	NORTH	51.58	-2.98	366.00	118378	17.32
NORTHAMPTON	UNITED KINGD	GBR	NORTH	52.25	-0.88	376.00	191973	17.28
NORWICH	UNITED KINGD	GBR	NORTH	52.63	1.30	381.00	172110	17.48
NOTTINGHAM	UNITED KINGD	GBR	NORTH	52.97	-1.17	383.00	273440	17.29
OLDHAM	UNITED KINGD	GBR	NORTH	53.55	-2.12	387.00	104263	16.70
OXFORD	UNITED KINGD	GBR	NORTH	51.75	-1.25	391.00	141962	17.50
PETERBOROUGH	UNITED KINGD	GBR	NORTH	52.58	-0.25	400.00	137316	17.45
PLYMOUTH	UNITED KINGD	GBR	NORTH	50.40	-4.12	403.00	242868	17.07
PORTSMOUTH	UNITED KINGD	GBR	NORTH	50.80	-1.08	413.00	185463	17.61
PRESTON	UNITED KINGD	GBR	NORTH	53.77	-2.72	418.00	182190	16.78
READING	UNITED KINGD	GBR	NORTH	51.43	-1.00	426.00	234535	17.46
ROTHERHAM	UNITED KINGD	GBR	NORTH	53.43	-1.35	435.00	119687	17.20
SHEFFIELD	UNITED KINGD	GBR	NORTH	53.37	-1.50	451.00	441129	17.20
SLOUGH	UNITED KINGD	GBR	NORTH	51.50	-0.58	459.00	124824	17.68
SOUTHAMPTON	UNITED KINGD	GBR	NORTH	50.90	-1.40	462.00	229804	17.61
SOUTHENDONSEA	UNITED KINGD	GBR	NORTH	51.53	0.70	464.00	160121	17.57
STOCKPORT	UNITED KINGD	GBR	NORTH	53.40	-2.15	477.00	131991	16.96
STOKEONTRENT	UNITED KINGD	GBR	NORTH	53.00	-2.18	480.00	262631	16.80
SUNDERLAND	UNITED KINGD	GBR	NORTH	54.91	-1.38	487.00	178163	16.77
SUTTONCOLDFIELD	UNITED KINGD	GBR	NORTH	52.57	-1.82	489.00	103928	17.10
SWANSEA	UNITED KINGD	GBR	NORTH	51.63	-3.97	493.00	171094	17.01
SWINDON	UNITED KINGD	GBR	NORTH	51.52	-1.78	495.00	152295	17.32
WALSALL	UNITED KINGD	GBR	NORTH	52.60	-2.00	516.00	171280	17.08
WATFORD	UNITED KINGD	GBR	NORTH	51.67	-0.40	522.00	120094	17.74
WESTBROMWICH	UNITED KINGD	GBR	NORTH	52.52	-2.00	527.00	143155	17.08
WOLVERHAMPTON	UNITED KINGD	GBR	NORTH	52.58	-2.13	548.00	251325	17.08
YORK	UNITED KINGD	GBR	NORTH	53.97	-1.08	556.00	134726	17.18

Appendix to Chapter 5

C

C.1 Data and result tables (digital format)

See attached CD for

- **Table** S1 showing City data for the ensemble-mean values in 2100 for MMT, EXD, MAG and their delta values ΔMMT, ΔEXD, ΔMAG.

  `Supplementary_Table_S1_city_data_ENSMEAN_2100_and_2090_2099_mmt_exd_mag_dlt_values_DECADE_20210820.xlsx`

- **Table** S2 showing a comparison of mean ensemble-mean statistics (P05, P95, Mean, Min, Max) for all 15 RCP/SSP combinations for MMT, EXD, MAG in 2000 and 2100 and their delta values ΔMMT, ΔEXD, ΔMAG.

  `Supplementary_Table_S2_compare_meanENSMEAN_2000_2100_and_1991_2000_to_2090_2099_dlt_mmt_exd_mag_DECADE_20210820.xlsx`

C.2 Scenario Matrix for changes in ΔMAG

Fig. C.1.: **Systematic overview of the change in adaptation and exposure magnitude (ΔMAG) for the city sample according to each RCP/SSP combination and the future socio-economic level per SSP.** Lower panel: The 2000–2100 ΔEXD (orange boxes) in context of ΔMAG (in-box text annotations) for all possible RCP/SSP combinations. Upper panel: Unique country-based GDP/capita per SSP in 2100 (mean from IIASA and OECD data). Green line in upper panel denotes the country-based GDP/capita as of 2000 [in 2011 int.$].

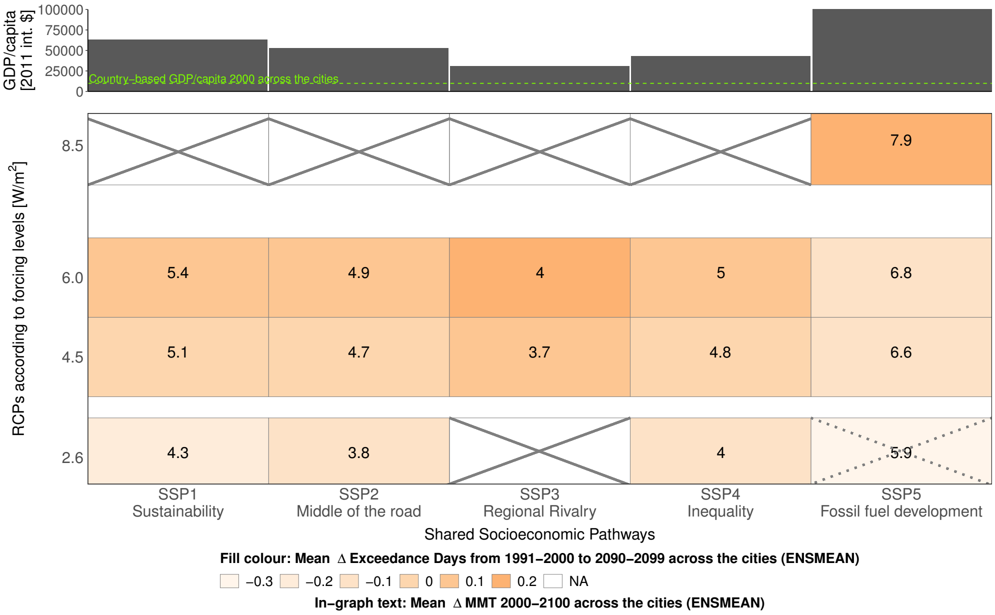

C.3 Supplementary Methods and Discussion

C.3.1 Methods previously used

Details on the previously developed MMT model

The model established in our prior study Krummenauer et al., 2019 approximates the MMT for cities without relying on daily mortality records as conventional studies do. It uses a set of city-specific climatic, topographic and socio-economic data instead. The model was systematically developed under the premise of simplicity and robustness, testing a multitude of model candidates containing different combinations of independent variables, which were gathered from previous literature. Collinearity among variables was restricted and for each model candidate individually, the significance of each model parameter was assessed via the likelihood-ratio test (LRT) with a significance level of 0.99. Model candidates that returned insignificant parameters according to our condition were removed. A further model selection criterion was the Akaike information criterion corrected for small sample sizes (AICc), which allows the comparison of non-nested models. The model candidate ranking lowest in the AICc was chosen. The model selection according to the combination of LRT and AICc consistently dismissed model candidates containing uninformative parameters while only exhibiting small increases in AICc scores (AICc difference < 2) compared to other model candidates without redundant parameters. We generally compared systematically the same variable setups in a linear model variant, segmented model variants with asymptotes and a sigmoid model variant. The latter showed the lowest and most optimal AICc of 1782 and a low RMSE of 2.81 ($^\circ$C) when employing five significant city-specific variables: the 30-year average of the daily mean temperature, the 30-year average of the annual amplitude, the elevation, the GPD/capita and improved urban water access. The other model variants showed less optimal AICc and RMSE values. The model was trained on 360 MMTs for cities across the globe and validated on 40 urban MMTs, the latter returned an RMSE of 2.63 ($^\circ$C). We did not find any systematic bias in any estimation subset for different climate zones and different world regions underlining the applicability of the model for cities across the globe. The performance of our model in estimating MMTs was better than using the most optimal temperature percentile, the 89th percentile in our daily mean temperature dataset, as suggested by previous studies. We used our model to estimate the MMT for current climate conditions for 600 European cities finding a pronounced decline in MMTs from southern European and Mediterranean cities to northern European cities, with the exception of cities in higher altitudes. The maximum MMT was 27.8°C in Sevilla (Spain).

C.3.2 Discussion of previous method

Advantages of the previous approach

A major advantage of our model is that it estimates MMTs as a measure of human heat adaptation independently from daily mortality records. In contrast to conventional studies analysing the heat-mortality relationship for cities based on daily mortality records, our method is in a twofold way a very flexible tool because it relies on freely available and robust, less error-prone city-specific data. First, the model employment is spatially flexible. It can be applied to any city around the globe and inform about the city-specific heat adaptation without having been subject to research using the conventional approach to derive MMTs on the basis of daily mortality records. The spatial appliance of the model has been successfully proven in our previous study on 600 European cities. The model performance was equally robust across different climate zones and world regions. Second, our model can be adjusted for usage for different time frames. This is due to the nature of the variables in the model. While topographic input data remains the same, for climate and socio-economic input variables, projections of climate and socio-economy can be used. Thus, the MMT for future time frames can be approached with our model. It even allows to compare MMTs for different time periods and calculate the delta changes in MMT. Such time independence cannot be achieved by the conventional method to derive the MMT, where usually observed mortality time series are replicated and continued into the future. Another principal advantage of our approach is that it allows to separate the shares of physiological acclimatisation and wealth-enabled measures to overall heat adaptation. The MMT is therefore more than a simple temperature index.

Limitations of the previous approach

We have to acknowledge that some degree of uncertainty in our model had been brought about by the original MMTs from the studies used in the previous work. It has to be noted that the MMTs gathered from the studies are commonly derived for all-cause mortality (excluding unnatural causes of death, such as murder or accidents) rather than only mortality specifically caused by direct heat exposure. The method therefore refers to a broader mortality and temperature association than using exclusively death cases caused from direct heat impact. A denser coverage of MMTs in the global south and warmer regions would possibly have increased precision of the model by decreasing the RMSE, even though the model performed equally well for data-rich regions across different climate zones.

C.3.3 Current Method

Coefficients

Tab. C.1.: Coefficients for the newly calibrated model, historic situation and new input data. Coefficients can be employed for historic and future gridded climate data as described in the Methods section in the article.

Mode	ENSMEAN
Time	2000
c	64.7446
d	0.545534305
30-year Tmean	0.672891536
30-year Amplitude	0.408054743
Elevation	0.006266229
GDP/capita	0.053298229
Water access (%)	-0.038787511
RMSE	3.2070

Bibliography

Abdulkareem, Haval A. (2016). 'Thermal Comfort through the Microclimates of the Courtyard. A Critical Review of the Middle-eastern Courtyard House as a Climatic Response'. In: *Procedia - Social and Behavioral Sciences* 216.October 2015, pp. 662–674. DOI: 10.1016/j.sbspro.2015.12.054. arXiv: arXiv:1011.1669v3 (cit. on p. 17).

Achebak, Hicham, Daniel Devolder and Joan Ballester (2018). 'Heat-related mortality trends under recent climate warming in Spain: A 36-year observational study'. In: *PLOS Medicine* 15.7. Ed. by Jonathan Alan Patz, e1002617. DOI: 10.1371/journal.pmed.1002617 (cit. on p. 35).

– (2019). 'Trends in temperature-related age-specific and sex-specific mortality from cardiovascular diseases in Spain: a national time-series analysis'. In: *The Lancet Planetary Health* 3.7, e297–e306. DOI: 10.1016/S2542-5196(19)30090-7 (cit. on p. 7).

Agard, John, Lisa E.F. Schipper, Jörn Birkmann, Maximiliano Campos, Carolina Dubeux, Yukihiro Nojiri, Lennart Olsson, Balgis Osman-Elasha, Mark Pelling, Michael J. Prather, Marta G. Rivera-Ferre, Oliver C. Ruppel, Asbury Sallenger, Kirk R. Smith and Asuncion L. St.Clair (2014). *Annex II: Glossary to the Fifth Assessment Report of the Intergouvernmental Panel on Climate Change (WGII AR5)*. Tech. rep. Geneva, Switzerland: IPCC (cit. on p. 2).

Ahima, Rexford S (2020). 'Global warming threatens human thermoregulation and survival'. In: *Journal of Clinical Investigation* 130.2, pp. 559–561. DOI: 10.1172/JCI135006 (cit. on p. 50).

Ahmadalipour, Ali and Hamid Moradkhani (2018). 'Escalating heat-stress mortality risk due to global warming in the Middle East and North Africa (MENA)'. In: *Environment International* 117.May, pp. 215–225. DOI: 10.1016/j.envint.2018.05.014 (cit. on p. 22).

Al Jazeera (2017). *Hotter and drier again in the Middle East and US desert* (cit. on p. 19).

Amirkhani Aryan, Zamani Ehsan, Saidian Amin and Khademi Masoud (2010). 'Wind Catchers: Remarkable Example of Iranian Sustainable Architecture'. In: *Sustainable Development* 3.2, pp. 89–97 (cit. on p. 17).

Anderson, Brooke G. and Michelle L. Bell (2009). 'Weather-Related Mortality'. In: *Epidemiology* 20.2, pp. 205–213. DOI: 10.1097/EDE.0b013e318190ee08 (cit. on p. 27).

Arbuthnott, Katherine G., Shakoor Hajat, Clare Heaviside and Sotiris Vardoulakis (2016). 'Changes in population susceptibility to heat and cold over time: assessing adaptation to climate change'. In: *Environmental Health* 15.S1, S33. DOI: 10.1186/s12940-016-0102-7 (cit. on pp. 4, 46, 50, 76, 80, 95, 99, 101).

Arbuthnott, Katherine G., Shakoor Hajat, Clare Heaviside and Sotiris Vardoulakis (2018). 'What is cold-related mortality? A multi-disciplinary perspective to inform climate change impact assessments'. In: *Environment International* 121, pp. 119–129. DOI: 10.1016/j.envint.2018.08.053 (cit. on p. 26).

– (2020). 'Years of life lost and mortality due to heat and cold in the three largest English cities'. In: *Environment International* 144.March, p. 105966. DOI: 10.1016/j.envint.2020.105966 (cit. on p. 7).

Arnold, Todd W. (2010). 'Uninformative Parameters and Model Selection Using Akaike's Information Criterion'. In: *Journal of Wildlife Management* 74.6, pp. 1175–1178. DOI: 10.2193/2009-367 (cit. on p. 40).

Åström, Daniel Oudin, Andreas Tornevi, Kristie L. Ebi, Joacim Rocklöv and Bertil Forsberg (2016). 'Evolution of Minimum Mortality Temperature in Stockholm, Sweden, 1901–2009'. In: *Environmental Health Perspectives* 124.6, pp. 740–744. DOI: 10.1289/ehp.1509692 (cit. on pp. 3, 7, 50).

Baccini, Michaela, Tom Kosatsky, Antonis Analitis, Hugh Ross Anderson, M. D'Ovidio, B. Menne, P. Michelozzi and A. Biggeri (2011). 'Impact of heat on mortality in 15 European cities: attributable deaths under different weather scenarios'. In: *Journal of Epidemiology & Community Health* 65.1, pp. 64–70. DOI: 10.1136/jech.2008.085639 (cit. on p. 2).

Baccini, Michela et al. (2008). 'Heat Effects on Mortality in 15 European Cities'. In: *Epidemiology* 19.5, pp. 711–719. DOI: 10.1097/EDE.0b013e318176bfcd (cit. on p. 94).

Bae, Jun-Sang, Jeong-Beom Lee, Takaaki Matsumoto, Timothy Othman, Young-Ki Min and Hun-Mo Yang (2006). 'Prolonged residence of temperate natives in the tropics produces a suppression of sweating'. In: *Pflügers Archiv - European Journal of Physiology* 453.1, pp. 67–72. DOI: 10.1007/s00424-006-0098-x (cit. on p. 7).

Bai, Li, Alistair Woodward, Cirendunzhu and Qiyong Liu (2016). 'County-level heat vulnerability of urban and rural residents in Tibet, China'. In: *Environmental Health* 15.1, p. 3. DOI: 10.1186/s12940-015-0081-0 (cit. on pp. 46, 95, 98, 99).

Ballester, Joan, Jean-Marie Robine, François Richard Herrmann and Xavier Rodó (2011). 'Long-term projections and acclimatization scenarios of temperature-related mortality in Europe'. In: *Nature Communications* 2.1, p. 358. DOI: 10.1038/ncomms1360 (cit. on pp. 38, 45, 50, 62, 95, 99).

Bao, Junzhe, Zhenkun Wang, Chuanhua Yu and Xudong Li (2016). 'The influence of temperature on mortality and its Lag effect: a study in four Chinese cities with different latitudes'. In: *BMC Public Health* 16.1, p. 375. DOI: 10.1186/s12889-016-3031-z (cit. on pp. 2, 43, 94).

Barreca, Alan, Karen Clay, Olivier Deschenes, Michael Greenstone and Joseph S. Shapiro (2016). 'Adapting to Climate Change: The Remarkable Decline in the US Temperature-Mortality Relationship over the Twentieth Century'. In: *Journal of Political Economy* 124.1, pp. 105–159. DOI: 10.1086/684582 (cit. on p. 35).

Beckmann, Sabrina and Michael Hiete (2020). 'Predictors Associated with Health-Related Heat Risk Perception of Urban Citizens in Germany'. In: *International Journal of Environmental Research and Public Health* 17.3, p. 874. DOI: 10.3390/ijerph17030874 (cit. on p. 4).

Benmarhnia, Tarik, Marie-France Sottile, Céline Plante, Allan Brand, Barbara Casati, Michel Fournier and Audrey Smargiassi (2014). 'Variability in Temperature-Related Mortality Projections under Climate Change'. In: *Environmental Health Perspectives* 122.12, pp. 1293–1298. DOI: 10.1289/ehp.1306954 (cit. on p. 36).

Boeckmann, Melanie and Ines Rohn (2014). 'Is planned adaptation to heat reducing heat-related mortality and illness? A systematic review'. In: *BMC Public Health* 14.1, p. 1112. DOI: 10.1186/1471-2458-14-1112 (cit. on pp. 7, 8).

Breitner, Susanne, Kathrin Wolf, Annette Peters and Alexandra Schneider (2014). 'Short-term effects of air temperature on cause-specific cardiovascular mortality in Bavaria, Germany'. In: *Heart* 100.16, pp. 1272–1280. DOI: 10.1136/heartjnl-2014-305578 (cit. on pp. 3, 26, 35, 72).

Bundeszentrale für Gesundheitliche Aufklärung (2020). *Infektionsschutz* (cit. on p. 73).

Burkart, Katrin, Alexandra Schneider, Susanne Breitner, Mobarak Hossain Khan, Alexander Krämer and Wilfried Endlicher (2011). 'The effect of atmospheric thermal conditions and urban thermal pollution on all-cause and cardiovascular mortality in Bangladesh'. In: *Environmental Pollution* 159.8-9, pp. 2035–2043. DOI: 10.1016/j.envpol.2011.02.005 (cit. on p. 94).

Burnham, K.P. and D.R. Anderson (2002). *Model Selection and Multimodel Inference. A Practical Information-Theoretic Approach.* 2nd ed. New York City, USA: Springer New York City (cit. on pp. 40, 42).

Burt, Christopher C (2017). *World's Hottest Nights/Highest Minimum Temperatures Yet Measured* (cit. on p. 19).

Carleton, Tamma et al. (2018). 'Valuing the Global Mortality Consequences of Climate Change Accounting for Adaptation Costs and Benefits'. In: *SSRN Electronic Journal*. DOI: 10.2139/ssrn.3224365 (cit. on p. 26).

Center for International Earth Science Information Network (CIESIN) at Columbia University (2016). *Gridded Population of the World, Version 4 (GPWv4): Population Density Adjusted to Match 2015 Revision UN WPP Country Totals*. Palisades, USA (cit. on pp. 96, 98, 99).

Center for International Earth Science Information Network (CIESIN) at Columbia University, International Food Policy Research Institute (IFPRI), The World Bank and The International Center for Tropical Agriculture (CIAT) (2008). 'Center for International Earth Science Information Network (CIESIN)'. In: *Choice Reviews Online* 45.05, pp. 45–2621–45–2621. DOI: 10.5860/CHOICE.45-2621 (cit. on pp. 64, 96, 97, 99).

Chen, Kai, Susanne Breitner, Kathrin Wolf, Masna Rai, Christa Meisinger, Margit Heier, Bernhard Kuch, Annette Peters and Alexandra Schneide (2019). 'Projection of Temperature-Related Myocardial Infarction in Augsburg, Germany'. In: *Deutsches Aerzteblatt Online* 116.31-32, pp. 521–527. DOI: 10.3238/arztebl.2019.0521 (cit. on pp. 3, 26, 72, 80).

Chen, Kai, Lian Zhou, Xiaodong Chen, Zongwei Ma, Yang Liu, Lei Huang, Jun Bi and Patrick L. Kinney (2016). 'Urbanization Level and Vulnerability to Heat-Related Mortality in Jiangsu Province, China'. In: *Environmental Health Perspectives* 124.12, pp. 1863–1869. DOI: 10.1289/EHP204 (cit. on pp. 43, 47, 95, 98, 99, 101).

Chen, Kai et al. (2021). 'Ambient carbon monoxide and daily mortality: a global time-series study in 337 cities'. In: *The Lancet Planetary Health* 5.4, e191–e199. DOI: 10.1016/S2542-5196(21)00026-7 (cit. on p. 72).

Christidis, Nikolaos, Dann Mitchell and Peter A. Stott (2019). 'Anthropogenic climate change and heat effects on health'. In: *International Journal of Climatology* 39.12, pp. 4751–4768. DOI: 10.1002/joc.6104 (cit. on pp. 50, 62).

Chung, Joo-youn, Yasushi Honda, Yun-chul Hong, Xiao-chuan Pan, Yue-leon Guo and Ho Kim (2009). 'Ambient temperature and mortality: An international study in four capital cities of East Asia'. In: *Science of The Total Environment* 408.2, pp. 390–396. DOI: 10.1016/j.scitotenv.2009.09.009 (cit. on p. 94).

Chung, Yeonseung, Youn-Hee Lim, Yasushi Honda, Yue-Liang Leon Guo, Masahiro Hashizume, Michelle L. Bell, Bing-Yu Chen and Ho Kim (2015). 'Mortality Related to Extreme Temperature for 15 Cities in Northeast Asia'. In: *Epidemiology* 26.2, pp. 255–262. DOI: 10.1097/EDE.0000000000000229 (cit. on pp. 38, 95).

Chung, Yeonseung, Heesang Noh, Yasushi Honda, Masahiro Hashizume, Michelle L Bell, Yue-Liang Leon Guo and Ho Kim (2017). 'Temporal Changes in Mortality Related to Extreme Temperatures for 15 Cities in Northeast Asia: Adaptation to Heat and Maladaptation to Cold'. In: *American Journal of Epidemiology* 185.10, pp. 907–913. DOI: 10.1093/aje/kww199 (cit. on pp. 46, 95).

Chung, Yeonseung, Daewon Yang, Antonio Gasparrini, Ana M. Vicedo-Cabrera, Chris Fook Sheng Ng, Yoonhee Kim, Yasushi Honda and Masahiro Hashizume (2018). 'Changing Susceptibility to Non-Optimum Temperatures in Japan, 1972–2012: The Role of Climate, Demographic, and Socioeconomic Factors'. In: *Environmental Health Perspectives* 126.5, p. 057002. DOI: 10.1289/EHP2546 (cit. on p. 35).

Ciavarella, Andrew, Daniel Cotterill, Peter Stott, Sarah Kew, Sjoukje Philip, Geert Jan van Oldenborgh, Amalie Skålevåg, Philip Lorenz, Yoann Robin, Friederike Otto, Mathias Hauser, Sonia I Seneviratne, Flavio Lehner and Olga Zolina (2021). 'Prolonged Siberian heat of 2020 almost impossible without human influence'. In: *Climatic Change* 166.1-2, p. 9. DOI: 10.1007/s10584-021-03052-w (cit. on p. 1).

Columbia University (2018). *Center for International Earth Science Information Network (CIESIN)* (cit. on p. 99).

Cook, Benjamin I., Kevin J. Anchukaitis, Ramzi Touchan, David M. Meko and Edward R. Cook (2016). 'Spatiotemporal drought variability in the Mediterranean over the last 900 years'. In: *Journal of Geophysical Research: Atmospheres* 121.5, pp. 2060–2074. DOI: 10.1002/2015JD023929 (cit. on p. 17).

Corobov, Roman, Scott Sheridan, Kristie Ebi and Nicolae Opopol (2013). 'Warm Season Temperature-Mortality Relationships in Chisinau (Moldova)'. In: *International Journal of Atmospheric Sciences* 2013.2013, pp. 1–9. DOI: 10.1155/2013/346024 (cit. on p. 94).

Coumou, Dim and Alexander Robinson (2013). 'Historic and future increase in the global land area affected by monthly heat extremes'. In: *Environmental Research Letters* 8.3, p. 034018. DOI: 10.1088/1748-9326/8/3/034018 (cit. on pp. 1, 50).

Coumou, Dim, Alexander Robinson and Stefan Rahmstorf (2013). 'Global increase in record-breaking monthly-mean temperatures'. In: *Climatic Change* 118.3-4, pp. 771–782. DOI: 10.1007/s10584-012-0668-1 (cit. on p. 1).

Crespo Cuaresma, Jesús (2017). 'Income projections for climate change research: A framework based on human capital dynamics'. In: *Global Environmental Change* 42, pp. 226–236. DOI: 10.1016/j.gloenvcha.2015.02.012 (cit. on p. 64).

Curriero, Frank C (2002). 'Temperature and Mortality in 11 Cities of the Eastern United States'. In: *American Journal of Epidemiology* 155.1, pp. 80–87. DOI: 10.1093/aje/155.1.80 (cit. on pp. 38, 46, 94, 95).

Damkjaer, Simon and Richard Taylor (2017). 'The measurement of water scarcity: Defining a meaningful indicator'. In: *Ambio* 46.5, pp. 513–531. DOI: 10.1007/s13280-017-0912-z (cit. on p. 22).

Dellink, Rob, Jean Chateau, Elisa Lanzi and Bertrand Magné (2017). 'Long-term economic growth projections in the Shared Socioeconomic Pathways'. In: *Global Environmental Change* 42, pp. 200–214. DOI: 10.1016/j.gloenvcha.2015.06.004 (cit. on p. 64).

Deschenes, Olivier (2014). 'Temperature, human health, and adaptation: A review of the empirical literature'. In: *Energy Economics* 46, pp. 606–619. DOI: 10.1016/j.eneco.2013.10.013 (cit. on pp. 8, 78).

Dewachi, Omar, Mac Skelton, Vinh-kim Nguyen, Fouad M Fouad, Ghassan Abu Sitta, Zeina Maasri and Rita Giacaman (2014). 'Changing therapeutic geographies of the Iraqi and Syrian wars'. In: *The Lancet* 383.9915, pp. 449–457. DOI: 10.1016/S0140-6736(13)62299-0 (cit. on pp. 18, 22, 23).

Dhingra, Mani and Subrata Chattopadhyay (2016). 'Advancing smartness of traditional settlements-case analysis of Indian and Arab old cities'. In: *International Journal of Sustainable Built Environment* 5.2, pp. 549–563. DOI: 10.1016/j.ijsbe.2016.08.004 (cit. on p. 17).

D'Ippoliti, Daniela et al. (2010). 'The impact of heat waves on mortality in 9 European cities: results from the EuroHEAT project'. In: *Environmental Health* 9.1, p. 37. DOI: 10.1186/1476-069X-9-37 (cit. on p. 3).

Ebi, Kristie L., Tomoko Hasegawa, Katie Hayes, Andrew Monaghan, Shlomit Paz and Peter Berry (2018). 'Health risks of warming of 1.5 °C, 2 °C, and higher, above pre-industrial temperatures'. In: *Environmental Research Letters* 13.6, p. 063007. DOI: 10.1088/1748-9326/aac4bd (cit. on pp. 26, 35).

Egondi, Thaddaeus, Catherine Kyobutungi, Sari Kovats, Kanyiva Muindi, Remare Ettarh and Joacim Rocklöv (2012). 'Time-series analysis of weather and mortality patterns in Nairobi's informal settlements'. In: *Global Health Action* 5.1, p. 19065. DOI: 10.3402/gha.v5i0.19065 (cit. on pp. 3, 41).

El Mundo (2019). *Un menor de 17 años muere por un golpe de calor cuando trabajaba en el campo en Córdoba* (cit. on p. 4).

El-Zein, Abbas, Mylene Tewtel-Salem and Gebran Nehme (2004). 'A time-series analysis of mortality and air temperature in Greater Beirut'. In: *Science of The Total Environment* 330.1-3, pp. 71–80. DOI: 10.1016/j.scitotenv.2004.02.027 (cit. on pp. 3, 41, 94).

European Environment Agency (2013). *EEA coastline for analysis* (cit. on p. 97).

FAO (2017). *AQUASTAT. Saudi Arabia* (cit. on p. 23).

Farajzadeh, M. and M. Darand (2009). 'Analyzing the influence of air temperature on the cardiovascular, respiratory and stroke mortality in Tehran'. In: *Journal of Environmental Health Science & Engineering* 6.4, pp. 261–270. DOI: na (cit. on p. 94).

Folkerts, Mireille A., Peter Bröde, W. J. Wouter Botzen, Mike L. Martinius, Nicola Gerrett, Carel N. Harmsen and Hein A. M. Daanen (2020). ‘Long Term Adaptation to Heat Stress: Shifts in the Minimum Mortality Temperature in the Netherlands’. In: *Frontiers in Physiology* 11.March, pp. 1–7. DOI: 10.3389/fphys.2020.00225 (cit. on pp. 2, 4, 50, 78, 80).

Follos, F., C. Linares, J.M. Vellón, J.A. López-Bueno, M.Y. Luna, G. Sánchez-Martínez and J. Díaz (2020). ‘The evolution of minimum mortality temperatures as an indicator of heat adaptation: The cases of Madrid and Seville (Spain)’. In: *Science of The Total Environment* 747, p. 141259. DOI: 10.1016/j.scitotenv.2020.141259 (cit. on pp. 3, 4, 50).

Fouillet, A., G. Rey, F. Laurent, G. Pavillon, S. Bellec, C. Guihenneuc-Jouyaux, J. Clavel, E. Jougla and D. Hémon (2006). ‘Excess mortality related to the August 2003 heat wave in France’. In: *International Archives of Occupational and Environmental Health* 80.1, pp. 16–24. DOI: 10.1007/s00420-006-0089-4 (cit. on p. 1).

Fouillet, A., G. Rey, V. Wagner, K. Laaidi, P. Empereur-Bissonnet, A. Le Tertre, P. Frayssinet, P. Bessemoulin, F. Laurent, P. De Crouy-Chanel, E. Jougla and D. Hémon (2008). ‘Has the impact of heat waves on mortality changed in France since the European heat wave of summer 2003? A study of the 2006 heat wave’. In: *International Journal of Epidemiology* 37.2, pp. 309–317. DOI: 10.1093/ije/dym253 (cit. on p. 8).

Freitas, Christopher de and Elena Grigorieva (2015). ‘Role of Acclimatization in Weather-Related Human Mortality During the Transition Seasons of Autumn and Spring in a Thermally Extreme Mid-Latitude Continental Climate’. In: *International Journal of Environmental Research and Public Health* 12.12, pp. 14974–14987. DOI: 10.3390/ijerph121214962 (cit. on pp. 7, 78).

Frieler, Katja et al. (2017). ‘Assessing the impacts of 1.5 °C global warming - simulation protocol of the Inter-Sectoral Impact Model Intercomparison Project (ISIMIP2b)’. In: *Geoscientific Model Development* 10.12, pp. 4321–4345. DOI: 10.5194/gmd-10-4321-2017 (cit. on pp. 26, 27).

Ganguly, Auroop R., Karsten Steinhaeuser, David J. Erickson, Marcia Branstetter, Esther S. Parish, Nagendra Singh, John B. Drake and Lawrence Buja (2009). ‘Higher trends but larger uncertainty and geographic variability in 21st century temperature and heat waves’. In: *Proceedings of the National Academy of Sciences* 106.37, pp. 15555–15559. DOI: 10.1073/pnas.0904495106 (cit. on pp. 1, 50, 80).

Gasparrini, Antonio, Ben Armstrong and Michael G. Kenward (2010). ‘Distributed lag non-linear models’. In: *Statistics in Medicine* 29.21, pp. 2224–2234. DOI: 10.1002/sim.3940 (cit. on pp. 12, 26, 29).

– (2012a). ‘Multivariate meta-analysis for non-linear and other multi-parameter associations’. In: *Statistics in Medicine* 31.29, pp. 3821–3839. DOI: 10.1002/sim.5471 (cit. on pp. 12, 26, 29).

Gasparrini, Antonio, Ben Armstrong, Sari Kovats and Paul Wilkinson (2012b). ‘The effect of high temperatures on cause-specific mortality in England and Wales’. In: *Occupational and Environmental Medicine* 69.1, pp. 56–61. DOI: 10.1136/oem.2010.059782 (cit. on p. 27).

Gasparrini, Antonio and Michela Leone (2014). ‘Attributable risk from distributed lag models’. In: *BMC Medical Research Methodology* 14.1, p. 55. DOI: 10.1186/1471-2288-14-55 (cit. on p. 29).

Gasparrini, Antonio et al. (2015). 'Mortality risk attributable to high and low ambient temperature: a multicountry observational study'. In: *The Lancet* 386.9991, pp. 369–375. DOI: 10.1016/S0140-6736(14)62114-0 (cit. on pp. 2, 3, 12, 27, 28, 30, 35, 38, 46, 71, 74, 76, 94).

Gasparrini, Antonio et al. (2017). 'Projections of temperature-related excess mortality under climate change scenarios'. In: *The Lancet Planetary Health* 1.9, e360–e367. DOI: 10.1016/S2542-5196(17)30156-0 (cit. on pp. 2, 3, 8, 26, 29, 30, 35, 36, 50, 61, 62, 73, 75–80).

Géoclimat (2018). *Records nationaux de température (mensuels et absolus) en 2017* (cit. on p. 19).

Glockmann, Manon, Yunfei Li, Tobia Lakes, Jürgen P Kropp and Diego Rybski (2021). 'Quantitative evidence for leapfrogging in urban growth'. In: *Environment and Planning B: Urban Analytics and City Science*, p. 239980832199871. DOI: 10.1177/2399808321998713 (cit. on p. 81).

Gosling, Simon N., David M. Hondula, Aditi Bunker, Dolores Ibarreta, Junguo Liu, Xinxin Zhang and Rainer Sauerborn (2017). 'Adaptation to Climate Change: A Comparative Analysis of Modeling Methods for Heat-Related Mortality'. In: *Environmental Health Perspectives* 125.8, p. 087008. DOI: 10.1289/EHP634 (cit. on pp. 2–4, 7, 8, 50, 62, 76, 78, 79).

Gosling, Simon N., Glenn R. McGregor and Jason A. Lowe (2009). 'Climate change and heat-related mortality in six cities Part 2: climate model evaluation and projected impacts from changes in the mean and variability of temperature with climate change'. In: *International Journal of Biometeorology* 53.1, pp. 31–51. DOI: 10.1007/s00484-008-0189-9 (cit. on p. 8).

Gosling, Simon N., Glenn R. McGregor and Anna Páldy (2007). 'Climate change and heat-related mortality in six cities Part 1: model construction and validation'. In: *International Journal of Biometeorology* 51.6, pp. 525–540. DOI: 10.1007/s00484-007-0092-9 (cit. on pp. 38, 94, 95).

Gouveia, Nelson, Shakoor Hajat and Ben Armstrong (2003). 'Socioeconomic differentials in the temperature–mortality relationship in São Paulo, Brazil'. In: *International Journal of Epidemiology* 32.3, pp. 390–397. DOI: 10.1093/ije/dyg077 (cit. on p. 94).

Guo, Yuming, Adrian G. Barnett and Shilu Tong (2013). 'Spatiotemporal model or time series model for assessing city-wide temperature effects on mortality?' In: *Environmental Research* 120, pp. 55–62. DOI: 10.1016/j.envres.2012.09.001 (cit. on pp. 97–99, 101).

Guo, Yuming et al. (2014). 'Global Variation in the Effects of Ambient Temperature on Mortality'. In: *Epidemiology* 25.6, pp. 781–789. DOI: 10.1097/EDE.0000000000000165 (cit. on pp. 38, 46, 76, 95).

Guo, Yuming et al. (2016). 'Temperature Variability and Mortality: A Multi-Country Study'. In: *Environmental Health Perspectives* 124.10, pp. 1554–1559. DOI: 10.1289/EHP149 (cit. on pp. 73, 75, 95, 99).

Guo, Yuming et al. (2018). 'Quantifying excess deaths related to heatwaves under climate change scenarios: A multicountry time series modelling study'. In: *PLOS Medicine* 15.7. Ed. by Jonathan Alan Patz, e1002629. DOI: 10.1371/journal.pmed.1002629 (cit. on pp. 3, 7, 50, 61).

Ha, Jongsik and Ho Kim (2013). 'Changes in the association between summer temperature and mortality in Seoul, South Korea'. In: *International Journal of Biometeorology* 57.4, pp. 535–544. DOI: 10.1007/s00484-012-0580-4 (cit. on pp. 94, 95, 99, 101).

Ha, Jongsik, Yongseong Shin and Ho Kim (2011). 'Distributed lag effects in the relationship between temperature and mortality in three major cities in South Korea'. In: *Science of The Total Environment* 409.18, pp. 3274–3280. DOI: 10.1016/j.scitotenv.2011.05.034 (cit. on p. 94).

Hajat, Shakoor and Tom Kosatky (2010). 'Heat-related mortality: a review and exploration of heterogeneity'. In: *Journal of Epidemiology & Community Health* 64.9, pp. 753–760. DOI: 10.1136/jech.2009.087999 (cit. on pp. 38, 39, 46, 95, 98, 99, 101).

Hajat, Shakoor, Sotiris Vardoulakis, Clare Heaviside and Bernd Eggen (2014). 'Climate change effects on human health: projections of temperature-related mortality for the UK during the 2020s, 2050s and 2080s'. In: *Journal of Epidemiology and Community Health* 68.7, pp. 641–648. DOI: 10.1136/jech-2013-202449 (cit. on p. 2).

Hales, Simon, Clare Salmond, G. Ian Town, Tord Kjellstrom and Alistair Woodward (2000). 'Daily mortality in relation to weather and air pollution in Christchurch, New Zealand'. In: *Australian and New Zealand Journal of Public Health* 24.1, pp. 89–91. DOI: 10.1111/j.1467-842X.2000.tb00731.x (cit. on p. 94).

Hanna, Elizabeth and Peter Tait (2015). 'Limitations to Thermoregulation and Acclimatization Challenge Human Adaptation to Global Warming'. In: *International Journal of Environmental Research and Public Health* 12.7, pp. 8034–8074. DOI: 10.3390/ijerph120708034 (cit. on pp. 7, 38).

Hanna, Joel M and Daniel E Brown (1983). 'Human Heat Tolerance: An Anthropological Perspective'. In: *Annual Review of Anthropology* 12, pp. 259–284 (cit. on p. 7).

Harlan, Sharon, Gerardo Chowell, Shuo Yang, Diana Petitti, Emmanuel Morales Butler, Benjamin Ruddell and Darren Ruddell (2014). 'Heat-Related Deaths in Hot Cities: Estimates of Human Tolerance to High Temperature Thresholds'. In: *International Journal of Environmental Research and Public Health* 11.3, pp. 3304–3326. DOI: 10.3390/ijerph110303304 (cit. on pp. 38, 46, 94, 95).

Haylock, M.R., N. Hofstra, A.M.G. Klein Tank, E.J. Klok, P. Jones and M. New (2008). 'A European daily high-resolution gridded data set of surface temperature and precipitation for 1950–2006'. In: *Journal of Geophysical Research* 113.D20, p. D20119. DOI: 10.1029/2008JD010201 (cit. on p. 96).

Health Authority Abu Dhabi (2011). *Health Authority Abu Dhabi. Occupational and Environmental Health Section & The Safety in the Heat Programme*. Abu Dhabi, Vereinigte Arabische Emirate (cit. on p. 22).

Heo, Seulkee, Eunil Lee, Bo Yeon Kwon, Suji Lee, Kyung Hee Jo and Jinsun Kim (2016). 'Long-term changes in the heat–mortality relationship according to heterogeneous regional climate: a time-series study in South Korea'. In: *BMJ Open* 6.8, e011786. DOI: 10.1136/bmjopen-2016-011786 (cit. on p. 46).

Honda, Yasushi, Masahide Kondo, Glenn McGregor, Ho Kim, Yue-Leon Guo, Yasuaki Hijioka, Minoru Yoshikawa, Kazutaka Oka, Saneyuki Takano, Simon Hales and R. Sari Kovats (2014). 'Heat-related mortality risk model for climate change impact projection'. In: *Environmental Health and Preventive Medicine* 19.1, pp. 56–63. DOI: 10.1007/s12199-013-0354-6 (cit. on p. 8).

Huang, Cunrui, Adrian G. Barnett, Xiaoming Wang and Shilu Tong (2012). 'The impact of temperature on years of life lost in Brisbane, Australia'. In: *Nature Climate Change* 2.4, pp. 265–270. DOI: 10.1038/nclimate1369 (cit. on p. 7).

Huang, Cunrui, Adrian G. Barnett, Xiaoming Wang, Pavla Vaneckova, Gerard FitzGerald and Shilu Tong (2011). 'Projecting Future Heat-Related Mortality under Climate Change Scenarios: A Systematic Review'. In: *Environmental Health Perspectives* 119.12, pp. 1681–1690. DOI: 10.1289/ehp.1103456 (cit. on pp. 2, 26).

Huang, Jixia, Jing Tan and Weiwei Yu (2017). 'Temperature and Cardiovascular Mortality Associations in Four Southern Chinese Cities: A Time-Series Study Using a Distributed Lag Non-Linear Model'. In: *Sustainability* 9.3, p. 321. DOI: 10.3390/su9030321 (cit. on p. 94).

Huber, Veronika, Linda Krummenauer, Cristina Peña-Ortiz, Stefan Lange, Antonio Gasparrini, Ana M. Vicedo-Cabrera, Ricardo Garcia-Herrera and Katja Frieler (2020). 'Temperature-related excess mortality in German cities at 2 °C and higher degrees of global warming'. In: *Environmental Research* 186.March. DOI: 10.1016/j.envres.2020.109447 (cit. on p. 80).

Hübler, Michael, Gernot Klepper and Sonja Peterson (2008). 'Costs of climate change'. In: *Ecological Economics* 68.1-2, pp. 381–393. DOI: 10.1016/j.ecolecon.2008.04.010 (cit. on pp. 26, 35).

Ibrahim, Iman (2016). 'Livable Eco-Architecture Masdar City, Arabian Sustainable City'. In: *Procedia - Social and Behavioral Sciences* 216.October 2015, pp. 46–55. DOI: 10.1016/j.sbspro.2015.12.070 (cit. on p. 18).

Independent (2017). *Temperatures in Iranian city of Ahvaz hit 129.2F (54C), near hottest on Earth in modern measurements* (cit. on p. 18).

Iñiguez, Carmen, Ferran Ballester, Juan Ferrandiz, Santiago Pérez-Hoyos, Marc Sáez and Antonio López (2010). 'Relation between Temperature and Mortality in Thirteen Spanish Cities'. In: *International Journal of Environmental Research and Public Health* 7.8, pp. 3196–3210. DOI: 10.3390/ijerph7083196 (cit. on pp. 2, 38, 46, 94, 95, 99, 101).

Jarvis, A., H.I. Reuter, A. Nelson and E. Guevara (2008). *Hole-filled SRTM for the globe Version 4. available from the CGIAR-CSI SRTM 90m Database* (cit. on pp. 64, 96, 98, 99).

Johansson, Erik and Rohinton Emmanuel (2006). 'The influence of urban design on outdoor thermal comfort in the hot, humid city of Colombo, Sri Lanka'. In: *International Journal of Biometeorology* 51.2, pp. 119–133. DOI: 10.1007/s00484-006-0047-6 (cit. on pp. 95, 99).

Johnson, Daniel P., Jeffrey S. Wilson and George C. Luber (2009). 'Socioeconomic indicators of heat-related health risk supplemented with remotely sensed data'. In: *International Journal of Health Geographics* 8.1, p. 57. DOI: 10.1186/1476-072X-8-57 (cit. on p. 6).

Jones, B. and B. C. O'Neill (2016). 'Spatially explicit global population scenarios consistent with the Shared Socioeconomic Pathways'. In: *Environmental Research Letters* 11.8, p. 084003. DOI: 10.1088/1748-9326/11/8/084003 (cit. on p. 81).

Kamal, Mohammad Arif (2014). 'The morphology of traditional architecture of Jeddah: Climatic design and environmental sustainability'. In: *Global Built Environment Review* 9.1, pp. 4–26 (cit. on p. 18).

Kan, Haidong, Jian Jia and Bing-Heng Chen (2003). 'Temperature and daily mortality in Shanghai: a time-series study.' In: *Biomedical and environmental sciences : BES* 16.2, pp. 133–9. DOI: na (cit. on p. 94).

Kark, Ruth and Seth J. Frantzman (2012). 'Empire, State and the Bedouin of the Middle East, Past and Present: A Comparative Study of Land and Settlement Policies'. In: *Middle Eastern Studies* 48.4, pp. 487–510. DOI: 10.1080/00263206.2012.682303 (cit. on p. 17).

Karlsson, Martin and Nicolas R Ziebarth (2018). 'Population health effects and health-related costs of extreme temperatures: Comprehensive evidence from Germany'. In: *Journal of Environmental Economics and Management* 91, pp. 93–117. DOI: 10.1016/j.jeem.2018.06.004 (cit. on pp. 7, 26, 35).

Kelley, Colin P., Shahrzad Mohtadi, Mark A. Cane, Richard Seager and Yochanan Kushnir (2015). 'Climate change in the Fertile Crescent and implications of the recent Syrian drought'. In: *Proceedings of the National Academy of Sciences* 112.11, pp. 3241–3246. DOI: 10.1073/pnas.1421533112 (cit. on pp. 17, 19).

Kendrovski, Vladimir, Michela Baccini, Gerardo Martinez, Tanja Wolf, Elizabet Paunovic and Bettina Menne (2017). 'Quantifying Projected Heat Mortality Impacts under 21st-Century Warming Conditions for Selected European Countries'. In: *International Journal of Environmental Research and Public Health* 14.7, p. 729. DOI: 10.3390/ijerph14070729 (cit. on p. 26).

Khalaf, Roha W. (2012). 'Traditional vs modern Arabian morphologies'. In: *Journal of Cultural Heritage Management and Sustainable Development* 2.1, pp. 27–43. DOI: 10.1108/20441261211223252 (cit. on pp. 17, 18).

Kim, E-Jin and Ho Kim (2017). 'Effect modification of individual- and regional-scale characteristics on heat wave-related mortality rates between 2009 and 2012 in Seoul, South Korea'. In: *Science of The Total Environment* 595, pp. 141–148. DOI: 10.1016/j.scitotenv.2017.03.248 (cit. on pp. 46, 95, 101).

Kim, Ho, Jongsik Ha and Jeongim Park (2006). 'High Temperature, Heat Index, and Mortality in 6 Major Cities in South Korea'. In: *Archives of Environmental & Occupational Health* 61.6, pp. 265–270. DOI: 10.3200/AEOH.61.6.265-270 (cit. on pp. 94, 95).

Kim, Young-Min, Soyeon Kim, Hae-Kwan Cheong and Eun-Hye Kim (2011). 'Comparison of Temperature Indexes for the Impact Assessment of Heat Stress on Heat-Related Mortality'. In: *Environmental Health and Toxicology* 26, e2011009. DOI: 10.5620/eht.2011.26.e2011009 (cit. on pp. 94, 99).

Kinney, Patrick L., Joel Schwartz, Mathilde Pascal, Elisaveta Petkova, Alain Le Tertre, Sylvia Medina and Robert Vautard (2015). 'Winter season mortality: will climate warming bring benefits?' In: *Environmental Research Letters* 10.6, p. 064016. DOI: 10.1088/1748-9326/10/6/064016 (cit. on p. 26).

Klenk, J., C. Becker and K. Rapp (2010). 'Heat-related mortality in residents of nursing homes'. In: *Age and Ageing* 39.2, pp. 245–252. DOI: 10.1093/ageing/afp248 (cit. on p. 7).

Kornhuber, Kai, Scott Osprey, Dim Coumou, Stefan Petri, Vladimir Petoukhov, Stefan Rahmstorf and Lesley Gray (2019). 'Extreme weather events in early summer 2018 connected by a recurrent hemispheric wave-7 pattern'. In: *Environmental Research Letters* 14.5, p. 054002. DOI: 10.1088/1748-9326/ab13bf (cit. on p. 1).

Krummenauer, Linda, Boris F. Prahl, Luís Costa, Anne Holsten, Carsten Walther and Jürgen P. Kropp (2019). 'Global drivers of minimum mortality temperatures in cities'. In: *Science of The Total Environment* 695, p. 133560. DOI: 10.1016/j.scitotenv.2019.07.366 (cit. on pp. 22, 50, 64, 65, 139).

Lange, Stefan (2017). *ISIMIP2b Bias-Correction Code*. Potsdam. DOI: 10.5281/zenodo.1069050 (cit. on p. 27).

Laschewski, G. and G. Jendritzky (2002). 'Effects of the thermal environment on human health: an investigation of 30 years of daily mortality data from SW Germany'. In: *Climate Research* 21.1, pp. 91–103. DOI: 10.3354/cr021091 (cit. on p. 26).

Lawrence, Mark G. (2005). 'The Relationship between Relative Humidity and the Dewpoint Temperature in Moist Air: A Simple Conversion and Applications'. In: *Bulletin of the American Meteorological Society* 86.2, pp. 225–234. DOI: 10.1175/BAMS-86-2-225 (cit. on p. 63).

Lee, Jae, Woo-Seop Lee, Kristie Ebi and Ho Kim (2019). 'Temperature-Related Summer Mortality Under Multiple Climate, Population, and Adaptation Scenarios'. In: *International Journal of Environmental Research and Public Health* 16.6, p. 1026. DOI: 10.3390/ijerph16061026 (cit. on p. 35).

Lee, Whanhee et al. (2020). 'Projections of excess mortality related to diurnal temperature range under climate change scenarios: a multi-country modelling study'. In: *The Lancet Planetary Health* 4.11, e512–e521. DOI: 10.1016/S2542-5196(20)30222-9 (cit. on pp. 2, 79, 80).

Lelieveld, J., P. Hadjinicolaou, E. Kostopoulou, C. Giannakopoulos, A. Pozzer, M. Tanarhte and E. Tyrlis (2014). 'Model projected heat extremes and air pollution in the eastern Mediterranean and Middle East in the twenty-first century'. In: *Regional Environmental Change* 14.5, pp. 1937–1949. DOI: 10.1007/s10113-013-0444-4 (cit. on p. 19).

Lelieveld, J., Y. Proestos, P. Hadjinicolaou, M. Tanarhte, E. Tyrlis and G. Zittis (2016). 'Strongly increasing heat extremes in the Middle East and North Africa (MENA) in the 21st century'. In: *Climatic Change* 137.1-2, pp. 245–260. DOI: 10.1007/s10584-016-1665-6 (cit. on p. 20).

Lenzholzer, Sanda, Gerrit Jan Carsjens, Robert D. Brown, Silvia Tavares, Jennifer Vanos, You Joung Kim and Kanghyun Lee (2020). 'Awareness of urban climate adaptation strategies –an international overview'. In: *Urban Climate* 34.November, p. 100705. DOI: 10.1016/j.uclim.2020.100705 (cit. on pp. 4, 6).

Leone, Michela, Daniela D'Ippoliti, Manuela De Sario, Antonis Analitis, Bettina Menne, Klea Katsouyanni, Francesca K. de'Donato, Xavier Basagana, Afif Ben Salah, Elsa Casimiro, Zeynep Dörtbudak, Carmen Iñiguez, Chava Peretz, Tanja Wolf and Paola Michelozzi (2013). 'A time series study on the effects of heat on mortality and evaluation of heterogeneity into European and Eastern-Southern Mediterranean cities: results of EU CIRCE project'. In: *Environmental Health* 12.1, p. 55. DOI: 10.1186/1476-069X-12-55 (cit. on pp. 94, 95, 99, 101).

Li, Dan, Weilin Liao, Angela J. Rigden, Xiaoping Liu, Dagang Wang, Sergey Malyshev and Elena Shevliakova (2019). 'Urban heat island: Aerodynamics or imperviousness?' In: *Science Advances* 5.4, eaau4299. DOI: 10.1126/sciadv.aau4299 (cit. on p. 5).

Li, Tiantian, Radley M. Horton and Patrick L. Kinney (2013). 'Projections of seasonal patterns in temperature- related deaths for Manhattan, New York'. In: *Nature Climate Change* 3.8, pp. 717–721. DOI: 10.1038/nclimate1902 (cit. on p. 26).

Li, Yixue, Guoxing Li, Qiang Zeng, Fengchao Liang and Xiaochuan Pan (2018). 'Projecting temperature-related years of life lost under different climate change scenarios in one temperate megacity, China'. In: *Environmental Pollution* 233, pp. 1068–1075. DOI: 10.1016/j.envpol.2017.10.008 (cit. on p. 26).

Li, Yonghong, Yibin Cheng, Guoquan Cui, Chaoqiong Peng, Yan Xu, Yulin Wang, Yingchun Liu, Jingyi Liu, Chengcheng Li, Zhen Wu, Peng Bi and Yinlong Jin (2014). 'Association between high temperature and mortality in metropolitan areas of four cities in various climatic zones in China: a time-series study'. In: *Environmental Health* 13.1, p. 65. DOI: 10.1186/1476-069X-13-65 (cit. on p. 94).

Li, Yunfei, Sebastian Schubert, Jürgen P. Kropp and Diego Rybski (2020). 'On the influence of density and morphology on the Urban Heat Island intensity'. In: *Nature Communications* 11.1, p. 2647. DOI: 10.1038/s41467-020-16461-9 (cit. on p. 81).

Liu, Cuiqing, Zubin Yavar and Qinghua Sun (2015). 'Cardiovascular response to thermoregulatory challenges'. In: *American Journal of Physiology-Heart and Circulatory Physiology* 309.11, H1793–H1812. DOI: 10.1152/ajpheart.00199.2015 (cit. on p. 46).

Liu, Jing, Fei Ma and Ying Li (2011). 'The Effect of Anthropogenic Heat on Local Heat Island Intensity and the Performance of Air Conditioning Systems'. In: *Advanced Materials Research* 250-253, pp. 2975–2978. DOI: 10.4028/www.scientific.net/AMR.250-253.2975 (cit. on p. 5).

Liu, Tao and Wenjun Ma (2019). 'Climate change and health: more research on adaptation is needed'. In: *The Lancet Planetary Health* 3.7, e281–e282. DOI: 10.1016/S2542-5196(19)30112-3 (cit. on pp. 4, 50, 76, 80).

Liu, Zhao, Bruce Anderson, Kai Yan, Weihua Dong, Hua Liao and Peijun Shi (2017). 'Global and regional changes in exposure to extreme heat and the relative contributions of climate and population change'. In: *Scientific Reports* 7.1, p. 43909. DOI: 10.1038/srep43909 (cit. on p. 50).

Lo, Y. T. Eunice, Daniel M. Mitchell, Antonio Gasparrini, Ana M. Vicedo-Cabrera, Kristie L. Ebi, Peter C. Frumhoff, Richard J. Millar, William Roberts, Francesco Sera, Sarah Sparrow, Peter Uhe and Gethin Williams (2019). 'Increasing mitigation ambition to meet the Paris Agreement's temperature goal avoids substantial heat-related mortality in U.S. cities'. In: *Science Advances* 5.6, eaau4373. DOI: 10.1126/sciadv.aau4373 (cit. on p. 26).

London School of Hygiene and Tropical Medicine (2021). *MCC Collaborative Research Network* (cit. on p. 3).

López-Bueno, J. A., J. Díaz, F. Follos, J.M. Vellón, M.A. Navas, D. Culqui, M.Y. Luna, G. Sánchez-Martínez and C. Linares (2021). 'Evolution of the threshold temperature definition of a heat wave vs. evolution of the minimum mortality temperature: a case study in Spain during the 1983–2018 period'. In: *Environmental Sciences Europe* 33.1, p. 101. DOI: 10.1186/s12302-021-00542-7 (cit. on pp. 3, 4, 50).

Lowe, Rachel, Joan Ballester, James Creswick, Jean-Marie Robine, François Herrmann and Xavier Rodó (2015). ‘Evaluating the Performance of a Climate-Driven Mortality Model during Heat Waves and Cold Spells in Europe’. In: *International Journal of Environmental Research and Public Health* 12.2, pp. 1279–1294. DOI: 10.3390/ijerph120201279 (cit. on pp. 43, 47).

Lu, Yun and Scott L. Zeger (2007). ‘On the equivalence of case-crossover and time series methods in environmental epidemiology’. In: *Biostatistics* 8.2, pp. 337–344. DOI: 10.1093/biostatistics/kxl013 (cit. on p. 39).

Luber, George and Michael McGeehin (2008). ‘Climate Change and Extreme Heat Events’. In: *American Journal of Preventive Medicine* 35.5, pp. 429–435. DOI: 10.1016/j.amepre.2008.08.021 (cit. on p. 6).

Martin, Sara Lauretta, Sabit Cakmak, Christopher Alan Hebbern, Mary-Luyza Avramescu and Neil Tremblay (2012). ‘Climate change and future temperature-related mortality in 15 Canadian cities’. In: *International Journal of Biometeorology* 56.4, pp. 605–619. DOI: 10.1007/s00484-011-0449-y (cit. on pp. 26, 43, 94).

Martinez, Gerardo Sanchez, Julio Diaz, Hans Hooyberghs, Dirk Lauwaet, Koen De Ridder, Cristina Linares, Rocio Carmona, Cristina Ortiz, Vladimir Kendrovski and Dovile Adamonyte (2018). ‘Cold-related mortality vs heat-related mortality in a changing climate: A case study in Vilnius (Lithuania)’. In: *Environmental Research* 166, pp. 384–393. DOI: 10.1016/j.envres.2018.06.001 (cit. on p. 26).

Masson-Delmotte, V. et al. (2021). *Climate Change 2021: The Physical Science Basis. Contribution of Working Group I to the Sixth Assessment Report of the Intergovernmental Panel on Climate Change*. Tech. rep. Cambridge: Cambridge University Press (cit. on pp. 1, 80).

McMichael, Anthony J et al. (2008). ‘International study of temperature, heat and urban mortality: the ‘ISOTHURM’ project’. In: *International Journal of Epidemiology* 37.5, pp. 1121–1131. DOI: 10.1093/ije/dyn086 (cit. on pp. 2, 38, 94, 95).

Medina-Ramon, M and J Schwartz (2007). ‘Temperature, temperature extremes, and mortality: a study of acclimatisation and effect modification in 50 US cities’. In: *Occupational and Environmental Medicine* 64.12, pp. 827–833. DOI: 10.1136/oem.2007.033175 (cit. on pp. 38, 46, 95, 98, 99, 101).

Meehl, Gerald A. (2004). ‘More Intense, More Frequent, and Longer Lasting Heat Waves in the 21st Century’. In: *Science* 305.5686, pp. 994–997. DOI: 10.1126/science.1098704 (cit. on pp. 1, 50).

Meng, Xia et al. (2021). ‘Short term associations of ambient nitrogen dioxide with daily total, cardiovascular, and respiratory mortality: multilocation analysis in 398 cities’. In: *BMJ* 39, n534. DOI: 10.1136/bmj.n534 (cit. on p. 72).

Mercereau, Luc, Nicolas Todd, Gregoire Rey and Alain-jacques Valleron (2017). ‘Comparison of the temperature-mortality relationship in foreign born and native born died in France between 2000 and 2009’. In: *International Journal of Biometeorology* 61.10, pp. 1873–1884. DOI: 10.1007/s00484-017-1373-6 (cit. on p. 7).

Michelozzi, Paola, Ursula Kirchmayer, Klea Katsouyanni, Annibale Biggeri, Glenn McGregor, Bettina Menne, Pavlos Kassomenos, Hugh Ross Anderson, Michela Baccini, Gabriele Accetta, Antonis Analytis and Tom Kosatsky (2007). 'Assessment and prevention of acute health effects of weather conditions in Europe, the PHEWE project: background, objectives, design'. In: *Environmental Health* 6.1, p. 12. DOI: 10.1186/1476-069X-6-12 (cit. on pp. 39, 46, 64, 95).

Milner, James, Colin Harpham, Jonathon Taylor, Mike Davies, Corinne Le Quéré, Andy Haines and Paul Wilkinson (2017). 'The Challenge of Urban Heat Exposure under Climate Change: An Analysis of Cities in the Sustainable Healthy Urban Environments (SHUE) Database'. In: *Climate* 5.4, p. 93. DOI: 10.3390/cli5040093 (cit. on p. 79).

Mishra, Vimal, Auroop R. Ganguly, Bart Nijssen and Dennis P. Lettenmaier (2015). 'Changes in observed climate extremes in global urban areas'. In: *Environmental Research Letters* 10.2, p. 024005. DOI: 10.1088/1748-9326/10/2/024005 (cit. on p. 50).

Mitchell, Daniel, Clare Heaviside, Nathalie Schaller, Myles Allen, Kristie L. Ebi, Erich M. Fischer, Antonio Gasparrini, Luke Harrington, Viatcheslav Kharin, Hideo Shiogama, Jana Sillmann, Sebastian Sippel and Sotiris Vardoulakis (2018). 'Extreme heat-related mortality avoided under Paris Agreement goals'. In: *Nature Climate Change* 8.7, pp. 551–553. DOI: 10.1038/s41558-018-0210-1 (cit. on p. 26).

Montero, J.C., I.J. Mirón, J.J. Criado-Álvarez, C Linares and J Díaz (2012). 'Influence of local factors in the relationship between mortality and heat waves: Castile-La Mancha (1975–2003)'. In: *Science of The Total Environment* 414.2012, pp. 73–80. DOI: 10.1016/j.scitotenv.2011.10.009 (cit. on p. 94).

Mora, Camilo, Chelsie W.W. Counsell, Coral R. Bielecki and Leo V. Louis (2017a). 'Twenty-Seven Ways a Heat Wave Can Kill You:' in: *Circulation: Cardiovascular Quality and Outcomes* 10.11. DOI: 10.1161/CIRCOUTCOMES.117.004233 (cit. on p. 73).

Mora, Camilo et al. (2017b). 'Global risk of deadly heat'. In: *Nature Climate Change* 7.7, pp. 501–506. DOI: 10.1038/nclimate3322 (cit. on p. 50).

Muthers, Stefan, Gudrun Laschewski and Andreas Matzarakis (2017). 'The Summers 2003 and 2015 in South-West Germany: Heat Waves and Heat-Related Mortality in the Context of Climate Change'. In: *Atmosphere* 8.12, p. 224. DOI: 10.3390/atmos8110224 (cit. on p. 26).

Ng, Chris Fook Sheng, Melanie Boeckmann, Kayo Ueda, Hajo Zeeb, Hiroshi Nitta, Chiho Watanabe and Yasushi Honda (2016). 'Heat-related mortality: Effect modification and adaptation in Japan from 1972 to 2010'. In: *Global Environmental Change* 39, pp. 234–243. DOI: 10.1016/j.gloenvcha.2016.05.006 (cit. on pp. 8, 95, 99, 101).

Ng, Edward (2012). 'Towards planning and practical understanding of the need for meteorological and climatic information in the design of high-density cities: A case-based study of Hong Kong'. In: *International Journal of Climatology* 32.4, pp. 582–598. DOI: 10.1002/joc.2292 (cit. on pp. 95, 99, 101).

NOAA National Climatic Data Center (2018). *Global Summary of the Day (GSOD)* (cit. on pp. 18, 19, 96, 97, 99).

Nunez, M. and T. R. Oke (1977). 'The Energy Balance of an Urban Canyon'. In: *Journal of Applied Meteorology* 16.1, pp. 11–19. DOI: 10.1175/1520-0450(1977)016<0011:TEBOAU>2.0.CO;2 (cit. on p. 5).

Odhiambo Sewe, Maquins, Aditi Bunker, Vijendra Ingole, Thaddaeus Egondi, Daniel Oudin Åström, David M. Hondula, Joacim Rocklöv and Barbara Schumann (2018). 'Estimated Effect of Temperature on Years of Life Lost: A Retrospective Time-Series Study of Low-, Middle-, and High-Income Regions'. In: *Environmental Health Perspectives* 126.1, p. 017004. DOI: 10.1289/EHP1745 (cit. on p. 7).

Oke, T.R. (1973). 'City size and the urban heat island'. In: *Atmospheric Environment (1967)* 7.8, pp. 769–779. DOI: 10.1016/0004-6981(73)90140-6 (cit. on pp. 1, 5, 95).

O'Neill, Brian C., Elmar Kriegler, Keywan Riahi, Kristie L. Ebi, Stephane Hallegatte, Timothy R. Carter, Ritu Mathur and Detlef P. van Vuuren (2014). 'A new scenario framework for climate change research: the concept of shared socioeconomic pathways'. In: *Climatic Change* 122.3, pp. 387–400. DOI: 10.1007/s10584-013-0905-2 (cit. on p. 51).

Ostberg, Sebastian, Jacob Schewe, Katelin Childers and Katja Frieler (2018). 'Changes in crop yields and their variability at different levels of global warming'. In: *Earth System Dynamics* 9.2, pp. 479–496. DOI: 10.5194/esd-9-479-2018 (cit. on p. 26).

Pal, Jeremy S. and Elfatih A.B. Eltahir (2016). 'Future temperature in southwest Asia projected to exceed a threshold for human adaptability'. In: *Nature Climate Change* 6.2, pp. 197–200. DOI: 10.1038/nclimate2833 (cit. on pp. 21, 22, 50, 61, 79).

Peng, Roger D., Jennifer F. Bobb, Claudia Tebaldi, Larry McDaniel, Michelle L. Bell and Francesca Dominici (2011). 'Toward a Quantitative Estimate of Future Heat Wave Mortality under Global Climate Change'. In: *Environmental Health Perspectives* 119.5, pp. 701–706. DOI: 10.1289/ehp.1002430 (cit. on pp. 1, 2).

Peretz, Chava, Annibale Biggeri, P. Alpert and Michaela Baccini (2012). 'The Effect of Heat Stress on Daily Mortality in Tel Aviv, Israel'. In: *National Security and Human Health Implications of Climate Change*. Ed. by H. J. S. Fernando, Z. Klaić and J.L. McCulley. NATO Science for Peace and Security Series C: Environmental Security. Dordrecht: Springer Netherlands, pp. 241–251. DOI: 10.1007/978-94-007-2430-3_20 (cit. on pp. 94, 95, 99).

Petkova, E. P., H. Morita and P. L. Kinney (2014). 'Health Impacts of Heat in a Changing Climate: How Can Emerging Science Inform Urban Adaptation Planning?' In: *Current Epidemiology Reports* 1.2, pp. 67–74. DOI: 10.1007/s40471-014-0009-1 (cit. on pp. 3, 7, 8, 76, 78).

Phung, Dung, Yuming Guo, Huong T.L. Nguyen, Shannon Rutherford, Scott Baum and Cordia Chu (2016). 'High temperature and risk of hospitalizations, and effect modifying potential of socio-economic conditions: A multi-province study in the tropical Mekong Delta Region'. In: *Environment International* 92-93.April, pp. 77–86. DOI: 10.1016/j.envint.2016.03.034 (cit. on pp. 95, 99, 101).

Qiao, Zhen, Yuming Guo, Weiwei Yu and Shilu Tong (2015). 'Assessment of Short- and Long-Term Mortality Displacement in Heat-Related Deaths in Brisbane, Australia, 1996–2004'. In: *Environmental Health Perspectives* 123.8, pp. 766–772. DOI: 10.1289/ehp.1307606 (cit. on p. 94).

Rai, Masna, Susanne Breitner, Kathrin Wolf, Annette Peters, Alexandra Schneider and Kai Chen (2019). 'Impact of climate and population change on temperature-related mortality burden in Bavaria, Germany'. In: *Environmental Research Letters* 14.12, p. 124080. DOI: 10.1088/1748-9326/ab5ca6 (cit. on pp. 3, 7, 26, 35, 72).

Raymond, Colin, Tom Matthews and Radley M. Horton (2020). 'The emergence of heat and humidity too severe for human tolerance'. In: *Science Advances* 6.19, eaaw1838. DOI: 10.1126/sciadv.aaw1838 (cit. on p. 61).

Reckien, Diana, Johannes Flacke, Marta Olazabal and Oliver Heidrich (2015). 'The Influence of Drivers and Barriers on Urban Adaptation and Mitigation Plans—An Empirical Analysis of European Cities'. In: *PLOS ONE* 10.8. Ed. by Kristie L Ebi, e0135597. DOI: 10.1371/journal.pone.0135597 (cit. on p. 102).

Research Data Centres of the Federation and the Federal States of Germany (2020). *Website Research Data Centres of the Federation and the Federal States of Germany* (cit. on p. 72).

Revich, Boris and Dmitri Shaposhnikov (2008). 'Temperature-induced excess mortality in Moscow, Russia'. In: *International Journal of Biometeorology* 52.5, pp. 367–374. DOI: 10.1007/s00484-007-0131-6 (cit. on p. 94).

Riahi, Keywan et al. (2017). 'The Shared Socioeconomic Pathways and their energy, land use, and greenhouse gas emissions implications: An overview'. In: *Global Environmental Change* 42, pp. 153–168. DOI: 10.1016/j.gloenvcha.2016.05.009 (cit. on pp. 51, 52, 54, 65, 81).

Robert Koch Institut (2021). *Hinweise zur Erfassung und Veröffentlichung von COVID-19-Fallzahlen* (cit. on p. 73).

Rohat, Guillaume, Olga Wilhelmi, Johannes Flacke, Andrew Monaghan, Jing Gao, Hy Dao and Martin van Maarseveen (2019). 'Characterizing the role of socioeconomic pathways in shaping future urban heat-related challenges'. In: *Science of The Total Environment* 695.August, p. 133941. DOI: 10.1016/j.scitotenv.2019.133941 (cit. on p. 61).

Romero-Lankao, Patricia and Daniel Gnatz (2019). 'Risk Inequality and the Food-Energy-Water (FEW) Nexus : A Study of 43 City Adaptation Plans'. In: *Frontiers in Sociology* 4.April, pp. 1–14. DOI: 10.3389/fsoc.2019.00031 (cit. on p. 102).

Rozell, Daniel (2017). 'Using population projections in climate change analysis'. In: *Climatic Change* 142.3-4, pp. 521–529. DOI: 10.1007/s10584-017-1968-2 (cit. on p. 81).

Sailor, D. J., T. B. Elley and M. Gibson (2011). 'Exploring the building energy impacts of green roof design decisions - a modeling study of buildings in four distinct climates'. In: *Journal of Building Physics* 35.4, pp. 372–391. DOI: 10.1177/1744259111420076 (cit. on p. 5).

Sailor, David J. and Lu Lu (2004). 'A top–down methodology for developing diurnal and seasonal anthropogenic heating profiles for urban areas'. In: *Atmospheric Environment* 38.17, pp. 2737–2748. DOI: 10.1016/j.atmosenv.2004.01.034 (cit. on p. 5).

Salama, Ashraf M. (2015). 'Urban Traditions in the Contemporary Lived Space of Cities on the Arabian Peninsula'. In: *International Association for the Study of Traditional Environments (IASTE)* 27.1, pp. 20–39 (cit. on p. 17).

Samad, Ziad Abdul (2008). *Millennium Development Goals. Lebanon Report 2008*. Tech. rep., p. 70 (cit. on pp. 97, 99).

Sanderson, Michael, Katherine G. Arbuthnott, Sari Kovats, Shakoor Hajat and Pete Falloon (2017). 'The use of climate information to estimate future mortality from high ambient temperature: A systematic literature review'. In: *PLOS ONE* 12.7. Ed. by Juan A. Añel, e0180369. DOI: 10.1371/journal.pone.0180369 (cit. on p. 26).

Sarath Chandran, M. A., A. V. M. Subba Rao, V. M. Sandeep, V. P. Pramod, P. Pani, V. U. M. Rao, V. Visha Kumari and Ch Srinivasa Rao (2017). 'Indian summer heat wave of 2015: a biometeorological analysis using half hourly automatic weather station data with special reference to Andhra Pradesh'. In: *International Journal of Biometeorology* 61.6, pp. 1063–1072. DOI: 10.1007/s00484-016-1286-9 (cit. on p. 1).

Schaeffer, Laura, Perrine de Crouy-Chanel, Vérène Wagner, Julien Desplat and Mathilde Pascal (2016). 'How to estimate exposure when studying the temperature-mortality relationship? A case study of the Paris area'. In: *International Journal of Biometeorology* 60.1, pp. 73–83. DOI: 10.1007/s00484-015-1006-x (cit. on p. 27).

Schleussner, Carl-Friedrich, Tabea K. Lissner, Erich M. Fischer, Jan Wohland, Mahé Perrette, Antonius Golly, Joeri Rogelj, Katelin Childers, Jacob Schewe, Katja Frieler, Matthias Mengel, William Hare and Michiel Schaeffer (2016). 'Differential climate impacts for policy-relevant limits to global warming: the case of 1.5 °C and 2 °C'. In: *Earth System Dynamics* 7.2, pp. 327–351. DOI: 10.5194/esd-7-327-2016 (cit. on p. 28).

Schwartz, Joel D, Mihye Lee, Patrick L Kinney, Suijia Yang, David Mills, Marcus C Sarofim, Russell Jones, Richard Streeter, Alexis St Juliana, Jennifer Peers and Radley M Horton (2015). 'Projections of temperature-attributable premature deaths in 209 U.S. cities using a cluster-based Poisson approach'. In: *Environmental Health* 14.1, p. 85. DOI: 10.1186/s12940-015-0071-2 (cit. on p. 26).

Semenza, Jan C., Carol H Rubin, Kenneth H. Falter, Joel D. Selanikio, W. Dana Flanders, Holly L. Howe and John L. Wilhelm (1996). 'Heat-Related Deaths during the July 1995 Heat Wave in Chicago'. In: *New England Journal of Medicine* 335.2, pp. 84–90. DOI: 10.1056/NEJM199607113350203 (cit. on p. 1).

Seposo, Xerxes T., Tran Ngoc Dang and Yasushi Honda (2016). 'Effect modification in the temperature extremes by mortality subgroups among the tropical cities of the Philippines'. In: *Global Health Action* 9.1, p. 31500. DOI: 10.3402/gha.v9.31500 (cit. on pp. 38, 94).

Sera, Francesco et al. (2019). 'How urban characteristics affect vulnerability to heat and cold: a multi-country analysis'. In: *International Journal of Epidemiology* 48.4, pp. 1101–1112. DOI: 10.1093/ije/dyz008 (cit. on p. 36).

Sherwood, Steven C. and Matthew Huber (2010). 'An adaptability limit to climate change due to heat stress'. In: *Proceedings of the National Academy of Sciences* 107.21, pp. 9552–9555. DOI: 10.1073/pnas.0913352107 (cit. on pp. 21, 22, 38, 39, 47).

Siebert, Hendrik, Helmut Uphoff and Henny Annette Grewe (2019). 'Monitoring hitzebedingter Sterblichkeit in Hessen'. In: *Bundesgesundheitsblatt - Gesundheitsforschung - Gesundheitsschutz* 62.5, pp. 580–588. DOI: 10.1007/s00103-019-02941-x (cit. on p. 73).

Song, Xuping, Shigong Wang, Yuling Hu, Man Yue, Tingting Zhang, Yu Liu, Jinhui Tian and Kezheng Shang (2017). 'Impact of ambient temperature on morbidity and mortality: An overview of reviews'. In: *Science of The Total Environment* 586, pp. 241–254. DOI: 10.1016/j.scitotenv.2017.01.212 (cit. on pp. 95, 99, 101).

Steadman, Robert G. (1984). 'A Universal Scale of Apparent Temperature'. In: *Journal of Climate and Applied Meteorology* 23.12, pp. 1674–1687. DOI: 10.1175/1520-0450(1984)023<1674:AUSOAT>2.0.CO;2 (cit. on pp. 39, 64).

Steul, Katrin, Hans-Georg Jung and Ursel Heudorf (2019). ‘Hitzeassoziierte Morbidität: Surveillance in Echtzeit mittels rettungsdienstlicher Daten aus dem Interdisziplinären Versorgungsnachweis (IVENA)’. In: *Bundesgesundheitsblatt - Gesundheitsforschung - Gesundheitsschutz* 62.5, pp. 589–598. DOI: 10.1007/s00103-019-02938-6 (cit. on p. 74).

Stewart, Ronald E., Daniel Betancourt, James B. Davies, Deborah Harford, Yaheli Klein, Robert Lannigan, Linda Mortsch, Erin O’Connell, Kathy Tang and Paul H. Whitfield (2017). ‘A multi-perspective examination of heat waves affecting Metro Vancouver: now into the future’. In: *Natural Hazards* 87.2, pp. 791–815. DOI: 10.1007/s11069-017-2793-7 (cit. on pp. 95, 99, 101).

Sun, Jing, Guo Xing Li, Rohan Jayasinghe, Ross Sadler, Glen Shaw and Xiao Chuan Pan (2012). ‘Time Course of Apparent Temperature Effects on Cardiovascular Mortality: A Comparative Study of Beijing, China and Brisbane, Australia’. In: *Public Health Research* 2.3, pp. 43–48. DOI: 10.5923/j.phr.20120203.02 (cit. on pp. 39, 46, 94).

Susca, T., S.R. Gaffin and G.R. Dell’Osso (2011). ‘Positive effects of vegetation: Urban heat island and green roofs’. In: *Environmental Pollution* 159.8-9, pp. 2119–2126. DOI: 10.1016/j.envpol.2011.03.007 (cit. on p. 5).

Taylor, Karl E., Ronald J. Stouffer and Gerald A. Meehl (2012). ‘An Overview of CMIP5 and the Experiment Design’. In: *Bulletin of the American Meteorological Society* 93.4, pp. 485–498. DOI: 10.1175/BAMS-D-11-00094.1 (cit. on p. 63).

The Inter-Sectoral Impact Model Intercomparison Project (ISIMIP) (2019). Potsdam (cit. on p. 63).

The World Bank (2017a). *GDP per capita, PPP (current international $)* (cit. on pp. 64, 96, 99).

– (2017b). *GINI index (World Bank estimate)* (cit. on pp. 97, 99).

– (2017c). *Health expenditure, total (% of GDP)* (cit. on pp. 97, 99).

– (2017d). *Improved water source (% of population with access)* (cit. on pp. 64, 97, 99).

– (2017e). *Life expectancy at birth, total (years)* (cit. on pp. 97, 99).

– (2017f). *Population ages 65 and above (% of total)* (cit. on pp. 97, 99).

– (2018). *Total Population. World Bank Open Data* (cit. on p. 16).

– (2019). *Urban Population (%)* (cit. on p. 3).

Tobías, Aurelio, Ben Armstrong and Antonio Gasparrini (2017). ‘Brief Report: Investigating Uncertainty in the Minimum Mortality Temperature: Methods and Application to 52 Spanish Cities.’ In: *Epidemiology* 28.1, pp. 72–76. DOI: 10.1097/EDE.0000000000000567 (cit. on pp. 38, 46, 95).

Tobías, Aurelio, Ben Armstrong, Ines Zuza, Antonio Gasparrini, Cristina Linares and Julio Diaz (2012). ‘Mortality on extreme heat days using official thresholds in Spain: a multi-city time series analysis’. In: *BMC Public Health* 12.1, p. 133. DOI: 10.1186/1471-2458-12-133 (cit. on p. 97).

Turek-Hankins, Lynée L. et al. (2021). ‘Climate change adaptation to extreme heat: a global systematic review of implemented action’. In: *Oxford Open Climate Change* 1.1, pp. 1–13. DOI: 10.1093/oxfclm/kgab005 (cit. on pp. 3, 7, 76, 78).

UN News (2016). *Temperature in Kuwait hits 54 Celsius, sets possible record amid Middle East heatwave – UN* (cit. on p. 18).

UNESCWA and WHO (2017). *Climate Change Adaptation in the Health Sector. Using Integrated Water Resources Management Tools*. Tech. rep. Beirut, Lebanon: United Nations Economic and Social Commission for Western Asia; World Health Organization, p. 99 (cit. on p. 22).

Urban, Aleš et al. (2021). 'Evaluation of the ERA5 reanalysis-based Universal Thermal Climate Index on mortality data in Europe'. In: *Environmental Research* 198, p. 111227. DOI: 10.1016/j.envres.2021.111227 (cit. on p. 72).

Valois, Pierre, Denis Talbot, David Bouchard, Jean-Sébastien Renaud, Maxime Caron, Magalie Canuel and Natacha Arrambourg (2020). 'Using the theory of planned behavior to identify key beliefs underlying heat adaptation behaviors in elderly populations'. In: *Population and Environment* 41.4, pp. 480–506. DOI: 10.1007/s11111-020-00347-5 (cit. on p. 4).

Vicedo-Cabrera, Ana M., Francesco Sera and Antonio Gasparrini (2019). 'Hands-on Tutorial on a Modeling Framework for Projections of Climate Change Impacts on Health'. In: *Epidemiology* 30.3, pp. 321–329. DOI: 10.1097/EDE.0000000000000982 (cit. on pp. 29, 30).

Vicedo-Cabrera, Ana M. et al. (2018). 'Temperature-related mortality impacts under and beyond Paris Agreement climate change scenarios'. In: *Climatic Change* 150.3-4, pp. 391–402. DOI: 10.1007/s10584-018-2274-3 (cit. on pp. 26, 29, 35, 36, 50, 80).

Vicedo-Cabrera, Ana M. et al. (2020). 'Short term association between ozone and mortality: global two stage time series study in 406 locations in 20 countries'. In: *BMJ* 368, p. m108. DOI: 10.1136/bmj.m108 (cit. on p. 72).

Vicedo-Cabrera, Ana M. et al. (2021). 'The burden of heat-related mortality attributable to recent human-induced climate change'. In: *Nature Climate Change* 11.6, pp. 492–500. DOI: 10.1038/s41558-021-01058-x (cit. on pp. 1, 50, 72, 73, 75, 80).

Vuuren, Detlef P. van, Jae Edmonds, Mikiko Kainuma, Keywan Riahi, Allison Thomson, Kathy Hibbard, George C. Hurtt, Tom Kram, Volker Krey, Jean-Francois Lamarque, Toshihiko Masui, Malte Meinshausen, Nebojsa Nakicenovic, Steven J. Smith and Steven K. Rose (2011). 'The representative concentration pathways: an overview'. In: *Climatic Change* 109.1-2, pp. 5–31. DOI: 10.1007/s10584-011-0148-z (cit. on p. 51).

Vuuren, Detlef P. van, Elmar Kriegler, Brian C. O'Neill, Kristie L. Ebi, Keywan Riahi, Timothy R. Carter, Jae Edmonds, Stephane Hallegatte, Tom Kram, Ritu Mathur and Harald Winkler (2014). 'A new scenario framework for Climate Change Research: scenario matrix architecture'. In: *Climatic Change* 122.3, pp. 373–386. DOI: 10.1007/s10584-013-0906-1 (cit. on pp. 51, 52, 65, 81).

Waha, Katharina et al. (2017). 'Climate change impacts in the Middle East and Northern Africa (MENA) region and their implications for vulnerable population groups'. In: *Regional Environmental Change* 17.6, pp. 1623–1638. DOI: 10.1007/s10113-017-1144-2 (cit. on pp. 16, 19, 20, 22, 23).

Wang, Yanjun, Anqian Wang, Jianqing Zhai, Hui Tao, Tong Jiang, Buda Su, Jun Yang, Guojie Wang, Qiyong Liu, Chao Gao, Zbigniew W. Kundzewicz, Mingjin Zhan, Zhiqiang Feng and Thomas Fischer (2019). 'Tens of thousands additional deaths annually in cities of China between 1.5 °C and 2.0 °C warming'. In: *Nature Communications* 10.1, p. 3376. DOI: 10.1038/s41467-019-11283-w (cit. on p. 26).

Weinberger, Kate R., Leah Haykin, Melissa N. Eliot, Joel D. Schwartz, Antonio Gasparrini and Gregory A. Wellenius (2017). 'Projected temperature-related deaths in ten large U.S. metropolitan areas under different climate change scenarios'. In: *Environment International* 107.July, pp. 196–204. DOI: 10.1016/j.envint.2017.07.006 (cit. on pp. 2, 26).

Weinberger, Kate R., Keith R. Spangler, Antonella Zanobetti, Joel D. Schwartz and Gregory A. Wellenius (2019). 'Comparison of temperature-mortality associations estimated with different exposure metrics'. In: *Environmental Epidemiology* 3.5, e072. DOI: 10.1097/ee9.0000000000000072 (cit. on p. 27).

Whitmee, Sarah et al. (2015). 'Safeguarding human health in the Anthropocene epoch: report of The Rockefeller Foundation–Lancet Commission on planetary health'. In: *The Lancet* 386.10007, pp. 1973–2028. DOI: 10.1016/S0140-6736(15)60901-1 (cit. on p. 80).

Wichmann, Janine (2017). 'Heat effects of ambient apparent temperature on all-cause mortality in Cape Town, Durban and Johannesburg, South Africa: 2006–2010'. In: *Science of The Total Environment* 587-588, pp. 266–272. DOI: 10.1016/j.scitotenv.2017.02.135 (cit. on pp. 38, 39, 46, 94, 95, 99, 101).

Wight, Daniel, Erica Wimbush, Ruth Jepson and Lawrence Doi (2016). 'Six steps in quality intervention development (6SQuID)'. In: *Journal of Epidemiology and Community Health* 70.5, pp. 520–525. DOI: 10.1136/jech-2015-205952 (cit. on pp. 7, 8).

Williams, Susan, Monika Nitschke, Thomas Sullivan, Graeme R Tucker, Philip Weinstein, Dino L Pisaniello, Kevin a Parton and Peng Bi (2012). 'Heat and health in Adelaide, South Australia: Assessment of heat thresholds and temperature relationships'. In: *Science of The Total Environment* 414, pp. 126–133. DOI: 10.1016/j.scitotenv.2011.11.038 (cit. on p. 94).

WMO (2018). *World Weather & Climate Extremes Archive* (cit. on p. 18).

World Income Inequality Database (WIID 3-4) (2017). *GINI Coeffients* (cit. on pp. 97, 99).

Wouters, Hendrik, Koen De Ridder, Lien Poelmans, Patrick Willems, Johan Brouwers, Parisa Hosseinzadehtalaei, Hossein Tabari, Sam Vanden Broucke, Nicole P. M. van Lipzig and Matthias Demuzere (2017). 'Heat stress increase under climate change twice as large in cities as in rural areas: A study for a densely populated midlatitude maritime region'. In: *Geophysical Research Letters* 44.17, pp. 8997–9007. DOI: 10.1002/2017GL074889 (cit. on pp. 5, 21).

Wu, Jianyong, Ying Zhou, Yang Gao, Joshua S. Fu, Brent A. Johnson, Cheng Huang, Young-Min Kim and Yang Liu (2014). 'Estimation and Uncertainty Analysis of Impacts of Future Heat Waves on Mortality in the Eastern United States'. In: *Environmental Health Perspectives* 122.1, pp. 10–16. DOI: 10.1289/ehp.1306670 (cit. on p. 2).

Wu, Wei, Yize Xiao, Guangchun Li, Weilin Zeng, Hualiang Lin, Shannon Rutherford, Yanjun Xu, Yuan Luo, Xiaojun Xu, Cordia Chu and Wenjun Ma (2013). 'Temperature–mortality relationship in four subtropical Chinese cities: A time-series study using a distributed lag non-linear model'. In: *Science of The Total Environment* 449, pp. 355–362. DOI: 10.1016/j.scitotenv.2013.01.090 (cit. on p. 94).

Xiao, Jianpeng, Ji Peng, Yonghui Zhang, Tao Liu, Shannon Rutherford, Hualiang Lin, Zhengmin Qian, Cunrui Huang, Yuan Luo, Weilin Zeng, Cordia Chu and Wenjun Ma (2015). 'How much does latitude modify temperature–mortality relationship in 13 eastern US cities?' In: *International Journal of Biometeorology* 59.3, pp. 365–372. DOI: 10.1007/s00484-014-0848-y (cit. on pp. 95, 99).

Yacobi, Haim and Relli Shechter (2005). 'Rethinking cities in the Middle East: political economy, planning, and the lived space'. In: *The Journal of Architecture* 10.5, pp. 499–515. DOI: 10.1080/13602360500285500 (cit. on p. 18).

Yang, Jun, Peng Yin, Maigeng Zhou, Chun-Quan Ou, Yuming Guo, Antonio Gasparrini, Yunning Liu, Yujuan Yue, Shaohua Gu, Shaowei Sang, Guijie Luan, Qinghua Sun and Qiyong Liu (2015). 'Cardiovascular mortality risk attributable to ambient temperature in China'. In: *Heart* 101.24, pp. 1966–1972. DOI: 10.1136/heartjnl-2015-308062 (cit. on pp. 43, 47, 94).

Yin, Qian, Jinfeng Wang, Zhoupeng Ren, Jie Li and Yuming Guo (2019). 'Mapping the increased minimum mortality temperatures in the context of global climate change'. In: *Nature Communications* 10.1, p. 4640. DOI: 10.1038/s41467-019-12663-y (cit. on p. 50).

Yu, Weiwei, Kerrie Mengersen, Xiaoyu Wang, Xiaofang Ye, Yuming Guo, Xiaochuan Pan and Shilu Tong (2012). 'Daily average temperature and mortality among the elderly: a meta-analysis and systematic review of epidemiological evidence'. In: *International Journal of Biometeorology* 56.4, pp. 569–581. DOI: 10.1007/s00484-011-0497-3 (cit. on pp. 95, 101).

Zacharias, Stefan, Christina Koppe and Hans-Guido Mücke (2015). 'Climate Change Effects on Heat Waves and Future Heat Wave-Associated IHD Mortality in Germany'. In: *Climate* 3.1, pp. 100–117. DOI: 10.3390/cli3010100 (cit. on p. 26).

Zaninović, Ksenija and Andreas Matzarakis (2014). 'Impact of heat waves on mortality in Croatia'. In: *International Journal of Biometeorology* 58.6, pp. 1135–1145. DOI: 10.1007/s00484-013-0706-3 (cit. on pp. 38, 46, 95, 99).

Zhao, Lei, Keith Oleson, Elie Bou-Zeid, E. Scott Krayenhoff, Andrew Bray, Qing Zhu, Zhonghua Zheng, Chen Chen and Michael Oppenheimer (2021a). 'Global multi-model projections of local urban climates'. In: *Nature Climate Change* 11.2, pp. 152–157. DOI: 10.1038/s41558-020-00958-8 (cit. on pp. 2, 72, 79).

Zhao, Qi et al. (2021b). 'Global, regional, and national burden of mortality associated with non-optimal ambient temperatures from 2000 to 2019: a three-stage modelling study'. In: *The Lancet Planetary Health* 5.7, e415–e425. DOI: 10.1016/S2542-5196(21)00081-4 (cit. on pp. 1, 72, 80).

Zheng, Zhonghua, Lei Zhao and Keith W. Oleson (2021). 'Large model structural uncertainty in global projections of urban heat waves'. In: *Nature Communications* 12.1, p. 3736. DOI: 10.1038/s41467-021-24113-9 (cit. on p. 79).

Zhou, Bin, Diego Rybski and Jürgen P Kropp (2013). 'On the statistics of urban heat island intensity'. In: *Geophysical Research Letters* 40.20, pp. 5486–5491. DOI: 10.1002/2013GL057320 (cit. on pp. 5, 81).

– (2017). 'The role of city size and urban form in the surface urban heat island'. In: *Scientific Reports* 7.1, p. 4791. DOI: 10.1038/s41598-017-04242-2 (cit. on pp. 5, 6, 21, 81).

Declaration

I hereby declare to have prepared this dissertation without illegitimate assistance. The work contained herein is original and my own except where explicitly stated otherwise by reference in the text or work which has formed part of jointly-authored publications. No part of the dissertation has been submitted for any other degree or professional qualification. This dissertation has not been presented to any other university for examination, neither in Germany nor in another country.

Potsdam, 23rd August 2022

Linda Krummenauer

Colophon

This thesis was typeset with $\LaTeX\ 2_\varepsilon$. It uses the *Clean Thesis* style developed by Ricardo Langner. The design of the *Clean Thesis* style is inspired by user guide documents from Apple Inc.

Download the *Clean Thesis* style at http://cleanthesis.der-ric.de/.